RST
RECENT SCIENCE AND TECHNOLOGY

Recent Science and Technology

ISSN 3057-0786 (Online)

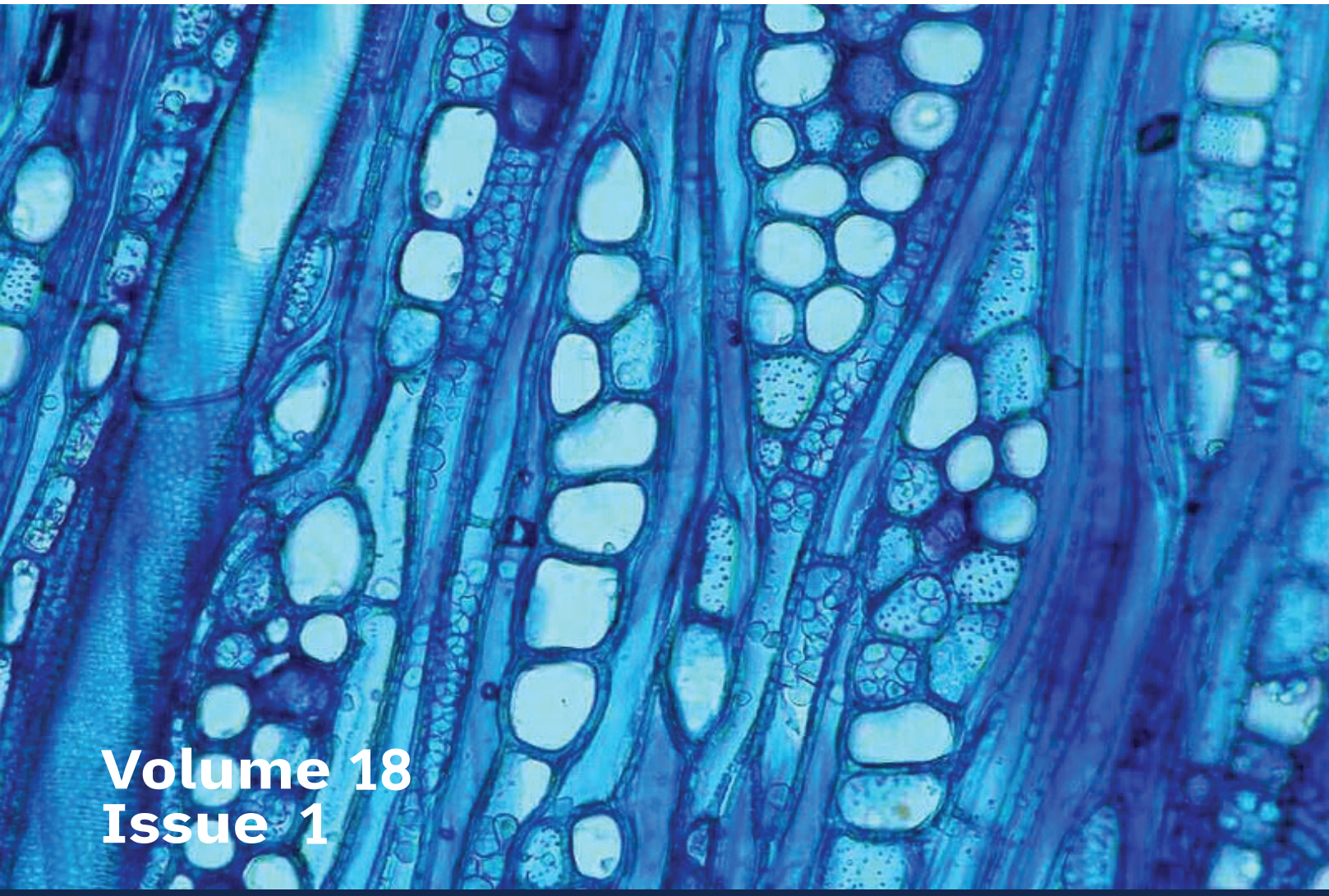

Volume 18
Issue 1

(January - April 2026)

Published by
Rajamangala University of Technology Srivijaya

TABLE OF CONTENTS

Recent Science and Technology

Journal homepage: https:// www.tci-thaijo.org/index.php/rmutsvrj/index

ISSN: 3057-0786 (Online)

Research Article

Infill Structure Analysis of 17-4 PH Materials Extrusion Additive Manufacturing based on Finite Element Method

Kaweewat Worasaen [a *] and Pasut Promsuwan [b]

[a] *Department of Information and Production Technology Management (IPTM), College of Industrial Technology, King Mongkut's University of Technology North Bangkok, Bangsue, Bangkok 10800, Thailand.*

[b] *Department of Manufacturing and Service Industry Management, Faculty of Business and Industrial Development, King Mongkut's University of Technology North Bangkok, Bangsue, Bangkok 10800, Thailand.*

Article history:

Received: 2024-12-16
Revised: 2025-06-16
Accepted: 2025-06-23

Keywords:

Digital manufacturing;
Additive manufacturing;
Infill structure design;
Finite element method

ABSTRACT

This study evaluates the mechanical performance of 17-4 precipitation-hardened (PH) stainless steel components fabricated via material extrusion additive manufacturing (MEAM), with a focus on the role of the infill structure. Finite element method (FEM) simulations and tensile testing were used to analyze how different infill patterns and densities affect structural integrity. The results show that increasing infill density improves mechanical strength and load distribution, reducing stress concentrations that lead to failure. A 30% infill density was identified as an effective balance between strength and material efficiency, making it suitable for high-pressure applications. However, this choice may limit weight reduction and material savings compared to lower infill densities. These findings highlight the importance of infill optimization in enhancing the reliability and cost-effectiveness of MEAM-produced 17-4 PH components for engineering use.

1. Introduction

The growth of additive manufacturing (AM) technologies in recent years has been a major driver in the reshaping of modern manufacturing, enabling them to produce parts with complex geometries and tailor-made properties. This technology has become a global sensation in the automotive industry because it can be used for many applications. AM can offer automated manufacturing processes, novel designs, as well as intricate shapes which are considered as part and parcel of Industry 4.0 (Wegner *et al*., 2018; Thompson *et al*., 2015). Material extrusion additive manufacturing (MEAM) is one of many forms of AM techniques that have been investigated extensively due to their flexibility and low-cost requirements.

The mechanical characteristics of 17-4 PH stainless steel are well known for their excellent qualities such as high strength, toughness, and high resistance to corrosion, achieved through the martensitic precipitation hardening process. Some studies have been carried out on 17-4 PH in AM pointing to the issue of thermal and mechanical behaviors during layer-by-layer fabrication. For instance, Buchanan and Gardner (2019) showed that the presence of Al_2O_3 ceramic in the metal matrix increased its wear resistance but caused a significant decrease in hardness. They also observed that porosities existed in processed metals than those expected from corresponding PM preforms, resulting into lower densities. MEAM part mechanical performance is defined by infill structures. Their impact can be felt on strength, mass, and material utilization. Wu *et al*. (2015)

* **Corresponding author.**

E-mail address: *kaweewat.w@cit.kmutnb.ac.th*

Cite this article as:

Worasaen, K. and Promsuwan, P. 2026. Infill Structure Analysis of 17-4 PH Materials Extrusion Additive Manufacturing based on Finite Element Method. **Recent Science and Technology** 18(1): 265687.

https://doi.org/10.65411/rst.2026.265687

examined different densities and patterns of infilling and found that optimized infill could significantly enhance the mechanical properties of printed components. Besides, Han *et al.* (2020) used FEM to analyze stress distribution in various types of infilling, thereby providing knowledge on how these patterns affect the overall performance of the part.

The Finite Element Method (FEM) is a robust technique used to evaluate mechanical characteristics of Additive Manufacturing (AM) parts. In 2014, Zhang *et al*. (2017) carried out FEM research to predict the AM stress distribution, deformation, and failure mechanisms. Crucially, FEM has been utilized in optimizing infill structures, as shown by Smith and Ritchie (2021), who used FEA to find the best infills for efficient, lightweight, high-strength components.

Connecting rods are essential components in internal combustion engines, with extremely high cyclic loads and stress. Common production methods such as forging and casting have been employed to fabricate these parts. Despite this, the recent development of AM technology has shown its promise in manufacturing connecting rods with complex geometries and improved properties. According to Kumar and Kumar (2022), research was conducted on AM used for the manufacture of a rod, in which they observed that weight reduction could be achieved by optimizing design features and materials. Knowing how a connecting rod behaves under tensile stress is significant since failure in this mode can result into severe engine destruction. Researchers indicate that tensile stress concentration areas around the small end and big end bores of the rod are critical zones for fatigue failure. Using FEM, Lee *et al*. (2019) simulated tension loading on connecting rods to determine stress concentration factors and possible points of breakage. However, limited research has addressed how infill pattern and density specifically affect the mechanical behavior of 17-4 PH stainless steel connecting rods produced using MEAM technology. This represents a key research gap that this study aims to address.

Therefore, the main goal of this research is to analyze the infill structures of 17-4 PH stainless steel MEAM parts, especially connecting rods using FEM. The objective of this study is to assess the mechanical behaviors of various patterns of infill, find out what influence is exerted by filling density on structural integrity and identify the best infill shapes that improve performance and lifespan under tensile stress conditions for connecting rods. When it comes to the results, it is expected that they will contribute to AM technologies development and adoption of 17-4 PH stainless steel in important engineering applications in general.

2. Materials and Methods

The material used for this test is 17-4PH stainless steel, which has tiny grain size and a thermoplastic organic binder. Composite materials like this one were made and used during the printing process to ensure maximum performance and precision. The chemical composition of the 17-4PH stainless steel specimens is given in Table 1 below.

Table 1 Chemical compositions of AM feedstock 17-4 PH.

Chemical compositions (%wt)				
Fe	**Cr**	**Ni**	**Cu**	**C**
70.98-77.28	15.5-17.75	3.00-5.00	3.00-5.00	0.007 (max)

2.1 Metal 3D printing process

To create the AM 17-4PH stainless steel specimens, Desktop Metal's studio system is used. This sophisticated material extrusion additive manufacturing (MEAM) process contains three main parts that are essential to the production procedure: a 3D printer, a debinding machine and, a sintering furnace. The green part is first obtained from the 3D printer and is referred to as the as-printed object. Thus, this green part was passed through debinding followed by sintering to enhance its mechanical strength and structural integrity.

The printing parameters for this study were set specifically with utmost care, including a nozzle diameter of 0.4 mm, a nozzle temperature of 165 °C, a chamber temperature of 50 °C, a stage temperature of 65 °C, a printing rate of 8 cc/hr and a layer thickness of approximately 4.5 millimeters. The construction of these green parts in a horizontal orientation ensured that uniformity and precision were maintained during the fabrication process alone.

2.2 Heat treatment process for 17-4PH stainless steel

In the heat treatment of experimental samples, two different methods were employed: solution treatment and aging treatment. Solution heat treatment was performed at 1038 °C for a time range of 15 to 30 minutes followed by quick air cooling to retain desired microstructure. The solution-treated specimens were subsequently aged for one hour at 482 °C and then, air-cooled. The purpose of this aging stage was to improve mechanical properties and stabilize the structure of the sample. The solution and aging protocols used in this study were modified from studies by Sun *et al.* (2018) and Yoo *et al.* (2006). Figure 1 shows the complete heat-treating diagram indicating temperature and duration of each stage.

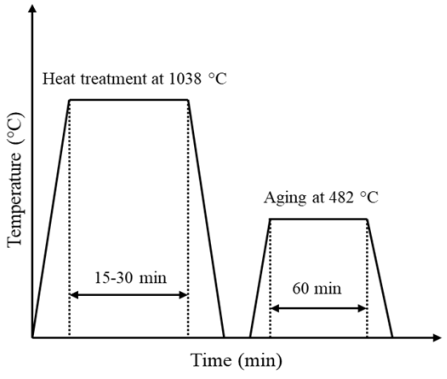

Figure 1 Heat treatment pattern of 17-4PH specimens.

2.3 Tensile testing

The tensile tests were conducted using a SHIMADZU AGS X 100 kN universal testing machine at room temperature with a strain rate of 0.00025 mm/(mm·sec) to avoid the effect of dynamic loading during the test, as recommended in the ASTM E8 standard. The specimen dimensions followed the ASTM E8 standard methods for tension testing of metallic materials, as shown in Figure 2(a).

2.4 Computer simulation setup and mesh convergence analysis

Using ANSYS Workbench, the numerical simulation was done with a license from King Mongkut's University of Technology North Bangkok (KMUTNB). In the simulation process, the material properties utilized were obtained from experimentally determined mechanical properties and stress-strain curves. Figure 2(a) displays the tensile specimen dimensions according to the ASTM E8 standard. In Figure 2 (b), region A is under displacement while region B is a fixed support with zero displacement in the simulation setup. During the entire simulation, a strain rate of 0.00025 mm/(mm·sec) developed by displacing 0.5 mm over approximately 80 seconds. To ensure an accurate and meaningful analysis, the CAD model meshing is shown in Figure 2 (c).

A mesh sensitivity study was performed to determine appropriate mesh size for this model and ensure reliable results when simulating it. Three-dimensional 10-node tetrahedral structural solid elements (SOLID187) were employed in this study using a nonlinear static analysis approach. The convergence of maximum equivalent stress in the gauge length area as a function of the number of mesh elements was analyzed. Simulation results began stabilizing after using approximately 356,420 tetrahedral elements (mesh size: 0.75 mm), as seen in Figure 3, which we adopted as our mesh configuration for this research. It should be borne in mind that if one compares the highest similar stresses between both meshes, where their sizes are respectively 0.25 mm and 0.75 mm there will be less than a one percent difference observed between them.

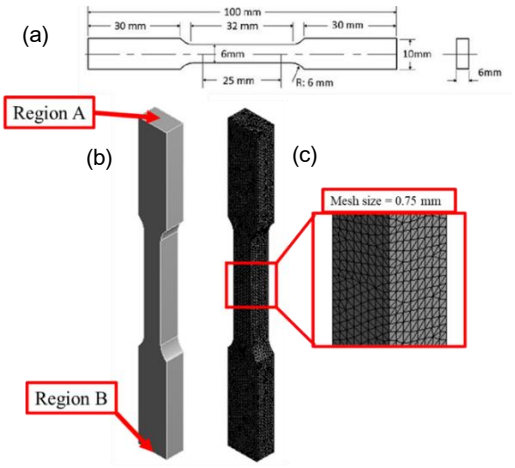

Figure 2 a) tensile specimen dimensions due to ASTM E8 standard, b) boundary condition finite element specimen and c) specimen mesh size.

2.5 Numerical model and design of connecting rod

The connecting rod design used in this research follows the standard size employed in commercial applications. The illustration of this particular connecting rod is included in Figure 4. This is equipment that has been designed to be operated under a pressure of 140 bar, as explained in the work by Witek and Zelek (2019). Cylinder support is used over region A to confine radial, rotational, and tangential movement of model. To find out how much maximum applied pressure the infill structure can withstand under working conditions, 14, 20, 25, 30, 35, 40, 45, and 50 MPa are applied on region B in –x direction. It means that there was an application of triangular-shaped infill structures with weight reductions at region C equalling about 15%, 20%, 25% and 30%, respectively.

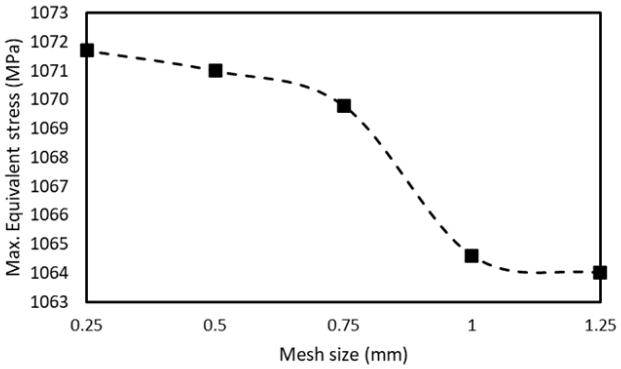

Figure 3 Mesh sensitivity analysis used in this model.

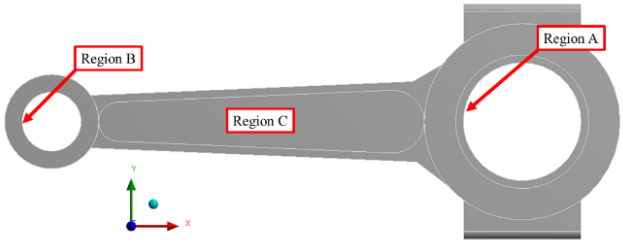

Figure 4 Boundary conditions defined in numerical model.

Figure 5 shows the infill structures having percentages equal to (a) 15%, (b) 20% (c) 25%, and (d) 30%, respectively. Nonlinear static analysis was utilized when calculating models because there were large deformations taking place at high applied loads. Considering numerical calculations, the maximum principal (σ1) stress distributions for the connecting rod were obtained at operational loads. Namely, tensile σ1 stress influences both fatigue crack initiation and crack propagation in fracture analysis.

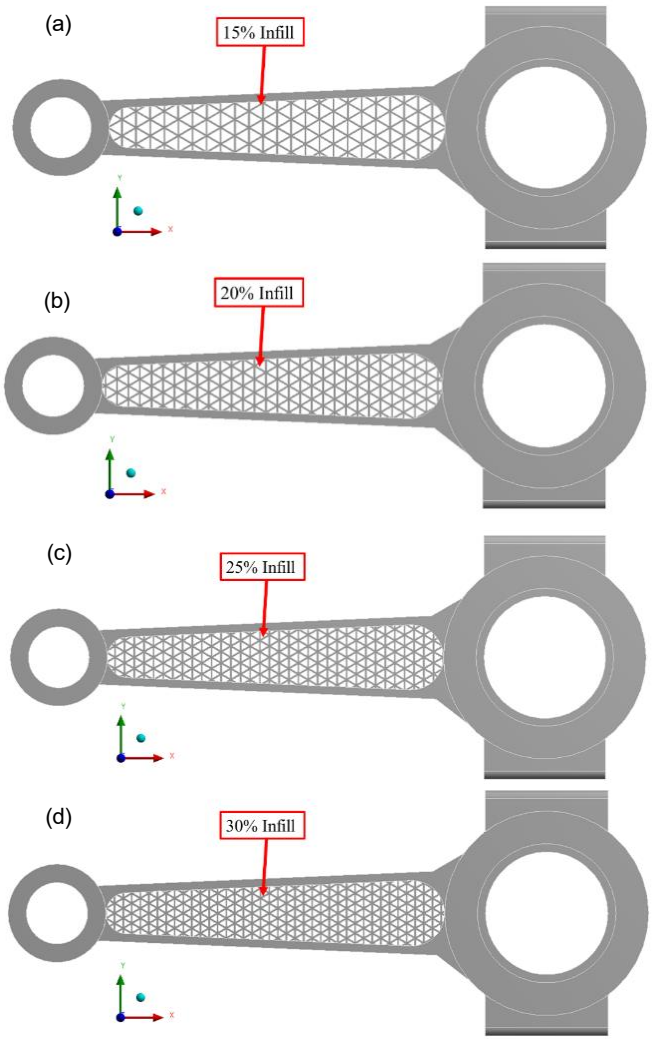

Figure 5 Infill structure design of connecting rod including a) 15%, b) 20%, c) 25% and d) 30% infill.

3. Results and Discussion

3.1 Tensile test

The engineering stress-strain curve of the AM 17-4PH stainless steel specimens is illustrated in Figure 6 and the tensile properties are shown in Table 2. Thus, when compared to the sintered specimen, it is observed that the samples revealed a higher strength in the elongation combination. A striking observation in this case was that this study sample had exceptional mechanical features, unlike MEAM 17-4PH steels mentioned in literature (Jones *et al*., 2023; Andreacola *et al*., 2021; Carneiro *et al*., 2019).

Table 2 Tensile properties of 17-4PH stainless steel.

Yield stress (MPa)	Young's modulus (GPa)	Ultimate tensile strength (MPa)	Elongation (%)
675	191	1014	4.1

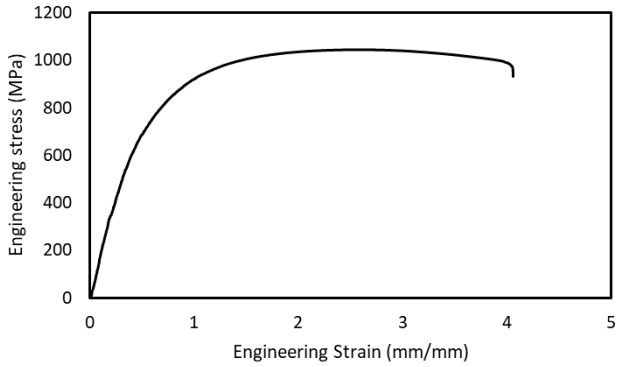

Figure 6 The engineering stress-strain curve of the AM 17-4PH stainless steel specimens.

3.2 Simulation results and experiment validation

The correlation between the simulation and direct measurements of the true stress-strain curve and true strain for the additive manufactured (AM) 17-4PH stainless steel specimen is shown in Figure 7. The figure provides an extensive comparison of the simulated data against the actual experimental results, displaying their link at different deformation stages. These validation outcomes prove that the simulation adheres to the experimentation, thereby showing how this technique is reliable and accurate.

The deviation between the experimental and numerical results remains under 5%, which proves a high accuracy of simulation procedure used. This minimal discrepancy emphasizes how well this method simulates true mechanical behaviour of AM 17-4PH stainless steel under given conditions. In addition, similarity level suggests that simulation is highly robust while also suggesting its applicability for predicting performance of AM materials within practical settings. A strong coincidence between the two shows that these simulations can be safely relied upon when undertaking further analysis on filling structure designs to optimize them as per requirements, due to their resemblance to the real process as indicated by the stress–strain curve.

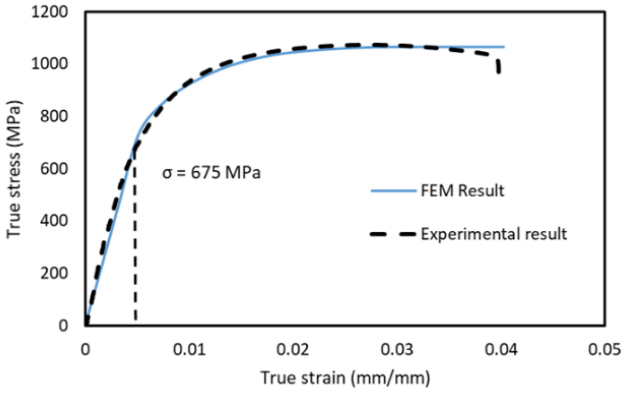

Figure 7 The validation between numerical simulation and experimental results of the true stress strain curve and the true strain for AM 17-4PH stainless steel specimen.

3.3 Influence of infill structure on stress distribution on connecting rod structures

Figure 8 presents the results of a nonlinear finite element simulation with respect to the maximum principal stress (σ1) distribution on the connecting rod model at 14MPa. Figure 8(a) depicts the σ1 stress distribution on the solid part. It is evident that, within the connection zone between the said body and rod head, a maximum of 335 MPa value is recorded for σ1 stress. This concentration of σ1 stress can cause crevices in this component. Infill development reduces the σ1 stress concentration within the joint area. However, there may still be some presence of σ1 stress concentration in the infill fin area of the 15% infill structure, as shown in Figure 8(b). The small proportion of infill structure appears to enhance significantly the concentration of σ1 stress. In figure 8 (c)-(e), starting from twenty up to thirty percent infill structures, tensile strength decreases gradually but steadily while all other parameters are constant. A large proportion of infill structure can reduce load concentrations by spreading loads more evenly over the materials under test so that weight bearing capacities are improved and localized stiffness peaks are avoided, thus contributing to global structural integrity (Thompson *et al*., 2015). Moreover, deformation modes caused by mechanical fracture mechanisms were observed predominantly along bonding interfaces between columns and horizontal layers rather than directly through any struts or nodes themselves as anticipated per their orientation within voids (Lee *et al*., 2019). Other researchers have reported similar findings; for example, Chou and Hong (2013) showed that increasing the density of fillers in three-dimensional printed objects leads to a more even spread pattern of stresses throughout them, resulting into reduced incidences of fatigue stresses and higher resistance levels among other things. Additionally, Zhang *et al*. (2022) have shown that increasing percentages used for filling materials improves load bearing ability, reducing risks associated with mechanical failure in additively fabricated products.

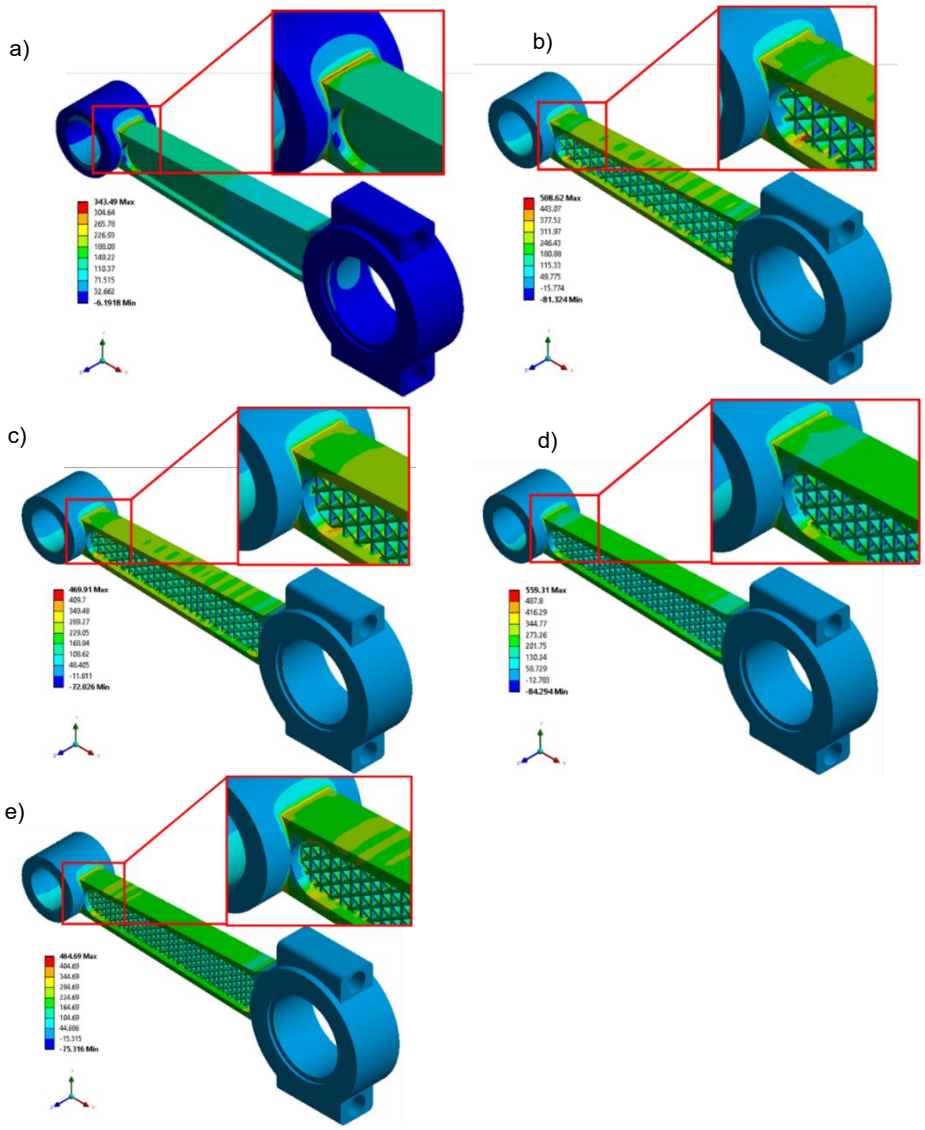

Figure 8 The maximum principal stress distribution of connecting rod under 14 MPa load in different designs including: a) solid, b) 15% infill, c) 20% infill, d) 25% infill and e) 30% infill

Various infill percentages and solid material are clearly related to applied pressure in Figure 9. Consequently, this leads to an increase in maximum principal stress with increasing applied pressure for all types of materials involved. It is the solid material that indicates consistently higher stress values. On the other hand, infill structures demonstrate a reduction in such stress levels with larger percentages, resulting into lower maximum principal stresses. The 30% infill structure shows the highest reduction in stress followed by the 25%, 20%, and 15% infills, amongst others. Hence it is clear that optimal distribution of applied loads by high density fillers helps to minimize local areas subjected to high levels of stress. Thus, infill percentage optimization is paramount for improving component mechanical performance and serviceability, especially at elevated pressures. Therefore, a better use of materials together with strength can be found on the thirty percent infill structure only. This discovery has a significant bearing on additive manufacturing as it concerns efficient application of materials for best performance results. Stress concentration may be minimized, and lifespan elongated by raising the amount of filling inside components.

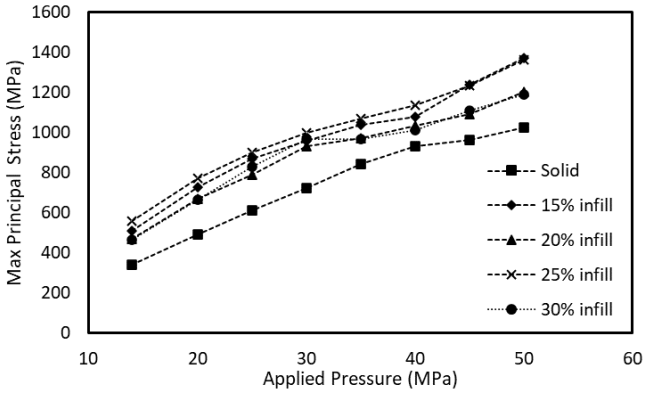

Figure 9 The relationship between applied pressure and maximum principal stress for different infill percentages and a solid material.

Figure 10 shows that the safety factor reduces as applied pressure increases among all materials. The solid sample indicates high safety factors at low pressures, but there is a remarkable decrease with an increase in pressure. Safety factors generally rise with the degree of infill; the higher the percentage of infill, the safer it is. In contrast, the 15% infill structure shows the opposite trend compared to the 30% infill structure as indicated by the lowest and highest safety factors, respectively. The difference between different filler fractions becomes prominent at lower applied pressures. However, at higher applied pressures, these differences diminish as they maintain their hierarchical order. The data suggest that an increasing percentage of infilling improves safety factor, hence offering more margin before failure. Similarly, the 30% infill provides a much greater level of protection than those with smaller proportions, thereby making it attractive for high-pressure applications. Although larger amounts of filling material result in improved protection levels, one needs to balance this requirement with manufacturing cost and time employed for production. Generally, it is important to optimize the percentage infill when making sure that these components can withstand extremely tough conditions like high pressure, thus enhancing their durability and safety features.

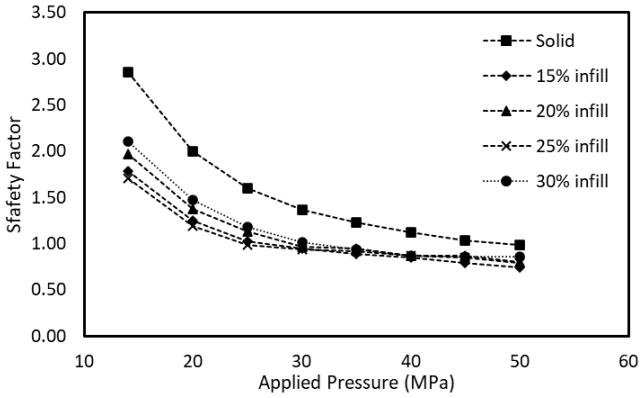

Figure 10 Relationship between safety factor and applied pressure of connecting rod in various designed conditions.

The identification of a 30% infill density as the optimal balance between mechanical strength and material efficiency has important implications for the real-world application of 17-4 PH stainless steel components produced by MEAM. In industries such as automotive, aerospace, and energy, where parts are frequently subjected to cyclic loading, it is essential to consider not only static strength but also performance under dynamic or fatigue conditions. Although this study focused primarily on tensile behaviour under quasi-static conditions, the improved stress distribution and reduced stress concentrations observed in the 30% infill structure suggest enhanced fatigue resistance. A more uniform load path reduces the risk of crack initiation, which is typically driven by local stress peaks in cyclic loading. Therefore, it is expected that the 30% infill configuration would provide superior fatigue life compared to lower-density infill structures, while still offering weight savings and reduced material use compared to solid parts. However, for applications involving high-frequency or long-duration loading cycles, further investigation is required. Real-world fatigue performance depends on factors such as build orientation, interlayer adhesion, and thermal history during processing. Future studies should evaluate the fatigue life of MEAM parts through experimental fatigue testing and life prediction modelling to fully validate their suitability for dynamic applications.

The findings of this study align closely with the objectives of Industry 4.0, particularly in promoting intelligent, resource-efficient, and digitally integrated manufacturing. By optimizing infill structures, such as the 30% density configuration in 17-4 PH stainless steel components, manufacturers can achieve a critical balance between mechanical performance and material efficiency, key principles of sustainable production. In the context of automotive applications, where weight reduction, structural

reliability, and cost control are pivotal, this research supports the adoption of material extrusion additive manufacturing (MEAM) for non-critical and semi-critical components like connecting rods, brackets, and housings. The ability to tailor internal geometries without compromising structural integrity enables design-driven performance enhancement, a hallmark of Industry 4.0's customization potential. Moreover, the validated use of finite element analysis (FEA) integrated with experimental data represents a data-driven design approach that enhances predictive maintenance and digital twin modelling. These capabilities contribute to shorter development cycles, reduced prototyping costs, and smarter production workflows, ultimately fostering more agile and adaptive manufacturing ecosystems.

4. Conclusion

This study shows that the infill pattern significantly influences the mechanical performance of 17-4 PH stainless steel components manufactured using the material extrusion additive manufacturing (MEAM) process. From the configurations tested, an infill density of 30% yielded the best combination of strength, efficiency, and durability, making it suitable for moderate to high mechanical loads. With a validated finite element method (FEM) model performing within 5% of experimental outcomes, simulation-driven design for internal structure optimization in additively manufactured parts can be trusted. These results bolster the case for utilizing MEAM to manufacture functionally critical components, particularly in automotive and aerospace industries where weight and performance are delicately balanced. From a practical standpoint, the 30% infill setting provides a static or quasi-static load enduring structure while remaining economical and maintaining sufficient strength. Further testing is needed to validate these assumptions in realistic use scenarios.

Future work should focus on evaluating the fatigue behaviour of MEAM fabricated 17-4 PH stainless steel components to understand their long-term durability under cyclic loading conditions. In addition, further investigations into performance under various environmental conditions, such as elevated temperatures, humidity, or corrosive environments, would provide valuable insights into their suitability for real-world engineering applications. These directions will help validate the robustness of optimized infill structures and extend the applicability of this manufacturing approach to more demanding and safety-critical industries.

5. Acknowledgments

The authors express their gratitude to King Mongkut's University of Technology North Bangkok (KMUTNB) for providing the ANSYS Workbench license, which was essential for the successful completion of this research.

6. References

Andreacola, F.R., Capasso, I., Pilotti, L. and Brando, G. 2021. Influence of 3D-printing parameters on the mechanical properties of 17-4PH stainless steel produced through selective laser melting. **Frattura ed Integrità Strutturale** 15(58): 282-295.

Buchanan, C. and Gardner, L. 2019. Metal 3D printing in construction: A review of methods, research, applications, opportunities and challenges. **Additive Manufacturing** 28: 704-718.

Carneiro, L., Jalalahmadi, B., Ashtekar, A. and Jiang, Y. 2019. Cyclic deformation and fatigue behavior of additively manufactured 17-4PH stainless steel. **International Journal of Fatigue** 123: 22-30.

Chou, T.H. and Hong, C.Y. 2013. Effects of infill density on mechanical properties of 3D-printed PLA parts. **Journal of Mechanical Engineering** 45(3): 279-284.

Han, D., Zhang, W., Li, P. and Fan, H. 2020. Numerical investigation of stiffness and buckling response of simple and optimized infill structures. **Structural and Multidisciplinary Optimization** 61(6): 2629-2639.

Jones, J., Vafadar, A. and Hashemi, R. 2023. A review of the mechanical properties of 17-4PH stainless steel produced by bound powder extrusion. **Journal of Manufacturing and Materials Processing** 7(5): 162.

Kumar, A. and Kumar, R. 2022. Additive manufacturing of optimized connecting rods for enhanced performance. **International Journal of Advanced Manufacturing Technology** 122(5): 3057-3070.

Lee, M.K., Lee, H., Lee, T.S. and Jang, H. 2019. Design of high duty diesel engine connecting rod based on finite element analysis. **Journal of the Brazilian Society of Mechanical Sciences and Engineering** 41: 2796-2803.

Smith, J. and Ritchie, M. 2021. Additive manufacturing infill optimization for automotive 3D-printed ABS components. **The International Journal of Advanced Manufacturing Technology** 114(6): 4207-4218.

Sun, Q., Wang, Y. and Zhang, X. 2018. Effect of solution temperature on the microstructure and properties of 17-4PH high-strength steel samples formed by selective laser melting. **Metals** 8(10): 1-14.

Thompson, S.M., Bian, L., Shamsaei, N. and Yadollahi, A. 2015. An overview of direct laser deposition for additive manufacturing; Part II: Mechanical behavior, process parameter optimization and control. **Additive Manufacturing** 8: 36-62.

Wegner, K., Meboldt, K., Klahn, R. and Breitenstein, E. 2018. Additive manufacturing of metallic materials in the context of industry 4.0. **IEEE Transactions on Industrial Informatics** 14(4): 1866-1873.

Witek, L. and Zelek, P. 2019. Stress and failure analysis of the connecting rod of diesel engine. **Engineering Failure Analysis** 97: 374-382.

Wu, W., Geng, P., Li, G., Zhao, D., Zhang, H. and Zhao, J. 2015. Influence of layer thickness and raster angle on the mechanical properties of 3D-printed PEEK and a comparative mechanical study between PEEK and ABS. **Materials** 8(10): 5834-5846.

Yoo, Y., Lee, J. and Kim, T. 2006. Microstructural evolution and mechanical properties of Ti-6Al-4V alloy subjected to solution and aging treatments. **Journal of Materials Processing Technology** 176(1-3): 162-169.

Zhang, S., Yang, F., Li, P., Bian, Y., Zhao, J. and Fan, H. 2022. A topologically gradient body-centered lattice design with enhanced stiffness and energy absorption properties. **Engineering Structures** 263: 114-384.

Zhang, W., Li, G., Wang, X. and Zhang, H. 2017. An improved prediction of residual stresses and distortion in additive manufacturing. **Computational Materials Science** 126: 360-372.

Recent Science and Technology

Journal homepage: https:// www.tci-thaijo.org/index.php/rmutsvrj/index

ISSN: 3057-0786 (Online)

Research Article

House Built with Interlocking Blocks Containing Para-Wood Ash

Premmanat Chumprom, Charoon Charoennatkul, Pornarai Boonrasi *, Chuthamat Laksanakit, Sommart Swasdi, Pongsak Sookmanee and Thaweesak Thongkhwan

Division of Civil Engineering, Faculty of Engineering, Rajamangala University of Technology Srivijaya, Mueang, Songkhla 90000, Thailand.

Article history:

Received: 2024-09-07
Revised: 2025-06-26
Accepted: 2025-09-05

Keywords:

Interlocking blocks;
Rubberwood ash;
Aggregates

ABSTRACT

This research aimed to determine the optimal mixing ratio of rubberwood ash in the aggregate of masonry blocks. The most suitable ratio was selected to construct a prototype house wall using masonry blocks mixed with rubber wood ash. The cement-to-aggregate ratios tested were 1:4, 1:5, 1:6, 1:7, and 1:8 by weight. The aggregate was a mixture of laterite and heavy rubber wood ash in ratios of 100:0, 90:10, 80:20, 70:30, 60:40, and 50:50 by weight of the aggregate. The blocks were molded using a small-scale industrial press. The results were compared to the Community Product Standard 602/2547, which specifies that the compressive strength of non-load-bearing masonry blocks must be at least 25 kg/cm², while load-bearing blocks must have a compressive strength of at least 70 kg/cm² and a water absorption rate not exceeding 288 kg/m³. All ratios met the criteria for non-load-bearing blocks, while only 11 ratios met the standard for load-bearing blocks. These included a cement-to-aggregate ratio of 1:4 with aggregate mixed with 0, 10, 20, 30, 40, and 50 percent of rubberwood ash; a cement-to-aggregate ratio of 1:5 with aggregate mixed with 0, 10, 20, and 30 percent of rubberwood ash; and a cement-to-aggregate ratio of 1:6 with aggregate mixed with 0 percent of rubberwood ash. Therefore, the cement-to-aggregate ratio of 1:8 with 50% heavy rubberwood ash was the most suitable ratio for constructing a prototype house wall. The resulting blocks exhibited a maximum heat resistance of 2.0 degrees Celsius, were 60% cheaper than commercial products, did not develop mold or mildew, and had no odor of rubberwood ash. The masonry blocks mixed with rubberwood ash could be successfully used to construct residential walls and were deemed a practical building material. This innovative building material offers a cost-effective solution and effectively converts industrial waste into a valuable product.

1. Introduction

Thailand currently ranks second globally in rubber plantation area, following Indonesia. In 2022, the country had approximately 24.23 million rai of rubber plantations, producing around 4.78 million metric tons of rubber. The northeastern and southern regions exhibited the highest rubber yield per tapped area. Once rubber trees become unproductive, farmers often resort to felling them for furniture manufacturing or as biomass fuel for electricity generation. The production of 22 megawatts of electricity requires approximately 750 metric tons of rubber wood chips, which are burned at a temperature of around 1,000 degrees Celsius. This combustion process results in approximately 15 metric tons of rubber wood ash (Dasaesamoh *et al.*, 2011). This results in a significant amount of rubber wood ash as a byproduct of the production process, posing a significant disposal challenge and requiring considerable storage space. A particleboard manufacturer in Hat Yai district, Songkhla province, is one such company facing this issue. The company generates over 10 metric tons of rubber wood ash per month. While the chemical contaminants in the ash fall within the permissible limits set by the Pollution Control Department, the predominant chemical composition is calcium oxide (CaO), accounting for 41.19%. This directly influences the compressive strength of the ash. Other components include silicon dioxide (SiO_2), aluminum oxide (Al_2O_3), and iron oxide (Fe_2O_3), at 2.57%, 0.53%, and 0.56%, respectively (Hawa and

* **Corresponding author.**

E-mail address: *Pornarai.b@rmutsv.ac.th*

Cite this article as:

Chumprom, P., Charoennatkul, C., Boonrasi, P., Laksanakit, C., Swasdi, S., Sookmanee, P. and Thongkhwan, T. 2026. House Built with Interlocking Blocks Containing Para-Wood Ash. **Recent Science and Technology** 18(1): 264615.

https://doi.org/10.65411/rst.2026.264615

Tonnayopas, 2008). When rubber wood ash is mixed with cement and water, a pozzolanic reaction occurs, enhancing the bonding properties and resulting in increased strength of the concrete block.

The utilization of recycled materials in interlocking concrete block production has been extensively studied by researchers from multiple countries. Researchers from Anna University, India, and Covenant University, Nigeria, developed an optimal mix design for interlocking blocks using fly ash and GGBS by applying an ANN model with the Levenberg-Marquardt algorithm in MATLAB to analyze data from 2,600 samples. Their study achieved 98% prediction accuracy, and the optimal mix composition resulted in 50% cost reduction with 10-fold faster construction speed (Krishna Prakash *et al*., 2021). Taking a different approach, researchers from Universitas Sumatera Utara investigated wood sawdust ash (WSA) as an eco-friendly additive in interlocking brick production by manufacturing 25×12.5×10 cm bricks with WSA replacement ratios of 0-10% and conducting comprehensive testing across multiple properties. Their results showed 20% weight reduction and enhanced sound insulation of 34.6 dB, though compressive strength decreased significantly from 13.54 to 0.81 MPa (Karolina *et al*., 2024). Meanwhile, Vietnamese researchers studied the use of municipal solid waste incineration fly ash (IFA) to replace 0-60% of cement in interlocking concrete bricks using the Densified Mixture Design Algorithm and 56-day testing protocols. Their findings demonstrated that all formulations met Vietnamese construction standards and were environmentally safe, despite compressive strength reduction from 45.04 to 28.01 MPa (Nguyen and Huynh, 2022). Finally, Ghanaian researchers tested burnt sawdust ash (BSDA) from seven timber species as partial cement replacement in laterite interlocking blocks by producing 396 blocks with 0-30% BSDA replacement and conducting 28-day testing according to British Standards. They found that 10% replacement level was optimal, with Wawa, Odum, and Mansonia species performing best (Assiamah *et al*., 2025). These research studies demonstrate the high potential of using recycled materials in interlocking concrete blocks for sustainable construction, though careful consideration must be given to the trade-offs between special properties and material strength.

Nonetheless, rubber wood ash can be incorporated as an aggregate in the production of non-loadbearing concrete blocks. Previous studies have shown that rubber wood ash can be mixed into concrete blocks at a cement-to-aggregate ratio of 1:6 and 1:8. Moreover, the optimal ratio of laterite to rubber wood ash in the aggregate mixture, based on previous research, is 50:50 or 75:25, which meets the Community Product Standards for Interlocking Blocks for non-loadbearing concrete blocks (Kuasakul *et al*., 2017). However, this research focused on load-bearing concrete blocks, using cement-to-aggregate ratios of 1:4, 1:5, 1:6, 1:7, and 1:8 by weight. The aggregate mixture consisted of various proportions of laterite to rubber wood ash, ranging from 100:0, 90:10, 80:20, 70:30, 60:40, and 50:50 by weight, with the aim of maximizing the amount of rubber wood ash in the aggregate while still meeting the Community Product Standards for Interlocking Blocks (Association of Block Manufacturers of Thailand, 2004), which stipulate a minimum compressive strength of 70 kg/cm² for load-bearing concrete blocks and 25 kg/cm² for non-loadbearing blocks, as well as a maximum water absorption of 288 kg/m³ for load-bearing blocks. The optimal ratio will be determined through experimentation by constructing a 3x4 meter prototype wall using the rubber wood ash-concrete blocks. This research may lead to the development of a new type of concrete block with a distinctive and aesthetically pleasing appearance compared to conventional concrete blocks available on the market.

2. Materials and Methods

2.1 Materials for interlocking block production

The primary constituents of the concrete blocks used in this study were a cement binder, and an aggregate mixture comprising of laterite and rubber wood fly ash. These three materials share similar chemical compositions, particularly the cement and rubber wood fly ash. The incorporation of rubber wood fly ash into the aggregate mixture served to introduce a pozzolanic material, which potentially enhanced the strength and durability of the concrete blocks. The materials used in this study are illustrated in Figure 1.

Figure 1 Materials used in research.

The objective of this study is to examine the fundamental properties of lateritic soil and rubber wood ash. To achieve this goal, several tests will be carried out, including particle size distribution analysis of Soil as per ASTM D 422-63 (ASTM, 2002a), specific gravity determination of Soil as per ASTM D 143-94 (ASTM, 1994), modified Proctor compaction as per ASTM D 1557-02 (ASTM, 2002b), and liquid limit determination as per ASTM D 2216-98 (ASTM, 1998). These tests will provide valuable insights into the engineering characteristics of the materials, which are essential for subsequent analysis and design.

The results of the sieve analysis showed that 90.76% of laterite and 93.23% of rubber wood fly ash passed through a No. 4 sieve, while 28.37% of laterite and 4.25% of rubber wood fly ash passed through a No. 200 sieve. The specific gravity of laterite and rubber wood fly ash was determined to be 2.62 and 2.25, respectively. The maximum dry density of laterite and rubber wood fly ash obtained from the standard Proctor test was 1.80 g/cm³ and 1.62 g/cm³, respectively, at optimum moisture contents of 10.60% and 7.60%, respectively. The liquid limit, plastic limit, and plasticity index of laterite were found to be 28.15%, 22.91%, and 5.24%, respectively. However, the liquid limit test could not be performed on rubber wood fly ash due to its non-plastic nature. The results of this study are generally consistent with previous research on the properties of laterite and rubber wood fly ash. The high percentage of fines in rubber wood fly ash may contribute to its pozzolanic properties and improve the long-term performance of concrete (Kuasakul *et al*., 2017). The results of the tests revealed significant variations in the properties of the materials. The particle size distribution showed a maximum difference of 37.65% between samples. The specific gravity of the laterite and rubber wood fly ash varied by a maximum of 4.44%. The standard Proctor test results indicated a maximum difference of 14.89% in dry density and 83.55% in optimum moisture content. The liquid limit test results for laterite showed a maximum variation of 155.61%. This significant variation is likely due to the different sources of laterite, indicating that the engineering properties of laterite can vary considerably depending on its origin.

2.2 Mix design for interlocking blocks

To investigate the optimal mix design, various cement-to-aggregate ratios 1:4, 1:5, 1:6, 1:7, and 1:8 by weight were tested. The aggregate consisted of varying proportions of laterite to rubber wood ash 100:0, 90:10, 80:20, 70:30, 60:40, and 50:50 by weight. Five specimens were prepared for each mix ratio, and compressive strength and water absorption tests were conducted at 7, 14, and 28 days of curing, following standard engineering practices. A total of 600 specimens were required for this study. To ensure accurate identification and prevent sample mix-ups, a labeling system was developed as follows

$$A - B - C \quad (1)$$

A : Cement-to-aggregate ratio
B : Laterite-to-rubber wood ash ratio
C : Curing age

Examples of interpreting the symbols and specifications of interlocking blocks

1:4 - 80:20 - 14 The interlocking blocks were composed of a 1:4 cement-to-aggregate ratio, where the aggregate consisted of 80:20 percent of rubberwood ash, and were cured for 14 days.

1:8 - 50:50 - 28 The interlocking blocks were composed of a 1:8 cement-to-aggregate ratio, where the aggregate consisted of 50:50 percent of rubberwood ash, and were cured for 28 days.

2.3 Molding of interlocking blocks with rubber wood ash

To accommodate the large-scale testing and construction of a sample house using interlocking blocks with rubber wood ash, a small-scale industrial molding process at a local block manufacturing plant in Hat Yai was deemed most suitable. The process began with (1) the preparation of raw materials, including laterite, rubber wood ash, cement, and water. Both the laterite and rubber wood ash were sieved through a 10-mesh sieve. (2) The mixture of laterite, rubber wood ash, and cement was thoroughly mixed using a large-scale plant mixer, followed by the addition of clean water via a spray nozzle. (3) The mixed soil was then conveyed by a conveyor belt to the molding machine. (4) After molding, the interlocking blocks were air-dried in the shade for approximately one day before curing. Curing involved sprinkling or spraying the blocks with water to keep them moist and covering them with plastic sheets to prevent moisture loss. This process was repeated for 7, 14, and 28 days, after which the blocks were subjected to standard testing procedures.

Figure 2 The molding of interlocking blocks with rubberwood ash mixture.

Figure 3 The compressive strength test of interlocking blocks.

Figure 4 Evaluation of water absorption capacity of interlocking blocks.

2.4 Testing of interlocking blocks

Prior to compressive strength and water absorption tests, interlocking blocks were subjected to a visual inspection to assess overall condition, including dimensions, cracks, and chipping, following the procedures outlined in Community Product Standard 602/2547. Only specimens that passed this initial visual inspection were then subjected to the compressive strength and water absorption tests.

3. Results and Discussion

3.1 The compressive strength of interlocking blocks

Compressive strength testing of interlocking blocks is a crucial step in evaluating the strength and quality of the binding material and aggregates. This ensures that interlocking blocks produced with rubber wood ash have sufficient and safe compressive strength, in accordance with Community Product Standard 602/2547, which specifies a minimum compressive strength of 70 kg/cm² for load-bearing blocks and 25 kg/cm² for non-load-bearing blocks. By varying the cement-to-aggregate ratio (1:4, 1:5, 1:6, 1:7, and 1:8 by weight) and the laterite-to-rubber wood ash ratio in the aggregate (100:0, 90:10, 80:20, 70:30, 60:40, and 50:50 by weight), and curing the specimens for 7, 14, and 28 days, it was found that all mixtures achieved their highest compressive strength at 28 days. The development of compressive strength for cement-to-aggregate ratios of 1:4, 1:5, 1:6, 1:7, and 1:8 was 59.63-79.76%, 64.78-83.45%, 49.67-56.13%, 26.16-32.28%, and 38.66-59.74% of the 7-day strength, respectively.

Since interlocking blocks rely on cement as a binding material, the observed increase in compressive strength with curing time is consistent with the well-established understanding of concrete hydration. Cement hydration reactions typically reach completion by 28 days, and while concrete strength continues to increase after this period, the rate of increase is significantly reduced (Thai Industrial Cement, 2014). Given the significant increase in compressive strength with curing time, this study focuses on reporting the average compressive strength of five interlocking blocks containing rubber wood ash at 28 days of curing, as presented in Table 1.

Table 1 The effect of cement-aggregate ratio on 28-day compressive strength.

Laterite to rubber wood ash ratio (%)	compressive strength (kg/cm^2)				
	cement-to-aggregate ratios 1:4	cement-to-aggregate ratios 1:5	cement-to-aggregate ratios 1:6	cement-to-aggregate ratios 1:7	cement-to-aggregate ratios 1:8
100 : 0	144.46	90.67	75.29	56.47	41.92
90 : 10	130.14	86.12	72.27	51.57	39.06
80 : 20	120.15	82.65	64.97	48.61	35.36
70 : 30	107.67	79.14	61.32	46.27	33.77
60 : 40	97.66	72.58	55.34	44.47	30.62
50 : 50	90.13	68.22	53.24	40.16	26.94

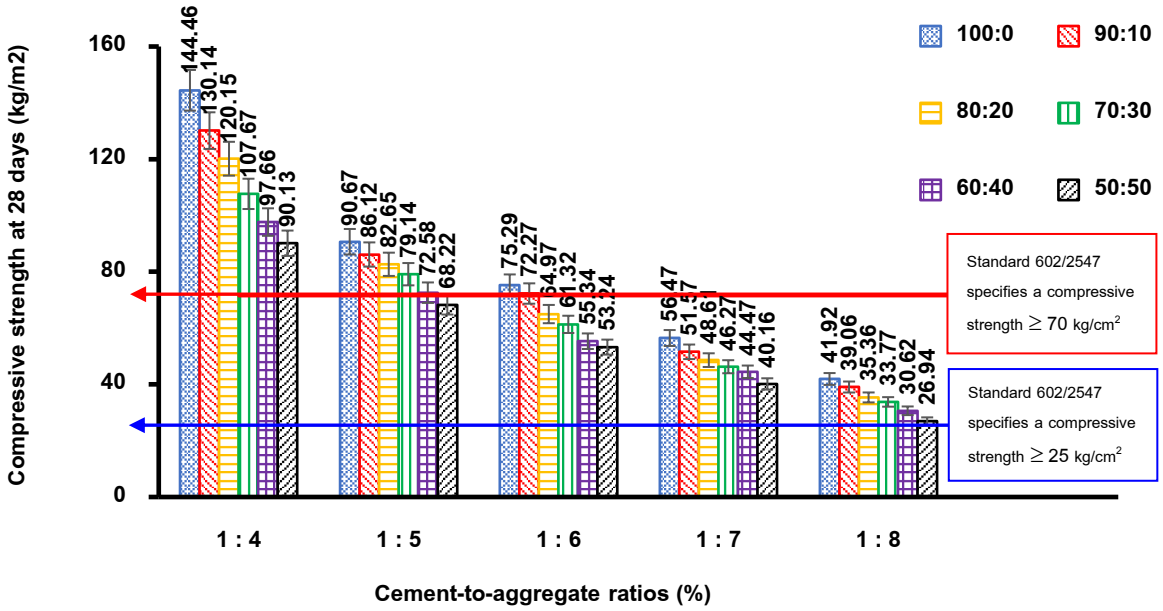

Figure 5 The effect of cement-aggregate ratio on 28-day compressive strength.

The compressive strength test results of interlocking blocks containing rubber wood ash after 28 days of curing showed that the mixture with a ratio of 1:4-100:0-28 exhibited the highest compressive strength at 144.46 kg/cm². The mixture with a ratio of 1:4-90:10-28 had the second-highest compressive strength at 130.14 kg/cm², while the mixture with a ratio of 1:8–50:50-28 had the lowest compressive strength at 26.94 kg/cm². These findings are consistent with previous research on the engineering properties of interlocking blocks containing rubber wood ash from a fishmeal factory (Kuasakul *et al.*, 2017). At a cement-to-aggregate ratio of 1:8 with a laterite-to-rubber wood ash ratio of 50:50, the compressive strength was approximately 47.50 ksc, representing a 76.32% difference, which may be attributed to the molding process. The study used a manual interlocking block machine, and when comparing the results to the Community Product Standard 602/2547, all mixtures passed the non-load-bearing criteria, while 12 mixtures passed the load-bearing criteria. These included 6 mixtures with a cement-to-aggregate ratio of 1:4, 5 mixtures with a ratio of 1:5, and 1 mixture with a ratio of 1:6. Considering compressive strength alone, a correlation equation between compressive strength and cement-to-aggregate ratio was developed, as shown in Figure 6.

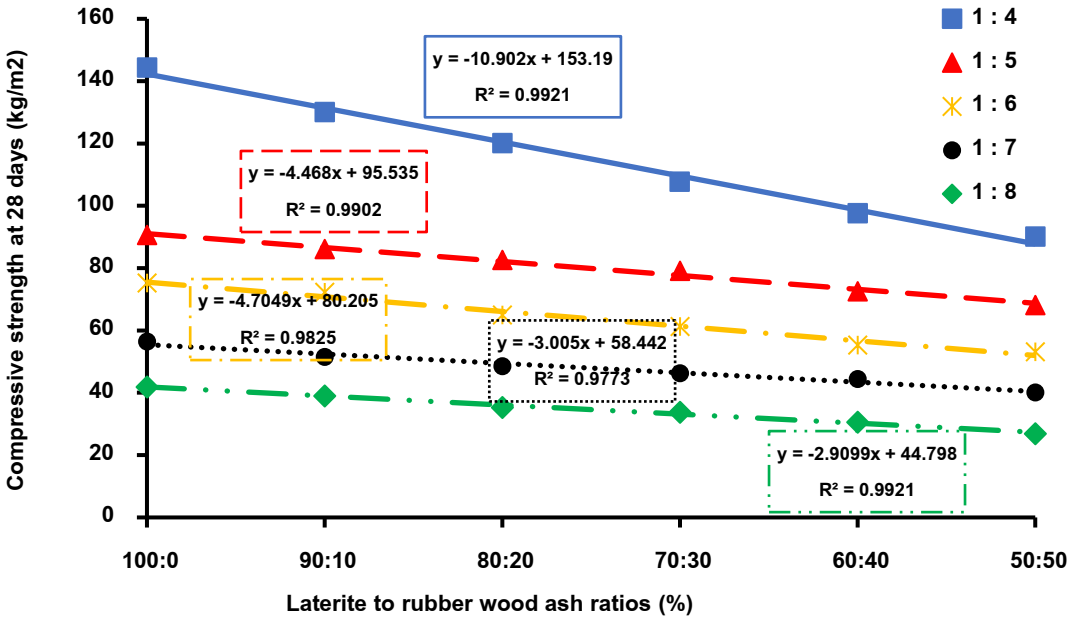

Figure 6 The relationship between cement-aggregate ratio and 28-day compressive strength.

Table 2 The equation of the relationship between compressive strength and cement-to-aggregate ratio.

Cement-to-aggregate ratios	Equation of relationship			R^2	Equation
1:4	$COMP_{1:4-28}$	=	$-10.902B_{S:A} + 153.19$	0.9921	1
1:5	$COMP_{1:5-28}$	=	$-4.468B_{S:A} + 95.535$	0.9902	2
1:6	$COMP_{1:6-28}$	=	$-4.7049B_{S:A} + 80.205$	0.9825	3
1:7	$COMP_{1:7-28}$	=	$-3.005B_{S:A} + 58.442$	0.9773	4
1:8	$COMP_{1:8-28}$	=	$-2.9099B_{S:A} + 44.798$	0.9921	5

When considering the correlation between the compressive strength equation and the cement-to-aggregate ratio, it was found that the equations of different ratios can be used to predict the compressive strength of interlocking blocks mixed with rubber wood ash. This can serve as a guideline for future research in selecting the cement-to-aggregate ratio and the mixture ratio between laterite and rubber wood ash in the aggregate.

3.2 Water absorption of interlocking blocks

Water absorption testing of interlocking blocks containing rubber wood ash is an essential component of quality control procedures for the production and utilization of interlocking blocks. This testing ensures that the blocks possess suitable properties for various applications and have a long service life. Excessive water absorption can lead to moisture accumulation, promoting the growth of mold and potentially causing deterioration or dissolution, especially in environments with extreme temperature fluctuations. To assess the water absorption properties of rubber wood ash-based interlocking blocks, an average of five samples is tested after 28 days of air curing. This curing period is selected because cement-based interlocking blocks typically reach their maximum strength within this timeframe (Thai Industrial Cement, 2014). The results are presented in Table 3.

Table 3 The average water absorption of interlocking blocks containing para-wood ash, measured over 5 samples, after a curing period of 28 days.

Laterite to rubber wood ash ratio (%)	Average water absorption of interlocking blocks after 28 days of curing (kg/m3)				
	cement-to-aggregate ratios 1:4	cement-to-aggregate ratios 1:5	cement-to-aggregate ratios 1:6	cement-to-aggregate ratios 1:7	cement-to-aggregate ratios 1:8
100 : 0	162.15	186.40	195.54	205.72	218.10
90 : 10	180.57	214.79	240.25	244.50	251.47
80 : 20	200.41	245.20	266.30	272.44	286.75
70 : 30	214.01	280.31	300.17	310.14	315.46
60 : 40	223.76	296.41	320.18	330.45	340.18
50 : 50	245.68	310.70	338.97	355.62	361.20

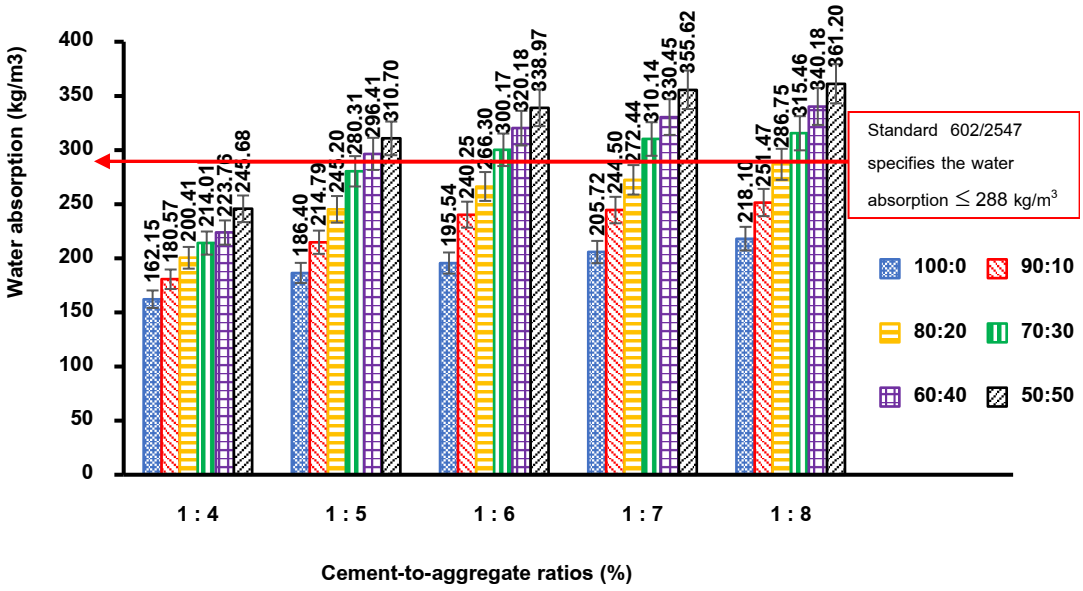

Figure 7 Average water absorption of rubber wood ash-blended interlocking blocks at 28 days.

The water absorption test results of interlocking blocks containing rubber wood ash revealed that mixtures with 50 percent of rubberwood ash exhibited the highest water absorption, ranging from 245.68 to 361.20 kg/m³. Mixtures with 40% rubber wood ash had the second-highest water absorption, ranging from 223.76 to 340.18 kg/m³, while mixtures without rubber wood ash had the lowest water absorption, ranging from 162.15 to 218.10 kg/m³. This indicates that increasing the proportion of rubber wood ash leads to higher water absorption. This phenomenon is likely due to the finer particle size of rubber wood ash compared to laterite, resulting in higher water absorption for blocks with higher proportions of rubber wood ash in the aggregate mixture. When compared to the standard for water absorption of load-bearing interlocking blocks, which is a maximum of 288 kg/m³, 19 mixtures met the standard. These included 6 mixtures with a cement-to-aggregate ratio of 1:4, 4 mixtures with a ratio of 1:5 (1:5-100:0-28 1:5-90:10-28 1:5-80:20-28 and 1:5-70:30-28), 3 mixtures with a ratio of 1:6 (1:6-100:0-28 1:6-90:10-28 and 1:6–80:20-28), 3 mixtures with a ratio of 1:7 (1:7-100:0-28 1:7-90:10-28 and 1:7-80:20-28), and 3 mixtures with a ratio of 1:8(1:8-100:0-28 1:8-90:10-28 and 1:8-80:20-28). The specific mixture proportions for these compliant blocks are listed in detail. The relationship between the proportion of laterite to rubber wood ash and water absorption was analyzed, and the resulting equation is shown in Figure 8.

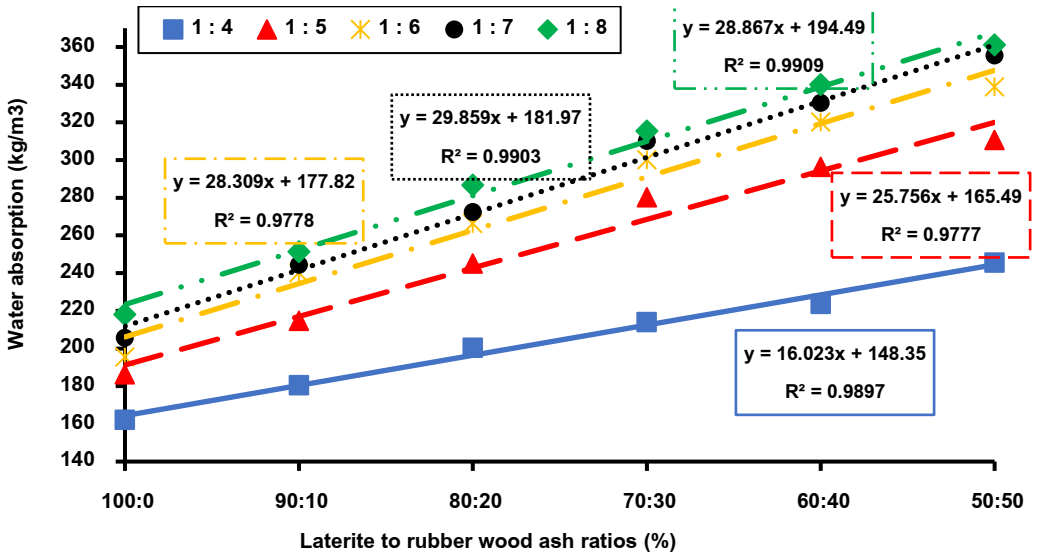

Figure 8 The relationship between average water absorption of rubber wood ash-blended interlocking blocks at 28 days.

Table 4 The equation of the relationship between average water absorption and the cement-to-aggregate ratio.

Cement-to-aggregate ratios	Equation of relationship	R^2	Equation
1 : 4	$ASB_{1:4\ -\ 28} = 16.023B_{S:A} + 148.35$	0.9401	6
1 : 5	$ASB_{1:5\ -\ 28} = 25.756B_{S:A} + 165.49$	0.9777	7
1 : 6	$ASB_{1:6\ -\ 28} = 28.309B_{S:A} + 177.82$	0.9778	8
1 : 7	$ASB_{1:7\ -\ 28} = 29.859B_{S:A} + 181.97$	0.9903	9
1 : 8	$ASB_{1:8\ -\ 28} = 28.867B_{S:A} + 194.49$	0.9909	10

Table 5 Density test results for interlocking blocks containing rubber wood ash at 28 days.

Laterite to rubber wood ash ratio (%)	Density test results for interlocking blocks containing rubber wood ash at 28 days (kg/m^3)				
	cement-to-aggregate ratios 1:4	cement-to-aggregate ratios 1:5	cement-to-aggregate ratios 1:6	cement-to-aggregate ratios 1:7	cement-to-aggregate ratios 1:8
100 : 0	1712.28	1701.95	1686.73	1673.63	1672.35
90 : 10	1692.44	1675.89	1660.10	1653.88	1650.67
80 : 20	1663.73	1654.98	1639.66	1632.68	1626.05
70 : 30	1643.66	1634.57	1614.95	1606.58	1602.00
60 : 40	1627.51	1607.68	1594.08	1586.23	1585.50
50 : 50	1598.78	1573.55	1568.08	1562.57	1562.08

When considering the correlation between the average water absorption equation and the cement-to-aggregate ratio, it was found that the equations of different ratios can be used to predict the water absorption of interlocking blocks mixed with rubber wood ash. This can serve as a guideline for future research in selecting the cement-to-aggregate ratio and the mixture ratio between laterite and rubber wood ash in the aggregate.

Results of density tests conducted on interlocking blocks. The density test of interlocking blocks with rubber wood ash was conducted to determine a key property of the samples. Given that rubber wood ash has a specific gravity of 2.05, which is lower than that of laterite at 2.29, incorporating rubber wood ash into the aggregate mixture can reduce the density of the interlocking blocks. The density of the rubber wood ash interlocking blocks was determined by averaging the values of five samples after 28 days of air curing. This curing period was chosen because interlocking blocks typically require at least 28 days to reach full strength. The results of the density tests are presented in Table 5.

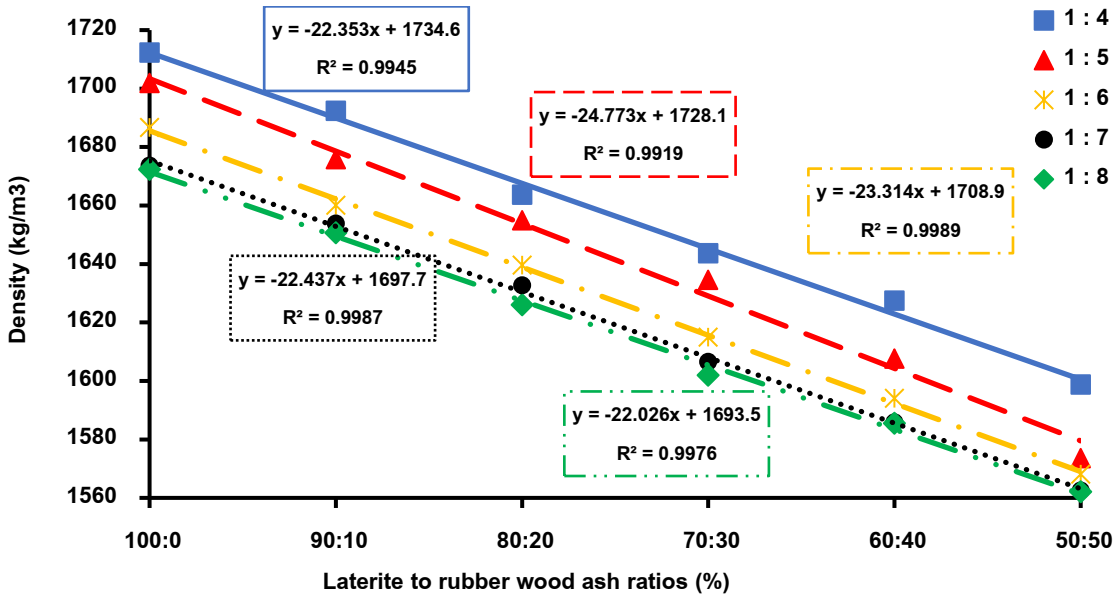

Figure 9 Density test results for interlocking blocks containing rubber wood ash at 28 days.

Density tests on interlocking blocks with rubber wood ash revealed that mixtures without rubber wood ash exhibited the highest density, ranging from 1672.35 to 1712.28 kg/m³. Mixtures with 10 percent of rubberwood ash had the second-lowest density, ranging from 1650.67 to 1692.44 kg/m³, while mixtures with 50% percent of rubberwood ash had the lowest density, ranging from 1562.08 to 1598.78 kg/m³. It is evident that increasing the proportion of rubber wood ash reduces the density of the interlocking blocks. This suggests that incorporating rubber wood ash into the aggregate mix can reduce the structural load on buildings, allowing for smaller structural elements such as beams, columns, and foundations. These findings are consistent with previous studies on interlocking blocks made with rubber wood ash and Narathiwat kaolin (Dasaesamoh *et al.*, 2014). The density values obtained from the 28-day curing test of interlocking blocks with varying mixture ratios ranged from 1532 to 1932 kg/m³. The correlation between density and mixture ratio was analyzed, and the resulting equation is presented in Figure 9.

3.3 Construction of a prototype House built with interlocking blocks containing para-wood ash

After 28 days of curing, compressive strength, water absorption, and density tests were conducted on all interlocking block mixtures. Results indicated that all mixtures met the non-load-bearing standards specified in the Community Product Standards for Interlocking Blocks (Association of Block Manufacturers of Thailand, 2004), which requires a minimum compressive strength of 25 kg/cm². Based on these findings, a cement-to-aggregate ratio of 1:8 with a 50:50 mixture of laterite and rubber wood ash (1:8-50:50-28) was selected for the prototype wall construction due to its lowest cement content and highest rubber wood ash content among all tested mixtures, making it the most cost-effective option. For load-bearing applications, a cement-to-aggregate ratio of 1:4 with a 50:50 mixture of laterite and rubber wood ash (1:4-50:50-28) was selected, as it met the minimum compressive strength requirement of 70 kg/cm² for load-bearing interlocking blocks and utilized the highest percentage of rubber wood ash among all suitable mixtures. A cost analysis of producing interlocking blocks with rubber wood ash revealed that non-load-bearing blocks have a production cost of 6.41 baht per block, which is 13.59 baht cheaper than the market price, representing a 67.95% reduction. Load-bearing blocks have a production cost of 8.00 baht per block, which is 12.00 baht cheaper than the market price, representing a 60.00% reduction. These cost comparisons do not include profit margins or marketing costs. However, it is evident that incorporating rubber wood ash into interlocking blocks can reduce production costs by at least 0.20-0.23 baht per block. Additionally, considering the environmental benefits of reducing industrial waste and mitigating air pollution, soil contamination, and water pollution, the production of interlocking blocks with rubber wood ash is both feasible and economically viable.

Therefore, based on the comprehensive analysis of data and components, it can be concluded that a cement-to-aggregate ratio of 1:8 with an aggregate mixture of 50:50 rubber wood ash (1:8-50:50-28) is the most suitable and cost-effective option for constructing a prototype wall using interlocking blocks made from rubber wood ash.

Figure 10 House built with interlocking blocks containing para-wood ash.

3.4 Initial data collection of the prototype house regarding thermal resistance and physical properties

This study presents the initial findings of a month-long monitoring of a prototype house constructed using interlocking blocks made from a mixture of cement, laterite, and rubber wood ash at a ratio of 50:50 (1:8-50:50-28), respectively. The primary focus was on assessing the thermal performance and physical properties of the blocks, including mold growth, color changes, and odors. Results showed that the interlocking blocks made from rubber wood ash were successfully used to construct the prototype house and provided a maximum heat resistance of 2.0 degrees Celsius. Since the prototype house was constructed behind a school building, where the ambient temperature is relatively low, the temperature difference between the interior and exterior of the house was not significant.

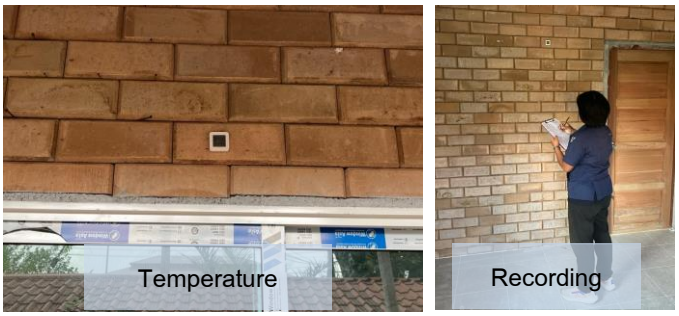

Figure 11 Temperature recording of a house built with interlocking blocks containing para-wood ash.

Visual observations of the interlocking blocks were conducted daily from July 17 to August 17, 2024, to monitor the occurrence of mold, color changes, and odors. No mold growth or rubber wood ash odor was observed on the interlocking blocks. The only detectable odor was that of cement, which is commonly associated with the construction process. While the interior interlocking blocks maintained their original grayish-brown color, the exterior blocks exhibited a color change from grayish-brown to reddish-brown after 31 days. This color change is likely attributed to the constant exposure to salt-laden aerosols carried by sea breezes, as the prototype house is located near the coast. Consequently, the exterior wall surface experienced color alteration before the interior surface.

Figure 12 Color of interlocking blocks with rubber wood ash admixture inside a house.

Figure 13 Changes in the surface color of interlocking blocks with rubber wood ash admixture on the exterior of a house.

4. Conclusion

The production of interlocking blocks using rubber wood ash by a particleboard manufacturer in Hat Yai district, Songkhla province, has proven to be a feasible endeavor. This initiative not only promotes the development and utilization of industrial waste but also contributes to the creation of environmentally friendly construction materials. By substituting traditional raw materials with rubber wood ash, production costs can be reduced, enhancing the product's competitiveness in the market. Based on tests conducted according to the Community Product Standards for Interlocking Blocks (Association of Block Manufacturers of Thailand, 2004), it was found that increasing the aggregate content while maintaining a constant cement ratio resulted in a decrease in compressive strength and an increase in water absorption. Similarly, increasing the proportion of rubber wood ash and decreasing the amount of laterite led to a reduction in compressive strength and an increase in water absorption. The optimal cement-to-aggregate ratios of 1:4, 1:5, and 1:6 by weight allowed for the incorporation of up to 50, 30, and 0 percent of rubberwood ash by weight, respectively, while still meeting the standards for load-bearing interlocking blocks. A cement-to-aggregate ratio of 1:4 by weight, with 50 percent

of the aggregate replaced by rubber wood ash, was found to be the optimal mix for producing load-bearing interlocking blocks. All block mixtures within the scope of this research met the standards for non-load-bearing interlocking blocks. Consequently, a cement-to-aggregate ratio of 1:8 by weight, with 50% of the aggregate replaced by rubber wood ash, was selected as the most suitable mixture for constructing a prototype wall using interlocking blocks made from rubber wood ash. This mixture resulted in a production cost of 6.41 baht per block, which is 13.59 baht cheaper than the market price, representing a 67.95 percent cost reduction. The resulting blocks exhibited a maximum heat resistance of 2.0°C, no mold growth, and no rubber wood ash odor. These findings demonstrate the feasibility and practicality of using interlocking blocks made from rubber wood ash for residential construction. The production of interlocking blocks from rubber wood ash offers a cost-effective and sustainable solution for converting industrial waste into a valuable product.

5. Recommendations

In this research, interlocking blocks made from rubber wood ash were produced using a manual interlocking block press in the Civil Engineering Department's laboratory. The optimal mixture ratio has been determined based on the previous study titled 'The Feasibility of Using Rubberwood Bottom Ash in The Mixture of Interlocking Block' (Chumprom *et al*., 2024). However, when the aforementioned mixture ratio was applied to a small-scale industrial interlocking block press at a local factory in Hat Yai, it was found that the blocks could not be successfully molded. Consequently, all mixture ratios were retested using the factory's equipment. Based on these findings, it is recommended that future research involving large-scale production of interlocking blocks should utilize industrial-scale molding equipment.

6. References

Assiamah, S., Kankam, C.K., Adinkrah-Appiah, K., Afrifa, R.O., Banahehe, O.J. and Agyeman, S. 2025. The impact of burnt sawdust ash from timber species as partial cement replacements on the durability properties for sustainable interlocking blocks. **Discover Civil Engineering** 2(20).

Association of Block Manufacturers of Thailand. 2004. **Community product standards for interlocking bricks (MPS 602/2547).** Association of Block Manufacturers of Thailand, Bangkok.

ASTM. 1994. **Standard test methods for specific gravity of soil solids by water pycnometer (D 143-94).** American Society for Testing and Materials, West Conshohocken, PA.

ASTM. 1998. **Standard test method for laboratory determination of water (moisture) content of soil and rock by mass1 (D 2216-98).** American Society for Testing and Materials, West Conshohocken, PA.

ASTM. 2002a. **Standard test methods for particle-size analysis of soils (D 422-63).** American Society for Testing and Materials, West Conshohocken, PA.

ASTM. 2002b. **ASTM D 1557-02 standard test methods laboratory compaction characteristics of soil using modified effort.** American Society for Testing and Materials, West Conshohocken, PA.

Chumprom, P., Charoennatkul, C., Boonrasi, P., Laksanakit, C., Swasdi, S., Sookmanee, P. and Thongkun, T. 2024. The feasibility of using rubberwood bottom ash in the mixture of interlocking block. **Research on Modern Science and Utilizing Technological: Innovation Journal (RMUTI Journal)** 17(1): 15-26. (inThai)

Dasaesamoh, A., Maming, J., Radeang, N. and Awae, Y. 2011. Physical roperties and mechanical properties of para rubber wood fly ash brick. **Journal of Yala Rajabhat University** 6(1): 25-35. (inThai)

Dasaesamoh, A., Maha, H. and Chebueraheng, H. 2014. Properties of interlocking block from para rubber wood fly ash mixed narathiwat kaolin. **Journal of Science, Technology, and Environment Research for Learning** 5(2): 202-208. (inThai)

Hawa, A. and Tonnayopas, D. 2008. Effects of rubber wood fly ash on the properties of pumice concrete, pp. 115-119. *In* **Proceedings of the 6th Chulalongkorn University Engineering Conference.** Chulalongkorn University, Bangkok.

Karolina, R., Fachrudin, H.T., Handana, M.A.P., Farhan, A. and Ritonga, S.I. 2024. Utilizing of wood sawdust ash in eco-friendly interlocking bricks: A sustainable approach. **E3S Web of Conferences** 519: 04006.

Krishna Prakash, A., Jane Helena, H. and Awoyera, P.O. 2021. Optimization of mix proportions for novel dry stack interlocking concrete blocks using ANN. **Advances in Civil Engineering** 2021(1): 9952781.

Kuasakul, T., Charoennatkul, C. and Lukjan, A. 2017. Engineering properties of interlocking blocks containing rubber wood ash of a fishmeal factor, pp. 384-392. *In* **The 14th National Kasetsart University Kamphaeng Saen Conference (The 14th KU-KPS) Conference.** Kasetsart University Kamphaeng Saen, Nakhon Pathom.

Nguyen, M.H. and Huynh, T.P. 2022. Turning incinerator waste fly ash into interlocking concrete bricks for sustainable development. **Construction and Building Materials** 321: 126385.

Thai Industrial Cement. 2014. Curing and formwork removal of concrete, pp. 241-243. *In* Sethabutra, C., Maenpimolchai, S., Jitwarodom, S. and Phanmicheaw, T., eds. **Cement and applications.** Bangkok.

Recent Science and Technology 18(1): 266514

Recent Science and Technology

Journal homepage: https:// www.tci-thaijo.org/index.php/rmutsvrj/index

ISSN: 3057-0786 (Online)

Research Article

Feature Analysis of Current Unbalance in Electrical Distribution Systems Using Random Forest

Santi Karisan [a]* and Sittisak Rojchaya [b]

[a] *Department of Engineering, College of Industrial Technology and Management, Rajamangala University of Technology Srivijaya, Khanom, Nokhon Si Thammarat 80210, Thailand.*

[b] *Department of Electrical Engineering, Faculty of Engineering and Technology, Rajamangala University of Technology Srivijaya, Sikao, Trang 92150, Thailand.*

Article history:

Received: 2025-02-28
Revised: 2025-09-04
Accepted: 2025-10-10

Keywords:

Current Unbalance;
Machine Learning;
Random Forest Regressor

ABSTRACT

The building sector accounts for more than 130 exajoules (EJ) of global energy consumption, representing approximately 30% of the total energy demand, with a continuous upward trend. Notably, energy demand in buildings surged during the COVID-19 crisis and increased by approximately 20% between 2000 and 2007. A significant portion of this energy consumption is attributed to lighting and air-conditioning systems. The rising electricity demand in buildings adversely impacts power quality, leading to issues such as harmonic distortion, voltage unbalance, and current unbalance in electrical distribution systems. This study investigates the application of the Machine Learning-based Random Forest Regressor model to analyze the causes of current unbalance in a building's power distribution system. A case study was conducted using electricity consumption data from a facility at the College of Industrial Technology and Management, Rajamangala University of Technology. The analysis results indicate that power features significantly influence current unbalance, with Power Phase A contributing the most at 74.73%, followed by Power Phase C at 10.98% and Power Phase B at 9.55%. These findings provide valuable insights for optimizing maintenance strategies and improving the efficiency of building power distribution systems.

1. Introduction

The building sector accounts for more than 130 exajoules (EJ) of global energy consumption, representing approximately 30% of total energy demand, with a continuously increasing trend. During the COVID-19 crisis, energy consumption in this sector surged beyond typical levels. Historical data from 2000 to 2007 indicate an approximate 20% increase in energy demand (Santamouris and Vasilakopoulou, 2021). A significant portion of this energy is utilized for lighting and air-conditioning systems, including heating, cooling, and ventilation (Melo *et al.*, 2023). The growing deployment of such systems has significantly contributed to the increasing electricity demand in buildings.

The rise in electricity demand negatively impacts power quality, leading to issues such as harmonic distortion, voltage unbalance, and current unbalance in electrical systems (Drovtar *et al.*, 2012). The degradation of power quality can result in increased energy losses in power transmission, excessive heat buildup in electrical components, and a reduced lifespan of connected equipment. Additionally, power quality disturbances may cause operational errors in industrial control devices such as Programmable Logic Controllers (PLC) and Variable Frequency Drives (VFD). To mitigate power quality issues in electrical distribution systems, previous studies have proposed various analytical approaches. For instance, Jove *et al.* (2021) applied machine learning techniques, including Principal Component Analysis (PCA), k-nearest neighbor (KNN), and Gaussian classifiers, to detect harmonic distortions in wind generator systems. Their results indicate that PCA demonstrated the highest detection efficiency, particularly for harmonic distortion variations ranging from 10% to 40% total harmonic distortion

* **Corresponding author.**

E-mail address: *santi.k@rmutsv.ac.th*

Cite this article as:

Karisan, S. and Rojchaya, S. 2026. Feature Analysis of Current Unbalance in Electrical Distribution Systems Using Random Forest. **Recent Science and Technology** 18(1): 266514.
https://doi.org/10.65411/rst.2026.266514

(THD) and exceeding 90% THD. In another study, Vinayagam *et al.* (2021) analyzed the impact of integrating renewable energy sources, such as solar power, into the electrical grid. Their comparison of two models one combining Bayesian networks with multilayer perceptron classifiers (Model 1) and another incorporating Bayesian networks, multilayer perceptrons, and J48 decision tree classifiers (Model 2) revealed that Model 2 achieved a classification accuracy of up to 100%. Furthermore, Wang and Chen (2019) introduced a convolutional neural network (CNN)-based system for power quality classification within multi-energy integration systems. Their results demonstrated that CNN achieved an accuracy of approximately 99.5% on validation data, with a training time of 191 minutes, outperforming long short-term memory (LSTM), ResNet50, and stacked autoencoder (SAE) models.

A review of existing research suggests that most power quality disturbance classification techniques rely on machine learning models combined with feature extraction methods based on signal processing (Chawda *et al.*, 2020). However, these approaches often focus on classification rather than identifying the root causes of power quality issues. Therefore, this study presents the application of the Random Forest Regressor model, a machine learning technique well-suited for analyzing nonlinear datasets of medium to large sizes (Schonlau and Zou, 2020). The proposed approach aims to identify the key factors contributing to current unbalance in building power distribution systems. The analysis is conducted using real-world electricity consumption data from the College of Industrial Technology and Management, Rajamangala University of Technology. The findings of this study will contribute to the development of optimized maintenance strategies for electrical distribution systems, ultimately improving energy efficiency and system reliability.

2. Theoretical Framework

2.1 Unbalanced Current

In a three-phase power supply system, the system is considered to be in a balanced current state when the current magnitudes in all three phases are equal and the phase shift between them is precisely 120°. However, any deviation from these conditions results in an unbalanced current state (Mahmoud, 2021). The degree of current unbalance is typically quantified by evaluating the ratio of the maximum deviation of phase currents from the average phase current to the total average current across all phases. This is commonly expressed as the Percentage Current Unbalance (PCU) in accordance with the IEEE 45-2002 standard (Sinuraya *et al.*, 2022). The general formulation for PCU is defined as follows: (1)

$$PCU = \frac{I_{Max}Dev}{I_{avg}} \times 100 \quad (1)$$

From (1), the Percentage Current Unbalance *PCU* is defined as the ratio of the maximum current deviation to the total average current across all phases. The maximum current deviation $I_{Max}Dev$ from the average current in each phase is determined using (2), while the total average current I_{avg} across all phases is calculated as shown in (3).

$$I_{Max}Dev = \max\left(\left|I_A - I_{avg}\right|, \left|I_B - I_{avg}\right|, \left|I_C - I_{avg}\right|\right) \quad (2)$$

$$I_{avg} = \frac{I_A + I_B + I_C}{3} \quad (3)$$

2.2 Correlation Matrix

The Correlation Matrix serves as a fundamental statistical tool for analyzing relationships among multiple features or variables (Wang *et al.*, 2022). The relationship between features is quantified using the Correlation Coefficient (R), which ranges from -1 to 1. When $R \approx 1$, it indicates a strong positive correlation, meaning the features change in the same direction. Conversely, when $R \approx -1$, the features exhibit an inverse relationship, changing in opposite directions. If R=0, it signifies no correlation, implying that changes in one feature do not correspond to changes in another (Hadd and Rodgers, 2020). The Correlation Coefficient (R) is computed using (4)–(6).

$$X = \begin{bmatrix} X_{1,1}X_{1,2}\cdots X_{1,m} \\ X_{2,1}X_{2,2}\cdots X_{2,m} \\ \vdots \\ X_{n,1}X_{n,2}\cdots X_{n,m} \end{bmatrix} \quad (4)$$

From (4), let X represent the dataset under analysis, where Observations are denoted as n and Variables as m. Each data point in the dataset is evaluated to determine the Correlation Coefficient (r) using the Pearson correlation coefficient equation, as defined in (5). In this context, $X_{i,j}$ represents the data at the i^{th} Observation and the j^{th} Feature within the dataset.

$$r_{X_i,X_j} = \frac{\sum(X_i - \overline{X}_i)(X_j - \overline{X}_j)}{\sqrt{\sum(X_i - \overline{X}_i)^2} \cdot \sqrt{\sum(X_j - \overline{X}_j)^2}} \quad (5)$$

From (5), let X_i and X_j represent the data points within the dataset at the specified positions, while $\overline{X}_i$ and $\overline{X}_j$ denote their respective mean values. Since equation (5) analyzes the relationship of a single feature within the dataset, the computation of the Correlation Coefficient (R) for all features within the dataset follows the matrix representation in equation (6).

$$R = \begin{bmatrix} r_{X_1,X_1} & r_{X_1,X_2} & \cdots & r_{X_1,X_m} \\ r_{X_2,X_1} & r_{X_2,X_2} & \cdots & r_{X_2,X_m} \\ \vdots & & & \\ r_{X_m,X_1} & r_{X_m,X_2} & \cdots & r_{X_m,X_m} \end{bmatrix} \quad (6)$$

From equation (6), r_{X_i,X_j} represents the Correlation Coefficient between X_i and X_j indicating the degree of relationship between the respective feature positions within the dataset.

2.3 Random Forest Regressor (RFR) Algorithm

The Random Forest Regressor (RFR) is a Machine Learning Model commonly employed for decision-making processes and target prediction based on independent and uncorrelated decisions. It operates using the Bagging Technique, incorporating Boot-strapping and Aggregation principles (Breiman, 2001). In the context of Feature Importance analysis using the RFR Algorithm, two primary approaches are utilized: Mean Decrease in Impurity (MDI) and Permutation Importance. The MDI value, defined in equation (7), quantifies the extent to which a feature contributes to reducing the model's variance. Meanwhile, Permutation Importance, as described in equation (9), measures the effect of randomly shuffling features on model performance (Hastie *et al*., 2009).

$$FI(X_j) = \frac{1}{T}\sum_{t=1}^{T}\sum_{s \hat{I} S_t, X_a = X_j} \Delta Var_s \quad (7)$$

As presented in equation (7), $FI(X_j)$ is defined as the Mean Decrease in Impurity (MDI), where S_t represents the set of nodes in tree T that utilize the corresponding feature. Additionally, ΔVar_s is defined based on Decision Tree Regression, which is computed using equation (8).

$$\Delta Var_s = Var(D) - \left[\frac{|D_L|}{|D|} Var(D_L) + \frac{|D_R|}{|D|} Var(D_R) \right] \quad (8)$$

As presented in equation (8), Var(D) represents the variance of the parent node, while $Var(D_L)$ and $Var(D_R)$ denote the variances of the left and right child nodes, respectively.

$$FI(X_i) = R(X) - R(X_{shuffled}) \quad (9)$$

From equation (9), Permutation Importance $FI(X_i)$ is defined as the difference between the model error before random shuffling R(X) and the model error after random shuffling of features $R(X_{shuffled})$.

3. Materials and Methods

3.1 Installation of Electrical Energy Meters in the Building Power Distribution System

To measure electrical energy consumption within the building, a Clamp Meter (CM) is installed to monitor the current in the range of 0.6–120 A (AC) with a measurement resolution of 0.03 A. The CM supports a maximum alternating current voltage of 600 V and includes the capability to measure the temperature of the transmission line. The device is integrated into the power transmission line within the Main Distribution Board (MDB) cabinet. The installation layout of the measuring device within the MDB cabinet is illustrated in Figures 1 and 2, which depict the experimental setup utilized in this study. Once the electrical energy measurement system acquires the current flowing through the power transmission line, the signal undergoes quality enhancement via a Signal Conditioner. Subsequently, all recorded electrical energy consumption data are transmitted via Bluetooth 4.1, operating in the 2.402 GHz to 2.48 GHz frequency band, to the Gateway for data logging and further analysis.

Figure 1 The Main Distribution Board (MDB) used for analyzing the relationship between features influencing the occurrence of unbalanced current.

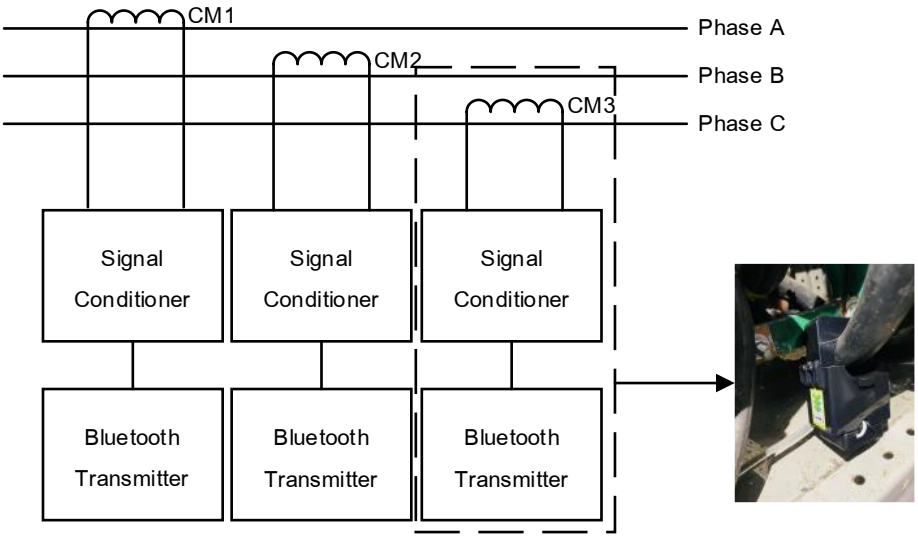

Figure 2 Diagram illustrating the installation of the Clamp Meter (CM) in the power transmission line inside the Main Distribution Board (MDB).

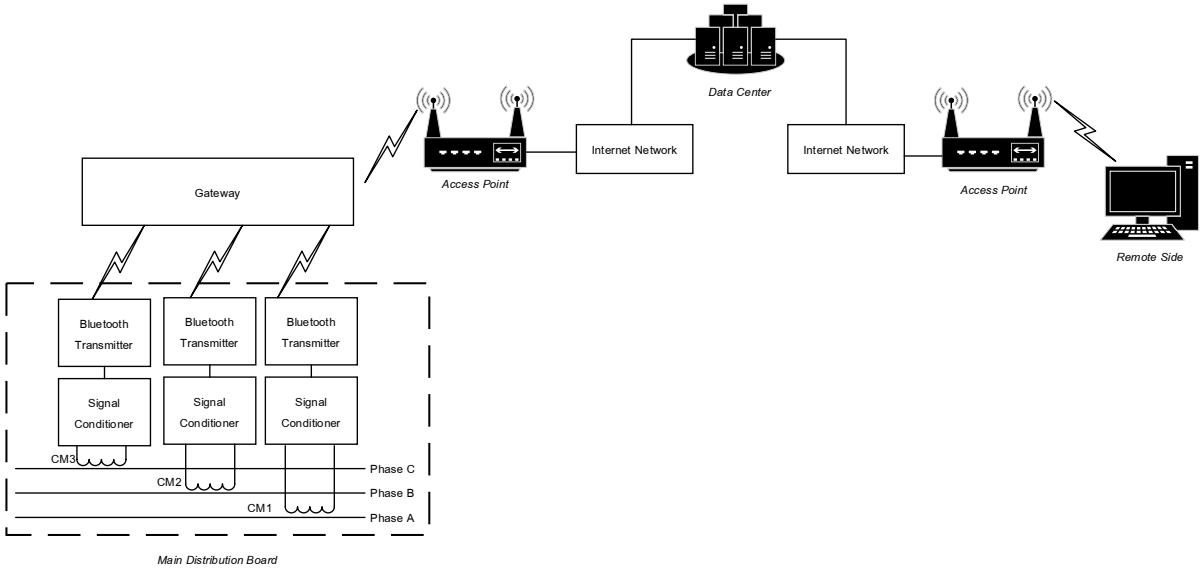

Figure 3 Overview diagram of the electrical energy usage recording system installed in the Main Distribution Board (MDB)

3.2 Electricity Usage Data Recording Process

The recording of electrical energy usage data from the Main Distribution Board (MDB) involves multiple stages. After the Clamp Meter (CM) measures the electrical parameters and undergoes the Signal Conditioning process, the processed data is transmitted to the Gateway. The Gateway serves as an intermediary, facilitating communication between field devices, specifically the Clamp Meter (CM), and the Internet via Bluetooth 4.1 operating within the 2.402 GHz to 2.48 GHz frequency range. The recorded electrical energy usage data is uploaded to the Data Center at one-minute intervals. The overall system architecture for data recording is illustrated in Figure 3. Access to the recorded electrical energy usage data is provided in CSV format, allowing for direct downloads from the Data Center. Remote-side equipment connected to the Internet, in conjunction with a Browser Engine, is utilized to retrieve and analyze the recorded data. The graphical user interface for data access and retrieval via the Browser Engine is depicted in Figure 4. For this study, electrical energy usage data was recorded continuously over one month, from December 1, 2024, to December 31, 2024. This dataset was sub-sequently used to analyze the relationship between various features influencing the occurrence of Un-balance Current.

3.3 Feature Extraction

After downloading the electrical power usage data in CSV format from the Data Center, the data is grouped into features for model training and analysis to identify relationships influencing the occurrence of Unbalance Current. The features used in this study are categorized into two groups. The first group consists of 12 features obtained from direct measurements inside the Main Distribution Board, as presented

in Table 1. The second group includes a single feature derived using an analytical equation for Unbalance Current, as defined in equation (1).

Table 1 Features of Measured Energy Consumption in the MDB Cabinet

Feature	Unit
Power Phase A	W
Energy Phase A	kWh
Current Phase A	A
Temperature Phase A	Celsius
Power Phase B	W
Energy Phase B	kWh
Current Phase B	A
Temperature Phase B	Celsius
Power Phase C	W
Energy Phase C	kWh
Current Phase C	A
Temperature Phase C	Celsius

Figure 4 Illustrating the electrical energy usage recording system.

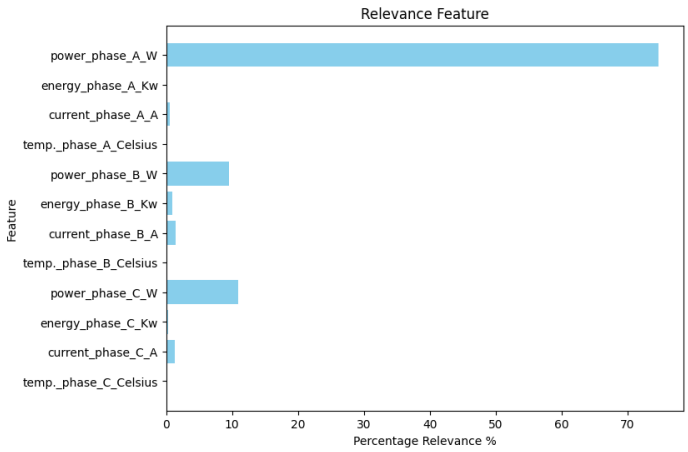

Figure 5 Comparison of relevance score percentages for each feature analyzed using the Random Forest Regressor.

4. Results and Discussion

4.1 Power

As shown in Figure 5, the power feature exerts the most significant influence on unbalanced current compared to other parameters. Phase A power alone accounts for approximately 74.73% of the observed unbalance, while Phases C and B contribute only 10.98% and 9.55%, respectively. Interestingly, the average power of Phase A is 1.56 kW, which is considerably lower than the values of Phase B (3.76 kW) and Phase C (1.80 kW), as depicted in Figure 6. This suggests that unbalanced current is not merely a function of absolute power magnitude but is strongly associated with the disproportionate loading conditions in Phase A. Further analysis of the unbalanced current distribution using histogram plots Figure 7 highlights this difference. The Phase A data exhibit a broader spread, indicating greater variability, while Phases B and C follow narrower, near- normal distributions with similar statistical characteristics. The estimated mean unbalance current in Phase A is 52.58%, significantly exceeding the 36.87% observed for Phases B and C. This wider distribution combined with the higher mean value confirms that the load imbalance in Phase A dominates the overall system unbalance. Therefore, the results demonstrate that although Phase A operates with lower average power than the other two phases, its disproportionate loading condition drives the highest unbalanced current. This finding emphasizes the importance of phase balancing in power distribution networks, as the concentration of load in a single phase can introduce substantial current imbalance, even when the overall system power is relatively low.

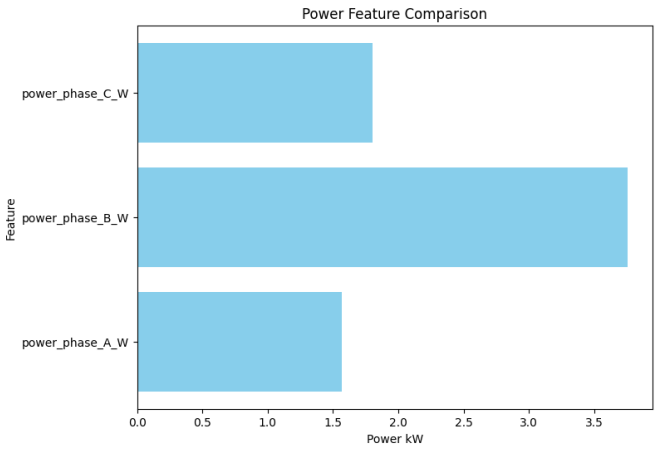

Figure 6 Comparison of power across each phase.

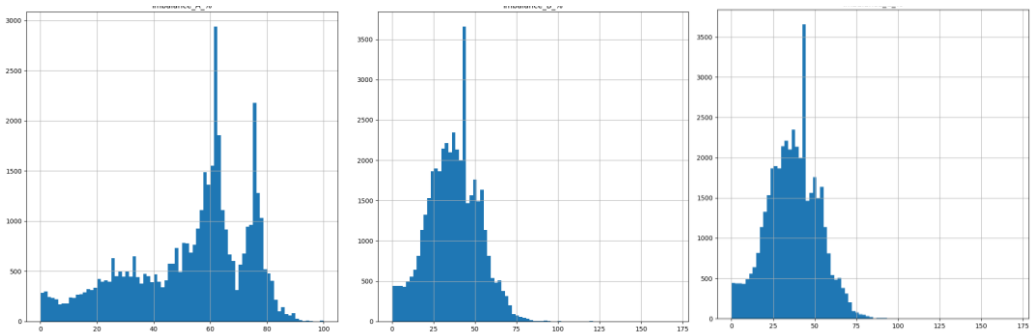

A) Unbalance current Phase A B) Unbalance current Phase B C) Unbalance current Phase C

Figure 7 Histogram of unbalance current in the power distribution system

4.2 Current

Figure 5 illustrates the contribution of electric current to the unbalance current, with Phases A, B, and C contributing 0.58%, 1.37%, and 1.21%, respectively. These results demonstrate that electric current has a minimal impact on the unbalance current compared to electric power. However, changes in electric current directly influence changes in electric power, as evidenced by the correlation matrix in Figure 8.

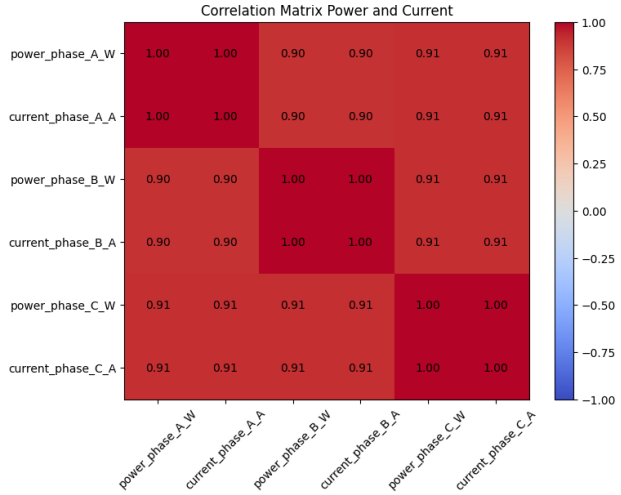

Figure 8 Correlation matrix of power and current.

The correlation matrix in Figure 8 demonstrates a perfect positive correlation (correlation coefficient = 1) between power and current across all three phases, indicating that changes in these features are directly proportional. Analysis of the current data reveals that Phase A contributes 75.17% to the unbalance current, significantly higher than Phase B (12.10%) and Phase C (12.72%). Figure 8 illustrates the percentage relevance scores of the current feature in influencing the unbalance current state.

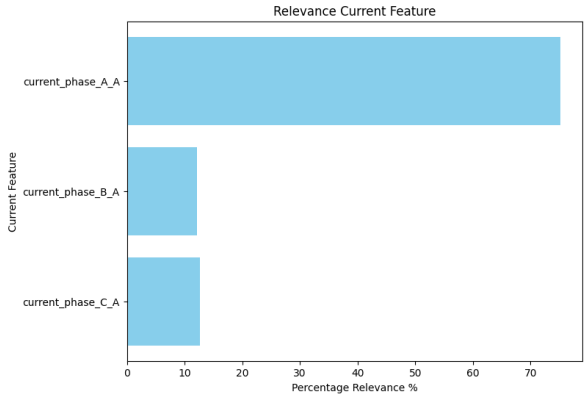

Figure 9 Comparison of relevance score percentages for the current feature analyzed using the Random Forest Regressor.

Phase A current has the highest impact on the unbalance current in the power distribution system, with an average current consumption of 4.12 A, lower than Phase C (4.74 A) and Phase B (9.89 A). Consequently, Phase A contributes the most to the unbalance current, as reflected in its higher weight in the three-phase current feature analysis. These results align with the histogram presented in Figure 7.

4.3 Energy

Analysis of the energy feature using the Random Forest Regressor indicates contributions to the unbalance current of 0.23%, 1.02%, and 0.39% for Phases A, B, and C, respectively. These values are significantly lower than those of the power and electric current features. The relationships between these features are further explored using the correlation matrix, as shown in Figure 10.

Figure 10 demonstrates that the energy feature directly influences changes in the power and current features, which are the primary drivers of the unbalance current in the power distribution system. The correlation coefficient between energy, power, and current is 1 for all phases (A, B, and C), reflecting a perfect positive relationship. This relationship arises because energy is a function of power and time, causing its variation to align directly with changes in power and current. Thus, while the energy feature does not directly impact the unbalance current, it indirectly affects it by influencing the power and current features.

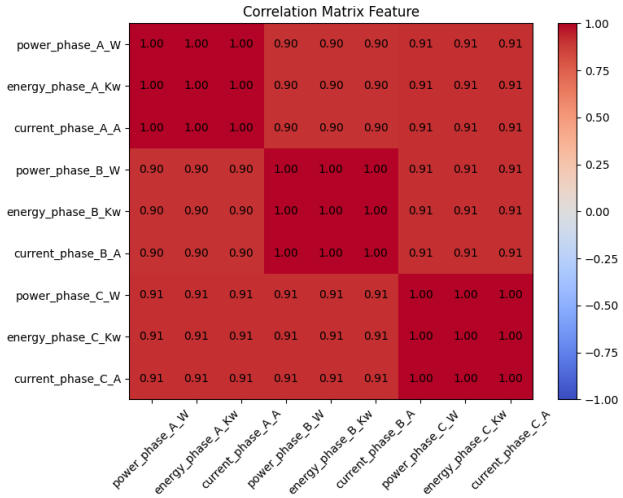

Figure 10 Correlation matrix of power, current, and energy features.

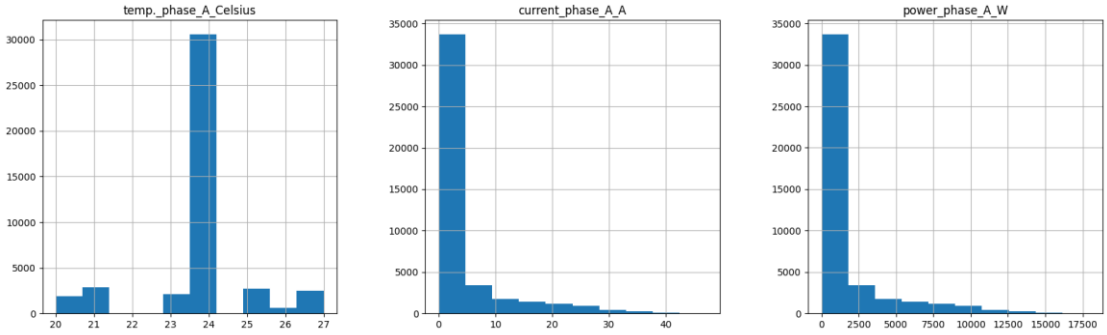

A) Temperature Phase A B) Current Phase A C) Power Phase A

Figure 11 Histogram of temperature, current, and power for Phase A.

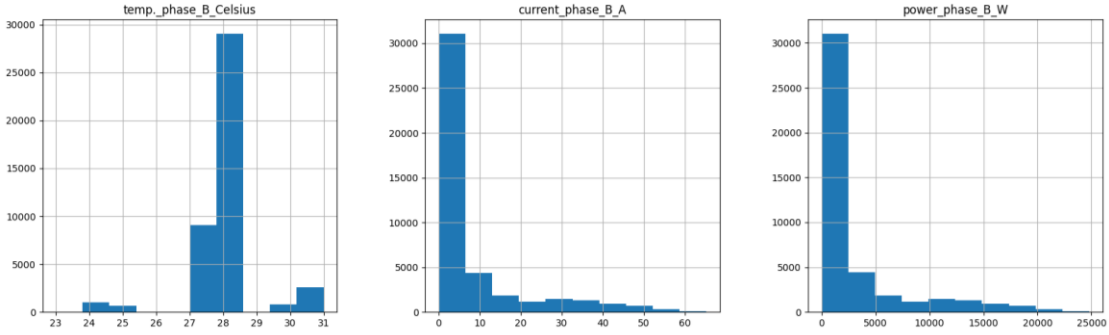

A) Temperature Phase B B) Current Phase B C) Power Phase B

Figure 12 Histogram of temperature, current, and power for Phase B.

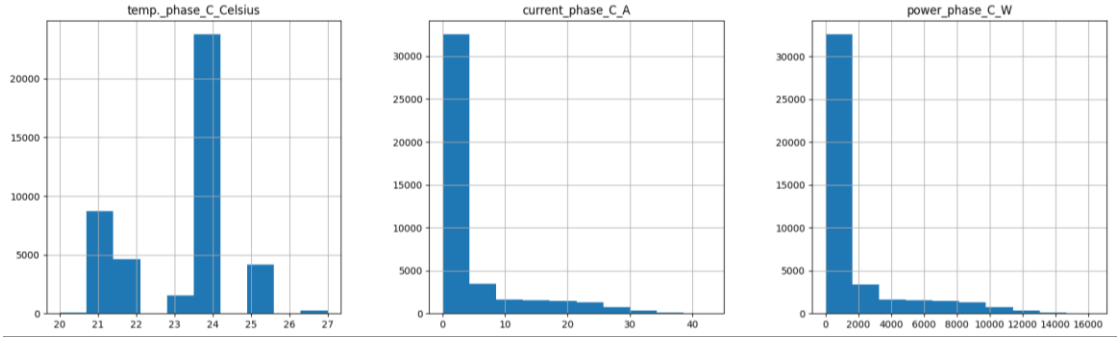

A) Temperature Phase C B) Current Phase C C) Power Phase C

Figure 13 Histogram of temperature, current, and power for Phase c.

4.4 Temperature

Temperature was identified as the feature with the least contribution to unbalanced current in the power distribution system when analyzed using the Random Forest Regressor model. As shown in Figure 5, the effect of temperature was quantified at approximately 0.07% in Phases A and C, and only 0.02% in Phase B. Compared to electrical power and current, which exhibited significantly higher contributions, temperature was determined to be a secondary factor in the development of unbalanced current conditions. A closer inspection of the histogram data provides further insight into this observation. For Phase B Figure 12, the system recorded a maximum power demand of 24.78 kW and a maximum current of 65.20 A. These operating conditions resulted in a peak conductor temperature of approximately 31 °C, which was higher than in the other phases. In contrast, Phase A Figure 11 reached a maximum power demand of 17.93 kW and a maximum current of 47.20 A, corresponding to a maximum temperature of about 27 °C. Phase C showed similar behavior, with a maximum power demand of 16.30 kW, a maximum current of 42.90 A, and a peak temperature of 27 °C, as illustrated in Figure 13. These results are consistent with findings reported in Beňa *et al*. (2021), which emphasize that conductor temperature is primarily driven by current loading. Although temperature had the smallest statistical contribution to unbalance prediction, it remains a valuable diagnostic parameter. Thermal variation across phases reflects differences in electrical loading and provides indirect information about conductor losses and efficiency. For example, elevated temperatures in Phase B suggest that this phase experiences higher energy stress, which may accelerate insulation aging and reduce equipment lifespan. Furthermore, localized heating can increase resistive losses, contributing to overall system inefficiency. This interpretation is supported by Moon and Lee (2019), who demonstrated that temperature rise in large electrical machines is strongly correlated with electromagnetic and copper losses. Therefore, while temperature by itself is not a dominant predictor of unbalanced current, its monitoring enhances the understanding of phase imbalance from a thermal perspective. Integrating temperature data with electrical features allows for improved condition monitoring, better prediction of component degradation, and more effective energy management strategies. From a system-level perspective, these insights contribute to optimizing load distribution, reducing technical losses, and enhancing the long-term reliability of power distribution networks.

5. Conclusion

The case study on the analysis of factors influencing Unbalance Current in the power distribution system at the College of Industrial Technology and Management, Rajamangala University of Technology, utilized a dataset comprising four key features: Power, Current, Energy, and Temperature. The Machine Learning Model Random Forest Regressor was employed to examine the relationship between these features and Unbalance Current. The analysis results indicate that electrical power has the highest impact on the occurrence of Unbalance Current, with Phase A Power contributing 74.73%, followed by Phase C Power (10.98%) and Phase B Power (9.55%). The primary cause of this imbalance is the significantly lower power consumption in Phase A, where small loads, such as lighting systems, are connected. In contrast, Phase B and Phase C are linked to large loads, including motors and air conditioning systems, leading to higher power demand in Phases B and C and contributing to the unbalance in Phase A. Other features, such as Current and Energy, have a relatively lower impact, contributing less than 1.5% in all cases, but show a direct correlation with the Power feature. The Temperature feature has the least impact, with values of 0.07% in Phases A and C and 0.02% in Phase B. The study concludes that Power is the most influential factor in Unbalance Current, and the application of Machine Learning for predictive analysis can support maintenance planning to mitigate power quality issues in building power systems, as highlighted by Popa *et al*. (2020). However, this approach has limitations due to the small dataset used for model training and testing, which may lead to miscalculations in practical applications. Additionally, the need to download data from Cloud systems for analysis adds complexity to the data processing workflow. To address these limitations, future research should focus on developing real-time Machine Learning models capable of running on embedded control devices or Cloud Computing systems. This would enable real-time anomaly detection, improve the accuracy of predictive models by increasing the training dataset size, and enhance the efficiency of power quality management in building and industrial applications.

6. Acknowledgments

The author would like to express gratitude to the Faculty of Engineering, College of Industrial Technology and Management, Rajamangala University of Technology Srivijaya, Thailand, for supporting this research through the 2025 fiscal year research fund and for providing access to facilities and equipment. Appreciation is also extended to the research team, faculty members, and staff for their valuable guidance and assistance. Additionally, heartfelt thanks go to family and colleagues for their encouragement and support throughout the research process.

7. References

Beňa, Ľ., Gáll, V., Kanálik, M., Kolcun, M., Margitová, A., Mészáros, A. and Urbanský, J. 2021. Calculation of the overhead transmission line conductor temperature in real operating conditions. **Electrical Engineering** 103: 769-780.

Breiman, L. 2001. **Random forest, Machine Learning.** Statistics Department, University of California, Berkeley.

Chawda, G.S., Shaik, A.G., Shaik, M., Padmanaban, S., Holm-Nielsen, J. B., Mahela, O. P. and Kaliannan, P. 2020. Comprehensive review on detection and classification of power quality disturbances in utility grid with renewable energy penetration. **IEEE Access** 8: 146807-146830.

Drovtar, I., Niitsoo, J., Rosin, A., Kilter, J. and Palu, I. 2012. Electricity consumption analysis and power quality monitoring in commercial buildings, pp. 1-6. *In* **Electric Power Quality and Supply Reliability.** Department of Fundamentals of Electrical Engineering and Electrical Machines, Tallinn, Estonia.

Hadd, A. and Rodgers, J.L. 2020. **Understanding correlation matrices.** Sage Publications.

Hastie, T., Tibshirani, R., Friedman, J., Hastie, T., Tibshirani, R. and Friedman, J. 2009. **The elements of statistical learning: data mining, inference, and prediction.** springer, New York.

Jove, E., González-Cava, J. M., Casteleiro-Roca, J. L., Alaiz-Moretón, H., Baruque, B., Leitão, P., Pérez, J. A. M. and Calvo-Rolle, J.L. 2021. An intelligent system for harmonic distortions detection in wind generator power electronic devices. **Neurocomputing** 456: 609-621.

Mahmoud, R. A. A. 2021. Detection and assessment scheme of voltage and current unbalance for three phase synchronous generators using dual numerical techniques based on correlation and deviation percentage concepts. **The Journal of Engineering** 2021(9): 477-495.

Melo, F.C., da Graça, G.C. and Panão, M.J.O. 2023. A review of annual, monthly, and hourly electricity use in buildings. **Energy and Buildings** 293: 113201.

Moon, S. and Lee, S. 2019. High-reliable temperature prediction considering stray load loss for large induction machine. **IEEE Transactions on Magnetics** 55(6): 1-5.

Popa, G.N., Iagăr, A. and Diniş, C.M. 2020. Considerations on current and voltage unbalance of nonlinear loads in residential and educational sectors. **Energies** 14(1): 102.

Santamouris, M. and Vasilakopoulou, K. 2021. Present and future energy consumption of buildings: Challenges and opportunities towards decarbonisation. **e-Prime-Advances in Electrical Engineering, Electronics and Energy** 100002(1): 1-14.

Schonlau, M. and Zou, R.Y. 2020. The random forest algorithm for statistical learning. **The Stata Journal** 20(1): 3-29.

Sinuraya, E., Soemantri, M. and Rafif, I. 2022. Evaluation and Mitigation of Voltage and Current Unbalance at MSTP Undip Jepara. **Journal of Physics: Conference Serie** 2406(1): 012013. 1-9.

Vinayagam, A., Veerasamy, V., Radhakrishnan, P., Sepperumal, M. and Ramaiyan, K. 2021. An ensemble approach of classification model for detection and classification of power quality disturbances in PV integrated microgrid network. **Applied Soft Computing** 106: 107294.

Wang, C., Du, J. and Fan, X. 2022. High-dimensional correlation matrix estimation for general continuous data with Bagging technique. **Machine Learning** 111(8): 2905-2927.

Wang, S. and Chen, H. 2019. A novel deep learning method for the classification of power quality disturbances using deep convolutional neural network. **Applied Energy** 235: 1126-1140.

Recent Science and Technology

Journal homepage: https:// www.tci-thaijo.org/index.php/rmutsvrj/index

ISSN: 3057-0786 (Online)

Research Article

RMUTTOBot: Transforming University Admission Services with a TAG-based RAG LLM Chatbot

Vipa Thananant [a] and Saowakhon Nookhao [b *]

[a] *Division of Information Technology, Faculty of Business Administration and Information Technology, Rajamangala University of Technology Tawan-ok : Chakrabongse Bhuvanarth Campus, Bangkok 10400, Thailand.*

[b] *Digital Transformation and Technology Management Program, KMITL Business School, Bangkok 10520, Thailand.*

Article history:

Received: 2025-05-13
Revised: 2025-10-15
Accepted: 2025-10-28

Keywords:

Large language models (LLM);
Retrieval-augmented generation (RAG);
Structured data retrieval;
BERTScore;
Domain-specific chatbot

ABSTRACT

Advancements in artificial intelligence, particularly in large language models (LLMs) and retrieval-augmented generation (RAG) techniques, have improved chatbot capabilities for more natural and domain-specific interactions. However, conventional RAG systems, which retrieve information from unstructured text sources like websites and PDFs, exhibit critical failures when applied to the dynamic and precise nature of university information. This research addresses these gaps through the design and development of RMUTTOBot, a domain-specific chatbot providing admissions support for prospective students at Rajamangala University of Technology Tawan-ok (RMUTTO). We propose a novel, lightweight table-augmented generation (TAG) approach that combines a curated, updatable knowledge base for general information with live database queries for real-time, dynamic data. Performance was evaluated using both automated metrics and human assessments across six criteria: semantic similarity, retrieval effectiveness, relevance, fluency, coverage, and consistency. Experimental results show that the TAG-based RAG system significantly outperformed both the baseline LLM-only configuration and PDF-based RAG system, achieving a 12.76% higher BERTF1 score compared to a PDF-based RAG. Human evaluation confirmed the system's high response relevance and linguistic fluency, with strong inter-rater reliability (Krippendorff's $\alpha > 0.835$). These findings demonstrate that combining structured data augmentation with RAG substantially enhances chatbot accuracy, contextual grounding, and completeness, offering a robust framework for intelligent conversational systems in academic domains. The source code and implementation details are publicly available at https://github.com/vipa-thananant/RMUTTOBot.

1. Introduction

This research is situated within the significant evolution of chatbots, which have transformed through distinct developmental stages from simple tools into powerful learning partners (Alkishri *et al*., 2025). Early systems relied on pattern-matching, while subsequent versions integrated AI and natural language processing (NLP) for more context-aware interactions. Today, generative AI and Large Language Models (LLMs) represent the state-of-the-art. Within the LLM paradigm, solutions generally fall into three categories: fine-tuned models, retrieval-augmented generation (RAG) systems, and hybrid approaches (Ren *et al*., 2025; Wan *et al*., 2025). Fine-tuning involves adapting a pre-trained model using domain-specific datasets to improve accuracy and tone alignment (Doumanas *et al*., 2025). RAG-based systems, in contrast, retrieve relevant external content during inference without requiring retraining (Liang *et al*., 2025; Uhm *et al*., 2025). RAG is particularly effective when dealing with unstructured sources such as documents, websites, and PDF files. It functions by encoding such content into embeddings stored in a vector database, enabling efficient semantic search and integration into the generation process (Fan *et al*., 2024;

* **Corresponding author.**

E-mail address: *saowakhon.no@kmitl.ac.th*

Cite this article as:

Thananant, V. and Nookhao, S. 2026. RMUTTOBot: Transforming University Admission Services with a TAG-based RAG LLM Chatbot. **Recent Science and Technology** 18(1): 267581.

https://doi.org/10.65411/rst.2026.267581

Arslan *et al*., 2024). Hybrid models combine both strategies, leveraging fine-tuning for personalization and tone consistency while using retrieval mechanisms to provide fresh, topic-specific information (Budakoglu and Emekci, 2025).

While RAG has advanced the capabilities of university chatbots, its foundational reliance on semantic search over unstructured documents creates critical failures in the precision and reliability required for this high-stakes domain (Barnett *et al*., 2024). This approach struggles significantly with queries that demand keyword-level accuracy, such as requests for a specific course code like CSE101. A search may incorrectly link this query to general "introduction to computer science" documents, misdirecting students and preventing them from finding essential information. Furthermore, the chunking process used to index documents fragments context, leading to incomplete answers. A retrieved passage stating, "A minimum GPA of 3.5 is required," is not just incomplete but actively misleading if the preceding, unretrieved chunk specifies, "For the Faculty of Engineering applicants," causing potential applicants to miss critical requirements. This ambiguity is compounded when students ask for broad information like the "admissions policy," where a standard RAG system often returns a generic policy without distinguishing between the distinct requirements for undergraduate, graduate, or international students.

Most critically, conventional RAG is ill-suited for the dynamic, multi-faceted queries common in a university setting. Its core weakness is its reliance on static documents, such as admissions brochures, which cannot be updated in real time. For example, consider a prospective student asking, "Is the Bachelor of Nursing program still accepting applications for the fall semester?" A RAG system retrieving from a brochure published months prior might incorrectly state that applications are open until the official deadline. However, if that popular program has already reached its capacity and closed early, the chatbot provides false hope and misleads the student into wasting time preparing an invalid application. An accurate response requires a real-time query to the live admissions database to check the program's current status. This limitation makes static document retrieval unreliable for the critical, time-sensitive needs of prospective students.

To address these specific failures, this research introduces RMUTTOBot, a domain-specific chatbot built on our novel table-augmented generation (TAG) approach. Unlike heavyweight systems that generate complex SQL or reason over graphs, our lightweight TAG-based RAG operates on a hybrid model. It retrieves foundational knowledge from a database of QA pairs and uses LLM-native function calling to trigger simple, pre-written queries for specific, real-time data. Our TAG-based RAG approach is an evolution of this RAG framework, specifically adapting it for the structured and dynamic data environment of a university, thereby addressing a key gap in current methodologies.

1.1 Related work

This section reviews the evolution of university chatbots to contextualize the contribution of our TAG-based RAG approach. The narrative traces the progression from traditional NLP systems to the current state-of-the-art in LLM-powered RAG, highlighting the persistent challenges that motivate our research.

Early university chatbots relied on traditional NLP techniques like intent recognition and entity extraction to handle user queries. Systems developed for Petrozavodsk State University (Shchegoleva *et al*., 2021) and Universitas Stikubank, which used the RASA framework (Hadiono *et al*., 2024), employed rule-based dialogue management to address frequently asked questions. While functional, these systems were limited in flexibility; as Pothuri (2024) notes, rule-based intent recognition struggles with linguistically diverse queries and often fails to maintain coherent multi-turn dialogue. The advent of LLMs marked a significant paradigm shift, offering more robust natural language understanding and adaptability that overcame these constraints (Karanikolas *et al*., 2025).

The predominant architecture in this new era is LLM-powered RAG, which enhances LLMs with external, domain-specific context. A common strategy in educational settings, as explored by Alsafari *et al*. (2024), is to build a knowledge base from unstructured documents like course materials, websites, and student handbooks. This approach is exemplified by systems like JayBot at Johns Hopkins University (Odede and Frommholz, 2024) and a similar chatbot at the University of Mosul (Sharief and Ersayyem, 2024). While these systems demonstrate increased flexibility, studies consistently highlight a critical shared vulnerability: their accuracy is entirely dependent on the currency of the static documents in their knowledge base, and they lack automated pipelines for ingesting new data. To address precision issues, some researchers have developed hybrid retrieval methods. URAG, for instance, combines semantic vector search with keyword-based search to retrieve precise terms (Nguyen and Quan, 2025), while a system at XJTLU integrated TF-IDF for the same purpose (Xu and Liu, 2024). However, these innovations still operate on text and inherit its fundamental limitations, particularly an inability to address personalized or confidential queries requiring database lookups.

Recognizing the limitations of text-only retrieval for factual precision, recent research has focused on adapting RAG for structured and tabular data. For instance, frameworks like Binder demonstrate how LLMs can be bound to symbolic languages, enabling them to execute SQL queries directly against relational databases for high-fidelity data retrieval (Cheng *et al*., 2023). Other approaches, such as StructGPT, construct knowledge graphs from structured data to perform complex, multi-hop reasoning across interconnected information (Jiang *et al*., 2023).

While these structured-data-aware architectures significantly improve factual accuracy, they introduce trade-offs in complexity, computational cost, and real-time adaptability that limit their practicality for chatbots. The complex pipelines required for on-the-fly text-to-SQL generation (Cheng *et al.*, 2023), dynamic graph construction (Jiang *et al.*, 2023), or iterative multi-stage retrieval are often computationally intensive and require significant engineering effort. They can also rely on static data representations, making them ill-suited for the dynamic university environment where information like course availability and admission statuses change frequently.

This leaves a critical gap for a system that can achieve the factual reliability of structured-data reasoning without the high overhead of these complex frameworks. Our research addresses this gap by proposing RMUTTOBot, a lightweight TAG-based RAG system that leverages LLM-native function calling. Instead of tasking the model with generating complex SQL or reasoning over a graph, our approach uses the LLM as an intelligent router to trigger pre-defined, highly-optimized database queries. This method provides a practical, scalable, and accurate solution tailored to the specific needs of university information systems by achieving factual reliability without the high engineering and computational overhead of more complex reasoning frameworks.

The structure of this paper is organized as follows. Section 2 describes the methodology of the study, including the design and components of the RMUTTOBot framework, as well as the evaluation strategies adopted to assess its effectiveness. Section 3 presents the results and discussion, incorporating both quantitative evaluations using automated metrics and qualitative assessments based on human judgment. Section 4 concludes the paper by summarizing key findings and suggesting directions for future research.

2. Materials and Methods

2.1 RMUTTOBot framework

The RMUTTOBot system utilizes a lightweight TAG-based RAG approach built on a hybrid, dual-source retrieval strategy. This architecture is designed to ensure both comprehensive context and real-time factual accuracy by distinguishing between two distinct but interconnected information sources: a knowledge base and a direct interface to live institutional databases.

The foundation of the system is a knowledge base of over 600 pre-verified QA pairs, which contains general, foundational information about the university. Critically, this is not a static repository. The QA pairs are stored in a database and are managed through an application that allows administrators to easily add, update, or remove questions and answers. This ensures the chatbot's foundational knowledge remains current without needing to retrain or re-index complex documents. For highly dynamic or volatile information, the system employs a dynamic data interface using LLM-native function calling. This allows the chatbot to query live institutional databases for real-time data such as course availability, admission statuses, or specific tuition fees.

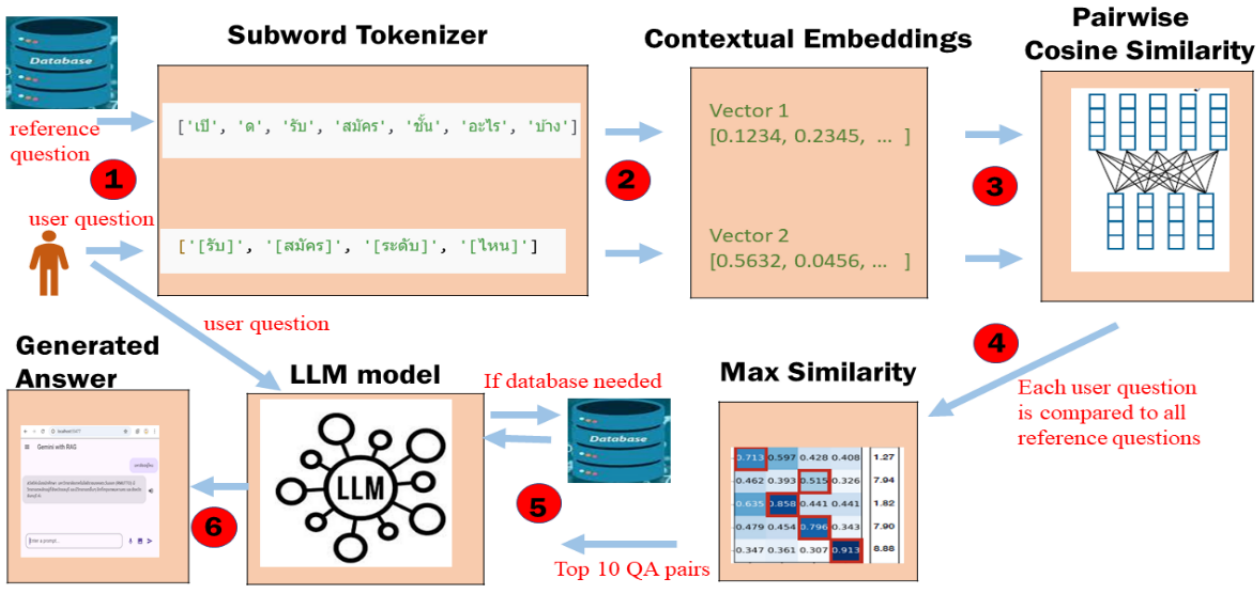

Figure 1 Over all Framework of the Proposed Methodology

The proposed methodology is comprised of four primary components: data preparation and tool definition, hybrid retrieval and query dispatch, context consolidation and prompt engineering, and response generation.

Step 1 Data Preparation and Tool Definition: The development process begins with the creation of the foundational knowledge base. Using the GPT-4 Turbo model, approximately 600 QA pairs were automatically generated. This state-of-the-art model was selected to ensure both scale and quality, enabling the rapid production of a comprehensive set of questions covering a wide range of university-specific topics and diverse linguistic phrasings for common inquiries. This automated generation provided a high-quality baseline for the initial knowledge base.

To enable the LLM to trigger database-related functions, we deliberately modified approximately 20% of the initially generated QA pairs. With a modified query such as "What is the tuition fee for computer engineering?", the LLM is designed to call the get_tuition_fee (major_name) function, which then retrieves tuition fee of computer engineering from the institutional database. This deliberate inclusion of function-triggering queries ensures that the system can effectively handle both knowledge-based and dynamic data-driven interactions, supporting real-time information retrieval through predefined database functions.

To ensure reliability and factual consistency, each generated QA pair underwent manual review by a team of three domain experts. These experts meticulously cross-checked every answer against verified institutional sources, including the university website, official databases, student handbooks, and admissions brochures. This rigorous verification process was designed to identify and correct hallucinated or inaccurate information, thereby guaranteeing alignment with official institutional data.

Following validation, the all QA pairs were stored in a Firebase Firestore database, forming the system's primary knowledge repository. In parallel, a set of function tools was defined for the LLM to support real-time data retrieval. These tools correspond to high-value database lookups, which allow the system to access dynamic institutional database as needed.

Step 2 Hybrid Retrieval and Query Dispatch: As shown in Figure 1, the retrieval process is initiated when a user question is submitted through the chatbot interface (① Figure 1). The system concurrently retrieves reference questions from the QA database and processes both inputs using a Subword Tokenizer (②), which decomposes text into subword units to accommodate linguistic variability across languages.

Next, the tokenized sequences are encoded into contextual embeddings (③) using the bert-base-multilingual-cased model. This model was selected over alternative embedding methods such as Sentence-BERT, word2vec, or fastText due to its strong multilingual capability including full support for the Thai language contextual sensitivity, and robustness across semantically diverse text corpora. Unlike static word embeddings, bert-base-multilingual-cased generates context-aware vector representations that maintain semantic meaning even in paraphrased or linguistically complex queries. Its multilingual pretraining ensures effective cross-lingual generalization, allowing the chatbot to process queries in both English and Thai, which are commonly used in the university context.

These embeddings capture the semantic meaning of each question, enabling robust cross-lingual matching. The system then calculates pairwise cosine similarity between the user question vectors and the stored reference vectors (④), facilitating semantic retrieval of the most relevant QA pairs.

The top 10 QA pairs with the highest similarity scores are selected (⑤). This threshold was empirically validated in a pilot evaluation of 50 paraphrased queries, where the correct reference consistently appeared within the top ten retrieved results. The chosen limit optimizes both accuracy and computational efficiency, ensuring a high signal-to-noise ratio, minimizing token length for prompt construction, and improving response latency.

Concurrently, the Gemini 1.5 Flash model serves as a reasoning engine that inspects the user query to determine whether real-time data retrieval is required. This model was selected over alternative LLMs due to its exceptional balance between reasoning performance, inference speed, and cost efficiency, making it well suited for real-time chatbot applications. Compared with larger or slower models such as Gemini Pro or GPT-4 Turbo, Gemini 1.5 Flash demonstrates significantly lower latency while maintaining competitive accuracy in structured reasoning and function-calling tasks. Its optimized architecture allows the system to process queries rapidly without compromising contextual understanding an essential factor in delivering responsive and reliable user interactions within the university chatbot environment.

If the query matches a predefined function tool (e.g., tuition fees or application deadlines), the system triggers the corresponding database function (⑤). Otherwise, the retrieved QA pairs proceed directly to the next stage (Step 3).

Step 3 Context Consolidation and Prompt Engineering: As shown in Figure 1, The system aggregates all relevant contextual information, consisting of the top ten retrieved QA pairs and, when applicable, real-time database outputs, into a structured input for the LLM. (⑤). This process ensures factual accuracy and prevents the generation of unsupported or outdated information.

The retrieved content and contextual information are consolidated into a structured prompt. This prompt design provides the model with rich contextual grounding while maintaining efficiency in token usage. In addition, system-level instructions and fallback directives are embedded within the prompt to control the model's reasoning behavior, ensuring consistent tone, factuality, and adherence to institutional guidelines. The

completed prompt is then forwarded to the response generation module for synthesis (⑥).

Step 4 Response Generation and Delivery: As depicted in Figure 1, the final stage involves submitting the structured prompt to the Gemini 1.5 Flash model for natural language synthesis (⑥). The model generates a coherent, contextually grounded, and factually reliable response that draws from both the QA knowledge base and any dynamic data obtained through database queries. The output is then delivered through the Flutter-based chatbot interface, providing the user with a seamless and interactive experience.

The flowchart illustrating from query input to response delivery is presented in Figure 2.

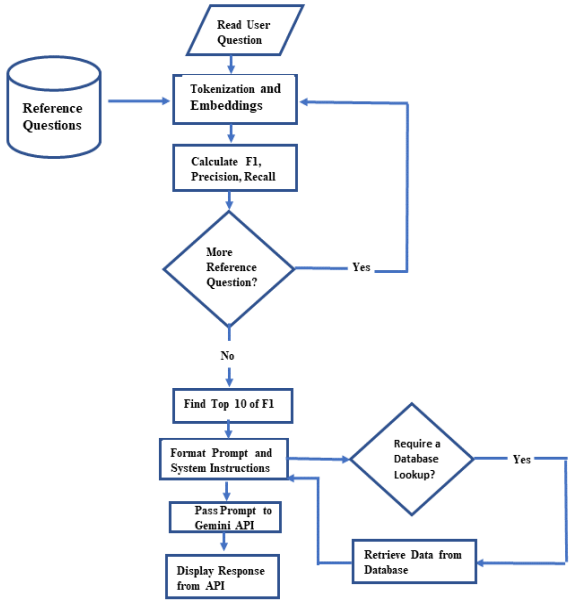

Figure 2 RMUTTOBot flow chart

2.2 Evaluation strategies

To ensure a fair and reproducible assessment of the proposed chatbot system (RMUTTOBot), a structured evaluation procedure was implemented. The evaluation was conducted in two phases automated testing and human evaluation under identical operating conditions. The chatbot was deployed on a controlled environment using the Gemini 1.5 Flash API integrated with a Firebase Firestore knowledge base. All evaluations were performed through the same user interface to eliminate bias introduced by differing platforms or communication modes.

Evaluating LLMs–based chatbots within a RAG framework requires a multidimensional approach to ensure both semantic fidelity and practical usability. Six key criteria provide a comprehensive foundation for assessing such systems: semantic similarity, retrieval effectiveness, response relevance and accuracy, linguistic fluency and coherence, content coverage and completeness, and robustness and consistency (Abeysinghe and Circi, 2024; Joshi, 2025; Oro *et al*., 2024).

Semantic similarity measures how closely the chatbot's responses preserve the intended meaning of the reference answers in the knowledge base. Retrieval effectiveness assesses the informativeness and relevance of the top-N retrieved texts that support answer generation an essential factor influencing factual precision. Response relevance and accuracy determine whether the generated output is factually correct and contextually aligned with the retrieved materials. Linguistic fluency and coherence capture grammaticality, readability, and logical flow, while content coverage and completeness gauge whether the system's output thoroughly addresses user questions using available information. Finally, robustness and consistency evaluate the chatbot's ability to generate stable, logically consistent answers across similar or ambiguous queries.

The following two assessment strategies, automated metrics and human evaluation, were used to address these criteria:

1. Automated metrics evaluation: The criteria of semantic similarity, retrieval effectiveness, and robustness and consistency were evaluated using automated metrics.

For the evaluation of semantic similarity and robustness and consistency, a representative of 200 reference questions was randomly selected from a pool of 600 QA entries in RMUTTOBot's structured QA database. Furthermore, to facilitate a thorough assessment of dynamic information retrieval, a 20% subset of these questions (40 in total) was specifically selected to activate the LLM's pre-defined database queries. To simulate realistic variations in user input, each selected question was paraphrased using GPT-4 Turbo, introducing lexical and syntactic diversity while preserving semantic intent. Each paraphrased query was then processed under three system configurations for comparison: (1) baseline LLM-only (Without RAG): The chatbot relied solely on its base language model without external data augmentation. This configuration, implemented using the Flutter framework, served as the baseline. (2) TAG-based RAG: This configuration employs a hybrid dual-source retrieval strategy, leveraging structured knowledge base and LLM-native function calling. It was implemented using the Flutter framework. (3) PDF-based RAG: In this configuration, retrieval relied exclusively on external PDF documents. The ChatDOC platform was used for evaluation due to its integration of retrieval-augmented generation (RAG) with high-quality semantic embeddings, citation mapping, and support for multi-document queries. ChatDOC's research-oriented design enables more reliable academic information retrieval compared to conventional PDF-QA tools.

Performance was measured using BERTScore, which evaluates semantic equivalence by comparing contextual embeddings (Zhang *et al*., 2019). This metric was chosen over traditional lexical overlap metrics like BLEU, METEOR, and ROUGE, which primarily evaluate text quality by counting the number of shared words and phrases (n-grams) between a

candidate and a reference sentence. A key limitation of these lexical methods is their inability to recognize synonyms or paraphrasing. BERTScore produces three key measures: BERTPrecision, BERTRecall, and BERTF1, computed as shown in Equations 1–4.

$$BERTPrecision = \frac{1}{m}\sum_{i=1}^{m} \max_{j} sim(c_i, r_j) \quad (1)$$

$$BERTRecall = \frac{1}{n}\sum_{j=1}^{n} \max_{i} sim(c_i, r_j) \quad (2)$$

$$BERTF1 = \frac{2PR}{P+R} \quad (3)$$

$$sim(c_i, r_j) = \cos\left(\phi(c_i), \phi(r_j)\right) \quad (4)$$

where c = [c1,c2,…,cm] = tokens of the candidate sentence
r = [r1,r2,…,rn] = tokens of the reference sentence
ϕ (c_i) and ϕ (r_j) = BERT embeddings of tokens c_i and r_j, respectively
$sim(c_i, r_j)$ = cosine similarity between two vectors ϕ (c_i) and ϕ (r_j)

For the evaluation of retrieval effectiveness, a test set of 50 paraphrased user queries was used to validate the retrieval stage of the TAG-based RAG framework. The system retrieved the top k most semantically similar reference questions for each query. Performance was measured using Top-k Accuracy and Mean Reciprocal Rank (MRR).

Top-k Accuracy measures the proportion of queries for which the correct reference question appears within the top-k retrieved candidates, defined in Equations 5:

$$Top - k\ Accuracy = \frac{\#\ correct\ results\ within\ top\ k}{N} \quad (5)$$

where N = the total number of test queries
k = the number of results being considered.

MRR evaluates how highly the correct reference question is ranked, computed in Equations 6:

$$MRR = \frac{1}{N}\sum_{i=1}^{N} \frac{1}{rank_i} \quad (6)$$

where $rank_i$ denotes the position of the correct reference question for the i-th query.

2. Human evaluation: The criteria of response relevance and accuracy, linguistic fluency and coherence, and content coverage and completeness were assessed through human evaluation. For this task, 25 high-school students from Surasakmontree school were recruited as raters. Each evaluator assessed 25 paraphrased queries, comparing the responses generated by the TAG-based RAG (RMUTTOBot Flutter Framework) and PDF-based RAG (ChatDOC) systems against reference answers.

Responses were rated using a 5-point Likert scale, with detailed scoring rubrics provided in Tables 1–3

Table 1 Detailed scoring procedures for response relevance and accuracy criterion.

Score	Description
1	The answer is completely irrelevant to the question and factually incorrect
2	The answer is mostly off-topic or contains significant factual inaccuracies
3	The answer is somewhat related to the question and includes some correct information, but it also contains notable errors or omissions
4	The answer is generally relevant and factually accurate, with only minor issues or inaccuracies
5	The answer is highly relevant and entirely accurate. It fully addresses the user's question using correct and well-grounded information

Table 2 Detailed scoring procedures for linguistic fluency and coherence criterion.

Score	Description
1	Poor grammar; hard to understand
2	Some grammar issues; awkward phrasing affects clarity
3	Understandable but contains some unnatural or disjointed language
4	Mostly fluent with minor readability issue
5	Clear, coherent, grammatically correct, and easy to read

Table 3 Detailed scoring procedures for content coverage and completeness criterion.

Score	Description
1	Completely incomplete; no meaningful content
2	Covers only a small part; key details missing
3	Partially complete; addresses the main point but lacks supporting information
4	Mostly complete; minor omissions
5	Fully complete; all parts of the question are answered thoroughly

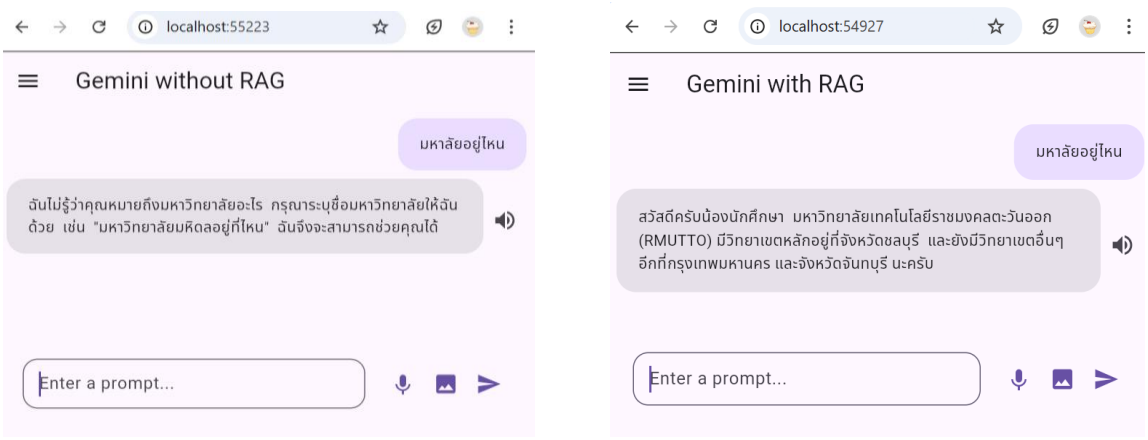

(a) without RAG (baseline LLM-only) (b) TAG-based RAG

Figure 3 Comparision Chatbot Responses: Without RAG vs. TAG-based RAG Approach via a Flutter Application

To ensure credibility and minimize subjective bias, the central tendency measures median and mode were computed for each criterion to capture consensus tendencies, while Krippendorff's Alpha (α) was calculated to assess inter-rater reliability, ensuring consistency and reliability across evaluators. Reliability interpretations followed established conventions: $\alpha \geq 0.80$ = strong agreement, $0.67 \leq \alpha < 0.80$ = acceptable agreement, and $\alpha < 0.67$ = low agreement (Krippendorff, 2011).

By integrating both automated and human evaluations, this mixed-method approach ensures breadth, depth, and reproducibility.

3. Results and Discussion

3.1 Evaluation of semantic similarity, robustness and consistency

To evaluate across two core criteria: semantic similarity, and robustness and consistency, the three system configurations Without RAG, PDF-based RAG, and TAG-based RAG were tested against a set of 200 paraphrased user queries. Qualitative comparisons revealed significant performance differences between these configurations. As illustrated in Figures 3 and 4, the without RAG baseline configuration (Figure 3a) failed to provide a substantive answer to the query "Where is the university located?". In contrast, both TAG-based RAG (Figure 3b) and PDF-based RAG (Figure 4) configurations successfully retrieved accurate information, demonstrating the core benefit of RAG. Further, Figure 5 highlights a key distinction in retrieval precision: when asked "How much is the tuition for Agricultural Engineering?", the PDF-based RAG (Figure 5a) produced an incorrect value of 12,700, despite the correct figure 13,500 being present in the PDF file. Conversely, the TAG-based RAG (Figure 5b) returned the correct answer, indicating superior retrieval precision.

The chatbot's responses across all three configurations were benchmarked against the reference answers using BERTScore. As shown in Table 4 and visualized in Figure 6, the integration of RAG markedly improved performance across all metrics. The baseline (without RAG) yielded the lowest scores. While the PDF-based RAG approach showed clear improvement, the TAG-based RAG approach demonstrated the most significant performance gains, achieving a BERTF1 score of 0.7361. The relative improvements of 13.44% in BERTPrecision, 11.92% in BERTRecall, and 12.76% in BERTF1 over the PDF-based approach underscore the advantage of structured data in facilitating more accurate and contextually relevant responses. These findings highlight that TAG-based RAG substantially enhances both semantic similarity and response robustness.

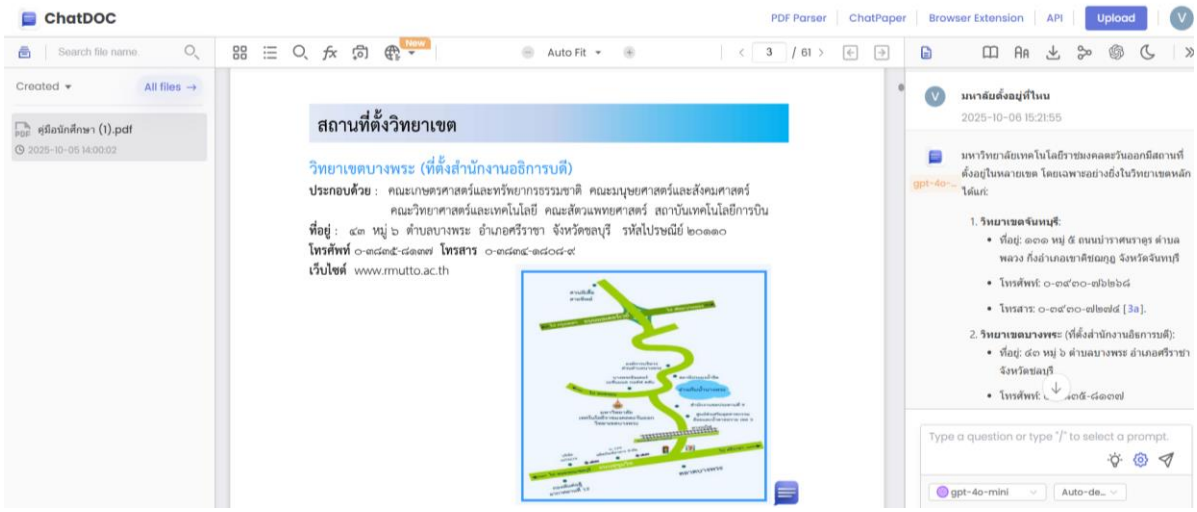

Figure 4 PDF-Based RAG Chatbot response via ChatDOC platform

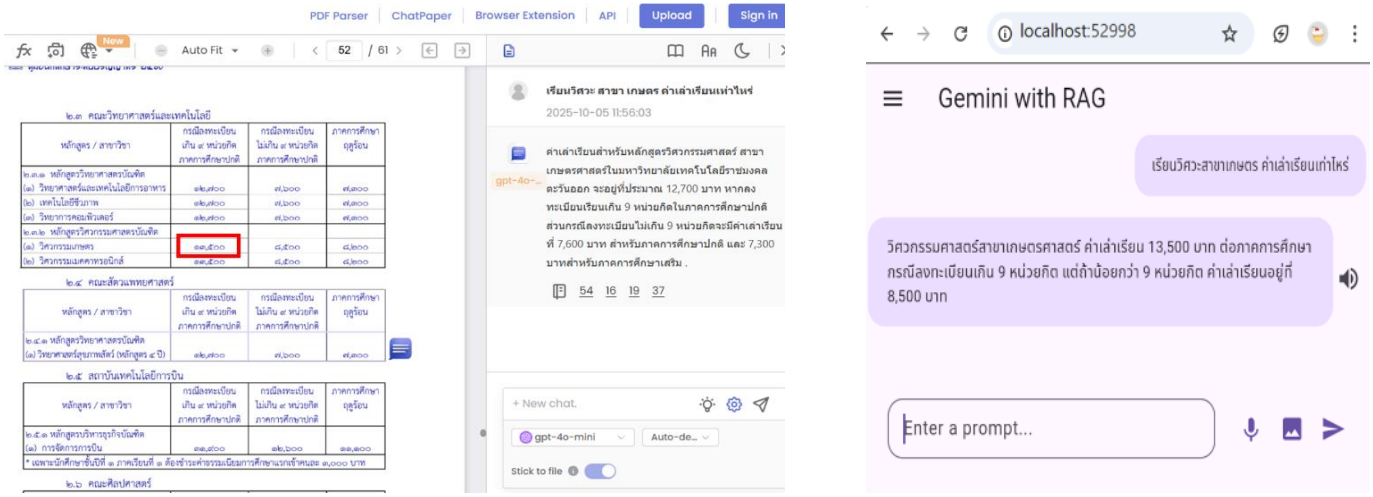

(a) PDF-based RAG (b) TAG-based RAG

Figure 5 Comparision Chatbot Responses: PDF-based RAG vs. TAG-based RAG Approach

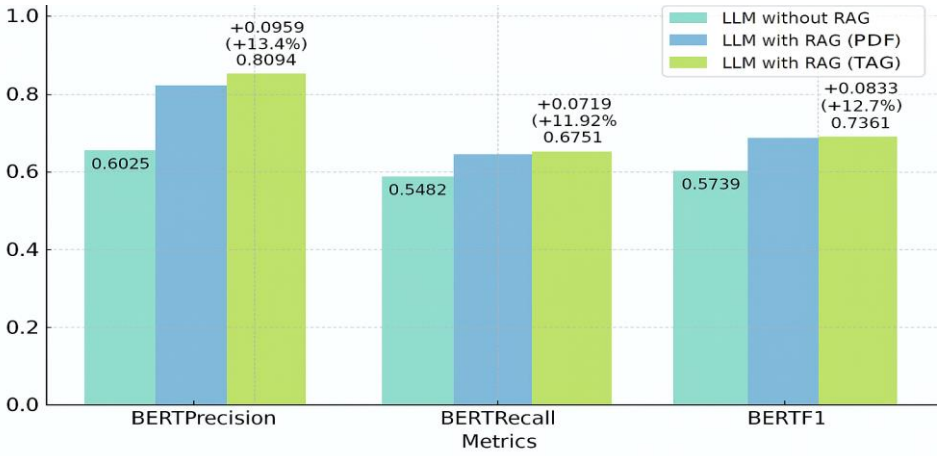

Figure 6 BERTScore Comparison: without RAG vs. PDF-based RAG vs. TAG-based RAG.

Table 4 BERTScore Comparison: without RAG vs. PDF-based RAG vs. TAG-based RAG.

Metric Score	without RAG	PDF-based RAG	TAG-based RAG	Difference TAG and PDF based	% Improvement TAG over PDF based
BERTPrecision	0.6025	0.7135	0.8094	+0.0959	+13.44%
BERTRecall	0.5482	0.6032	0.6751	+0.0719	+11.92%
BERTF1	0.5739	0.6528	0.7361	+0.0833	+12.76%

Table 5 Summary of Rank Distribution Across 50 Queries

Rank of Correct Reference Question	Number of Queries	Reciprocal Rank (1/rank)	Weighted Contribution
1	35	1.0000	35.0000
2	7	0.5000	3.5000
3	3	0.3333	1.0000
4	2	0.2500	0.5000
5	1	0.2000	0.2000
6	1	0.1667	0.1667
7-10	1	0.1250	0.1250
Total	**50**	**-**	**40.4917**

3.2 Evaluation of retrieval effectiveness

To evaluate TAG-based RAG retrieval performance, a test set of 50 paraphrased user queries was selected. The semantic similarity between each paraphrased query and all reference questions in the QA database was calculated using BERTScore. For each query, the system retrieved the top 10 most semantically similar reference questions, ranked by descending similarity scores. To provide a more comprehensive evaluation, two additional retrieval effectiveness metrics were applied: Top-10 Accuracy and MRR.

As presented in Table 5, the retrieval system achieved a Top-10 accuracy of 100%, indicating that the correct reference question was consistently identified within the top ten retrieved results for all 50 paraphrased queries. This result demonstrates the robustness of the semantic retrieval component in maintaining contextual equivalence despite variations in query phrasing.

Examination of the rank distribution in Table 5 shows that the correct reference question appeared at Rank 1 in 70% of cases and within the top four ranks in 94% of cases, reflecting strong ranking precision and stability. Only three queries (6%) were ranked between fifth and tenth positions, suggesting minimal retrieval deviation. The mean reciprocal rank (MRR) was 0.8098 (40.4917/50 Table 5), indicating that, on average, the correct match appeared within the top two retrieved results. Overall, these findings confirm the high reliability and semantic discrimination capability of the retrieval mechanism, supporting its effectiveness as a foundation for accurate and contextually grounded response generation within the TAG-based RAG framework.

Two representative examples are presented to illustrate retrieval behavior. Table 6 displays the results for the query "What are the available admission channels?". The corresponding reference question, "Which channels can be used to apply for admission?", was retrieved at rank 6 with a BERTF1 score of 0.8099. Although several higher-ranked items were not exact matches, they remained topically related (e.g., required documents, admission rounds), indicating that the retrieval model effectively grouped semantically coherent content.

Similarly, Table 7 presents the retrieval results for the query "Which educational programs are open for admission?". The correct reference question, "What levels of study are open for admission?", was ranked first, achieving a BERTF1 score of 0.7835, reflecting optimal semantic alignment.

To compare the retrieval effectiveness of the PDF-based and TAG-based RAG systems, both configurations were evaluated using the same set of 50 paraphrased user queries and BERTScore metrics, as shown in Table 8. Across all measures BERTPrecision, BERTRecall, and BERTF1 the TAG-based configuration outperformed the PDF-based one.

BERTPrecision improved from 0.7835 to 0.8272 (+5.58%), indicating that TAG retrieves more semantically aligned context. BERTRecall showed a modest increase of 0.57%, while BERTF1 rose from 0.7326 to 0.7534 (+2.85%), reflecting balanced gains in both precision and recall.

These results collectively demonstrate that integrating structured data within the TAG-based RAG framework leads to more precise and semantically consistent retrieval compared to traditional unstructured PDF-based methods. The findings reinforce that TAG-based RAG enhances contextual relevance and retrieval robustness key factors that contribute to downstream improvements in the accuracy and reliability of the chatbot's generated responses.

Table 6 Top 10 Retrieval Results for Query “What are the available admission channels?”

Rank	Reference Question	BERTF1
1	การสมัครเรียนต้องใช้เอกสารอะไรบ้าง	0.8675
2	เอกสารที่ต้องใช้ในการสมัครมีอะไรบ้าง	0.8372
3	ทุนเรียนดีมีอะไรบ้าง	0.8323
4	เปิดรับสมัครชันอะไรบ้าง	0.8243
5	รอบการรับสมัครมีช่วงไหนบ้าง	0.8157
6	**สามารถสมัครเรียนผ่านช่องทางไหนได้บ้าง**	**0.8099**
7	ทุนการศึกษาต้องใช้เอกสารอะไรบ้าง	0.8088
8	ต้องใช้คะแนนสอบอะไรบ้างในการสมัคร	0.7969
9	มหาวิทยาลัยมีกิจกรรมทางวิชาการอะไรบ้าง	0.7943
10	ใช้คะแนนสอบอะไรบ้าง	0.7926

Table 7 Top 10 Retrieval Results for Query “Which Educational Programs Are Open for Admission?”

Rank	Reference Question	BERTF1
1	**เปิดรับสมัครชันอะไรบ้าง**	**0.7835**
2	รอบการรับสมัครมีช่วงไหนบ้าง	0.7824
3	มีกำหนดการรับสมัครช่วงไหนบ้าง	0.7780
4	สามารถสมัครเรียนผ่านช่องทางไหนได้บ้าง	0.7645
5	นักศึกษาสามารถฝึกงานได้ที่ไหนบ้าง	0.7615
6	การสมัครเรียนต้องใช้เอกสารอะไรบ้าง	0.7549
7	มีทุนการศึกษาสำหรับนักศึกษาใหม่หรือไม่	0.7527
8	นักศึกษาสามารถเข้าร่วมโครงการสังคมหรือจิตอาสาได้ไหม	0.7483
9	นักศึกษาสามารถฝึกงานได้ที่ไหนบ้าง	0.7459
10	ทุนการศึกษาต้องใช้เอกสารอะไรบ้าง	0.7441

Table 8 BERTScore Retrieval Effectiveness Comparison: PDF-based RAG vs. TAG-based RAG.

Metric Score	PDF-based RAG	TAG-based RAG	Difference TAG and PDF based	% Improvement TAG over PDF based
BERTPrecision	0.7835	0.8272	+0.0437	+5.58%
BERTRecall	0. 6883	0.6922	+0.0039	+0.57%
BERTF1	0.7326	0.7534	+0.0209	+2.85%

3.3 Evaluation of response relevance and accuracy, linguistic fluency and coherence, content coverage and completeness

A human evaluation was conducted to compare the qualitative performance of the two RAG-based systems PDF-based RAG and TAG-based RAG across three core criteria: response relevance and accuracy, linguistic fluency and coherence, and content coverage and completeness.

A total of 25 high school students participated as independent evaluators. Each rater assessed 25 representative queries for both systems, resulting in 625 ratings per evaluation. For each query, paraphrased inputs were submitted to both the RMUTTOBot (TAG-based RAG) and ChatDOC (PDF-based RAG) systems. The generated responses were compared against the reference answers using a 5-point Likert scale, where higher scores indicated stronger performance.

Table 9 summarizes the quantitative results and corresponding qualitative interpretations.

The evaluation results demonstrate that both systems achieved high overall performance, with almost perfect inter-rater reliability (Krippendorff's $\alpha \geq 0.90$) for most criteria, underscoring the robustness and objectivity of the findings.

For response relevance and accuracy, both RAG configurations were rated at the highest level, achieving median and mode scores of 5, corresponding to “highly relevant and entirely accurate” answers. This indicates that both systems were equally effective in retrieving and presenting correct, on-topic responses aligned with the reference answers.

In terms of linguistic fluency and coherence, both systems maintained strong performance. The median score of 4 (“mostly fluent with minor readability issues”) alongside a mode of 5 (“clear and coherent”) suggests that while the generated responses were generally well-structured and readable, occasional phrasing or grammatical inconsistencies were noted.

Table 9 Summary of Human Evaluation Results across Three Criteria

Criterion	System	Median	Mode	Krippendorff's Alpha	Key Finding
response relevance and accuracy	PDF-based RAG	5	5	0.912 (Almost Perfect)	Excellent performance with very high rater agreement.
	TAG-based RAG	5	5	0.904 (Almost Perfect)	Excellent performance, comparable to the PDF system.
linguistic fluency and coherence	PDF-based RAG	4	5	0.908 (Almost Perfect)	High fluency, though not consistently rated as perfect.
	TAG-based RAG	4	5	0.912 (Almost Perfect	High fluency, with performance similar to the PDF system.
content coverage and completeness	PDF-based RAG	4	4	0.904 (Almost Perfect)	Good performance, but responses were typically rated 'mostly' complete.
	TAG-based RAG	5	5	0.835 (Substantial)	Excellent performance, outperforming the PDF system on this criterion.

A more distinct difference emerged in content coverage and completeness. The TAG-based RAG system exhibited superior performance, achieving median and mode scores of 5, indicating that its responses were consistently judged as “fully complete.” By contrast, the PDF-based RAG configuration achieved median and mode scores of 4, suggesting that its responses were “mostly complete” but occasionally omitted supplementary details.

Overall, these findings affirm that while both systems perform strongly across relevance, fluency, and completeness, the TAG-based RAG approach offers a notable advantage in delivering comprehensive, contextually enriched, and factually complete answers demonstrating the value of structured data integration in enhancing RAG system.

3.4 Overall Discussion

Collectively, the evaluation results demonstrate the clear superiority of the TAG-based RAG framework. The strong performance in retrieval effectiveness (Section 3.2), evidenced by a high MRR of 0.8098 and 100% Top-10 accuracy, serves as the foundation for the system's overall success. This highly precise retrieval of structured information directly contributed to the significant improvements in semantic similarity and robustness, as measured by BERTScore (Section 3.1), where the TAG-based RAG approach outperformed both the baseline and the PDF-based RAG. This quantitative superiority was corroborated by the human evaluation (Section 3.3). While both RAG systems were perceived as accurate and fluent, the ability of the TAG-based RAG to consistently provide "fully complete" answers highlights its key advantage. The structured nature of the TAG-based RAG ensures that all relevant data points are retrieved and synthesized, preventing the information omissions sometimes observed in the PDF-based RAG. This synthesis of automated and human evaluations confirms that integrating a robust, TAG-based RAG mechanism with a powerful LLM creates a system that is not only semantically aligned but also factually precise, comprehensive, and reliable

4. Conclusion

This research presented the design, development, and evaluation of RMUTTOBot, integrating a TAG-based RAG framework that employs dynamic data interfaces and LLM-native function calling to enable real-time retrieval from institutional databases. The performance of RMUTTOBot was rigorously assessed using a combination of automated metrics and human evaluations across six criteria: semantic similarity, robustness and consistency, retrieval effectiveness, response relevance and accuracy, linguistic fluency and coherence, and content coverage and completeness.

The experimental findings demonstrate that RAG substantially improves the quality and reliability of chatbot responses compared with a baseline language model operating without retrieval support. Quantitative results based on BERTScore metrics indicated that the TAG-based RAG configuration achieved the highest overall performance, with increases of 13.44%, 11.92%, and 12.76% in BERTPrecision, BERTRecall, and BERTF1, respectively, compared to the PDF-based RAG approach. The semantic retrieval evaluation further confirmed that the TAG-based RAG framework consistently identified semantically equivalent questions, successfully locating the correct reference question within the top 10 retrieved results for all test cases.

Human evaluation results corroborated these findings. Both RAG configurations demonstrated strong performance with high inter-rater reliability ($\alpha > 0.835$). While the PDF-based and TAG-based RAG systems performed comparably in response relevance and linguistic fluency, the TAG-based model outperformed in content coverage and completeness, reflecting its ability to dynamically access structured data for more

comprehensive answers. These results collectively validate the effectiveness of the TAG-based RAG framework in improving retrieval precision, contextual grounding, and overall response quality in chatbot systems.

Although the findings confirm the efficacy of the proposed framework, several directions remain for future research. First, scaling and generalization should be explored by extending the TAG-based RAG framework to other institutional domains and integrating multilingual support to enhance accessibility. Second, improvements in retrieval ranking algorithms and context filtering could further optimize performance, reducing redundancy and ensuring that only the most relevant information is provided to the LLM. Third, incorporating user interaction analytics and reinforcement learning from human feedback (RLHF) may enable adaptive refinement of chatbot responses based on real usage patterns. Finally, future iterations of RMUTTOBot could leverage knowledge graphs or structured ontologies to enable more interpretable, explainable, and semantically grounded responses.

Overall, the study contributes a practical, empirically validated framework for developing domain-specific chatbots. The proposed TAG-based RAG approach demonstrates that combining structured data augmentation with dynamic retrieval significantly enhances both the accuracy and completeness of LLM-generated responses an important step toward more intelligent, reliable, and context-aware conversational systems for academic institutions.

5. Acknowledgements

The authors would like to express sincere gratitude to Rajamangala University of Technology Tawan-ok (RMUTTO) for providing valuable data and institutional support used in the development and evaluation of the chatbot system for university admission services. This research would not have been possible without their contributions.

6. References

Abeysinghe, B. and Circi, R. 2024. **The challenges of evaluating LLM applications: An analy sis of automated, human, and LLM-based approaches.** Computation and Language. Available Source: https://doi.org/10.48550/arXiv.2406.03339, October 1, 2025.

Alkishri, W., Yousif, J.H., Al Husaini, Y.N. and Al-Bahri, M. 2025. Conversational AI in Education: A General Review of Chatbot Technologies and Challenges. **Journal of Logistics, Informatics and Service Science** 12(3): 264-282.

Alsafari, B., Atwell, E., Walker, A. and Callaghan, M. 2024. Towards effective teaching assistants: From intent-based chatbots to LLM-powered teaching assistants. **Natural Language Processing Journal** 8: 100-101.

Arslan, M., Ghanem, H., Munawar, S. and Cruz, C. 2024. A survey on RAG with LLMs. **Procedia Computer Science** 246: 3781-3790.

Barnett, S., Kurniawan, S., Thudumu, S., Brannelly, Z. and Abdelrazek, M. 2024. Seven failure points when engineering a retrieval augmented generation system, pp. 194-199. *In* **Proceedings of the IEEE/ACM 3rd International Conference on AI Engineering – Software Engineering for AI (CAIN '24).** Association for Computing Machinery.

Budakoglu, G. and Emekci, H. 2025. Unveiling the power of large language models: A comparative study of retrieval-augmented generation, fine-tuning, and their synergistic fusion for enhanced performance. **IEEE Access** 13: 30936-30951.

Cheng, Z., Xie, T., Shi, P., Li, C., Nadkarni, R., Hu, Y., Xiong, C., Radev, D., Ostendorf, M., Zettlemoyer, L., Smith, N. and Yu, T. 2023. **Binding language models in symbolic languages.** Computation and Language. Available Source: https://doi.org/10.48550/arXiv.2210.02875, October 1, 2025.

Doumanas, D., Soularidis, A., Spiliotopoulos, D., Vassilakis, C. and Kotis, K. 2025. Fine-Tuning Large Language Models for Ontology Engineering: A Comparative Analysis of GPT-4 and Mistral. **Applied Sciences** 15(4): 2146.

Fan, W., Ding, Y., Ning, L., Wang, S., Li, H., Yin, D., Chua, T.S. and Li, Q. 2024. A survey on RAG meeting LLMs: Towards retrieval-augmented large language models, pp. 6491-6501. *In* **The 30th ACM SIGKDD Conference on Knowledge Discovery and Data Mining (KDD '24).** Association for Computing Machinery, United States.

Hadiono, K., Andreas, F., Supriyanto, A. and Irawan, S. 2024. Chatbots implementation for students admission. **Journal of Software Engineering and Simulation** 10: 44-52.

Jiang, J., Zhou, K., Dong, Z., Ye, K., Zhao, X. and Wen, J.R. 2023. StructGPT: A general framework for large language model to reason over structured data, pp. 9237- 9251. *In* **Proceedings of the 2023 Conference on Empirical Methods in Natural Language Processing.** Association for Computational Linguistics.

Joshi, S. 2025. **Evaluation of large language models: Review of metrics, applications, and methodologies.** Artificial Intelligence and Machine Learning. Available Source: https://www.preprints.org/manuscript/202504.0369/v1, October 1, 2025.

Karanikolas, N.N., Manga, E., Samaridi, N., Stergiopoulos, V., Tousidou, E. and Vassilakopoulos, M. 2025. Strengths and Weaknesses of LLM-Based and Rule-Based NLP Technologies and Their Potential Synergies. **Electronics** 14(15): 3064.

Krippendorff, K. 2011. **Computing Krippendorff's alpha-reliability.** Computer Science. Available Source: https://www.researchgate.net/publication/260282682_Computing_Krippendorff's_Alpha-Reliability, October 1, 2025.

Liang, H., Zhou, Y. and Gurbani, V.K. 2025. Efficient and verifiable responses using retrieval augmented generation (RAG), pp. 1-6. *In* **The 4th International Conference on AI-ML Systems (AIMLSystems '24).** Association for Computing Machinery (ACM).

Nguyen, L.S.T. and Quan, T.T. 2025. URAG: Implementing a Unified Hybrid RAG for Precise Answers in University Admission Chatbots – A Case Study at HCMUT, pp. 82-93. *In* **Proceedings of the 2024 International Symposium Information and Communication Technology.** Springer.

Odede, J. and Frommholz, I. 2024. JayBot Aiding university students and admission with an LLM-based chatbot, pp. 391-395. *In* **Proceedings of the 2024 Conference on Human Information Interaction and Retrieval (CHIIR '24).** Association for Computing Machinery.

Oro, E., Granata, F.M., Lanza, A., Bachir, A., Grandis, L.D. and Ruffolo, M. 2024. **Evaluating Retrieval-Augmented Generation for Question Answering with Large Language Models.** Available Source: https://ceur-ws.org/Vol-3762/495.pdf, January 27, 2025.

Pothuri, V. 2024. Natural language processing and conversational AI. **International Research Journal of Modernization in Engineering Technology and Science** 6: 436-440.

Ren, R., Ma, J. and Zheng, Z. 2025. Large language model for interpreting research policy using adaptive two-stage retrieval augmented fine-tuning method. **Expert Systems with Applications** 278: 127330.

Sharief, B. and Ersayyem, Y. 2024. LLM and RAG powered chatbot for the College of Computer Science and Mathematics at the University of Mosul. **International Research Journal of Innovations in Engineering and Technology** 8: 59-61.

Shchegoleva, L., Burdin, G. and Attia, A. 2021. Chatbot for Applicants on University Admission Issues, pp. 491-494. *In* **Proceedings of the 29th Conference of Open Innovations Association.** FRUCT.

Uhm, M., Kim, J., Ahn, S., Jeong, H. and Kim, H. 2025. Effectiveness of retrieval augmented generation-based large language models for generating construction safety information. **Automation in Construction** 170: 105926.

Wan, Y., Chen, Z., Liu, Y., Chen, C. and Packianather, M. 2025. Empowering LLMs by hybrid retrieval-augmented generation for domain-centric Q&A in smart manufacturing. **Advanced Engineering Informatics** 65(B): 103212.

Xu, L. and Liu, J. 2024. A chat bot for enrollment of Xi'an Jiaotong-Liverpool University based on RAG, pp. 125-129. *In* **Proceedings of the 2024 International Workshop on Control Engineering and Advanced Algorithms (IWCEAA).** IEEE.

Zhang, T., Kishore, V., Wu, F., Weinberger, K.Q. and Artzi, Y. 2019. BERTScore: Evaluating text generation with BERT. *In* **Proceedings of the International Conference on Learning Representations.** ICLR.

Recent Science and Technology

Journal homepage: https:// www.tci-thaijo.org/index.php/rmutsvrj/index

ISSN: 3057-0786 (Online)

Research Article

Implementation of Lean Principles and QR Code Technology to Enhance Durable Articles Management System at Rattaphum College: A Process Efficiency Analysis

Wanpracha Nuansoi, Supawadee Mak-on and Supachai Maduea *

Department of Industrial, Rattaphum College, Rajamangala University of Technology Srivijaya, Rattaphum, Songkhla 90180, Thailand.

Article history:

Received: 2025-01-17
Revised: 2025-05-28
Accepted: 2025-06-12

Keywords:

Lean principles;
Durable articles management system;
QR Code;
Application

ABSTRACT

Rattaphum College, Rajamangala University of Technology Srivijaya, previously managed its durable articles through a document-based system, leading to frequent issues such as data loss, redundancy, and difficulty in searching and editing information. This research aimed to (1) develop a durable articles management application using QR Code technology, (2) analyze operational efficiency after applying lean principles, and (3) assess user satisfaction with the new system. The research was conducted using lean principles to reduce steps and time in the operation. The efficiency was calculated from the ratio of total working time to the sum of valuable time. The developed application includes features for QR Code scanning, searching, adding, and editing durable articles, as well as user management. Results showed that, for staff, the application reduced work processes by one step, saved 12.84 minutes, and increased efficiency by 56%. For general users, work steps were reduced by three, with the same time savings and a 72.22% increase in efficiency. User satisfaction was also evaluated, with application design receiving a very good rating ($\bar{x}$ = 4.50, S.D. = 0.70), and overall system usability rated as good ($\bar{x}$ = 4.46, S.D. = 0.69). The study also revealed that an easy-to-use user interface design and the perceived usefulness of the system are important factors influencing its acceptance. This system demonstrates significant improvements in efficiency and usability and can serve as a model for implementation in other educational institutions with similar needs.

1. Introduction

The management information system in educational institutions is a structured system that stores and manages the data necessary for decision-making. The system can facilitate efficient operations in various areas such as academic management, student affairs, finance, durable articles management, and human resources by providing accurate, timely, and integrated information (Colarika and Zahro, 2023). These systems support educational goals and increase the overall efficiency of the management process. The durable articles management information system is an important system for managing resources within the university. The Rajamangala University of Technology Srivijaya, Rattaphum College, still manages durable articles through a document system and records data in Microsoft excel. Currently, the number of durable articles is increasing. The old system is ineffective because there is a delay and lack of speed in searching for information, no search system, the need to travel to ask for information, and wasted time; data loss occurs due to no system to check for duplicate data and no data storage system; there is a lack of flexibility in use since information cannot be viewed all the time and someone must manage the system; and it causes waste by using excessive paper and requiring staff to provide services.

From the above problems, it can be seen that the system is inefficient. If the lean principle is applied to reduce the time and steps in the unimportant work process (Smith *et al*., 2012; Ghelani, 2021; Lojarernrat *et al*., 2024). the lean principle focuses on cost-effectiveness, avoiding losses in work, increasing efficiency in system operations, and enhancing ease of use. The use of lean principles can be done by writing the current work

* **Corresponding author.**

E-mail address: *suppachai.m@rmutsv.ac.th*

Cite this article as:

Nuansoi, W., Mak-on, S. and Maduea, S. 2026. Implementation of Lean Principles and QR Code Technology to Enhance Durable Articles Management System at Rattaphum College: A Process Efficiency Analysis. **Recent Science and Technology** 18(1): 265995.

https://doi.org/10.65411/rst.2026.265995

steps, timing each step, analyzing the necessity of each step, then calculating the efficiency, and proposing a new work approach by cutting out unnecessary steps and calculating the efficiency according to the new process. The convenience of use can be increased if QR Code technology is used, which is a convenient and popular channel for using the system today. QR Code can store more information than the original barcode and is fast in reading data (Moonsrikaew *et al*., 2021). It is an important tool that increases the convenience of retrieving durable articles quickly. This format is accepted in warehouse management. For example, in research (Krajungduang *et al*., 2021), a QR code scanning application was developed to record product code data. It is used to record data instead of the old way of writing. This allows for a reduction in the time and accuracy of recording product code numbers. Research by Kongmuang and Kandee (2023) has developed a system for applying QR code technology to verify durable articles. Research by Pitjamit *et al*. (2024) has applied the principles of Lean and Kaizen, where Kaizen refers to the continuous improvement of the work process. It presents the integration of technology with the concept of Lean-Kaizen. This research uses IoT and Automation systems to reduce waste and improve the production process. Research by Fomina and Yumatova (2022) applies the principles of Lean Production with information systems to increase the efficiency of organizational management and production processes. Research by Amit and Cholli (2021) applies Lean principles to the software development process, focusing on reducing waste and increasing the efficiency of the development team. Research by Monserrat *et al*. (2023) applies Lean principles to improve the teaching process in a software project management course to analyze the value chain and eliminate non-value-added processes in teaching.

From the above research, it can be seen that Lean principles are applied to reduce the steps and time of the operation. QR Code is applied to the information system, and both Lean principles and information system development are applied. This research focuses on solving the problems of the original system as mentioned above. It also integrates lean principles, applications, and QR Code technology to manage equipment in an educational context. It also adds a highlight of easy-to-use system design to achieve a high level of system acceptance. The research aims to 1) solve the problem of inefficient manual durable articles management at Rattaphum College by using Lean principles to increase the efficiency of the durable articles management system and develop it into an application that uses QR Codes; 2) analyze the efficiency of the process; and 3) evaluate the satisfaction of using the system. This research can reduce work steps, decrease the use of documents, reduce data redundancy, increase the speed of searching durable articles, and provide convenience for use at all times. It is beneficial to the departments, procurement officers, and personnel at Rattaphum College.

2. Materials and Methods

2.1 Research methodology

2.1.1 Research Scope

In terms of system capabilities, there are two types of users: administrators and general users. The administrators can scan and search for durable articles, add durable articles, edit durable articles, and add users. As for users, they can search for durable articles. The data will be stored in a relational database. The sample group is 30 personnel of Rattaphum College, Rajamangala University of Technology Srivijaya, using a purposive sampling method (Phoksawat *et al*., 2025) who use the durable articles management system, consisting of procurement officers, lecturers, and staff. The research team explained the details of the research project and protected the rights of the research participants. They also explained the rights of the sample group to refuse to participate in the study without affecting the services they will receive. All data are confidential and only the overall results are presented.

2.1.2 Development of the Rattaphum College Durable articles Management System using QR Code via Mobile Application was developed using System Development Life Cycle (SDLC) Waterfall Model.

The waterfall model is a traditional approach to the systems development life cycle (SDLC), characterized by linear and sequential steps, often used for projects where requirements are well understood and unlikely to change. The model is ideal for general systems or software, where the development process can follow a structured path from planning to maintenance as shown in Figure 1. The structured nature of the waterfall model ensures that each step is completed before the next task begins, which can help maintain quality and reduce errors (Wusidagama and Marikkar, 2024).

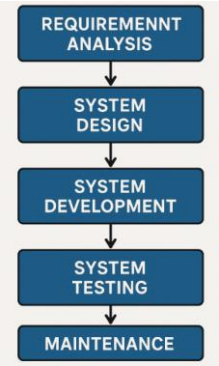

Figure 1 System Development Life Cycle (SDLC) waterfall model

2.1.2.1 Requirement Analysis

The needs of users of the system in the organization were analyzed through interviews. It was found that a durable articles management system that can be used via mobile phones, scanned by QR codes to search for durable articles,

add new durable articles, and edit durable article information, was needed.

2.1.2.2 System Design

System design includes overall system design, data flow diagram design, database design, and process design and performance analysis before applying lean principles.

From Figure 2, the system is designed using a client-server architecture by first developing a website system, which uses PHP (Mothongkul and Namcode, 2019) for development and a MySQL database (Satjabundanjai *et al*., 2023) that is fast to use and free to use. The user interface design uses the Technology Acceptance Model (TAM), which focuses on designing for perceived ease of use and perceived usefulness (Scherer *et al*., 2019; Natasia *et al*., 2022) to achieve higher system acceptance. Draw.io is used to help design, which is free to use. Users can use the website using various devices such as PCs, smartphones, and tablets on the ethernet network within the organization. For portable devices, the application was developed using Android Studio via the WebView method, which retrieves data from the website to display in the application. The advantage is that the system can be updated quickly. When the website is updated, the application will be updated immediately without having to edit it in the application.

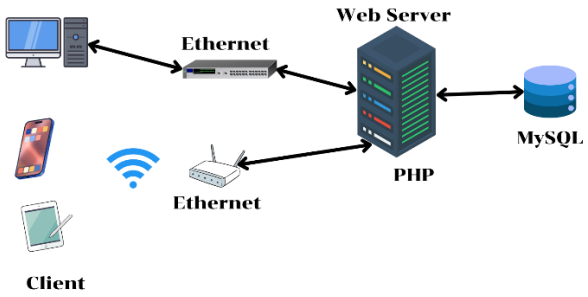

Figure 2 System Design

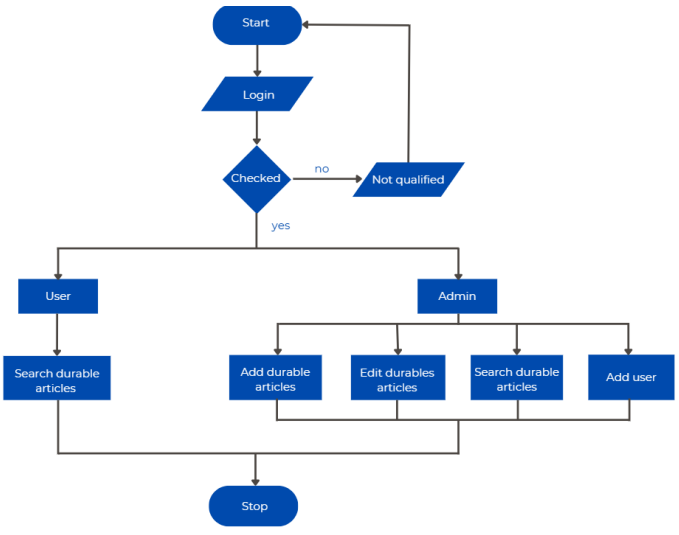

Figure 3 Flow chart showing the operation of the system

Figure 3 is a flow chart showing the operation of the system, starting from logging in to the system, filling in the username and password. The system will check with the database. If there is no username or the password is incorrect, the system will ask you to log in again. But if the username and password are correct, the system will check the type of user. If you are a user, you can scan the QR Code to search for durable articles. If you are an administrator, you can add durable articles, edit durable articles, search for durable articles, and add users.

(1) Data Flow Diagram (DFD) design

DFD is a representation of the flow of data within the system and the operations that occur in the system. The information in the diagram shows where the data comes from, where the data goes, where the data is stored, and what events happen to the data along the way. The data flow diagram shows the overall picture of the system from external factors flowing into the system through various work steps through data collection, showing data according to the direction of data flow. DFD Level 0 is the overall data flow, also called context diagram.

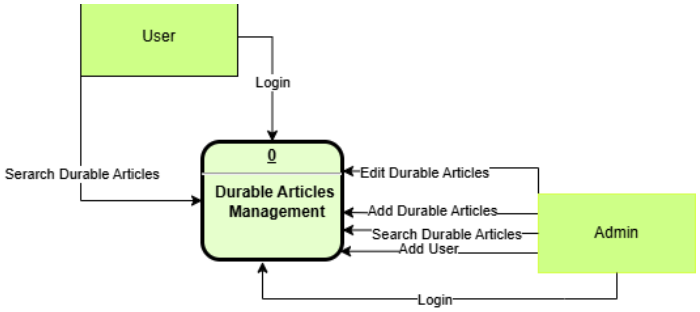

Figure 4 Data Flow Diagram level 0 or Context Diagram

From Figure 4, it is a context diagram showing the main process of durable articles management system, which is a central system that links the data exchange between external entities, namely user and admin, with clear data input and output characteristics for each role.

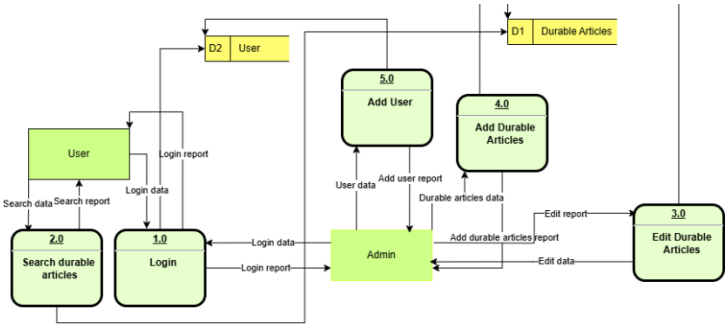

Figure 5 Data Flow Diagram level 1

From Figure 5, it is a DFD level 1 showing the breakdown of the sub-processes within the durable articles management system. The details are extracted from the context diagram (level 0) to clearly show the internal structure of the system,

especially the data flow between users, administrators, and the database.

(2) Database Design

The database design uses ER-Diagram, which is an easy-to-use and understandable database design tool. It is the main tool used in designing relational databases (Jaimez-González and Martínez-Samora, 2020). ER-Diagram is used to represent the structure of the data, show the relationship between entities, and define attributes and primary keys. Figure 6 is a model of the relationship between entities. It consists of 2 main entities: user and durable articles, which are related through a relationship called 'have' with a cardinality of 1: M, meaning that one user can own many items of durable articles, but each item of durable articles can be associated with only one user. Each entity has a clear primary key: User ID for the user entity and Durable articles ID for the durable articles entity.

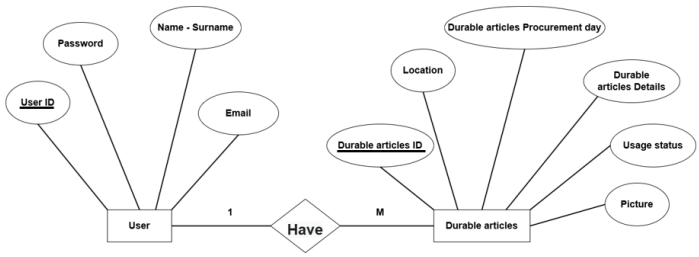

Figure 6 ER- Diagram

(3) Process and efficiency before using lean principles (Pre-LEAN)

Lean is a strategic concept that aims to increase the efficiency of the organization by eliminating waste and improving the process to meet customer needs. It is based on the Toyota Production System (TPS) and has been further developed with theoretical concepts such as Kaizen (continuous improvement), Just-In-Time (JIT) (just in time) and Theory of Constraints (TOC) (management of constraints) to be applied to all types of organizations, not limited to the manufacturing sector (Shah and Ward, 2007).

The Lean principle has the following methods:

Step 1: Write the current work process from the beginning to the end of the work process in detail, called Pre-Lean, by visiting the field to observe the actual work steps and interviewing staff to understand all steps.

Step 2: Time each work process, including the distance between steps and the waiting time at each step, using a timer application.

Step 3: Analyze the activities that occur to determine which activities are necessary or not necessary to do, or not necessary but must be done, by defining them as symbols as follows:

Necessary

Not necessary

Not necessary but must be done

Conduct meetings with operators to analyze activities together.

Step 4: Calculate the efficiency of the Pre-Lean work process using the formula:

$$\text{Efficiency} = \frac{\text{Sum of valuable time}}{\text{Total time}} \text{ X } 100$$

Step 5: Hold a meeting with the operators to analyze and find a new way of working (Post-Lean) by cutting out unnecessary processes (Waste) and cutting out unnecessary processes that must be done (Necessary non-value) or to the minimum, and collecting real data according to the new method to find efficiency.

Step 6: Calculate efficiency according to the new process or Post-LEAN that will have only things that do not need to be done but must be done and things that need to be done.

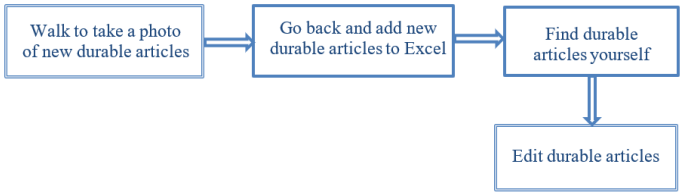

Figure 7 Durable articles management process for staffs before using lean principles

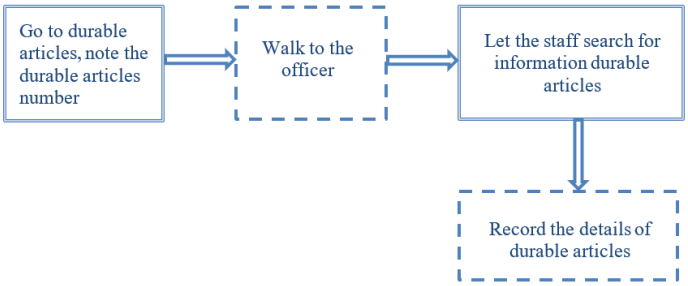

Figure 8 Durable articles management process for users before using lean principles

Durable articles management procedures for staff

1. Walk to take a photo of new durable articles. It takes 10 minutes.
2. Go back and add new durable articles to Excel. It takes 12 minutes.
3. Find durable articles yourself. It takes 2 minutes.
4. Edit durable articles. It takes 1 minute.

Steps 1 and 4 are necessary steps and therefore represent valuable time. Step 2 is unnecessary, while Step 3 is unnecessary but currently required. Step 3 can be eliminated if a digital application system is developed to replace the existing system. Therefore, the total valuable time for Steps 1 and 3 combined is 11 minutes.

$$\text{Efficiency} = \frac{10+1}{25} \times 100$$
$$\text{Efficiency} = 44.00\ \%$$

Durable articles management procedures for users

1. Go to durable articles and note the durable articles number. It takes 5 minutes.
2. Walk to the officer. It takes 10 minutes.
3. Let the staff search for information durable articles. It takes 2 minutes.
4. Record the details of durable articles. It takes 1 minute.

Step 1 is necessary and therefore represents valuable time. Steps 2 and 3 are unnecessary, while Step 4 is unnecessary but currently required. Step 4 can be eliminated if a digital application system is developed to replace the existing system. Therefore, the valuable time for Step 1 is 5 minutes.

$$\text{Efficiency} = \frac{5}{18} \times 100$$
$$\text{Efficiency} = 27.77\ \%$$

2.1.2.3 System development

After designing the data flow in the system, the user interface, and the database, the database system was developed using MySQL, and the system website was developed using PHP so that the system can be used via a web application. For mobile devices, to make the usage smoother, the application was developed using Android Studio (Tewari and Singh, 2021) in the form of using WebView to retrieve data from the website in the developed system. This method allows for fast system updates. If the website is updated, it will affect the application immediately. However, the display format may not be as beautiful as a native application.

2.1.2.4 System Testing

When the system development was completed, the system usage was tested under the rights of the Admin user, from adding durable articles information, scanning QR codes to search for durable articles, editing and updating information, and adding new users and users to scan QR codes to search for durable articles. When errors were found, the system was returned to the system development process to be improved.

2.1.2.5 Maintenance

During actual usage, user satisfaction was evaluated to guide further development and improvement. System training was also provided.

2.2 Creating a satisfaction questionnaire for durable articles management systems using QR codes via android applications.

1. A closed-ended questionnaire divided into two sections with 12 questions: Section 1: Personal information of the respondent, a 2-item survey: gender and age; and Section 2: Satisfaction with the development of the Rattaphum College durable articles management system using QR codes via mobile applications. The questionnaire was in the form of a rating scale, divided into two dimensions with 10 questions: application design and durable articles management system usage.

2. The questionnaire was examined for content validity by five experts, with an average validity ranging from 0.60-1.00.

3. The system users were asked to test the system and collect data.

4. Statistical data analysis used a ready-made statistical program to help with the analysis to find the arithmetic mean (Arithmetic Mean: $\bar{X}$ and standard deviation (Standard Deviation: S.D.) (Carifio and Perla, 2008), which uses a 5-level Likert scale as follows: 5 = most satisfied, 4 = very satisfied, 3 = moderately satisfied, 2 = slightly satisfied, 1 = least satisfied. The interpretation uses the following levels: 4.50-5.00 most satisfied, 3.50-4.49 very satisfied, 2.50-3.49 moderately satisfied, 1.50-2.49 slightly satisfied, and 1.00-1.49 least satisfied.

3. Results and Discussion

The research results and discussions are presented in three parts: the first part is the results of developing a durable articles management application using QR Code, the next is the results of analyzing the efficiency of the process after using lean principles, and the last is the results of evaluating the satisfaction of using the system, which is divided into application design and system use.

3.1 System Development Results

System development results include the system, login, adding durable articles, editing durable articles, scanning for durable articles, and adding users. From Figure 9, it is the system login page. When the user and password information is entered, the system will check the user database. If there is information, the system will continue to log in. If no information is found, the system will ask you to try logging in again.

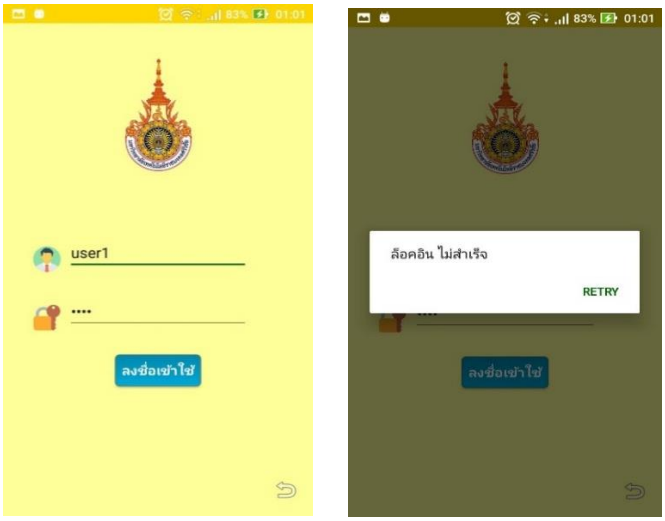

Figure 9 Login system

To scan QR codes for durable articles search, when users tap the QR code scan button, the system requests permission to access the mobile device's camera. Upon scanning, the system retrieves the durable article code as shown in Figure 10a. As illustrated in Figure 10b, users then press the search button. If the item exists in the database, its details are displayed on screen as shown in Figure 10c. If no matching item is found, the system notifies the user.

To add durable articles information, fill in the durable articles details, select a picture or take a photo, and press the add information button. The information will be added to the database system. You can also create a QR code to attach to the durable articles for further searching, as shown in Figure 11a. After scanning to search for durable articles, you can edit the durable articles information as desired. The system will save the information in the database as shown in Figure 11b.

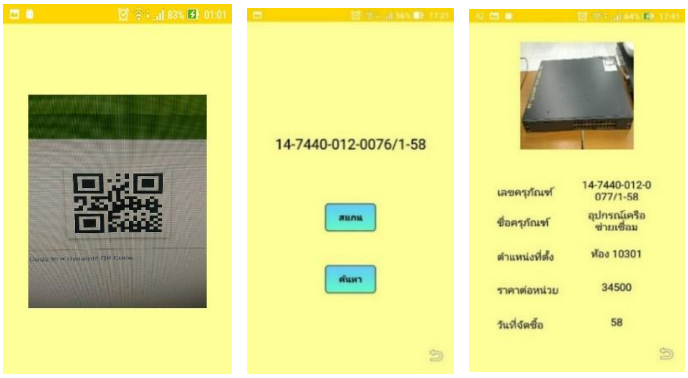

a b c

Figure 10 Scan QR code to search for durable articles

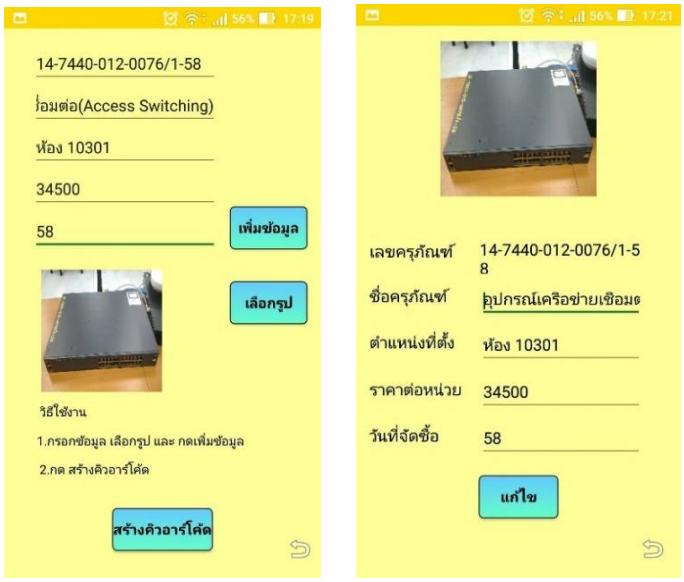

a b

Figure 11 Adding and editing durable articles data

The system design in this research focuses on simplicity but has the ability to manage data effectively. The database design separates data into different tables, namely, durable articles table and user table, so that it is possible to add, search, edit durable articles and add user data. There is a clear link between data. This approach is consistent with the concept of (Aleryani, 2024) who proposed that a relational database structure should be designed together with a data flow diagram (Data Flow Diagram: DFD) to help understand the flow of data in the system more clearly, especially in information systems that must support access to multiple functions.

3.2 Process and efficiency after using lean principles (Post-LEAN)

Figure 12 Durable articles management process for staff after applying lean principles

Durable articles management procedures for staff

1. Walk to take a photo of new durable articles. It takes 10 minutes.
2. Find durable articles yourself. It takes 2 minutes.
3. Edit durable articles. It takes 1 minute.

After implementing the lean principles (post-lean), steps 1 through 3 were identified as essential steps in the process, with a total combined duration of 12.16 minutes.

$$\text{Efficiency} = \frac{11+0.16+1}{12.16} \times 100$$

Efficiency = 100.00 %

Durable articles management procedures for users

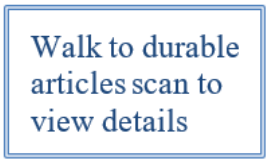

Figure 13 Durable articles management process for users after using lean principles

1.Walk to durable articles section to scan and view details. It takes 5 minutes.

Following the post-lean implementation, the process was streamlined to a single essential step, requiring only 5.16 minutes to complete.

$$\text{Efficiency} = \frac{5.16}{5.16} \times 100$$

Efficiency = 100 %

Table 1 Comparison of performance between pre-lean and post-lean

List	Pre-Lean: Staff	Post-Lean: Staff	Pre-Lean: Users	Post-Lean: Users
Process	4	3	4	1
Duration (minutes)	25	12.16	18	5.16
Efficiency (%)	44	100	27.77	100

Table 2 Application design satisfaction assessment results

Assessment Topics	$\bar{x}$	S.D.	Level
The screen design is suitable	4.67	0.56	Highest
Font and text layout	4.43	0.79	High
Able to understand the display of system information	4.76	0.43	Highest
Application background	4.14	0.77	High
Total	4.50	0.70	Highest

Table 3 Assessment of satisfaction with system usage

Assessment Topics	$\bar{x}$	S.D.	Level
Ease of use of the system	4.71	0.55	Highest
Appropriateness of font selection	4.43	0.66	High
System suitability	4.19	0.59	High
Accuracy of data verification via the system	4.48	0.66	High
Accuracy of data correction via the system	4.24	0.75	High
Speed of system use	4.71	0.70	Highest
Total	4.46	0.69	High

From Table 1, the comparison results between Pre-Lean and Post-Lean found that it helped reduce the staff's work steps by 1 step from 4 steps to 3 steps, reduced the time by 12.84 minutes from 25 minutes to 12.16 minutes, and increased the system efficiency from 44 to 56 to 100 because the staff still had many steps to do, resulting in not much improvement in efficiency. For general users, it helped reduce the work steps by 3 steps from 4 steps to 1 step, reduced the time by 12.84 minutes from 18 minutes to 5.16 minutes, and increased the system efficiency from 66.67 to 33.33 because the users had many steps that did not need to be done, resulting in a significant increase in efficiency.

The application of lean principles in this research focuses on reducing unnecessary steps in the durable articles management process, such as duplicate data entry, manual document search, and unsupported counting. The research results are in the same direction as the two (Krajungduang *et al*., 2021; Lojarernrat *et al*., 2024), who used lean principles to reduce steps and work time in developing an information system for managing warehouse and parcel work. And it is consistent with the by Teerapraipruek and Supakul (2024), which used lean principles to reduce work steps and increase efficiency in drug warehouse management. It is consistent with the research by Smith *et al*. (2012), which used lean principles to reduce waste, reduce waiting time for patients and personnel, reduce redundant paperwork, and increase personnel satisfaction. It is also consistent with the research by Contreras Castañeda *et al*. (2024), who used lean principles to reduce waste and improve the process in the production of raw sugar from sugarcane.

In addition, research by Marques *et al*. (2022), which applied lean principles in retail stores and e-commerce systems, also showed a reduction in waste in order and inventory management processes using digital systems combined with value stream mapping, similar to the approach in this research that analyzed the original process before improvement (Pre-Lean) to find waste and design a new system using lean tools such as timing, activity classification, and process efficiency assessment.

3.3 Satisfaction evaluation results

It is divided into two aspects: application design and system usage, as shown in Table 2-3.

According to Table 2, the satisfaction analysis of the Rattaphum College durable articles management system using QR codes via mobile application, regarding application design, shows that overall satisfaction was at the highest level ($\bar{x}$ = 4.50, S.D. =0.70). When considering individual items, the system's information display comprehensibility received the highest satisfaction ($\bar{x}$ = 4.67, S.D. =0.43), followed by appropriate screen design ($\bar{x}$ = 4.67, S.D. =0.56), and text and message layout ($\bar{x}$ = 4.43, S.D. =0.79).

The evaluation results are in the same direction as the research by Kongmuang and Kandee (2023), which evaluated the development of the QR code technology application system for checking durable articles in terms of meeting the needs of the

system users at the highest level. It is also consistent with the research by Nadee (2022), which has evaluation results showing satisfaction with the application design at a very satisfactory level as well.

According to Table 3, the satisfaction analysis of the Rattaphum College durable articles management system using QR codes via mobile application, regarding system usage reports, shows overall satisfaction at a high level ($\bar{X}$ = 4.46, S.D. =0.69). When considering individual items, system ease of use and system speed received the highest satisfaction ($\bar{X}$ = 4.71, S.D. =0.55), followed by accuracy in system data verification ($\bar{X}$ = 4.48, S.D. =0.66), and appropriateness of font selection ($\bar{X}$ = 4.43, S.D. =0.66).

From the evaluation results, the ease of use of the system and its speed resulted in users having a positive attitude towards the use of technology and accepting its use, which is consistent with the research by Phoksawat *et al*. (2025). The increased satisfaction of users after using the new system reflects the system's ability to meet the needs of actual use, especially in terms of fast access to information via QR Code and reducing redundant steps, which is different from the original system that required filling in paper files and searching manually. This research result is consistent with the study by Jaroenchart and Phookanngam (2023), which used QR code technology to check the safety system of forklifts and found a satisfaction evaluation result in terms of ease of use, convenience, and simplicity at a very good level as well.

Problems and obstacles found during the operation are that it is difficult for users to accept the use. Therefore, it is necessary to design the system to be easy to use and fast to use. And from the results of the research that applied lean principles and information system development to manage durable articles, it reduces the steps and time of work, increases convenience in using the system, and can be applied to other educational institutions.

4. Conclusion

The durable articles management system has the ability to add durable articles, scan and search for durable articles, edit durable articles, and add new users. There are 2 types of system users: general users can scan and search for durable articles, while administrators can use all systems. In developing the system, the database system was developed using MySQL and PHP was used to develop various systems. The mobile application was developed using Android Studio. In terms of the results of the evaluation of satisfaction with the system, it was found that satisfaction with the application design was at the highest level, while satisfaction with the use of system reports was at a high level. Satisfaction in terms of ease and speed of using the system was at the highest level, and the perception of the benefits of the system, both in terms of reduced work steps and increased efficiency, resulted in greater acceptance of its use. The research results clearly achieved the objectives of using lean principles to reduce steps and time in working, eliminate redundancy, and increase work efficiency. However, the research still has limitations: it was used by only one department and is also a small-scale example of use. However, it can be applied to other asset management systems. The future development guidelines will include developing a database to be stored in the cloud system that offers better flexibility in use, testing the system in a larger department to evaluate its efficiency, accuracy, and precision, and studying artificial intelligence technology to reduce the steps of the system, making it more automatic and more efficient.

5. Acknowledgments

This research was successfully completed. We would like to thank the Research Review Committee at Rattaphum College, Rajamangala University of Technology Srivijaya, and research assistants Mr. Sukrit Khadlae and Mr. Pathomporn Saelim. Finally, the research team would like to thank Rajamangala University of Technology Srivijaya for providing the budget and income to support this research.

6. References

Aleryani, A.Y. 2024. Analyzing data flow: A comparison between data flow diagrams (DFD) and user case diagrams (UCD) in information systems development. **European Modern Studies Journal** 8(1): 313-320.

Amit, R. and Cholli, N.G. 2021. Application of Lean Principles in Software Development Processes, pp. 38-42. *In* **2021 International Conference on Disruptive Technologies for Multi-Disciplinary Research and Applications (CENTCON).** IEEE, India.

Carifio, J. and Perla, R.J. 2008. Resolving the 50-year debate around using and misusing Likert scales. **Medical Education** 42(12): 1150-1152.

Colarika, S. and Zahro, F. 2023. Konsep dasar dalam sistem informasi manajemen dalam pendidikan. **ASCENT: Al-Bahjah Journal of Islamic Education Management** 1(2): 51-60.

Contreras Castañeda, E.D., Gordillo Galeano, J.J. and Olaya Rodríguez, K.J. 2024. Lean-Kaizen startup in panela production processes: the case of a trapiche. **Cogent Engineering** 11(1): 1-18.

Fomina, I.G. and Yumatova, K.V. 2022. Implementation of Lean Production Principles Using Information Systems, pp. 1654-1657. *In* **2022 Conference of Russian Young Researchers in Electrical and Electronic Engineering (ElConRus).** IEEE, Russia.

Ghelani, H.J. 2021. Advances in lean manufacturing: Improving quality and efficiency in modern production systems.

International Journal of Scientific Research and Management 9(6): 611-625.

Jaimez-González, C.R. and Martínez-Samora, J. 2020. DiagrammER: A Web Application to Support the Teaching-Learning Process of Database Courses Through the Creation of E-R Diagrams. **International Journal of Emerging Technologies in Learning (iJET)** 15(19): 4-21.

Jaroenchart, P. and Phookanngam, P. 2023. Development on a QR Code Technology system for Safety Inspection of Forklifts: the case of a warehousing company in Phranakhon Si Ayutthaya Province. **Journal of Management Science review** 25(3): 79-90. (in Thai)

Kongmuang, S. and Kandee, M. 2023. Application of QR-Code Technology for Equipment Inventory in College of Industrial Technology and Management. **Science and Technology Research Journal Nakhon Ratchasima Rajabhat University** 8(1): 1-12. (in Thai)

Krajungduang, K., Singhdong, P. and Weerapong, P. 2021. Improving Warehouse Operations with Mobile Applications and ECRS Concepts Case Study of Yusen Logistics (Thailand) Co. Ltd. **Journal of Learning Innovation and Technology (JLIT)** 1(2): 62-69. (in Thai)

Lojarernrat, J., Yathongchai, W. and Wannatrong, N. 2024. The Development of Supply Management Information System Based on Lean Concept: A Case Study of Buriram Provincial Administrative Organization. **Journal of Science and Technology Buriram Rajabhat University** 8(2): 109-123. (in Thai)

Marques, P.A., Jorge, D. and Reis, J. 2022. Using lean to improve operational performance in a retail store and e-commerce service: A Portuguese case study. **Sustainability** 14(10): 5913.

Moonsrikaew, P., Sitawan, S. and Chatsermsak, P. 2021. Online asset monitoring system using QR Code technology. **Mahasarakham Journal** 12(1): 117-128. (in Thai)

Monserrat, M., Mas, A., Mesquida Calafat, A.L. and Clarke, P. 2023. Applying Lean to Improve Software Project Management Education. **IEEE Transactions on Engineering Management** 71(1): 7496-7510.

Mothongkul, K. and Namcode, M. 2019. A development of meeting room reservation online system the office of disease prevention and control 7 Khon Kaen. **SciTech Research Journal** 2(2): 7-12. (in Thai)

Nadee, T. 2022. Android Operating System Applications About choosing a disease-specific diet. **Industrial Technology Journal** 2(2): 7-12. (in Thai)

Natasia, S.R., Wiranti, Y.T. and Parastika, A. 2022. Acceptance analysis of NUADU as e- learning platform using the Technology Acceptance Model (TAM) approach. **Procedia Computer Science** 197: 512-520.

Phoksawat, K., Chanakot, B., Phoksawat, E., Kongyarit, N., Laimnimitr, N. and Unjan, R. 2025. Data and geospatial information management web application for enhancing the competitiveness of Trang pepper large agricultural plot of community enterprise. **TEM Journal** 14(1): 117-128.

Pitjamit, S., Jewpanya, P. and Nuangpirom, P. 2024. Enhancing Lean-Kaizen practices through IoT and automation: A comprehensive analysis with simulation modeling in the Thai food industry. **Engineering and Applied Science Research** 51(3): 286-299.

Satjabundanjai, P., Panich, W. and Manosuttirit, A. 2023. Development of online active learning in computer programming on database with PHP and MySQL for undergraduate students in educational technology. **HRD Journal** 1(2): 62-69. (in Thai)

Scherer, R., Siddiq, F. and Tondeur, J. 2019. The Technology Acceptance Model (TAM): A meta-analytic structural equation modeling approach to explaining teachers' adoption of digital technology in education. **Computers & Education** 128: 13-35.

Shah, R. and Ward, P.T. 2007. Defining and developing measures of lean production. **Journal of Operations Management** 25(4): 785-805.

Smith, G., Poteat-Godwin, A., Harrison, L.M. and Randolph, G.D. 2012. Applying Lean principles and Kaizen rapid improvement events in public health practice. **Journal of Public Health Management and Practice** 18(1): 52-54.

Teerapraipruek, C. and Supakul, S. 2024. Optimization of Pharmacy Inventory Management by Applying LEAN Thinking in Nan Hospital. **Thai Journal of Pharmacy Practice** 16(1): 248-262. (in Thai)

Tewari, A. and Singh, P. 2021. Android App Development: A Review. **Journal of Management and Service Science** 1(2): 1-6.

Wusidagama, N.S. and Marikkar, F. 2024. Waterfall model over PcD.UcT model review. **Automation of Technological and Business Processes** 16(3): 133-138.

Recent Science and Technology

Journal homepage: https:// www.tci-thaijo.org/index.php/rmutsvrj/index

ISSN: 3057-0786 (Online)

Research Article

Impact of Stocking Density on Bioeconomic Performances of Blue Swimming Crab (*Portunus pelagicus*) Culture in Grow-Out Ponds

Vutthichai Oniam * **and Wasana Arkronrat**

Klongwan Fisheries Research Station, Faculty of Fisheries, Kasetsart University, Mueang, Prachuap Khiri Khan 77000, Thailand.

Article history:

Received: 2025-02-28
Revised: 2025-08-27
Accepted: 2025-10-15

Keywords:

Crab aquaculture;
Crab growth;
Crab survival;
Optimal stocking density;
Economic profitability

ABSTRACT

The blue swimming crab (BSC) is a commercially important species with high consumer demand, but escalating exploitation has negatively impacted its natural populations. Establishing effective cultivation methods for BSC offered a promising long-term solution to this issue. This study aimed to enhance stocking density in grow-out ponds by analyzing the effects on bioeconomic performance of BSC farming. The research involved rearing juvenile BSC in 1,600 m² earthen ponds at three stocking densities: low (1 crab/m²), medium (3 crabs/m²), and high (5 crabs/m²). Each group had three replicates (n = 3). BSC were fed an artificial shrimp feed (38% protein) at 5% of body weight per day, with feedings occurring twice daily. Over a 90-day period, survival rate (SR), weight gain (WG), average daily growth (ADG), specific growth rate (SGR), and feed conversion ratio (FCR) were assessed, alongside economic metrics such as total revenue (TR), break-even point (BEP), and payback period (PBP). Results indicated that stocking density significantly (p<0.05, one-way ANOVA) influenced the SR, WG, ADG, SGR, and revenue in BSC cultivation. As density increased, SR declined, and higher densities resulted in lower growth rates, reduced TR, and elevated FCR. In terms of culture efficiency, the densities of 1 and 3 crabs/m² proved to be more suitable for BSC culture compared to 5 crabs/m². However, economically, it was determined that rearing BSC at these three densities was not a worthwhile investment, with the density of 5 crabs/m² having the highest BEP (1.08 kg/m²) and PBP (7.5 years), while 1 crab/m² had the lowest BEP (0.38 kg/m²) and PBP (3.9 years). Therefore, appropriate BSC rearing guidelines should consider a density of no more than 3 crabs/m^2 for future production.

1. Introduction

Global food and nutrition security depended on the growth and development of aquaculture production systems, as fisheries and aquaculture contributed approximately 17% of total animal-source protein for human consumption. Among these, crustaceans held second place in importance (Boyd *et al*., 2022). Cai and Galli (2021) reported that marine crabs accounted for 447,372 tons of the 120 million tons of aquaculture produced worldwide in 2019, reflecting a 3.74% increase over 2018.

The blue swimming crab, *Portunus pelagicus* (BSC), is a valuable commercial species widespread across the tropical coastal waters of the western Indian Ocean and eastern Pacific. Thailand ranked as one of the world's leading producers of marine crabs (e.g., *Portunus pelagicus*, *Scylla serrata*), exporting about 42.2 million tons of BSC annually, valued at USD 35 million. Unfortunately, overexploitation led to decreasing crab populations, resulting in a decline in BSC landings and exports over the past few decades. In 2020, fishery trends showed that BSC catches remained at their highest levels. Notably, the demand for seafood is increasing, while natural marine resources are decreasing, due to overexploitation and habitat destruction, with the BSC being one of the species under threat in many Asian countries (FAO, 2022; Yulianto *et al*., 2024). Culture development of the BSC is one potential and promising long-term solution to cope with this problem. BSC culture development is a potential and promising long-term strategy to address the challenges

* **Corresponding author.**

E-mail address: *ffisvco@ku.ac.th*

Cite this article as:

Oniam, V. and Arkronrat, W. 2026. Impact of Stocking Density on Bioeconomic Performances of Blue Swimming Crab (*Portunus pelagicus*) Culture in Grow-Out Ponds. **Recent Science and Technology** 18(1): 266519.

https://doi.org/10.65411/rst.2026.266519

facing the aquaculture sector. It offers a viable pathway to increase seafood production while reducing pressure on wild stocks, enhancing food security, and supporting rural livelihoods. By expanding culture systems ranging from hatchery-reared juveniles to grow-out operations and value-added products, this approach can improve production efficiency, enable resource diversification, and promote responsible management of coastal ecosystems.

Recently, technologies associated with BSC aquaculture had been developed or improved, including broodstock rearing (Oniam and Arkronrat, 2022; Efrizal *et al*., 2024), nursing (Konsantad *et al*., 2024; Leearam *et al*., 2024), and grow-out culture (Phinrub *et al*., 2023). However, in most of the research studies conducted up to that point, it became evident that the economic sustainability of BSC farming remained a significant issue that needed further investigation to build confidence among farmers and establish tangible sustainability in commercial crab farming.

Bioeconomic and profitability analyses were crucial for understanding the dynamics of aquaculture, as these assessments employed mathematical models to evaluate the economic benefits of productivity enhancements, such as growth, survival, and feed efficiency, while also considering broader impacts on ecosystems and economies (Rabassó and Hernández, 2015; Llorente and Luna, 2016).

Bioeconomic studies provided valuable insights by examining the interactions between biological processes, economic factors, and environmental conditions in aquaculture systems (Llorente and Luna, 2016; Boyd *et al*., 2020). For crab aquaculture, stocking density was a critical factor that influenced the success of production, yet the optimal level for crab cultivation remained uncertain, with studies reporting varying outcomes (Mugwanya *et al*., 2022; Gençer, 2023; Zhang *et al*., 2023). Determining the ideal stocking density for aquatic animal cultivation proved complex, requiring a balance of factors such as species, growth rates, behavior, water quality, and the overall welfare of the animals (Farhaduzzaman *et al*., 2020). These factors impacted the bioeconomic and profitability outcomes of the cultured species (Llorente and Luna, 2016).

Although advances in BSC culture technology have been made, there is still no clear data on the stocking density that is appropriate from a bioeconomic perspective. The current study aimed to investigate the effects of varying stocking densities on bioeconomic parameters (growth rate, survival rate, and feed conversion ratio) and profitability, with the objective of optimizing production while ensuring the health and well-being of the cultured BSC.

2. Materials and Methods

2.1 Experimental design and set-up

The study was conducted at the Klongwan Fisheries Research Station (KFRS) in Thailand. Juvenile blue swimming crabs, *Portunus pelagicus* (BSC), with a carapace width of 1.5-2.0 cm (about 40-45 days after hatching) were transferred from the KFRS hatchery to be reared in a 1,600 m² grow-out pond. This experiment was designed (CRD) to investigate the impact of three stocking densities on BSC cultivation: low (1 crab/m²), medium (3 crabs/m²), and high (5 crabs/m²). Each treatment group had three replicates (n = 3). The duration of the study was from April 2022 to March 2024.

BSCs were fed artificial shrimp feed according to Oniam *et al*. (2012). In the first 30 days, crabs received shrimp feed No. 2 (pellet size 0.8 – 1 mm, 38% protein) at 30% of body weight/day. From days 31 to 60, BSCs were given shrimp feed No. 4S (pellet size 3.5 mm, 38% protein) at 5% of body weight/day, followed by 3% until day 90. Throughout the experiment, BSCs were fed twice a day at 0900 and 1700 hours.

2.2 Data collection

During the experiments, approximately half of the pond water was exchanged weekly, and water quality parameters were monitored twice a week. Salinity was measured using a refractometer (Prima Tech), and pH was assessed with a portable pH meter (Cyber Scan pH 11). Dissolved oxygen and temperature were recorded with an oxygen probe (YSI 550A), while total ammonia, nitrite, and alkalinity were determined according to the standard methods of APHA, AWWA and WEF (2023).

Over a 90-day period, for bioeconomic considerations, survival (SR), growth rates such as weight gain (WG), average daily growth (ADG) and specific growth rate (SGR), as well as feed conversion ratio (FCR) were calculated using Equations 1, 2, 3, 4 and 5, respectively:

$$\text{SR}\ (\%) = \left(\frac{\text{Number of crab surviving}}{\text{Number of crab stocked}}\right) \times 100 \quad (1)$$

$$\text{WG}\ (\text{g}) = \text{Final BW} - \text{Initial BW} \quad (2)$$

$$\text{ADG}\ (\text{g/day}) = \frac{\text{Final BW} - \text{Initial BW}}{\text{t}} \quad (3)$$

$$\text{SGR}(\%\text{day}) = \left(\frac{ln\ \text{final BW} - ln\ \text{initial BW}}{\text{t}}\right) \times 100 \quad (4)$$

$$\text{FCR} = \frac{\text{Total feed given}}{\text{Total crab weight gain}} \quad (5)$$

where BW is the mean body weight, t is the growth period in days and *ln* is the Napierian logarithm.

For profitability factors, we evaluated several economic indicators, total cost (TC) of BSC farming was divided into production cost (PC) and marketing cost (MC). PC included fixed costs (FC) like land, labor, tools and equipment depreciation, and variable costs (VC) such as seeds, feed, and transportation. MC covered distribution, packaging, and advertising expenses. Total revenue (TR) and net return (NR) represented sales values, with TR calculated by subtracting TC from gross returns at various stocking densities. The break-even point (BEP) indicated when TR equaled TC, showing no profit or loss,

and helped determine the quantity of BSC needed to cover all costs. Including, the payback period (PBP) is the amount of time that is expected before an investment will be returned in the form of income.

TC, PC, TR, NR, BEP and PBP were calculated using Equations 6, 7, 8, 9, 10 and 11, respectively:

$$\mathrm{TC} = \mathrm{PC} + \mathrm{MC} \quad (6)$$

$$\mathrm{PC} = \mathrm{TFC} + \mathrm{TVC} \quad (7)$$

$$\mathrm{TR} = \mathrm{P} \times \mathrm{Q} \quad (8)$$

$$\mathrm{NR} = \mathrm{TR} - \mathrm{TC} \quad (9)$$

$$\mathrm{BEP\ (kg/pond)} = \frac{\mathrm{TFC}}{(\mathrm{P} - \mathrm{VCU})} \quad (10)$$

$$\mathrm{PBP\ (year)} = \frac{\mathrm{Initial\ investment}}{\mathrm{TR\ per\ year}} \quad (11)$$

where TFC is the total fixed costs, TVC is the total variable costs, P is the price per unit of BSC/kg, Q is the total quantity of BSC in kg and VCU is the variable cost per unit of yield = TVC / Q measured in cost per kilograms, where all costs are in THB.

2.3 Data analysis

Statistical analysis was conducted using IBM SPSS Statistics (version 26.0; IBM Corp.; Armonk, NY, USA). Group differences were assessed with one-way ANOVA and Duncan's multiple range test at the 95% confidence level. Data were presented as mean ± SD values, and key measures (average, percentage, and ratios) were summarized in tables to evaluate economic characteristics, while profitability was assessed using a quantitative method.

3. Results and Discussion

3.1 Stocking density on growth and survival

The initial size of blue swimming crab *Portunus pelagicus* (BSC) released into ponds was similar across all density groups (body weight ranged between 0.08±0.02 and 0.10±0.03 g), as shown in Table 1. It was apparent that stocking densities affected the weight gain of BSC reared; density-dependent growth was evident, with low-density (1 crab/m^2) (85.47±10.21 g BW) and medium-density (3 crabs/m^2) (77.37±6.22 g BW) groups being the largest (p<0.05) followed by high-density group (5 crabs/m^2) (55.94±6.42 g BW). Likewise, ADG and SGR decreased with high-density group (p<0.05). The survival rate of low-density group (45.50±5.91%) was significantly higher (p<0.05) than that of the medium-density group (18.51±1.29%) meanwhile the lowest survival (p<0.05) was noted in the high-density group (10.17±1.21%) (Table 1).

3.2 Stocking density on bioeconomic performance

The yield and bioeconomic data of BSC harvested after 90 days of rearing showed that an increase in FCR was observed in the high-density group. The most favorable FCR was recorded in the low-density (1.48±0.24) and medium-density (2.24±0.14) groups, while the highest FCR (5.44±1.43) (p<0.05) was observed in the high-density group. As expected, the high-density group yielded the lowest yield. However, the yields of the low- and medium-density groups were similar and higher than those of the high-density group (Table 1).

The mean water conditions in the rearing ponds of BSC showed no significant differences among treatments (p>0.05). Water quality parameters, including salinity (31.25±1.15 – 32.82±0.75 ppt), temperature (29.18±0.94 – 30.15±0.73°C), dissolved oxygen (4.35±0.46–5.01±0.63 mg/L), pH (7.89±0.16 – 8.12±0.22), total ammonia (0.21±0.16 – 0.32±0.11 mg-N/L), nitrite (0.00±0.01 – 0.01±0.01 mg-N/L), and alkalinity (117.98±12.42 – 124.56±16.80 mg/L as $CaCO_3$), remained within suitable ranges and did not impact BSC rearing (Oniam and Arkronrat, 2022; Phinrub *et al*., 2023; Efrizal *et al*., 2024). Thus, the differences in BSC productivity in grow-out ponds were attributed to stocking density rather than water quality.

For profitability, the expenses and profits related to rearing BSC in this study are detailed in Table 2. The production costs, especially for variable costs, such as seed and feed, tended to increase with higher stocking densities. Based on the results, rearing BSC at high-density had the highest total cost (THB 95,897) compared to the medium-density and low-density groups. The highest average total revenue per pond (per crop) was also achieved with the medium-density group (THB 17,152), suggesting that an optimum density might lead to increased revenue. However, for BSC farming at these three densities, the returns received were still not worth the investment which yielded a negative net return of -34.55 to -52.81 THB/m^2 of pond (Table 2). Farming at group incurred the highest capital cost per production unit, followed by medium density, while low-density group experienced the least losses.

In terms of break-even points, the BSC farming operations at low-, medium-, and high-density groups reported values of 0.38, 0.72, and 1.08 kg/m^2, respectively. These figures highlighted a clear need for substantial mass production in order to reach a break-even status. Furthermore, the payback periods for the different farming densities were also notable, with periods of 3.9 years for low-density, 4.2 years for medium-density, and a significantly longer 7.5 years for high density groups (Table 2). The payback periods in aquaculture were highly context-specific (species, system, scale, location, input costs, market prices). There was no single "ideal" payback that applied universally to marine crabs or other aquaculture. In practice, operators aimed for payback ranges of about 2–5 years for intensive systems and 3–7 years for semi-intensive or extensive setups, but these

varied widely (Llorente and Luna, 2016; Farhaduzzaman *et al*., 2020; Arkronrat *et al*., 2024).

The current study showed that, despite efforts to optimize BSC farming at three different densities, the returns ultimately fell short of justifying the investment made. Among the various farming densities, high density proved to incur the highest capital costs per production unit. This was followed closely by medium-density, while low-density operations, although less profitable, experienced the least financial losses. These results underscore the challenges faced in achieving profitability within the BSC farming sector, particularly at higher densities where the financial risks and capital investments were markedly elevated.

Stocking density, the number of aquatic organisms per unit area or volume, played a pivotal role in the success of aquaculture operations (Boyd *et al*., 2020). The optimal stocking density varied among species, with each having a specific range that maximized growth (Farhaduzzaman *et al*., 2020). For crustacean, such as crabs, shrimps, and lobsters, at higher densities, competition for food and space hindered individual growth rates and led to size disparities within population. While the initial production rate may have increased at high density, the long-term effects often included reduced growth and higher mortality (Madzivanzira *et al*., 2020; Liew *et al*., 2024). From an economic standpoint, higher densities reduced per-unit production costs due to increased output. However, this had to be weighed against potential costs related to culture management and the need for improved water quality (Farhaduzzaman *et al*., 2020; Arkronrat *et al*., 2024). The market demand for specific sizes and qualities of crab also significantly influenced economic viability; overcrowding led to smaller, less marketable crabs (Liew *et al*., 2024). High stocking densities elevated stress levels among aquatic animals, making them more vulnerable to diseases. Stress negatively impacted feed conversion ratios and resulted in increased mortality rates (Boyd *et al*., 2020).

In the present study, it was observed that varying the density of the BSC during grow-out pond cultivation affected bioeconomic outcomes. As the stocking density increased, growth performance parameters (AG, ADG and SGR) declined, and the FCR worsened. The effects of stocking density on crab culture were multifaceted and varied with several factors: species, life stage, culture system and environmental conditions (Mugwanya *et al*., 2022; Gençer, 2023; Zhang *et al*., 2023). In crustacean cultivation, at lower stocking densities, they demonstrated diminished cannibalism, decreased resource competition (such as food and shelter), and reduced stress levels, thereby potentially enhancing their growth and survival rates (Farhaduzzaman *et al*., 2020; Madzivanzira *et al*., 2020; Manh *et al*., 2023).

Table 1 Bioeconomic data after 90 days of rearing in terms of growth, survival, feed conversion ratio, and yield of blue swimming crab (*Portunus pelagicus*) cultivated in 1,600 m^2 earthen pond at different stocking densities (n = 3).

Parameters	Density		
	Low (1 crab/m^2)	Medium (3 crabs/m^2)	High (5 crabs/m^2)
Initial body weight (g)	0.09±0.03^a	0.10±0.03^a	0.08±0.02^a
Weight gain (g)	85.47±10.21^a	77.37±6.22^a	55.94±6.42^b
Average daily growth (g/day)	0.95±0.11^a	0.86±0.07^a	0.62±0.07^b
Specific growth rate (%/day)	7.61±0.13^a	7.50±0.09^a	7.14±0.12^b
Survival rate (%)	45.50±5.91^a	18.51±1.29^b	10.17±1.21^c
Feed conversion ratio	1.48±0.24^a	2.24±0.14^a	5.44±1.43^b
Yield (kg/pond)	62.14±10.26^a	68.63±5.44^a	45.61±7.90^b

Means in each row followed by different letters indicate a significant difference (p<0.05).

Table 2 Fixed, variable, average production, and marketing costs and total costs and benefits for blue swimming crab (*Portunus pelagicus*) cultivated in 1,600 m^2 earthen pond at different stocking densities after 90 days (n = 3).

Parameters	Density		
	Low (1 crab/m^2)	Medium (3 crabs/m^2)	High (5 crabs/m^2)
Fixed cost			
Land cost (THB)[(1)]	2,500	2,500	2,500
Labor cost (THB)	27,000	27,000	27,000
Tools (THB)	30,000	30,000	30,000
Equipment depreciation (THB)[(2)]	2,466	2,466	2,466
Total (THB)	61,966	61,966	61,966

Table 2 (Continuous)

Parameters	Density		
	Low (1 crab/m^2)	Medium (3 crabs/m^2)	High (5 crabs/m^2)
Variable cost			
Seed cost (THB)	4,800	14,400	24,000
Feed cost (THB)	3,545	6,042	9,431
Other miscellaneous costs (THB)	200	200	200
Total (THB)	8,545	20,642	33,631
Production cost (THB)	70,511	82,608	95,597
Marketing cost (THB)(3)	300	300	300
Total cost (THB)	70,811	82,908	95,897
Initial investment (THB/year)	177,969	214,159	253,126
Benefit			
Total quantity of crab (kg/pond)	62.14	68.63	45.61
Price per unit of crab (THB/kg)	250	250	250
Total revenue (THB/pond/crop)	15,536	17,152	11,408
Net return (THB/m^2 of pond)	-34.55	-41.09	-52.81
Break-even point (kg/ m^2 of pond)	0.38	0.72	1.08
Pay back period (year)	3.9	4.2	7.5

Note: (1) Typically, farmers pay rental fees for pond areas, which vary based on factors such as area size, location, and government regulations. On average, fees are in the range of THB 5,000–20,000/rai/year, with an average of approximately THB 10,000/year. (2) Annual depreciation calculated using (cost of asset - salvage value) / useful life, with a service life of 3 years. (3) MC derived from shipping and packaging expenses associated with transporting crab per pond.

In the present study, it was observed that varying the density of the BSC during grow-out pond cultivation affected bioeconomic outcomes. As the stocking density increased, growth performance parameters (AG, ADG and SGR) declined, and the FCR worsened. The effects of stocking density on crab culture were multifaceted and varied with several factors: species, life stage, culture system and environmental conditions (Mugwanya *et al*., 2022; Gençer, 2023; Zhang *et al*., 2023). In crustacean cultivation, at lower stocking densities, they demonstrated diminished cannibalism, decreased resource competition (such as food and shelter), and reduced stress levels, thereby potentially enhancing their growth and survival rates (Farhaduzzaman *et al*., 2020; Madzivanzira *et al*., 2020; Manh *et al*., 2023).

Several studies examined the relationship between stocking density and various performance indicators in crab cultivation. For instance, Gençer (2023) reported that a stocking density of 5 crabs per 0.7 L tank resulted in the highest growth and survival rates for the blue crab (*Callinectes sapidus*) compared to densities of 10 and 15 crabs per 0.7 L tank. Similarly, research on the Chinese mitten crab (*Eriocheir sinensis*) by Zhang *et al*. (2023), the mud crab (*Scylla* spp.) by Liew *et al*. (2024), and other crustaceans (Bardera *et al*., 2021; Arkronrat *et al*., 2024) indicated that optimum stocking densities contributed to better overall welfare and enhanced physiological functioning, including reduced stress hormone levels and improved immune function.

These studies suggested that the optimal stocking density for crab cultivation varied significantly depending on the specific species and their respective life stages. Additionally, it was noted that other critical factors, such as the availability of shelter and the implemented feeding strategies, also needed to be taken into account in order to achieve the best results in crab farming practices.

4. Conclusion

Increasing the stocking density of blue swimming crab (*Portunus pelagicus*) in the pond reduced their survival and growth rates while increasing the FCR. Although the three stocking densities (1, 3, and 5 crabs/m²) in this study did not yield a return on investment, the most cost-effective density was the one that provided the highest biomass per unit area, the lowest break-even point, and the highest net income. It was clear that a stocking density of 1-3 crabs/m^2 was the most profitable of the densities tested. The interaction between stocking density and bioeconomic efficiency proved complex, requiring careful balance to ensure the growth and economic success of this crab. Emphasizing sustainable and cost-effective crab farming practices remained essential and warranted further research.

5. Acknowledgment

This study was part of the Project for the Potential Development of Blue Swimming Crab (*Portunus pelagicus* Linnaeus, 1758) Broodstock and Seed Production for Conservation and Crab Culture Implementation, funded by a grant from the Kasetsart

University Research and Development Institute (KURDI), Bangkok, Thailand under research grant No. P-2.3(D)7.11.61.

6. References

American Public Health Association, American Water Works Association and Water Environment Federation (APHA, AWWA and WEF). 2023. **Standard methods for the examination of water and wastewater** (24th ed). American Public Health Association, Washington, DC.

Arkronrat, W., Konsantad, R., Leearam, C., Deemark, P., Srisupawadee, C. and Oniam, V. 2024. Impacts of stocking densities on bioeconomics and profitability of mud spiny lobster (*Panulirus polyphagus* Herbst, 1793) cultivation in sea cages. **Agriculture and Natural Resources** 58(6): 707-716.

Bardera, G., Owen, M.A.G., Facanha, F.N., Alcaraz-Calero, J.M., Alexander, M.E. and Sloman. K.A. 2021. The influence of density and dominance on Pacific white shrimp (*Litopenaeus vannamei*) feeding behavior. **Aquaculture** 531: 735949.

Boyd, C.E., D'Abramo, L.R., Glencross, B.D., Huyben, D.C., Juarez, L.M., Lockwood, G.S., McNevin, A.A., Tacon, A.G.J., Teletchea, F., Tomasso, J.R., Tucker, C.S. and Valenti, W.C. 2020. Achieving sustainable aquaculture: Historical and current perspectives and future needs and challenges. **Journal of the World Aquaculture Society** 51: 578-633.

Boyd, C.E., McNevin, A.A. and Davis, R.P. 2022. The contribution of fisheries and aquaculture to the global protein supply. **Food Security** 14: 805-827.

Cai, J. and Galli, G. 2021. **Top 10 species groups in global aquaculture 2019.** FAO, Rome.

Efrizal, Rusnam, Nurmiati, Munzir, A. and Lubis, A.S. 2024. Enhancing the growth and survival rate of broodstock female *Portunus pelagicus* with formulated feed enriched with amaranth (*Amaranthus hybridus*) extract and vitamin E. **AACL Bioflux** 17(4): 1697-1709.

Farhaduzzaman, A.M., Hanif, M.A., Khan, M.S., Osman, M.H., Hasan, M.N., Shovon, Rahman, M.K. and Ahmed, S.B. 2020. Perfect stocking density ensures best production and economic returns in floating cage aquaculture system. **Journal of Aquaculture Research & Development** 11: 607.

Food and Agriculture Organization of the United Nations (FAO). 2022. **The state of world fisheries and aquaculture 2022.** FAO, Rome.

Gençer, Ö. 2023. The effects of using different stocking volumes on the development of broodstocks of the blue crab, *Callinectes sapidus* Rathbun, 1896 (*Brachyura, Portunidae*). **Crustaceana** 96(11-12): 1173-1181.

Konsantad, R., Oniam, V., Arkronrat, W. and Leearam, C. 2024. Effect of feeding frequency on larval stage index and survival rate of blue swimming crab (*Portunus pelagicus*) larvae from zoea I to IV stages. **Khon Kaen Agriculture Journal** 52(suppl.1): 82-87. (in Thai)

Leearam, C., Konsantad, R., Arkronrat, W. and Oniam, V. 2024. Effects of artificial water color (colors and concentration levels) to reduce the mortality rate due to cannibalism of blue swimming crab (*Portunus pelagicus*) larvae in First crab stage. **Agriculture & Technology RMUTI Journal** 5(2): 40-50. (in Thai)

Liew, K.S., Yong, F.K.B. and Lim, L.S. 2024. An overview of the major constraints in *Scylla* mud crabs grow-out culture and its mitigation methods. **Aquaculture Studies** 24(1): AQUAST993.

Llorente, I. and Luna, L. 2016. Bioeconomic modelling in aquaculture: An overview of the literature. **Aquaculture International** 24: 931-948.

Madzivanzira, T.C., South, J., Wood, L.E., Nunes, A.L. and Weyl, O.L.F. 2020. A review of freshwater crayfish introductions in Africa. **Reviews in Fisheries Science & Aquaculture** 29(5): 1-24.

Manh, N.V., Thang, N.Q., Uyen, D.M. and Thai, T.Q. 2023. Effects of stocking density and diets on survival and growth of lavi-cultured slipper lobster (*Thenus orientalis* Lund, 1793). Vietnam. **Journal of Marine Science and Technology** 23: 81-92.

Mugwanya, M., Dawood, M.A.O., Kimera, F. and Sewilam, H.A.N. 2022. A review on recirculating aquaculture system: influence of stocking density on fish and crustacean behavior, growth performance, and immunity. **Annals of Animal Science** 22(3): 873-884.

Oniam, V. and Arkronrat, W. 2022. Growth rate and sexual performance of domesticated blue swimming crab, *Portunus pelagicus* (Linnaeus, 1758) in earthen ponds. **Trend in Sciences** 19(20): 6235.

Oniam, V., Arkronrat, W. and Wechakama, T. 2012. Feed intake and survival rate assessment of blue swimming crab (*Portunus pelagicus*) raised in earthen pond. **Journal of Agriculture** 28: 83-91. (in Thai)

Phinrub, W., Khamcharoen, M., Songrak, A. and Wongsnansilp, T. 2023. Effect of foods on growth and survival rate of Blue swimming crab (*Portunus pelagicus* Linnaeus, 1758) in the vertical stacked boxes. **Khon Kaen Agriculture Journal** 51(3): 512-523. (in Thai)

Rabassó, M. and Hernández, J.M. 2015. Bioeconomic analysis of the environmental impact of a marine fish farm. **Journal of Environmental Management** 158: 24-35.

Yulianto, H., Ihsan, Y., Sumiarsa, D., Ansari, A. and Hendarmawan, H. 2024. Assessing the sustainability of the blue swimming crab (*Portunus pelagicus*) on the Eastern Coast of Lampung: a holistic approach to conservation and resource stewardship. **Frontiers in Marine Science** 11: 1304838.

Zhang, G., Jiang, X., Zhou, W., Chen, W., Levy, T. and Wu, X. 2023. Stocking density affects culture performance and economic profit of adult all-female Chinese mitten crabs (*Eriocheir sinensis*) reared in earthen ponds. **Aquaculture** 581: 740352.

Recent Science and Technology

Journal homepage: https:// www.tci-thaijo.org/index.php/rmutsvrj/index

ISSN: 3057-0786 (Online)

aaAResearch Article

Encapsulated Freeze-Dried Lactic Acid Bacteria Enhance Immune Response and Support Growth of *Penaeus monodon* (Fabricius, 1798) in Hatchery and Earthen Pond Culture

Narongchai Chupoon *, Nomchit Kaewthai Andre, Sirinat Srionnual and Thanikan Thorasin

Department of Food Innovation and Management, Faculty of Agro-Industry, Rajamangala University of Technology Srivijaya, Thung Yai, Nakhon Si Thammarat 80240, Thailand.

Article history:

Received: 2024-05-07
Revised: 2025-11-05
Accepted: 2025-11-27

Keywords:

Lactic acid bacteria (LAB);
Encapsulation;
Immune response;
Vibrio parahaemolyticus;
Shrimp aquaculture;
Microbiota profiling

ABSTRACT

This study investigated the effects of dietary supplementation with freeze-dried encapsulated *Lactobacillus* spp. (FEL) on the immune response, intestinal microbiota, and growth performance of black tiger shrimp (*Penaeus monodon*) under both hatchery and pond conditions. FEL, prepared with four lactic acid bacteria (LAB) strains and encapsulated in sodium alginate, was incorporated into diets at concentrations of 0%–1.0% (w/w). In hatchery trials, juvenile shrimp fed FEL-supplemented diets (0.2–1.0%) exhibited significantly enhanced total hemocyte count, phenoloxidase activity, and clearance of *Vibrio parahaemolyticus*, achieving 100% survival compared with 82.22 ± 8.02% in controls ($p < 0.001$). Shrimp fed 0.2% FEL also showed a significantly higher specific growth rate (1.94% day^{-1}) compared with controls (1.33% day^{-1}, $p < 0.05$). Moreover, FEL supplementation promoted LAB colonization and reduced intestinal *Vibrio* densities. In pond trials, shrimp were cultured for 100 days, with growth monitoring conducted from day 60 to day 100. Microbiota analysis by 16S rRNA gene sequencing revealed an increased abundance of beneficial Firmicutes and *Phaeobacter inhibens* and a decreased abundance of Proteobacteria and *Photobacterium damselae* in FEL-fed shrimp. Shrimp receiving 0.2% FEL supplementation also exhibited consistently greater body weight and length than the control group, with significant differences observed at later sampling points ($p < 0.05$). These findings demonstrate that FEL supplementation can enhance innate immunity, modulate the gut microbiota, and promote shrimp growth, highlighting its potential as a sustainable probiotic feed additive for shrimp aquaculture.

1. Introduction

Thailand, once a leading global exporter of black tiger shrimp (*P. monodon*), has experienced a marked decline in production due to recurring disease outbreaks, particularly white spot syndrome virus (WSSV) and early mortality syndrome (EMS) (Han *et al*., 2022; Leano and Mohan, 2020). These challenges highlight the urgent need for sustainable disease management strategies in shrimp aquaculture. Among various alternatives to antibiotics, probiotics have gained increasing attention due to their ability to enhance growth, improve immune responses, and reduce disease susceptibility (Hai, 2015; Hosein *et al*., 2021; Kesarcodi-Watson *et al*., 2012). Recent research indicates that dietary probiotic supplementation modulates the shrimp gut microbiota, improving nutrient uptake and stimulating host immune functions (Chin *et al*., 2024a; Lulijwa *et al*., 2020).

Within the broad range of probiotic candidates, LAB are the most widely studied due to their antimicrobial properties and immunostimulatory effects, including the suppression of pathogenic *Vibrio* spp. (Zhou *et al*., 2023; Huisakul *et al*., 2007). However, the practical application of LAB faces challenges, particularly maintaining viability during feed processing and gastrointestinal passage.

To address this, microencapsulation using biopolymers such as sodium alginate has emerged as a promising approach,

* **Corresponding author.**

E-mail address: *Narongchai.c@rmutsv.ac.th*

Cite this article as:

Chupoon, N., Andre, N.K., Srionnual, S. and Thorasin, T. 2026. Encapsulated Freeze-Dried Lactic Acid Bacteria Enhance Immune Response and Support Growth of *Penaeus monodon* (Fabricius, 1798) in Hatchery and Earthen Pond Culture. **Recent Science and Technology** 18(1): 267534.

https://doi.org/10.65411/rst.2026.267534

improving probiotic stability, targeted release, and colonization in the intestinal tract (Afzaal *et al*., 2020; Anal and Singh, 2021).

Despite these advances, most research on encapsulated probiotics has been confined to controlled laboratory settings. Field trials validating their effects in commercial aquaculture remain scarce, particularly when integrated with advanced microbiome profiling techniques. Addressing this gap is essential for translating laboratory success into practical implementation (Martínez-Porchas *et al*., 2021; Fan *et al*., 2023; Khanjani *et al*., 2024; Vieira *et al*., 2021).

Therefore, this study tested the hypothesis that dietary supplementation with FEL enhances the immune response, survival, growth, and gut microbiota stability of *P. monodon*. To evaluate this, experiments were conducted under both laboratory conditions, including pathogen challenge tests, and field conditions in earthen ponds. Practical application was assessed at a 0.2% FEL inclusion level, and gut microbiota dynamics were analyzed using 16S rRNA gene sequencing.

2. Materials and Methods

2.1 Experimental design overview

This study was conducted in two phases. Phase 1, conducted as a hatchery trial, employed a completely randomized design (CRD) with six dietary treatments of FEL ranging from 0 to 1.0% (w/w). Growth performance, survival during the feeding period, immune responses, and the intestinal LAB and *Vibrio* spp. were evaluated, along with resistance to *V. parahaemolyticus* challenge. Phase 2, a pond trial, validated the optimal FEL inclusion level of 0.2% identified in Phase 1. Two earthen ponds were used, each subdivided into cages, and shrimp were reared under farm-like conditions. Growth performance and intestinal microbiota composition were assessed, with statistical comparisons between the control and 0.2% FEL groups performed using independent-samples *t*-tests.

2.2 FEL preparation

This study utilized four strains of LAB: *Lactobacillus acidophilus* TISTR 236, *L. plantarum* TISTR 542, *L. casei* TISTR 389, and *L. bulgaricus* TISTR 451, obtained from the Thailand Institute of Scientific and Technological Research (TISTR, Thailand), for cell mass production and encapsulation. Pure freeze-dried cells of LAB activated by inoculating them into de Man, Rogosa and Sharpe (MRS) broth and incubating at 37 °C for 24 h. The fermentation process was conducted in a 5-L bioreactor (Bioflo III System, New Brunswick Scientific Co. Inc., NJ, USA) containing 3 L of sterilized MRS broth. After cooling, the activated inoculum was added. Each fermentation batch was inoculated with 5% (v/v) LAB culture, previously grown in MRS broth, at an initial concentration of approximately 1×10^5 CFU mL^{-1}.

Fermentation was maintained at 43 ± 2 °C with an agitation rate of 50 rpm. The pH was regulated at 5.0 throughout fermentation using a base pump with 4.0 mol L^{-1} NaOH. The process was carried out under anaerobic conditions for 48 h, after which the cell suspension was harvested for encapsulation. The harvested LAB suspension was co-encapsulated using sodium alginate microgels, following the method described by Afzaal *et al*. (2020). Briefly, the LAB culture suspension was mixed with a sodium alginate solution for 5 min to achieve a final concentration of 1×10^9CFU mL^{-1}. The mixture was then injected into a 0.1 M calcium chloride hardening solution to form beads. The beads were collected by filtration, washed with sterile deionized water, and stored in physiological saline solution at 4 °C until freeze-drying.

The diameter of freshly prepared alginate gel beads was 2.41 ± 0.07 mm (n = 10; range: 2.3–2.5 mm). Size distribution analysis revealed that 20% of the beads were between 2.3–2.4 mm, 60% between 2.4–2.5 mm, and 20% between 2.5–2.6 mm, indicating a narrow and uniform distribution. Finally, the FEL powder was incorporated into the experimental diets, as described in Section 2.3.

2.3 Shrimp husbandry and feeding protocol

Two independent cohorts of *P. monodon* were used in this study: one cohort for the hatchery feeding and challenge trial (Phase 1) and a second cohort for the earthen-pond validation trial (Phase 2). *P. monodon* post-larvae (PL-5) were purchased from a certified pathogen-free hatchery in Ranod District, Songkhla Province, Thailand. Upon arrival, the post-larvae were acclimatized and reared in nursery tanks at the Aquaculture Research Facility, Faculty of Science and Fisheries Technology, Trang Campus, Rajamangala University of Technology Srivijaya (RUTS), Thailand. The shrimp were maintained under standard aquaculture conditions with continuous aeration and daily water-quality monitoring to ensure optimal rearing. During the nursery phase (PL-5 to PL-30), shrimp were fed a commercial starter diet formulated for early juvenile shrimp (Phoca Starter P5–P30; Phoca Feed Co., Ltd., Thailand) containing approximately 40–42% crude protein.

After the nursery stage, shrimp were transferred to 1,000-L fiberglass tanks equipped with a recirculating seawater system and continuous aeration (150 shrimp $tank^{-1}$). Animals were fed a basal Phoca Feed diet for 20 days, after which six experimental diets containing FEL at 0, 0.2, 0.4, 0.6, 0.8, or 1.0% (w/w) were administered following Zhang *et al*. (2018) and Argue *et al*. (2002). For FEL diet preparation, soybean oil (2% of feed weight) was used as a binder; FEL powder was top-coated onto finished pellets, gently tumbled to ensure uniform adhesion, and air-dried at $\leq$ 35 °C to restore surface dryness. Diets were broadcast at 5–6% of body weight per day in five equal feedings (06:00, 10:00, 14:00, 18:00, and 22:00 h), with three replicate tanks per treatment.

Proximate composition analyses were conducted in triplicate following AOAC (2016) standard methods for crude protein,

lipid, fiber, moisture, and ash determinations. Nitrogen-free extract (NFE) was calculated by difference.

2.4 Challenge trials

At the end of the 50-day feeding period, juvenile *P. monodon* (mean weight 5.0 ± 0.20 g) from each dietary treatment were transferred to the Biotechnology Laboratory, Faculty of Agro-Industry, RUTS, Nakhon Si Thammarat Campus, Thailand, for the challenge trial. Upon arrival, shrimp were distributed into 100-L aquaria (15 shrimp per aquarium; three replicate aquaria per treatment) and acclimated for 10 days under standard laboratory conditions.

After acclimation, shrimp were challenged with *V. parahaemolyticus.* The bacterial strain was cultured in tryptic soy broth (TSB) supplemented with 1.5% NaCl at 30 °C for 18 h. The bacterial suspension was harvested by centrifugation, washed twice with sterile saline, and resuspended in 1.5% saline solution. The concentration was adjusted to 2×10^7 CFU mL^{-1} using a spectrophotometer and confirmed by plate counts on thiosulfate citrate bile salts sucrose (TCBS) agar. Each shrimp was injected intramuscularly in the third abdominal segment with 0.1 mL of the bacterial suspension, whereas control shrimp were injected with sterile saline. Following injection, shrimp were maintained under the same conditions for 9 days, and mortality was recorded twice daily.

Colony counts were expressed as $\log_{10}$ colony-forming units (CFU g^{-1}) of intestinal tissue. Homogenates were kept at 4 °C and processed within 24 h to maintain microbial viability. All procedures were performed aseptically to preserve sample integrity.

2.5 Sampling and analyses

Samples of hemolymph and intestinal tissue were collected in triplicate from challenged shrimp on day 9 at the time points described in Section 2.4. These samples were subjected to immunological, microbiological, and growth performance analyses. Total hemocyte count (THC), clearance ability (CA), and phenoloxidase (PO) activity were determined to assess the shrimp's immune response to *V. parahaemolyticus* challenge, while intestinal microbiological parameters and growth performance were also evaluated.

2.5.1 Immune Response

Hemolymph samples were randomly collected on day 9 of the challenge for immune analyses. THC, CA, and PO activity were measured as described below.

THC was measured using a hemocytometer under a light microscope. Hemolymph was diluted 1:1 with an anticoagulant solution, and hemocyte counts were performed in triplicate to ensure accuracy. The mean cell count for each sample was calculated and expressed as cells mL^{-1} of hemolymph.

The CA of *V. parahaemolyticus* in the hemolymph of *P. monodon* was evaluated following a modified method of van de Braak *et al*. (2002). Shrimp were injected intramuscularly in the third abdominal segment with 100 µL of a *V. parahaemolyticus* suspension ($\approx 1 \times 10^5$ CFU mL^{-1}) prepared in sterile 0.9% (w/v) saline. Hemolymph was collected from the ventral sinus at 0 and 3 h post-injection using a sterile syringe containing anticoagulant solution (10 mM sodium citrate, 450 mM NaCl, pH 7.3). Serial dilutions were plated on TCBS and incubated at 37 °C for 24 h. Bacterial densities were expressed as $\log_{10}$ CFU mL^{-1} of hemolymph. CA was calculated according to Equation (1):

$$\text{CA (\%)} = \frac{(N_0 - N_t)}{N_0} \times 100 \quad (1)$$

where N_0 and N_t are bacterial counts (CFU mL^{-1}) in hemolymph at 0 h and 3 h post-injection, respectively.

PO activity was assayed using L-DOPA as substrate. Hemolymph was centrifuged at 3,000 × g for 10 min to obtain cell-free plasma, which was incubated with 10 mM L-DOPA at 28 °C. Optical density at 490 nm was recorded every minute for 10 min, and PO activity expressed as the rate of absorbance change (OD_{490} min^{-1}).

2.5.2 Microbiological analysis and enumeration of LAB and Vibrio spp.

Intestinal samples were collected from juvenile *P. monodon* (≈69 days old; mean weight 6.26 ± 0.21 g) at the end of the *V. parahaemolyticus* challenge trial (Day 9) to quantify LAB and *Vibrio* spp. Shrimp were euthanized in ice-cold seawater, and intestines were aseptically dissected using sterile scissors and forceps.

For each dietary treatment (FEL 0, 0.2, 0.4, 0.6, 0.8, and 1.0% w/w), three biological replicates were prepared by pooling intestines from 4–6 shrimp to obtain approximately 0.20 g wet tissue per replicate. Pooled tissues were placed in sterile 2 mL tubes containing 1.8 mL of sterile 0.85% NaCl to yield a 1:10 (w/v) homogenate and homogenized with a stomacher. Serial ten-fold dilutions were plated on TCBS agar for enumeration of *Vibrio* spp. and on MRS agar for LAB. TCBS plates were incubated at 37 °C for 24 h, and MRS plates at 37 °C for 24–48 h under anaerobic conditions.

Colony counts were expressed as $\log_{10}$ colony-forming units (CFU g^{-1}) of intestinal tissue. Homogenates were kept at 4 °C and processed within 24 h to maintain microbial viability. All procedures were performed aseptically to preserve sample integrity.

2.5.2.1 Intestinal microbiota profiling

For pond-reared shrimp, the intestinal microbial community was profiled using 16S rRNA gene amplicon sequencing. Shrimp were reared in three replicate cages per dietary treatment (≈200 individuals per cage). For each

treatment, intestines from five shrimp per cage were pooled to obtain approximately 100 mg of wet tissue, yielding three biological replicates per treatment (control and 0.2% FEL). All dissections were performed aseptically on ice. Composite intestinal samples were immediately placed in 2 mL screw-cap tubes containing zirconia/silica beads, snap-frozen in liquid nitrogen, and stored at -80 °C until DNA extraction.

DNA was extracted using the QIAamp Fast DNA Stool Mini Kit (Qiagen, Germany) and quantified with a NanoDrop spectrophotometer (NanoDrop Technologies, USA). The V3–V4 hypervariable regions of the 16S rRNA gene were amplified by polymerase chain reaction (PCR) using Illumina overhang adapter primers and Phusion High-Fidelity DNA polymerase (Bio-Rad, UK) under the following thermal cycling conditions: initial denaturation at 95 °C for 3 min; 25 cycles of denaturation at 95 °C for 30 s, annealing at 55 °C for 30 s, and extension at 72 °C for 30 s; followed by a final extension at 72 °C for 5 min.

Amplicons were purified with AMPure XP magnetic beads (Beckman Coulter, USA), indexed using the Nextera XT Index Kit v2 (Illumina, USA), and pooled at equimolar concentrations. The pooled library was spiked with 5% PhiX control and sequenced on an Illumina MiSeq platform (2 × 300 bp paired-end reads) using the MiSeq Reagent Kit v3 (600-cycle). Raw sequence data were processed using MiSeq Reporter Software (Illumina, USA).

2.5.3 Growth performance evaluation

Following a 10-day acclimation period and a 50-day feeding phase, shrimp were subjected to a 9-day *Vibrio* challenge test. After the challenge, shrimp were weighed to determine specific growth rate (SGR) and survival rate. The calculations were performed using the following formulas, as described by Soundarapandian and Velmurugan (2008).

The SGR was calculated as:

$$\text{SGR (\% day}^{-1}) = \frac{(ln\, W_t - ln\, W_0)}{t} \times 100 \qquad (2)$$

where W_t is the final mean weight (g), W_0 is the initial mean weight (g), and t is the rearing period (days).

2.6 Field trial methods

The pond trial (Phase 2) was conducted at the shrimp-farming facility of the Faculty of Science and Fisheries Technology, RUTS, Trang Province, Thailand (Mai Fad Subdistrict, Sikao District; 7.5186 °N, 99.2682 °E). Two earthen ponds (1,600 m²; 1.8 m depth) were used: one served as the control (standard diet) and the other received the diet supplemented with 0.2% FEL. Each pond contained three replicate net cages (4 × 4 m; ≈ 6–7 shrimp m^{-3}) and was continuously aerated by four 0.75-kW paddlewheel aerators paddlewheel to maintain dissolved oxygen above 5 mg L^{-1}.

Shrimp stocking and transfer procedures followed the protocol described in Section 2.3, including the nursery phase and acclimation. Fifty-day-old shrimp (initial mean weight = 4.7 ± 0.2 g, mean ± SD) were acclimated in the ponds for 10 days prior to the start of the 40-day feeding period (days 60–100 of the culture cycle). At day 60, the control pond received the standard diet, whereas the treatment pond received the diet supplemented with 0.2% FEL.

Growth performance was monitored on days 60, 70, 80, 90, and 100. At each sampling point, ten shrimp were randomly collected from each cage to determine body weight (± 0.5 g; Sartorius Practum 2102-1S, Germany) and total length (± 0.1 cm) using a digital caliper. SGR was calculated as described in Section 2.5.3. At the end of the 100-day culture period, intestinal samples were collected for microbiota profiling as outlined in Section 2.5.2.1.

2.6.1 Water Quality Monitoring

Water quality was monitored daily throughout the trial. Salinity was maintained at 15–20 ppt by regular exchange with brackish water and measured with a Salinity Refractometer (MASTER-S/MillM, Atago, Japan). Dissolved oxygen (DO) and pH were measured using a multi-parameter water-quality meter (HI9829; pH/ISE/EC/DO/Turbidity, Hanna Instruments, USA), with DO kept above 5 mg L^{-1} and pH maintained between 7.5 and 8.5. Nitrite–nitrogen was kept below 0.1 mg L^{-1} and analyzed using a Hach NI-12 Nitrate–Nitrite Water Test Kit. Temperature was recorded with a digital thermometer.

All experimental procedures involving shrimp were conducted in accordance with the institutional guidelines for the care and use of aquatic animals of RUTS.

2.7 Statistical Analysis

The hatchery trial (Phase 1) followed a CRD with six dietary treatments (0–1.0% FEL, w/w) and three replicates each. Data were analyzed by one-way ANOVA, and means were compared using Tukey's HSD ($p < 0.05$). For the pond trial (Phase 2), growth and microbiota data were compared between the control and 0.2% FEL groups using an independent-samples *t*-test ($p < 0.05$).

3. Results and Discussion

3.1 Proximate Composition of Experimental Diets

The proximate composition of shrimp diets supplemented with different levels FEL is summarized in Table 1. Crude protein, lipid, fiber, ash, NFE, and moisture contents were comparable among all treatments, with crude protein ranging from 45.2 to 45.7%, lipid from 7.1 to 7.4%, and moisture from 11.2 to 11.9%. Negligible variations indicate that FEL inclusion up to 1.0% (w/w) did not affect the basic nutritional composition of the diets.

3.2 Immune Enhancement in Shrimp Challenged with *V. parahaemolyticus*

As shown in Table 2, shrimp fed 0.2–1.0% (w/w) FEL exhibited significantly higher THC, CA, and PO activities than the control group. THC peaked in the 1.0% FEL treatment at 10.10 ± 0.25 × 10^6 cells mL^{-1}, compared with 4.97 ± 0.09 × 10^6 cells mL^{-1} in controls ($p < 0.001$, $n = 3$). CA increased dose-dependently, reaching 22.53 ± 0.66% at 1.0% FEL ($p < 0.001$, $n = 3$), indicating a strong enhancement in cellular immune response. PO activity rose to 0.43 ± 0.009 OD min^{-1} at 0.8 % FEL ($p < 0.01$, $n = 3$) and remained elevated at 0.42 ± 0.018 OD min^{-1} in the 1.0% group ($p < 0.05$, $n = 3$). Dose-dependent increases in THC, CA, and PO indicate robust activation of cellular and enzymatic immune defenses, with PO activity plateauing beyond 0.8%, suggesting this level as the optimal immunostimulatory dose. These results are consistent with previous studies demonstrating that probiotic supplementation enhances immune response and resistance to *Vibrio* infection in *P. monodon* (Zokaeifar *et al*., 2012).

The observed responses agree with previous reports that LAB enhance shrimp immunity by stimulating hemocyte production and the prophenoloxidase cascade (Nguyen *et al*., 2025b; Kongnum and Hongpattarakere, 2012a; Feng *et al*., 2020). Similar effects were observed by Zheng *et al*. (2017) in Pacific white shrimp (*Litopenaeus vannamei*), where dietary probiotics significantly reduced intestinal *Vibrio* counts, supporting the application of FEL as a functional feed additive for disease-resilient aquaculture.

3.3 Effect of FEL Supplementation on Intestinal LAB and *Vibrio* spp.

FEL supplementation significantly influenced the intestinal microbiota of *P. monodon* during the *V. parahaemolyticus* challenge. As illustrated in Figure 1, shrimp fed FEL diets at 0.2–1.0% (w/w) exhibited a clear, dose-dependent decline in intestinal Vibrio density, with mean counts decreasing from 5.2 ± 0.4 log CFU g^{-1} in the control group to 1.1 ± 0.2 log CFU g^{-1} in shrimp receiving 0.8% FEL ($p < 0.001$). Conversely, the results presented in Figure 2 show that total LAB populations increased significantly across all FEL treatments ($p < 0.001$), reaching the highest density in the 1.0% group. These quantitative shifts confirm successful colonization of beneficial LAB while suppressing opportunistic *Vibrio* spp., demonstrating that FEL supports a more stable and health-promoting intestinal community.

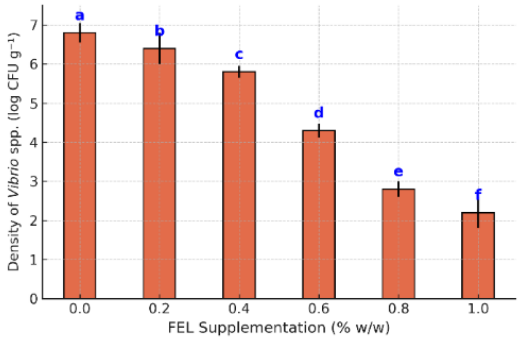

Figure 1 Density of intestinal *Vibrio* spp. in *P. monodon* fed FEL-supplemented diets after *V. parahaemolyticus* challenge. Note. Different letters indicate significant differences ($p < 0.001$)

Table 1 Proximate composition of shrimp diets supplemented with FEL (0–1.0% w/w).

FEL (% w/w)	Crude Protein (%)	Crude Lipid (%)	Crude Fiber (%)	Ash (%)	NFE (%)	Moisture (%)
0.0	45.2 ± 0.27	7.2 ± 0.20	3.8 ± 0.14	9.6 ± 0.15	22.4 ± 0.65	11.8 ± 0.11
0.2	45.2 ± 0.23	7.2 ± 0.17	3.7 ± 0.11	9.3 ± 0.15	22.6 ± 0.43	11.8 ± 0.14
0.4	45.2 ± 0.22	7.1 ± 0.15	3.9 ± 0.14	9.0 ± 0.16	22.7 ± 0.45	11.7 ± 0.14
0.6	45.3 ± 0.26	7.3 ± 0.14	3.4 ± 0.17	9.0 ± 0.18	22.5 ± 0.38	11.9 ± 0.15
0.8	45.5 ± 0.27	7.2 ± 0.13	3.6 ± 0.12	9.4 ± 0.17	22.3 ± 0.41	11.2 ± 0.14
1.0	45.7 ± 0.24	7.4 ± 0.17	3.6 ± 0.12	9.0 ± 0.16	22.1 ± 0.60	11.2 ± 0.13

Note. Values are expressed as mean ± standard deviation ($n = 3$).

Table 2 Immune responses of *P. monodon* fed 0–1.0% FEL diets after 9 days of *V. parahaemolyticus* challenge.

FEL Level (%)	THC (×10^6 cells mL^{-1})	CA (%)	PO activity (OD_{490} min^{-1})
0	4.97 ± 0.09^{d}	2.67 ± 0.55^{d}	0.06^{d}
0.2	7.53 ± 0.32^{c}	4.37 ± 0.84^{cd}	0.26^{c}
0.4	8.80 ± 0.34^{bc}	13.97 ± 0.47^{bc}	0.31^{c}
0.6	10.00 ± 0.50^{ab}	15.30 ± 0.93^{b}	0.37^{b}
0.8	9.73 ± 0.41^{ab}	21.33 ± 0.58^{a}	0.43^{a}
1.0	10.10 ± 0.25^{a}	22.53 ± 0.66^{a}	0.42^{a}

Note. Values are expressed as mean ± SE (n = 3). Different superscript letters within columns indicate significant differences among treatments ($p < 0.05$).

The pronounced reduction in *Vibrio* coupled with enrichment of LAB suggests that encapsulation protected probiotic viability during feed processing and gastrointestinal transit, enabling efficient colonization and competitive exclusion of pathogens. A stable and dominant LAB population enhances nutrient absorption and strengthens host resistance by producing antimicrobial metabolites and modulating intestinal pH. Such mechanisms are critical for maintaining microbial balance and host resilience under disease pressure.

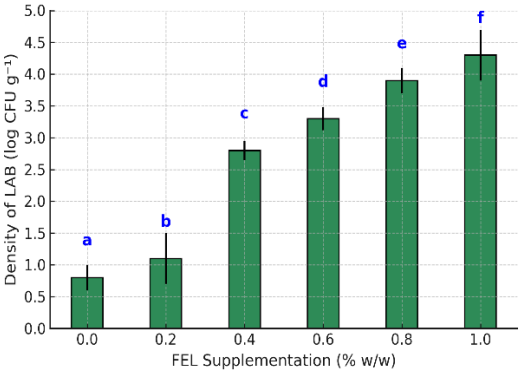

Figure 2 Density of intestinal LAB in *P.monodon* fed FEL-supplemented diets after *V. parahaemolyticus* challenge.
Note. Different letters indicate significant differences ($p < 0.001$).

Our results corroborate previous studies showing that LAB inhibit Gram-negative pathogens through organic acid production and immune stimulation (Ringø *et al*., 2020; Vieira *et al*., 2021). Comparable reductions in *Vibrio* loads and increases in LAB abundance have been reported in shrimp and other aquaculture species supplemented with encapsulated probiotics (Zheng *et al*., 2017; Kim *et al*., 2022), supporting FEL's potential as a functional microbial modulator in intensive shrimp farming.

The stability of LAB populations observed in FEL-treated groups during *V. parahaemolyticus* infection indicates enhanced probiotic colonization and survivability, likely attributed to the encapsulated form of the probiotics. Encapsulation has been reported to protect LAB from harsh gastrointestinal conditions, enabling them to reach the distal gut and establish more effectively (Vieira *et al*., 2021). Such gut microbiota modulation improves intestinal health and may also enhance systemic immunity, including phagocytic activity and disease resistance.

Therefore, FEL supplementation represents a promising strategy for microbiota management in shrimp aquaculture, offering both preventive and stabilizing effects on beneficial intestinal bacteria, while simultaneously suppressing opportunistic pathogens such as *V. parahaemolyticus*.

3.4 Effects of FEL on Growth and Survival under Pathogen Challenge

The findings confirm that dietary supplementation with FEL significantly enhanced both growth performance and survival of *P. monodon* under *V. parahaemolyticus* challenge. SGR was markedly improved in all FEL-supplemented groups compared with the control ($p < 0.05$), with the highest value observed in the 0.2% FEL group (1.94 ± 0.01% day^{-1}), whereas the control group exhibited the lowest growth (1.33 ± 0.06% day^{-1}). These results align with previous studies reporting that probiotic supplementation can elevate SGR in shrimp under pathogenic stress (Nguyen *et al*., 2025b; Zheng *et al*., 2017; Kim *et al*., 2022).

FEL supplementation likely promoted intestinal colonization, enzyme activity, and nutrient assimilation, thereby contributing to improved physiological resilience. Encapsulation may have protected probiotic viability during digestion, enabling effective gut colonization. All FEL-treated groups achieved 100% survival, which was significantly higher than the control (82.22 ± 8.02%), indicating strong immunomodulatory effects. Previous studies have shown that dietary lactic acid bacteria can enhance immune responses and improve disease resistance in *P. monodon* (Nguyen *et al*., 2019). These improvements suggest that FEL helps maintain gut health under pathogen stress. Hemocytes play a key role in bacterial clearance through phagocytosis and encapsulation, particularly against Vibrio spp., which may explain the improved survival observed in this study (van de Braak *et al*., 2002).

Overall, FEL supplementation at 0.2–1.0% enhanced both growth and disease resistance, with 0.2% being the most effective for growth, as summarized in Table 3. These findings support the application of FEL as a practical dietary additive to improve shrimp performance and resilience in commercial aquaculture.

Table 3 SGR and survival of *P. monodon* at 9 days after *V. parahaemolyticus* challenge under FEL-supplemented diets.

FEL Level (%)	Mean SGR (% day^{-1})	Survival Rate (%)
0	1.33 ± 0.06^{b}	82.22 ± 8.02^{b}
0.2	1.94 ± 0.01^{a}	100.00 ± 0.00^{a}
0.4	1.92 ± 0.01^{a}	100.00 ± 0.00^{a}
0.6	1.89 ± 0.02^{a}	100.00 ± 0.00^{a}
0.8	1.84 ± 0.01^{ab}	100.00 ± 0.00^{a}
1.0	1.79 ± 0.02^{b}	100.00 ± 0.00^{a}

Note. Values are expressed as mean ± SE ($n = 3$). Different superscript letters within columns indicate significant differences among treatments ($p < 0.05$ for SGR; $p < 0.001$ for survival rate).

Survival analysis confirmed the protective effect of FEL supplementation, with all treated groups exhibiting 100% survival at 9 days post-*V. parahaemolyticus* challenge, compared with 82.22 ± 8.02% in the control group. This marked difference is attributed to the synergistic action of four *Lactobacillus* spp. in FEL, which not only function as probiotics but also produce extracellular polymeric substances (EPSs) with prebiotic-like properties. EPSs can enhance host immunity and suppress pathogen colonization in the shrimp gut. Nguyen *et al*. (2025a) reported that EPSs derived from *L. plantarum* and

Bifidobacterium bifidum improved gut microbiota balance, reduced *V. parahaemolyticus* levels, and increased immune responses, including THC and PO activity. These effects likely contributed to the complete protection observed in FEL-fed shrimp.

Moreover, recent studies highlight the synergistic benefits of synbiotic approaches. For example, Khanjani *et al*. (2024) reported improved immunity and survival in *P. vannamei* fed synbiotic diets, while Nguyen *et al*. (2025a) also demonstrated enhanced immune responses and resistance to *V. parahaemolyticus* in shrimp supplemented with EPS derived from LAB. Taken together, these findings suggest that the protective effects of FEL may be associated with EPS-mediated mechanisms reported in other studies (Nguyen *et al*., 2025a), though EPS was not directly quantified in this study. The incorporation of such functional additives represents a sustainable alternative to antibiotics in intensive shrimp aquaculture.

Interestingly, no mortality was observed in any FEL-supplemented groups with 0.2–1.0% w/w following *V. parahaemolyticus* challenge. Although this clearly demonstrates the protective efficacy of FEL, the observed survival may also be influenced by the virulence characteristics of the bacterial strain employed. The *V. parahaemolyticus* isolate in this study is an AHPND-associated strain that primarily targets the hepatopancreas and induces acute tissue damage (Lai *et al*., 2015). The absence of mortality in FEL-fed shrimp suggests that FEL supplementation may effectively mitigate the pathogenic effects of AHPND-related strains through enhanced gut immunity and beneficial microbial modulation. Nevertheless, further studies using multiple *V. parahaemolyticus* strains with differing virulence profiles are recommended to more comprehensively determine the extent of FEL's protective capabilities.

3.5 Evaluation of 0.2% FEL Supplementation on Growth Performance of P. monodon in Earthen Pond Culture

The growth trajectories of *P. monodon* in the pond trial are presented in Figure 3, showing that shrimp fed 0.2% FEL consistently exhibited greater body weight than the control group, particularly during the latter part of the 100-day culture period. These weight trajectories formed the basis for calculating the SGR during the 40-day monitoring period (days 60–100). The calculated SGR was 4.16 ± 0.031% day^{-1} in the control group and 4.48 ± 0.015% day^{-1} in the 0.2% FEL-supplemented group, representing a statistically significant improvement ($p < 0.001$).

Although the absolute increase was moderate, this enhancement is biologically meaningful and consistent with previous reports on *P. monodon* and related penaeid shrimp cultured under semi-intensive pond conditions, where SGR typically ranges from 3.5–4.5% day^{-1} depending on initial size and culture conditions (Fan *et al*., 2023; Nguyen *et al*., 2025b; Sung *et al*., 2021). Importantly, the growth-promoting effect observed in the FEL group (≈ 0.3% increase in SGR) is comparable to outcomes reported for dietary probiotics and microbial-derived feed additives, where improvements of 0.1–0.4% day^{-1} are common (Tran *et al*., 2023). This alignment with the broader literature strengthens the evidence that FEL can function as a practical functional additive in shrimp farming.

As illustrated in Figure 4, in addition to body weight, shrimp fed with 0.2% FEL also exhibited significantly greater body length compared to the control group at the end of the pond trial. This result further supports the growth-promoting effect of FEL under practical culture conditions. Moreover, shrimp fed with 0.2% FEL also exhibited significantly greater body length at multiple time points, particularly on days 70, 80, and 100. These improvements in length growth align with the enhanced body weight observed in the same treatment group, suggesting that FEL supplementation supports balanced somatic growth by promoting both weight and length gain. The consistency of these trends across both parameters suggests that FEL may promote balanced growth by improving nutrient uptake, stimulating digestive efficiency, and enhancing gut microbial stability.

The selection of 0.2% FEL was based on both its demonstrated biological efficacy and economic feasibility, with an estimated production cost of approximately 1,000 THB per kilogram. Although the improvement in SGR was modest, the findings support the practical application of FEL as a functional feed additive in shrimp aquaculture. To extend its applicability, long-term studies under commercial farming conditions should be undertaken to confirm its cost-effectiveness and scalability.

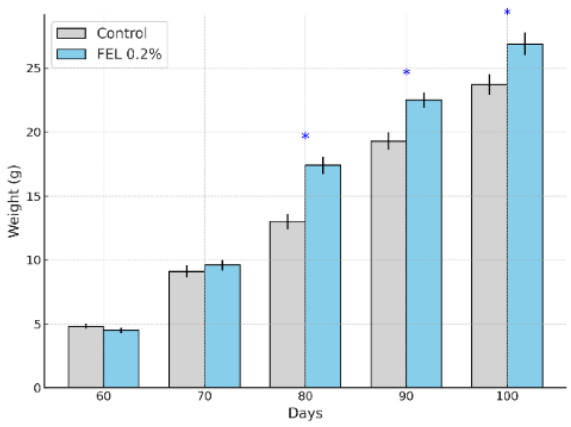

Figure 3 Effects of dietary 0.2% FEL supplementation on the body weight of *P. monodon* cultured in earthen ponds from days 60 to 100.

Note. Values are mean ± SD (n = 10). Asterisks (*) indicate significant differences between groups at each sampling point ($p < 0.05$, t-test).

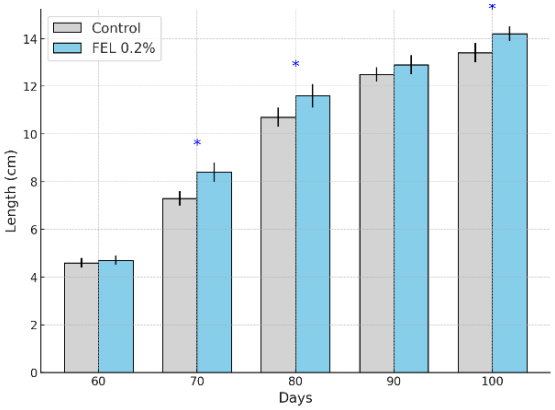

Figure 4 Effects of dietary 0.2% FEL supplementation on the body length of *P. monodon* cultured in earthen ponds from days 60 to 100.

Note. Values are mean ± SD (n = 10). Asterisks (*) indicate significant differences between groups at each sampling point (p < 0.05, t-test).

Visual observation indicated that shrimp in both control and FEL-supplemented groups exhibited comparable physical robustness and activity levels throughout the culture period. At harvest, the body weight of shrimp in both groups met the commercial market standard, indicating that FEL supplementation did not negatively affect shrimp morphology or growth uniformity. These findings support the practical applicability of 0.2% FEL in field conditions without compromising product quality or marketability.

Similar effects were reported by Sung *et al*. (2021), who demonstrated that dietary administration of LAB enhanced disease resistance and improved growth performance in *Litopenaeus vannamei* through modulation of immune parameters and intestinal microbiota. Likewise, Kongnum and Hongpattarakere (2012b) observed improved survival and growth in *P. monodon* fed with *L. plantarum*, underscoring the role of gut probiotics in promoting feed efficiency and physiological resilience. More recent studies (Li *et al*., 2022; Tran *et al*., 2023) further confirm that encapsulated probiotics enhance growth performance and gut health under both laboratory and field conditions.

Despite the positive outcomes observed, the limited pond replication warrants caution in interpretation. Future studies involving multiple farms and production cycles are recommended to substantiate these results.

3.6 Intestinal Microbiota Composition

3.6.1 Phylum-level analysis

Figure 5 presents the results of 16S rRNA sequencing at the phylum level, revealing that the intestinal microbiota of *P. monodon* was notably altered following supplementation with 0.2% FEL. Specifically, the relative abundance of Proteobacteria a phylum often associated with pathogenic bacteria and gut dysbiosis was significantly reduced in the FEL group compared to the control (p < 0.05). Conversely, the proportions of Actinobacteria and Firmicutes, both of which are commonly linked with beneficial functions such as immune modulation and gut barrier enhancement, were significantly increased (p < 0.05).

The observed changes in the gut microbiota suggest that FEL supplementation contributes to a more balanced and health-promoting intestinal ecosystem. Similar findings have been reported by Chin *et al*. (2024b) and Xiong (2024), who demonstrated that dietary probiotics can favorably modulate the intestinal microbiome of shrimp. Moreover, Gao *et al*. (2021) highlighted that an increase in Firmicutes abundance was associated with improved feed conversion efficiency and gut integrity in *L. vannamei*, while Nguyen *et al*. (2025b) showed that reducing *Proteobacteria* abundance via probiotic intervention could significantly lower the incidence of *Vibrio*-related infections.

This evidence is further supported by the work of Vieira *et al*. (2021) and Fan *et al*. (2023), who linked increased Firmicutes and Actinobacteria with enhanced immunity and digestive efficiency. Likewise, the decline in Proteobacteria is consistent with previous studies showing that probiotic-driven modulation can suppress pathogenic taxa such as *Vibrio* spp. (Nguyen *et al*., 2025b; Vega-Carranza *et al*., 2024), underscoring the functional role of FEL in promoting disease resilience in shrimp.

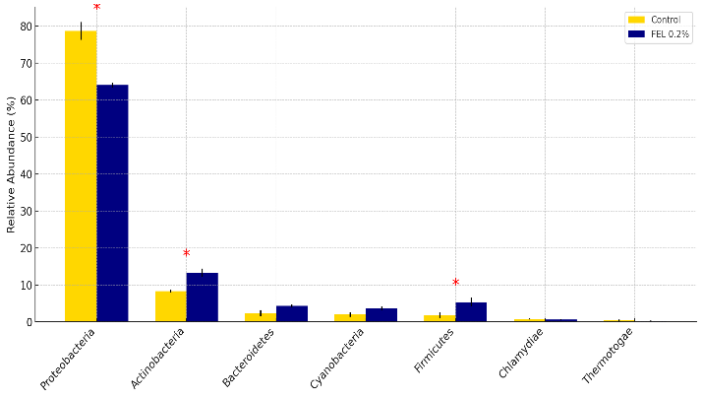

Figure 5 Phylum-level intestinal microbiota of *P.monodon* fed 0.2% FEL versus the control diet, based on 16S rRNA sequencing analysis (Illumina MiSeq).

Note. Data are presented as mean ± SD from three replicates. Asterisks (*) indicate phyla with significant differences between FEL and control groups (p < 0.05, t-test).

3.6.2 Species-level analysis

As depicted in Figure 6, at the species level, supplementation with 0.2% FEL significantly reduced the relative abundance of *P. damselae* (p < 0.05), a known shrimp pathogen, while increasing *P. inhibens* (p < 0.05). Notably, *P. inhibens* is a commensal species associated with enhanced immune regulation and pathogen suppression, which may contribute to improved disease resistance. This targeted microbial modulation suggests that FEL helps suppress harmful bacteria

while promoting beneficial taxa that support intestinal resilience. These findings align with previous studies reporting the probiotic benefits of encapsulated *Bacillus* and *Lactobacillus* spp. in enhancing shrimp immunity and intestinal health (Zhou *et al*., 2023; Ringø *et al*., 2020; Sirikharin *et al*., 2022).

The specific effect observed in *P. inhibens* underscores the importance of precision-targeted probiotics in modulating shrimp gut microbiota (Khanjani *et al*., 2024). Future studies should investigate the functional genomics and metabolomic interactions of dominant commensal species to clarify their roles in host immunity and performance. Additionally, long-term trials under commercial farming conditions are recommended to validate FEL's efficacy and microbial stability over extended culture periods (Tran *et al*., 2023).

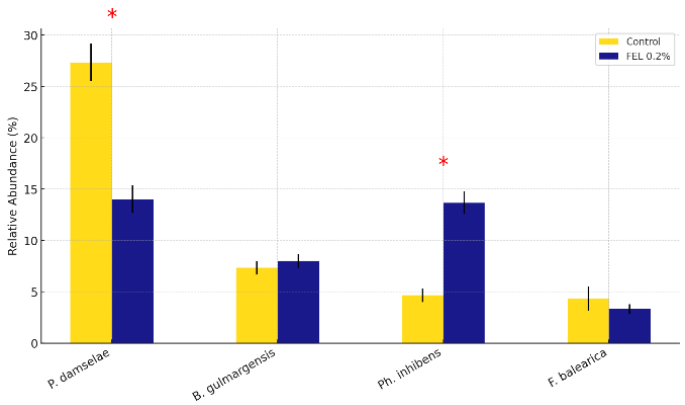

Figure 6 Relative abundance (%) of selected intestinal bacterial species in *P. monodon* fed the control and 0.2% FEL diets.

Note. Data are presented as mean ± SD from three replicates. Asterisks (*) indicate species with significant differences between FEL and control groups ($p < 0.05$, *t*-test).

P. damselae (Photobacterium damselae), B. gulmargensis (Blastochloris gulmargensis), Ph. inhibens (Phaeobacter inhibens), F. balearica (Ferrimonas balearica).

The enrichment of *P. inhibens* may also improve mucosal immunity and microbial competition, creating a more stable gut environment. The use of next-generation sequencing (NGS) enabled precise detection of both dominant and rare taxa, facilitating deeper insight into host–microbiota interactions and supporting the development of targeted probiotic strategies in shrimp aquaculture. The ability of FEL to selectively enrich beneficial species like *P. inhibens* while suppressing pathogens such as *P. damselae* demonstrates its potential as a precision microbiome modulator.

This targeted effect may result from enhanced probiotic viability and delivery efficiency provided by encapsulation technology (Andriani *et al*., 2022; Anal and Singh, 2021). Unclassified bacterial taxa detected in this study further emphasize the need for metagenomic and functional characterization to uncover the roles of currently unidentified microorganisms in shrimp gut ecology. Continued research into species-level interactions, including gene expression and metabolite production, will advance our understanding of FEL's long-term benefits and facilitate its application in commercial aquaculture (Khanjani *et al*., 2024; Tran *et al*., 2023).

While these findings are promising, they are based on observations from only two ponds with three replicate cages and should therefore be interpreted with caution.

4. Conclusion

Dietary supplementation with FEL enhanced immune responses, reduced intestinal *Vibrio* loads, and improved the growth performance of *P. monodon* under both laboratory and preliminary field conditions. FEL also modulated the intestinal microbiota by increasing beneficial Firmicutes and decreasing pathogenic taxa, underscoring its potential as a cost-effective and sustainable feed additive for shrimp health and productivity.

Further research should include larger-scale and multi-site trials across diverse aquaculture environments to validate its effectiveness under commercial conditions and to evaluate its safety, effects on meat quality, and economic feasibility for large-scale application.

5. Acknowledgments

The authors wish to express their sincere gratitude to the National Research Council of Thailand (NRCT) for funding this research under the fiscal year 2017 budget. Special thanks are also extended to the Faculty of Science and Technology of Fisheries, RUTS, Trang Campus, for providing access to the aquaculture laboratory and scientific equipment necessary for conducting this research. The authors would also like to thank the Office of Scientific Instrument and Testing, Prince of Songkla University, for performing the NGS analysis of the microbial community.

6. References

Afzaal, M., Saeed, F., Hussain, S., Mohamed, A.A., Alamri, M. S., Ahmad, A., Ateeq, H., Tufail, T. and Hussain, M. 2020. Survival and storage stability of encapsulated probiotic under simulated digestion conditions and on dried apple snacks. **Food Science & Nutrition** 8(5): 5392-5401.

AOAC. 2016. **Official Methods of Analysis, 20th ed.** AOAC International, Gaithersburg, MD, USA.

Anal, A.K. and Singh, H. 2021. Recent advances in microencapsulation of probiotics for applications in functional foods: A review. **Critical Reviews in Food Science and Nutrition** 61(5): 748-763.

Andriani, Y., Widanarni, W. and Ekasari, J. 2022. Encapsulation of probiotics for improved stability and efficacy in aquaculture: A review. **Aquaculture Reports** 24: 101088.

Argue, B.J., Arce, S.M., Lotz, J.M. and Moss, S.M. 2002. Selective breeding of Pacific white shrimp (*Litopenaeus vannamei*) for growth and resistance to Taura Syndrome Virus. **Aquaculture** 204(3-4): 447-460.

Chin, Y.K., Chin, Y.K., Haifa-Haryani, W.O., Nazarudin, M.F., Ahmad, M.I., Azzam-Sayuti, M., Mohamad, A., Ida-Muryany, M.Y., Karim, M.M., Annas, S., Azmai, M.N.A., Amal, M.N.A., Mohd Nor, N. and Ina-Salwany, M. 2024a. The synergistic *Lactobacillus plantarum* L20 and *Sargassum polycystum*-added diet for improvement of black tiger shrimp *Penaeus monodon's* growth, immune responses, bacterial profiles, and resistance against *Vibrio harveyi*. **Aquaculture Reports** 34: 101903.

Chin, Y.Y., Liew, H.C. and Ooi, P.T. 2024b. Dietary supplementation with *Lactobacillus plantarum* L20 and Sargassum polycystum enhances shrimp gut microbiota and disease resistance. **Aquaculture Reports** 29: 101601.

Fan, Y., Zhang, H., Liu, W., Zhang, Y. and Wang, W. 2023. Characterizing gut microbiota dynamics in *Penaeus monodon* fed probiotics using 16S rRNA sequencing. **Microbial Biotechnology** 16(2): 407-419.

Feng, Y., Liu, Y., Zhang, M. and Wang, J. 2020. Dietary supplementation of probiotics improves immune response and disease resistance in shrimp. **Aquaculture Reports** 17: 100361.

Gao, X., Zhang, J., Li, Y. and Chen, L. 2021. Dietary probiotics modulate gut microbiota and enhance feed conversion and intestinal integrity in *Litopenaeus vannamei.* **Aquaculture Reports** 21: 100812.

Hai, N.V. 2015. The use of probiotics in aquaculture. **Journal of Applied Microbiology** 119(4): 917-935.

Han, J.E., Tang, K.F.J. and Lightner, D.V. 2022. Field and experimental evidence of *Vibrio parahaemolyticus* causing shrimp disease. **Journal of Invertebrate Pathology** 186: 107637.

Hosein, S.H., Khalili, M., Esteban, M.A. and Ringø, E. 2021. Probiotics as means of diseases control in aquaculture, a review of current knowledge and future perspectives. **Frontiers in Microbiology** 12: 634973.

Huisakul, M., Chaitanawisuti, N. and Natsukari, Y. 2007. Influence of dietary *Lactobacillus* spp. on gut microbiota in *Penaeus monodon*. **Journal of the World Aquaculture Society** 38(2): 201-209.

Kesarcodi-Watson, A., Kaspar, H., Lategan, M.J. and Gibson, L. 2012. Probiotics in aquaculture: The need, principles, and mechanisms of action and screening processes. **Aquaculture** 274(1-4): 1-14.

Khanjani, M.H., Mozanzadeh, M.T. and Gisbert, E. 2024. Probiotics, prebiotics, and synbiotics in shrimp aquaculture: Their effects on growth performance, immune responses, and gut microbiome. **Aquaculture Reports** 38: 102362.

Kim, Y.J., Kim, S.W. and Lee, S.M. 2022. Modulation of gut microbiota and immune response in shrimp by dietary lactic acid bacteria. **Aquaculture Reports** 25: 101073.

Kongnum, K. and Hongpattarakere, T. 2012a. Effect of probiotic bacteria isolated from the gastrointestinal tract of wild shrimp on immune response and disease resistance. **Fish & Shellfish Immunology** 32(1): 67-76.

Kongnum, K. and Hongpattarakere, T. 2012b. Effect of *Lactobacillus plantarum* isolated from digestive tract of wild shrimp on growth and survival of white shrimp (*Litopenaeus vannamei*) challenged with *Vibrio harveyi*. **Fish & Shellfish Immunology** 32(2): 170-177.

Lai, H.C., Ng, T.H., Ando, M., Lee, C.T., Chen, I.T., Chuang, J.C., Mavvel, D., Chang, S.H., Huang, Y.T. and Wang, H.C. 2015. Pathogenesis of acute hepatopancreatic necrosis disease caused by *Vibrio parahaemolyticus* in shrimp. **Developmental & Comparative Immunology** 52: 77-84.

Leano, E.M. and Mohan, C.V. 2020. Early mortality syndrome in shrimp: A review. **Asian Fisheries Science** 33(2): 85-96.

Li, W., Li, X., Chen, Y. and Zhang, Y. 2022. Effects of dietary encapsulated probiotics on growth, intestinal health and immune response in shrimp. **Fish & Shellfish Immunology** 125: 220-228.

Lulijwa, R., Rupia, E.J. and Alfaro, A.C. 2020. Probiotics and their effects on gut microbiota of aquatic animals. **Applied Microbiology and Biotechnology** 104(17): 7255-7271.

Martínez-Porchas, M., Vargas-Albores, F. and Miranda-Baeza, A. 2021. Next-generation sequencing in aquaculture: Application and perspectives. **Aquaculture Reports** 19: 100611.

Nguyen, T.H., Vo, H.T., Pham, T.L. and Doan, H.V. 2019. Effects of dietary lactic acid bacteria on immune response and disease resistance in black tiger shrimp (*Penaeus monodon*). **Aquaculture Research** 50(5): 1218-1229.

Nguyen, H.T., Trinh, T.L., Nguyen, T.T.H., Nguyen, H.Y.N. and Nguyen, P.T. 2025a. Effect of dietary extracellular polymeric substances on shrimp immune responses. **Veterinary Integrative Sciences** 23(3): e2025061-1-16.

Nguyen, H.T., Trinh, T.L., Nguyen, T.T.H., Nguyen, H.Y.N. and Nguyen, P.T. 2025b. Probiotic supplementation enhances resistance against *Vibrio* in shrimp. **Aquaculture Reports** 28: 101298.

Ringø, E., Hoseinifar, S.H., Ghosh, K., Van Doan, H., Beck, B.R. and Song, S.K. 2020. Probiotic use in aquaculture: Importance of gut microbiota modulation. **Reviews in Aquaculture** 12(2): 234-256.

Sirikharin, R., Thitamadee, S. and Limsuwan, C. 2022. Effects of encapsulated *Bacillus* spp. on gut microbiota and disease resistance in *Penaeus monodon* under semi-intensive culture. **Thai Journal of Aquatic Animal Health** 16(2): 45-56.

Soundarapandian, P. and Velmurugan, C. 2008. Biochemical composition of the white shrimp *Litopenaeus vannamei* (Boone) collected from pond culture. **American-Eurasian Journal of Scientific Research** 3(5): 191-194.

Sung, H.H., Lin, Y.C., Chen, C.K. and Chiang, S.R. 2021. Dietary supplementation of lactic acid bacteria improves resistance to *Vibrio* in shrimp. **Aquaculture Reports** 19: 100580.

Tran, D.T., Nguyen, T.Q., Pham, H.L. and Le, H.V. 2023. Encapsulated probiotics enhance growth and intestinal health in Pacific white shrimp under intensive farming conditions. **Aquaculture** 570: 739418.

van de Braak, C.B.T., Botterblom, M.H.A., Taverne, N., Rombout, J.H.W.M., Huisman, E.A. and van der Knaap, W.P.W. 2002. The roles of haemocytes and the lymphoid organ in the clearance of injected *Vibrio* bacteria in *Penaeus monodon* shrimp. **Fish & Shellfish Immunology** 13(4): 293-309.

Vega-Carranza, A.S., Escamilla-Montes, R., Fierro-Coronado, J.A., Diarte-Plata, G., Guo, X., García-Gutiérrez, C. and Luna-González, A. 2024. Investigating the effect of bacilli and lactic acid bacteria on water quality, growth, survival, immune response, and intestinal microbiota of cultured *Litopenaeus vannamei*. **Animals** 14(18): 2676.

Vieira, F.N., Buglione-Neto, C.C., Ferrarezi, J.V. and Seiffert, W.Q. 2021. Encapsulated probiotics improve intestinal microbiota stability and disease resistance in shrimp. **Fish & Shellfish Immunology** 114: 56-63.

Xiong, J.B. 2024. Updated roles of the gut microbiota in exploring shrimp etiology and health management. **Microbiology Spectrum** 12(2): e00965-24.

Zhang, Y., Liu, W., Chen, X. and Wang, Q. 2018. Effects of dietary probiotic supplementation on growth and immune response of *Penaeus monodon*. **Aquaculture Research** 49(10): 3478-3486.

Zheng, Y., Yu, M., Liu, J., Qiao, Y. and Wu, S. 2017. Effects of dietary probiotics on gut microbiota composition and growth performance in aquaculture species. **Microbial Biotechnology** 10(6): 1345-1356.

Zhou, Q., Zhang, Q., Wang, Y. and Xia, X. 2023. Probiotic *Lactobacillus* improves immunity and disease resistance in black tiger shrimp. **Aquaculture International** 31(1): 175-188.

Zokaeifar, H., Balcázar, J.L., Saad, C.R., Kamarudin, M.S., Sijam, K., Arshad, A. and Nejat, N. 2012. Effects of dietary probiotic supplementation on the immune response and disease resistance of *Penaeus monodon*. **Fish & Shellfish Immunology** 32(5): 750-755.

Recent Science and Technology

Journal homepage: https:// www.tci-thaijo.org/index.php/rmutsvrj/index

ISSN: 3057-0786 (Online)

Research Article

Impact of Seaweed Species and Density on Mitigating Cannibalism in Blue Swimming Crab (*Portunus pelagicus*) Juvenile

Chonlada Leearam *, Rungtiwa Konsantad and Wasana Arkronrat

Klongwan Fisheries Research Station, Faculty of Fisheries, Kasetsart University, Mueang, Prachuap Khiri Khan 77000, Thailand.

Article history:

Received: 2025-07-01
Revised: 2025-09-19
Accepted: 2025-10-10

Keywords:

Cannibalism mitigation;
Crab nursing;
Portunus pelagicus;
Seaweed shelter

ABSTRACT

Cannibalism poses a major challenge in the aquaculture of crustaceans, particularly during the early nursery stages of the blue swimming crab (*Portunus pelagicus*), an economically important species that often experiences high mortality rates due to this behavior. This study investigated the effects of varying densities of *Caulerpa lentillifera* (CL), and *Chaetomorpha crassa* (CC), two green seaweed species, on reducing cannibalism in juvenile C2-stage crabs during their nursery phase. A two-factor experimental design was applied to crabs reared in controlled-environment indoor tanks for 30 days, based on seaweed density (0.5, 1, and 2 kg/m²) and species presence, with a negative control group lacking shelter. Based on the findings, while the seaweed species did not significantly influence growth parameters, the density of 0.5 kg/m² promoted higher growth rates, although these were not significantly different from the negative control. Conversely, the 2 kg/m² density of CC resulted in a substantial reduction in cannibalism, particularly from day 20 onward, with the lowest mortality rates observed under this treatment. These results underscore the importance of optimizing seaweed density and species type to enhance survival rates in crab juveniles, suggesting that CC at 0.5 kg/m² was optimal for growth, while CC at 2 kg/m² was most effective in minimizing cannibalism.

1. Introduction

Global food and nutrition security depend on the growth and development of aquacultural production systems because fisheries and aquaculture contribute approximately 17% of the total animal-source protein amounts of the major animal groups, with crustaceans being the second largest from capture fisheries and aquaculture (Boyd *et al*., 2022). Cai and Galli (2021) reported that marine crabs accounted for 447,372 t of the 120 million t of aquaculture produced worldwide in 2019-a 3.74% increase over 2018. Unfortunately, overexploitation has led to decreasing crab populations, which has resulted in a decline in *P. pelagicus* landings and exports over the past few decades. Thus, blue swimming crab cultivation has grown in importance. In 2023, Thailand had 5,176 productive sea crab farms, an increase of 13 farms or 0.25 percent from 2022. The value of sea crab farming was 1,257.74 million baht, an increase of 301.58 million baht or 31.54 percent from 2022 (Department of Fisheries, 2024). Although research and knowledge regarding the cultivation of crabs are constantly expanding, the most frequent difficulty with caring for crablets is their low survival rate, caused by cannibalism (Leearam *et al*., 2023).

Often, cannibalism constitutes the largest cause of mortality, affecting up to 90% of the young crabs (Oniam *et al*., 2011; Leearam *et al*., 2023). One of the many strategies applied to reduce cannibalism in the nursery phase has been the provision of appropriate shelters or substrates, which minimize physical encounters and, consequently, cannibalism. Since shelters provide an abiotic element, they are essential for lowering cannibalism-related mortality and reducing biota stress levels (Ly Van *et al*., 2020). Several studies have found that providing the provision of both natural shelters and artificial ones during

* **Corresponding author.**

E-mail address: *cld.leearam.77180@gmail.com*

Cite this article as:

Leearam, C., Konsantad, R. and Arkronrat, W. 2026. Impact of Seaweed Species and Density on Mitigating Cannibalism in Blue Swimming Crab (*Portunus pelagicus*) Juvenile. **Recent Science and Technology** 18(1): 268215.

https://doi.org/10.65411/rst.2026.268215

the nursery grow-out phases increased survivability and decreased cannibalism (Mirera and Moksnes, 2013; Oniam *et al*., 2015; 2020; Ly Van *et al*., 2020; Leearam *et al*., 2023).

In aquaculture farms, seaweeds used as shelters for juvenile crabs have had strongly positive effects on crab survival due to seaweed generally being a natural food source and providing habitat, shelter, and a nursery ground (Mirera and Moksnes, 2013; Al-Hafedh *et al*., 2015; Mantri *et al*., 2020; Kang *et al*., 2021). The green seaweed *Caulerpa* spp., belonging to the family Caulerpaceae, is common along the Andaman coast and the Gulf of Thailand. It is economically important as human food, as well as for health, cosmetics, bio-remediation, and commercial aquaculture production (Kamleshbhai *et al*., 2022). *Chaetomorpha* sp., the green filamentous seaweed inhabitant of stagnant coastal waters of central Thailand. It was abundant throughout the year that serving as a shelter for settling blue swimming crabs during the first instar stage. This genus has high biofiltration capacity, which can improve water quality and increase aquaculture productivity through integrated aquaculture systems. (Arumugam *et al*., 2018; Xu *et al.,* 2018; Roleda and Hurd, 2019; Zubia *et al*., 2019; Mahamad *et al*., 2023).

It has been suggested that the integration of aquaculture with green seaweed positively reduced cannibalism rates among blue swimming crab during the juveniles. Therefore, the goal of the present study was to assess the effects of different density levels of *Caulerpa lentillifera* and *Chaetomorpha crassa* on the mortality and growth of blue swimming crab (*P. pelagicus)* in the nursery stage using indoor rearing tanks.

2. Materials and Methods

2.1 Sources of experimental crab and seaweed

Samples of the blue swimming crab (BSC), *Portunus pelagicus*, in the juvenile were obtained from the hatchery at the Klongwan Fisheries Research Station (KFRS), Prachuap Khiri Khan province, Thailand. *Caulerpa lentillifera* and *Chaetomorpha crassa* are fast-growing, complex green seaweed that provide shelter and reduce cannibalism in crab larvae, as shown in Figure 1, were harvested from an improved earthen pond within the KFRS.

Figure 1 Characteristics of two green seaweeds as shelter for rearing BSC (*Portunus pelagicus*) in juveniles: (a) *Caulerpa lentillifera*; (b) *Chaetomorpha crassa*

2.2 Experimental design and management

A two-factor experiment was randomly established with three densities of seaweed (0.5, 1, and 2 kg/m^2) and without any seaweed as shelter (negative control) in separate tanks each having a bottom area of 0.13 m^2 (The dimensions are 0.32 × 0.47 × 0.30 meters) water volume 40 liters, combined with two species of seaweed *Caulerpa lentillifera* and *Chaetomorpha crassa*; denoted as CL and CC, respectively). Each treatment contained three replicates. Uniformly sized crabs were selected for the experiment, with mean ± standard deviation (SD) values for the initial carapace width (CW) and body weight (BW) of 0.31 ± 0.09 cm, and 0.03 ± 0.01 g, respectively. In this paper, seaweed densities of 0.5, 1, and 2 kg/m² are designated as D0.5, D1, and D2, respectively.

The rearing system was established at the KFRS, with all fiber tanks exposed to a natural photoperiod. The C2 crabs were reared in the filtered tanks at a density of 300 individuals/m2 (40 crabs/tank) with constant aeration. Frozen Artemia biomass was used as food for the crabs who were fed twice daily between 09:00 and 16:00 hours, at 20% of their biomass/day (Ly Van *et al*., 2020). Water exchange occurred in each tank every 5 days, replacing approximately 50% of the water volume. The crabs were raised for a total of 30 days. Every 15 days, the harvested seaweed biomass is weighed and measured. After using a cloth to wipe away extra water, the wet weight was recorded using a precision balance accurate to 0.1 g.

2.3 Data collection and analysis

Water quality was analyzed every 5 days. Salinity was measured using a refractometer (Master-S10 alpha; Atago, Japan), pH using a pH meter (pH Testr30; Eutech; Singapore), temperature, and dissolved oxygen (DO) concentration using an oxygen meter (Pro20i; YSI; USA), total ammonia based on Koroleff's indophenol blue method, nitrite using the colorimetric method, and alkalinity using the titration method according to APHA, AWWA, and WEF (2023).

The initial CW and BW statistics of the crabs were determined by randomly sampling 50 individuals from the acclimation tank. The weight of each crab was measured using a precision balance with an accuracy of 0.01 g, while CW was measured using calipers. The growth and mortality of each BSC were recorded every 10 days, during which four crabs were randomly sampled from each tank to assess their BW and CW. After measurement, each BSC was returned to its original tank. At the conclusion of the experiment, all surviving crabs in each tank were measured. Before weighing the crabs, excess water was removed using cloth, and the wet weight of the crabs was recorded to calculate growth rates. The average daily growth (ADG) in terms of BW (ADGBW) and CW (ADGCW) were calculated, along with the specific growth rate (SGR) for BW (SGRBW) and CW (SGRCW), using formulas 1–4, respectively. And show the size variation (CV) in terms of BW (CVBW) and CW (CVCW), using formula 5.

$$\text{ADGBW (g/day)} = \frac{(\text{final BW} - \text{initial BW})}{t} \quad (1)$$

$$\text{ADGCW (cm/day)} = \frac{(\text{final CW} - \text{initial CW})}{t} \quad (2)$$

$$\text{SGRBW (\%/day)} = \frac{(ln\text{final BW} - ln\text{initial BW})}{t} \times 100 \quad (3)$$

$$\text{SGRCW (\%/day)} = \frac{(ln\text{final CW} - ln\text{initial CW})}{t} \times 100 \quad (4)$$

$$\text{Coefficient of variation (\%)} = \frac{\text{SD}}{\text{Mean}} \times 100 \quad (5)$$

where t = culture period (days), and ln indicates the Napierian logarithm.

2.4 Statistical analysis

The experimental data were examined for normal distribution using the Kolmogorov-Smirnov test. When the data were found to be normally distributed, the variance of the data was examined using the Levene's test. Data meeting these assumptions were analyzed using two-way ANOVA (F test, p<0.05) to identify the influence of species and density of seaweed and their interaction on growth performance and mortality rate of cannibalism on crabs. Duncan's multiple range test at a 95 percent confidence level was applied to evaluate significant differences among treatments utilizing the IBM SPSS Statistics for Windows software (Version 24.0; IBM Corp.; Armonk, NY, USA). Data were presented as mean ± standard deviation values.

3. Results and Discussion

3.1 Cannibalism of BSC juveniles

The utilization of the seaweeds, *Caulerpa lentillifera* (CL) and *Chaetomorpha crassa* (CC) as shelters significantly decreased the cannibalism mortality of the BSC juveniles during the first 20 days only (p<0.05), with the mortality rate due to cannibalism being notably reduced from day 10 of the rearing onward compared to those reared without shelter (negative control), as shown in Figure 2a. In addition, the density of seaweed per unit area had a direct effect on the reduction of cannibalistic mortality, with the shelter at a density of 2 kg/m^2 having the best reduction in mortality compared to the other densities (p=0.003) at over 30 days (Figure 2b).

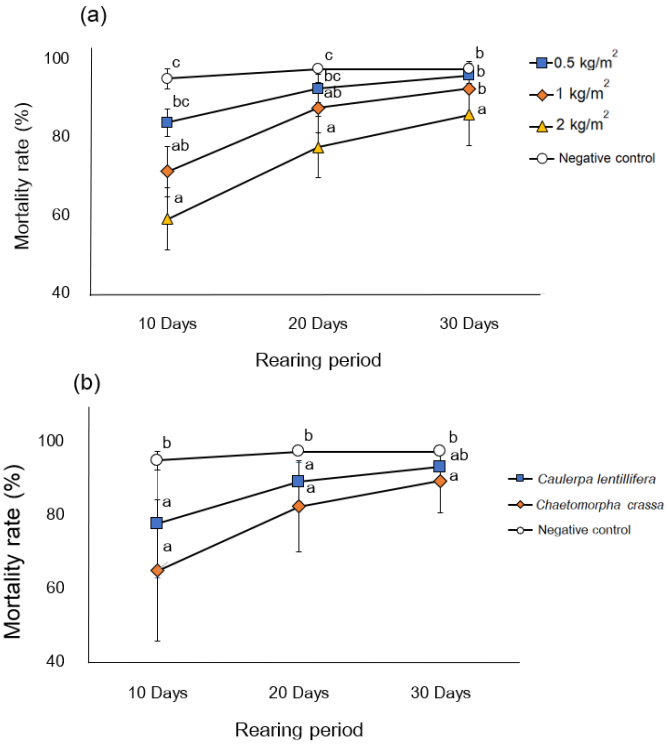

Figure 2 Mortality rates of BSC (*Portunus pelagicus*) juveniles reared with *Caulerpa lentillifera* and *Chaetomorpha crassa* (a) and across different seaweed densities used as shelter (b), compared to juveniles reared without any seaweed shelter (negative control). Error bars represent the mean±SD, and different lowercase letters at the symbols indicate significant differences (p<0.05).

Furthermore, examination of the interaction between seaweed species and densities on the mortality rate due to cannibalism in BSC juveniles indicated that these two factors collectively resulted in the significant reduction of cannibalism from day 20 onwards (p<0.05). The juveniles reared with UL as shelters at a density of 2 kg/m2 had the lowest cannibalistic mortality rate (79.16 ± 7.21%) at 30 days, of all treatments (Table 1).

Table 1 Mortality rate (MR), carapace width (CW), and body weight (BW) of BSC (*Portunus pelagicus*) juveniles reared in shelters with *Caulerpa lentillifera* (CL) and *Chaetomorpha crassa* (CC) at various densities, as well as in negative control group without shelter. Different superscript letters within same column indicated significant differences among treatments (p<0.05).

Treatment code	Species	Density (kg/m^2)	MR (%)			CW (cm/day)			BW (g/day)		
			10 Days	20 Days	30 Days	10 Days	20 Days	30 Days	10 Days	20 Days	30 Days
Individual treatment means (n=3)											
	Negative control		95.00±2.50^a	97.50±0.00^a	97.50±0.00^a	0.79±0.31^a	1.54±0.34^a	1.74±0.00^a	0.10±0.10^a	0.54±0.22^a	0.69±0.14^a
CL + D0.5	*Caulerpa lentillifera*	0.5	84.16±14.64^a	93.33±1.44^a	95.00±0.00^a	0.50±0.22^a	0.89±0.36^a	1.34±0.08^b	0.09±0.03^a	0.26±0.08^a	0.44±0.01^b
CC + D0.5	*Chaetomorpha crassa*	0.5	83.33±5.20^a	91.66±6.29^a	96.66±1.44^a	0.34±0.02^a	1.15±0.40^a	2.12±0.38^a	0.11±0.11^a	0.49±0.10^a	1.26±0.27^a
CL + D1	*Caulerpa lentillifera*	1	74.16±12.8 ^{a}	87.50±6.61^a	92.50±6.61^a	0.44±0.23^a	0.77±0.09^a	1.35±0.63^b	0.07±0.02^a	0.14±0.05^a	0.47±0.35^b
CC + D1	*Chaetomorpha crassa*	1	68.33±13.76^a	87.50±2.50^a	92.50±0.00^a	0.32±0.15^a	0.71±0.08^a	1.04±0.08^b	0.04±0.01^a	0.16±0.01^a	0.32±0.02^b
CL + D2	*Caulerpa lentillifera*	2	75.00±19.84^a	86.66±5.20^a	92.50±4.33^a	0.37±0.03^a	0.84±0.07^a	1.14±0.09^b	0.08±0.01^a	0.19±0.04^a	0.43±0.17^b
CC + D2	*Chaetomorpha crassa*	2	43.33±7.21^b	68.33±10.10^b	79.16±7.21^b	0.38±0.14^a	0.61±0.16^a	0.82±0.26^b	0.04±0.01^a	0.14±0.07^a	0.23±0.15^b
Two-way ANOVA P-values											
	Seaweed species (1)		0.044	0.025	0.063	0.331	0.936	0.749	0.741	0.193	0.114
	Seaweed density (2)		0.013	0.001	0.003	0.913	0.115	0.002	0.651	0.004	0.001
	Interaction (1) × (2)		0.099	0.025	0.013	0.728	0.282	0.009	0.852	0.091	0.001

D0.5 = seaweed densities of 0.5 kg/m²; D1 seaweed densities of 1 kg/m²; D2 = seaweed densities of 2 kg/m².

3.2 Growth rate of BSC

The seaweed species had no significant impact on CW and BW throughout the rearing period. Seaweed density at 1 and 2 kg/m^2 had a significant influence on both CL and BW, which was evident on day 30, with the significantly lowest growth of the C-stage BSC juveniles. Although seaweed species did not significantly affect CW or BW, there was a significant interaction effect between species and density on day 30 for CW and BW. Furthermore, CC at a density of 0.5 kg/m² produced CW and BW values of 2.12 ± 0.38 cm/day and 1.26 ± 0.27 g/day, respectively, which were greater than the other treatments. In addition, CC at 0.5 kg/m² was not significantly different from the negative control (Table 1).

The seaweed species did not significantly affect ADG and SGR based on all parameters of the BSC juveniles throughout the culture period. However, the seaweed density influenced the growth; compared to the other densities, the crabs reared at 0.5 kg/m^2 had higher growth for ADGCW, ADGBW, SGRCW, and SGRBW with values of 0.05 ± 0.01 cm/day, 0.02 ± 0.01 g/day, 5.13 ± 0.73 %/day, and 10.81 ± 1.89 %/day, respectively. In addition, there were significant interaction effects between species and density in both ADG and SGR for all parameters. CC at a density of 0.5 kg/m² produced higher growth than in the other experimental treatments. However, there was no significant difference for CC at 0.5 kg/m^2 in ADG and SGR in CW compared to the negative control (Table 2).

The coefficient of variation (CV) of CW and BW was used to assess growth uniformity among treatments at 10, 20, and 30 days (Table 3). Overall, the CV values for both CW and BW tended to decrease during the rearing period in most treatments, indicating improved size uniformity as the crabs grew. The lower CV values were found in tanks containing CC at 0.5-1 kg/m². By day 30, the lowest size variation in CW (6.46%) and BW (2.88%) was recorded in the CL at 0.5 kg/m², suggesting enhanced growth uniformity under this condition. In contrast, higher CV values were detected in the CC at 2 kg/m² with 31.71% for CW and 65.11% for BW, indicating greater size disparity at higher seaweed density. These results suggest that moderate seaweed coverage (0.5 kg/m²) promotes more uniform growth, whereas excessive density may lead to competition or reduced space availability, resulting in higher variation among individuals.

Table 2 Average daily growth (ADG) and specific growth rate (SGR) of BSC (*Portunus pelagicus*) juveniles reared in shelters with *Caulerpa lentillifera* (CL) and *Chaetomorpha crassa* (CC) at various densities, as well as in negative control group without shelter. Different superscript letters within same column indicated significant differences among treatments (p<0.05).

Treatment code	Species	Density (kg/m^2)	ADG_{CW} (cm/day)	SGR_{CW} (%/day)	ADG_{BW} (g/day)	SGR_{BW} (%/day)
Individual treatment means (n = 3)						
Negative control			0.06±0.00^a	5.22±0.00^a	0.02±0.00^b	10.56±0.71^b
CL + D0.5	*Caulerpa lentillifera*	0.5	0.04±0.00^b	4.54±0.16^b	0.01±0.00^b	9.14±0.09^b
CC + D0.5	*Chaetomorpha crassa*	0.5	0.07±0.01^a	5.72±0.52^a	0.04±0.01^a	12.48±0.74^a
CL + D1	*Caulerpa lentillifera*	1	0.04±0.02^b	4.44±1.15^{bc}	0.01±0.01^b	8.86±2.30^b
CC + D1	*Chaetomorpha crassa*	1	0.03±0.00^b	3.93±0.19^{bc}	0.01±0.00^b	8.19±0.24^b
CL + D2	*Caulerpa lentillifera*	2	0.04±0.00^b	4.16±0.19^{bc}	0.01±0.00^b	8.95±1.19^b
CC + D2	*Chaetomorpha crassa*	2	0.02±0.01^b	3.37±0.64^c	0.00±0.00^b	6.89±1.89^b
Two-way ANOVA P-values						
Seaweed species (1)			0.821	0.876	0.214	0.740
Seaweed density (2)			0.005	0.002	0.003	0.004
Interaction (1) × (2)			0.008	0.016	0.002	0.007

D0.5 = seaweed densities of 0.5 kg/m²; D1 seaweed densities of 1 kg/m²; D2 = seaweed densities of 2 kg/m².

Table 3 Size variation of BSC (*Portunus pelagicus*) juveniles reared in shelters with *Caulerpa lentillifera* (CL) and *Chaetomorpha crassa* (CC) at various densities, as well as in negative control group without shelter.

Treatment code	Species	Density (kg/m^2)	Coefficient of variation (%CV) $_{CW}$			Coefficient of variation (%CV) $_{BW}$		
			10 Days	20 Days	30 Days	10 Days	20 Days	30 Days
Individual treatment means (n=3)								
Negative control			39.53	22.49	0	83.23	41.41	21.02
CL + D0.5	*Caulerpa lentillifera*	0.5	45.3	41.17	6.46	39.22	28.94	2.88
CC + D0.5	*Chaetomorpha crassa*	0.5	7.35	35.21	18.29	98.66	21.21	21.85
CL + D1	*Caulerpa lentillifera*	1	54.5	12.24	46.67	25.13	37.58	75.42
CC + D1	*Chaetomorpha crassa*	1	47.24	12.61	8.48	39.95	6.15	7.93

Table 3 (Continuous)

Treatment code	Species	Density (kg/m^2)	Coefficient of variation (%CV) $_{CW}$			Coefficient of variation (%CV) $_{BW}$		
			10 Days	20 Days	30 Days	10 Days	20 Days	30 Days
CL + D2	*Caulerpa lentillifera*	2	8.97	8.11	7.86	24.66	20.88	40.65
CC + D2	*Chaetomorpha crassa*	2	36.08	27.44	31.71	26.75	49.33	65.11

D0.5 = seaweed densities of 0.5 kg/m²; D1 seaweed densities of 1 kg/m²; D2 = seaweed densities of 2 kg/m².

3.3 Water quality factors

During the 30 days of raising the crabs, the salinity, DO, temperature, pH, total ammonia, nitrite, and alkalinity levels in the culture tanks fluctuated in the ranges 31.3–33.7 ppt, 3.5–4.1 mg/L, 25.8–28.9 °C, 7.4–7.7, 0.04–0.24 mg-N/L, 0.00–0.22 mg-N/L, and 173–203 mg/L $CaCO_3$, respectively. These ranges in water quality parameters did not affect the growth or survival rate of BSC as they were within the ranges reported as suitable for crablet culture (Syafaat *et al*., 2021).

Reducing cannibalism in crustaceans, particularly crabs, is crucial to the success of commercial aquaculture, as cannibalism, especially in the BSC, has emerged as a major cause of failure during cultivation and this behavior has resulted in low yields that were deemed unprofitable (Oniam *et al*., 2011). Other studies have shown that the use of shelter for rearing BSC resulted in a lower mortality rate compared to conditions without shelter (Haemasaton and Pisuttharachai, 2017; Fatihah *et al*., 2017; Oniam *et al*., 2020; Leearam *et al*., 2023). In addition, the physical characteristics of the shelter influenced survival rates (Oniam *et al*., 2015; Zhang *et al*., 2021). Specifically, the use of plants as shelter is not only decreased mortality but also improved water quality and food availability (Arumugam *et al*., 2018; Roleda and Hurd, 2019).

Based on the results of the present study, throughout the experiment, the seaweed species did not significantly affect cannibalism in BSC; however, the seaweed density of 2 kg/m^2 clearly produced the best reduction in crab mortality from 20 days onward. Notably, from 20 days onward, considering the interaction between species and density of seaweed, the crab mortality rate in the CA-cultured crabs was higher than for the UL-cultured crabs for the density of 2 kg/m^2. This difference could be attributed to the distinct morphologies of the two species. For example, the genus *Caulerpa* features a simple structure consisting of long branching horizontal stolons and numerous simple or branched erect portions (Zubia *et al*., 2019; Lagourgue *et al*., 2024). Whereas *Chaetomorpha* is a common green seaweed genus characterized by it consists of uniseriate, unbranched filaments growing to 50–60 cm when fully developed. Lateral rhizoidal filaments are not observed at any time during the year, which provides better shelter (Xu *et al*., 2018; Mahamad *et al*., 2023). The present results were consistent with the findings of Toi *et al.* (2023), where all *Cladophora* sp. treatments had lower crab survival rates, biomass, and productivity than those in *Gracilaria tenuistipitata* treatments, likely due to differences in morphology and structural complexity of these seaweeds used as shelter. There was a reduced mortality rate for the BSC reared with a seaweed density of 2 kg/m². Other studies have reported that increasing the shelter complexity in crab culture could add surface area and interstitial spaces, thereby reducing encounter rates and cannibalism (Daly *et al*., 2009; Oniam *et al*., 2020; Leearam *et al*., 2023). Mirera and Moksne (2013) reported that cannibalism rates could be further reduced by providing shelters that diminished encounter rates among crabs, with such shelters being particularly important in mitigating cannibalism by offering refugia to smaller or molting crabs.

The seaweed species did not affect the crab growth throughout the culture experiment. However, at the end of the experiment, the seaweed densities of 1 and 2 kg/m^2 resulted in the lowest growth performance of BSC compared with the density of 0.5 kg/m^2 and the negative control. Budzałek *et al*. (2021) reported that Macroalgae in marine environments; Ulvophyceae, Chlorophyta (green algae), Florideophyceae, Rhodophyta (red algae), and Phaeophyceae, Ochrophyta (brown algae), with confirmed allelopathic activity against other heterotrophic organisms, which are synthesized as a defense strategy against coexisting aquatic competitors (Cnidaria) and herbivores (Annelida, Echinodermata, Arthropoda, Mollusca, and Chordata). Considering the interaction between species and density, UL with 0.5 kg/m^2 as a cover provided better growth for BSC than the other treatments and was not significantly different from the negative control. Therefore, the use of seaweed as a shelter has provided a positive effect on crabs, i.e., the crabs received additional food from the decaying algae, and a negative effect was that if the algae density was high, allelopathic compounds were synthesized, which affected the growth performance. In this experiment, the growth of crabs in terms of CW and BW was related to survival. For example, there were no significant differences between experiments in the size and growth rate of the BSC during the first 10 days because there was low mortality during this period in all treatments. Conversely, providing too much shelter might block the crabs from consuming primary foods (*Artemia* sp.). Daly *et al.* (2009) found that providing artificial substrate for the red king crab (*Paralithodes camtschaticus*) increased their survival but reduced the growth of juveniles, likely due to reduced cannibalism and increased time spent foraging. Arumugam *et al*. (2018), and Roleda and Hurd (2019) reported that seaweeds

helped to improve water quality and have been used commonly in integrated mariculture systems to absorb inorganic nutrient wastes. Thus, seaweed is a simple bio-filter, low-footprint aquaculture species that can be used for wastewater treatment and creating a habitat conducive habitat for crab development. Chaiyawat *et al.* (2009) revealed that crab fed only red seaweed (*Gracilaria edulis*) had the lowest percentage of body weight; however, as a dietary supplement for crabs, it increased the astaxanthin, red color, seaweed odor, and flavor of the meat and this was suitable for improving the meat quality of these crabs during short feeding periods. Shelley and Lovatelli (2011) reported that crabs were opportunistic omnivores so their aggression and associated cannibalism resulted in those surviving crabs in the tank eating both the experimental food and any recently molted crabs (Leearam *et al*., 2023). This was similar to the finding of Islam *et al.* (2018), who revealed that the cannibalistic nature of Scylla paramamosain gave them additional nutrition, which increased their growth rate. As shown by the results in the present study, the seaweed not only provided cover for crabs, but was also a food source. Chaiyawat *et al.* (2009) also reported on cultivating crabs (*P. pelagicus*) using red seaweed (*Gracilaria edulis*). According to Phinrub *et al.* (2019), crabs are animals that consume both plants and animals, both living and non-living. In their study, crabs were raised beside seagrass and it was reported that the crabs consumed the seagrass leaves, while those in green seaweed (*Caulerpa lentillifera*) shelters had the best growth performance and survival. This improvement was likely attributable to the supplementary food sources provided, as well as the algae that grew on the shelter structures, which served as an additional dietary component. Furthermore, as reported by Shelley and Lovatelli (2011), juvenile Scylla serrata consumed seagrass and algae, constituting approximately 13.05% of their total diet.

4. Conclusion

The use of seaweed shelters, particularly *Chaetomorpha crassa* (CC) at a density of 2 kg/m², significantly reduced cannibalism-induced mortality in the C-stage BSC juveniles of the BSC (*Portunus pelagicus*), especially after day 10 of rearing. The seaweed species did not significantly affect growth parameters. The seaweed density of 0.5 kg/m² promoted higher growth rates in terms of average daily growth and specific growth rate in the juveniles, although these results were not significantly different from the negative control. Notably, the interaction between species and density of seaweed further enhanced these outcomes, indicating that optimal combinations exist. To balance growth performance with cannibalism prevention, we recommend applying CC at 0.5 kg/m² when the goal is to improve BSC larval growth, and increasing CC to 2 kg/m² when the priority is to reduce mortality and boost survival. Using these two density regimes according to production stage can substantially increase the success rate of BSC larval seaweed cultivation.

5. References

Al-Hafedh, Y.S., Alam, A. and Buschmann, A.H. 2015. Bioremediation potential, growth and biomass yield of the green seaweed, *Ulva lactuca* in an integrated marine aquaculture system at the Red Sea coast of Saudi Arabia at different stocking densities and effluent flow rates. **Reviews in Aquaculture** 7(3): 161-171.

APHA, AWWA and WEF. 2023. **Standard methods for the examination of water and wastewater** (24th ed). American Public Health Association.

Arumugam, N., Chelliapan, S., Kamyab, H., Thirugnana, S., Othman, N. and Noor, N.S. 2018. Treatment of wastewater using seaweed: A review. **International Journal of Environmental Research and Public Health** 15: 2851.

Boyd, C.E., McNevin, A.A. and Davis, R.P. 2022. The contribution of fisheries and aquaculture to the global protein supply. **Food Security** 14: 805-827.

Budzałek, G., Śliwińska-Wilczewska, S., Wiśniewska, K., Wochna, A., Bubak, I., Latała, A. and Wiktor, J.M. 2021. Macroalgal Defense against Competitors and Herbivores. **International Journal of Molecular Sciences** 22(15):7865.

Cai, J. and Galli, G. 2021. **Top 10 Species Groups in Global Aquaculture 2019.** Available Source: https://openknowledge.fao.org/server/api/core/bitstreams/b9490d89-4bb7-4895-a994-4252ca70dbcd/content, October 16, 2025.

Chaiyawat, M., Eungrasamee, I. and Raksakulthai, N. 2009. Meat quality of blue swimming crab (*Portunus pelagicus*, Linnaeus 1758) fattened with different diets. **Kasetsart Journal (Natural Science)** 43: 132-142.

Daly, B., Swingle, J.S. and Eckert, G.L. 2009. Effects of diet, stocking density, and substrate on survival and growth of hatchery-cultured red king crab (*Paralithodes camtschaticus*) juveniles in Alaska, USA. **Aquaculture** 293(1-2): 68-73.

Department of Fisheries. 2024. **Statistics of sea crabs culture survey 2023.** Fishery Statistics Group, Fisheries Development Policy and Planning Division, Bangkok. (in Thai)

Fatihah, S.N., Julin H.T. and Chen C.A. 2017. Survival, growth and molting frequency of mud crab *Scylla tranquebarica* juveniles at different shelter conditions. **AACL Bioflux** 10(1): 1581-1589.

Haemasaton, T. and Pisuttharachai, D. 2017. Productivity improvement of mud crabs *Scylla sarrata* (Forskal) in cage-pond using different sheltering materials. **Thaksin Journal** 20(3): 1-7.

Islam, M., Siddiky, M.N.S.M. and Yahya, K. 2018. Growth, survival and intactness of green mud crab (*Scylla paramamosain*) broodstock under different captive grow out protocols. **Saarc Journal of Agriculture** 16(1): 169-180.

Kamleshbhai, B.P., Joshi, N.H., Tiwari, A. and Shaji, S. 2022. Seaweed classification, source and uses. **Agriculture India Today** 2(5): 54-57.

Kang, Y.H., Kim, S., Choi, S.K., Lee, H.J., Chung, I.K. and Park, S.R. 2021. A comparison of the bioremediation potential of five seaweed species in an integrated fish-seaweed aquaculture system: Implication for a multi-species seaweed culture. **Aquaculture** 13(1): 353-364.

Lagourgue, L., Sauvage, T., Zubia, M., Draisma, S.G.A., Vieira, C., Engelen, A. and Payri, C.E. 2024. Taxonomic insights into *Caulerpa* (Bryopsidales, Chlorophyta) species in French Polynesia: confirmation of 13 species and reinstatement of *C. pickeringii* Harvey and Bailey. **Diversity** 16(4): 243.

Leearam, C., Konsantad, R. and Arkronrat, W. 2023. Effect of shelter area ratio on mortality rate of blue swimming crab (*Portunus pelagicus*) due to cannibalism in young crab stage, pp. 248-255. *In* **The 20th Kasetsart University Kamphaeng Saen National Conference.** Kasetsart University, Nakhon Pathom. (in Thai)

Ly Van, K., Arsa, C.P., Nguyen Thi, N.A. and Ngoc, H.T. 2020. Use of different seaweeds as shelter in nursing mud crab, *Scylla paramamosain*: Effects on water quality, survival, and growth of crab. **Journal of the World Aquaculture Society** 53(1): 485-499.

Mahamad, H., Ruangchuay, R. and Bovornruangroj, N. 2023. Effect of salinity on growth of epiphytic green algae, *Chaetomorpha crassa* and *Rhizoclonium riparium*. **Khon Kaen Agriculture Journal SUPPL** 1: 48-54. (in Thai)

Mantri, V.A., Kavale, M.G. and Kazi, M.A. 2020. Seaweed biodiversity of India: Reviewing current knowledge to identify gaps, challenges, and opportunities. **Diversity** 12(1): 13.

Mirera, D.O. and Moksnes, P.O. 2013. Cannibalistic interactions of juvenile mud crab *Scylla serrata*: The effect of shelter and crab size. **African Journal of Marine Science** 35: 545-553.

Oniam, V., Arkronrat, W. and Binti Mohamed, N. 2015. Effect of feeding frequency and various shelter of blue swimming crab larvae, *Portunus pelagicus* (Linnaeus, 1758). **Songklanakarin Journal of Science and Technology** 37(2): 129-134.

Oniam, V., Taparhudee, W., Tunkijjanukij, S. and Musig, Y. 2011. Mortality rate of blue swimming crab (*Portunus pelagicus*) caused by cannibalism. **Kasetsart University Fisheries Research Bulletin** 35(2): 1-13.

Oniam, V., Taparhudee, W. and Yoonpundh, R. 2020. Installation of shelters on growth and survival of blue swimming crab (*Portunus pelagicus*) for development of its culture. **Songklanakarin Journal of Science and Technology** 42(1): 139-145.

Phinrub, W., Na Ranong, S. and Khamcharoen, M. 2019. Growth performance of blue swimming crab (*Portunus pelagicus* Linnaeus, 1758) in difference shelter. **Journal of Science and Technology, Ubon Ratchathani University** 22(3): 82-91. (in Thai)

Roleda, M.Y. and Hurd, C.L. 2019. Seaweed nutrient physiology: Application of concepts to aquaculture and bioremediation. **Phycologia** 58: 552-562.

Shelley, C. and Lovatel, A. 2011. **Mud Crab Aquaculture: A Practical Manual.** FAO Fisheries and Aquaculture, Rome, Italy.

Syafaat, M.N., Waiho, K., Azra, M.N., Abol-Munafi, A.B, Syahnon, M., Azmie, G., Ma, H. and Ikhwanuddin, M. 2021. Nursery culture of mud crab, genus *Scylla*, a review: The current progress and future directions. **Animals** 11(7): 2034.

Toi, H.T., Anh, N.T.N., Ngan, P.T.T., Nam, T.N.H. and Hai, T.N. 2023. Effects of stocking densities and seaweed types as shelters on the survival, growth, and productivity of juvenile mud crabs (*Scylla paramamosain*). **Egyptian Journal of Aquatic Research** 49(1): 401-407.

Xu, G., Endo, E. and Agatsuma, Y. 2018. Comparative study on the physiological differences between three *Chaetomorpha* species from Japan in preparation for cultivation. **Journal of Applied Phycology** 30: 1167-1174.

Zhang, H., Zhu, B., Yu, L., Liu, D., Wang, F. and Lu, Y. 2021. Selection of shelter shape by swimming crab (*Portunus trituberculatus*). **Aquaculture Reports** 21: 100908.

Zubia, M., Draisma, S.G.A., Morrissey, K.L., Varela-álvarez, E. and De Clerck, O. 2019. Concise review of the genus *Caulerpa* J.V. Lamouroux. **Journal of Applied Phycology** 32(1): 1-17.

Recent Science and Technology

Journal homepage: https:// www.tci-thaijo.org/index.php/rmutsvrj/index

ISSN: 3057-0786 (Online)

Research Article

Efficacy of Ethanol Extract of Leftover Chili (*Capsicum annuum* var. *frutescens* L.) on Weed Control, Growth and Yield of Thai Eggplants (*Solanum xanthocarpum* Schrad. & Wendl.)

Nalin-on Nuiplot *

Office of General Education, Valaya Alongkorn Rajabhat University under the Royal Patronage, Khlong Luang, Pathum Thani 13180, Thailand.

Article history:

Received: 2024-11-19
Revised: 2025-07-08
Accepted: 2025-08-13

Keywords:

Ethanol extract;
Weed control;
Leftover chili;
Thai eggplant;
Capsaicinoids

ABSTRACT

Weeds pose major problems for farmers as they compete for essential factors for plant growth, thereby affecting crop yields. Currently, natural methods are increasingly popular for weed control. In the study area where vegetables like chili and eggplant are grown for consumption and sale, a significant weed problem in the eggplant plots led to low quality and insufficient yields. This prompted the researcher to investigate using leftover chili extract to control weeds. This study aimed to evaluate the efficacy of ethanol extracts of leftover chili in controlling weeds. The extract was prepared using a 70% ethanol solution, filtered to separate pulp, then diluted with water to a 30% alcohol concentration, and poured into a spray bottle. Three treatment groups were tested: Control Group 1 (pulling weeds by hand), Control Group 2 (spraying with 30% ethanol), and Experimental Group (spraying with chili extracts). Treatments were applied around the base of eggplant plants every 10 days for 90 days. The growth of both Thai eggplant and weeds was measured by assessing height above the soil surface, counting weed growth, and counting eggplant fruit after spraying. Statistical analyses included mean and analysis of variance. The results showed that the chili extract significantly reduced weed germination and growth (dry weight), performing comparably to manual weeding. Notably, eggplant yields in the chili extract group were the highest, significantly outperforming the ethanol control and matching manual weeding. This indicates the extract's potential for effective, chemical-free weed control that supports crop growth.

1. Introduction

Weeds represent a formidable challenge in agriculture, directly competing with cultivated plants for essential resources such as sunlight, water, and nutrients. This competition inevitably leads to reduced crop yields and diminished quality, significantly impacting agricultural productivity and profitability (Radosevich *et al.*, 2007; Sardana *et al.*, 2017) In conventional farming, chemical herbicides are widely used for weed control; however, their persistent residues in agricultural products, potential environmental contamination, and rising costs (Tosena *et al.*, 2018) necessitate the exploration of sustainable and environmentally benign alternatives. Consequently, there is a growing global trend towards natural weed management methods, particularly crucial for the expansion of organic production systems, which strictly prohibit synthetic chemicals (IFOAM Organics International, 2024).

Chili (*Capsicum* spp.) is a vital shrub in the Solanaceae family. It is not only a staple in Asian diets and an economically significant crop in Thailand, but its fruits also contain capsaicinoids, a group of active compounds known for their pungency (Sayun and Suwanprateep, 2015). While chili fruit is primarily utilized for culinary, cosmetics, and medicinal purposes, significant amounts of leftover chili fruit often become agricultural waste, particularly in high-production areas like Thailand's central region. Despite existing research on valorizing chili waste, such

* **Corresponding author.**

E-mail address: *nalin-on@vru.ac.th*

Cite this article as:

Nuiplot, N. 2026. Efficacy of Ethanol Extract of Leftover Chili (*Capsicum annuum* var. *frutescens* L.) on Weed Control, Growth and Yield of Thai Eggplants (*Solanum xanthocarpum* Schrad. & Wendl.). **Recent Science and Technology** 18(1): 265348.

https://doi.org/10.65411/rst.2026.265348

as converting chili leaves into probiotic fermentation products (Urit, 2020), there remains a gap in research exploring in beneficial uses of discarded chili fruits.

The inherent properties of capsaicinoids suggest their potential as a natural bio pesticide. Previous studies have demonstrated the efficacy of chili extracts in controlling various insect pest like aphids and beetles by causing cellular irritation (Jirapong, 1999) and even inhibiting bacterial growth in laboratory settings (Soiklom *et al*., 2013). While these studies primarily focused on pests and bacteria, the fundamental irritant and cellular disruption properties of capsaicinoids suggest a plausible mechanism for inhibiting plant cell functions, which could extend the weed seed germination and growth. Specifically, capsaicinoids are polar hydrocarbons that readily dissolve in alcohol, ether, and acetone rather than in water (Salzer, 1997). This characteristic indicates that an ethanol-based extraction would be more effective in isolating these active compounds, potentially yielding a higher concentration of capsaicinoids compared to water-based extracts. Moreover, ethanol itself can contribute to weed control by inducing cellular dehydration in plants, a mechanism observed in other alcohol-containing natural weed suppressants (Sila-on, 2021; Nicholson, 2022).

In the study area, local farmers cultivating Thai eggplant (*Solanum xanthocarpum* Schrad. & Wendl.) for consumption and sale face a persistent challenge from common weeds like barnyard grass (*Echinochloa crus-galli* (L.) P.Beauv.) and sensitive plant (*Mimosa pudica* L.). These weeds severely impede eggplant production, leading to reduced yields and unprofitability, despite recommendations for pre-emergence weed control combined with manual weeding or mulching (Kongsaengdao *et al*., 2010). Given the escalating costs of synthetic herbicides and the increasing demand for organic and chemical-free produce, exploring effective and accessible natural alternatives is paramount for supporting local farmers and promoting sustainable agricultural practices.

Therefore, this research aimed to investigate the potential of utilizing leftover bird's eye chili (*Capsicum annuum* var. *frutescens* L.) extract as a natural weed control agent for eggplant cultivation. Specifically, the objectives of this study were to: 1) evaluate the efficacy of ethanol extract of leftover chili in inhibiting weed seed germination in an eggplant plot; and 2) assess its impact on the growth and yield of Thai eggplant, aiming to provide farmers with a cost-effective, environmentally friendly, and easily implementable weed management solution that aligns with organic production principles.

2. Materials and Methods

2.1 Plant Material and Extract Preparation

Fresh, bright red or orange, leftover bird's eye chili fruits harvested within 48 hours, were collected from the study area in Krachaeng Subdistrict, Bang Sai District, Phra Nakhon Si Ayuttaya Province, Thailand during May 2023. The chili fruits were washed thoroughly with clean water, had their stems removed, and were then stored at room temperature.

For extract preparation, 200 grams of chili fruits were finely chopped into small pieces, approximately 1 cm cube. While grinding the chili into a paste might potentially yield a more concentrated extract by increasing the surface area for solvent interaction, this study opted for chopping to simplify the extraction process, making it more accessible for farmers to replicate without specialized equipment. The chopped chili samples were then subjected to a maceration process, adapted from methods described by Preedapattarapong (1994), Kaewnoi *et al*. (2018), and Saeung and Punya (2022). Specifically, 200 grams of the chopped chili were soaked in 1000 mL of 70% ethanol at room temperature (25-30°C) for 24-72 hours.

Following the maceration, the mixture was filtered using fine-mesh cloth to separate the solid chili residue. From the resulting filtrate, 430 mL was diluted in 570 mL of distilled water to achieve a final concentration of 30% (v/v) alcohol. This specific alcohol concentration was selected based on preliminary trials and the adapted review literature above suggesting that a 30% ethanol solution provides an optimal balance between efficient extraction of capsaicinoids, which are alcohol-soluble, and a sufficient level of alcohol-induced dehydration for effective weed control, while minimizing potential phytotoxic to the target crop. The diluted solution was left to stand for 15 minutes at room temperature to ensure thorough mixing. The physical characteristics of the prepared chili extract, including color, clarity or separation, and smell, were observed, and its pH value was measured before storage in a spray bottle for subsequent efficacy evaluation.

2.2 Effect of Chili Extract on Weed Control, Growth, and Yield of Thai Eggplant

This study was conducted as a pot experiment under ambient conditions, utilizing a Completely Randomized Design (CRD). To ensure statistical validity, five replicates were used for each of the three treatment groups, with one pot representing each experimental unit.

2.2.1 Pot Preparation and Plant Establishment

Each experimental unit consisted of a plastic pot with a diameter of 20 cm and a height of 25 cm, filled with a pre-sterilized potting soil. The soil was screened to remove pre-existing weed seeds and contaminants, ensuring consistency across all pots. Thirty-day-old Thai eggplant seedlings were transplanted, one per pot. Immediately after transplanting, weed seeds of barnyard grass (*Echinochola crus-galli* (L.) P.Beauv.) and sensitive plants (*Mimosa pudica* L.) were intentionally sown into each pot at a density of 5 seeds per weed species, ensuring a controlled and consistent weed challenge. Plants were consistently watered every three days to maintain adequate soil moisture (Adapted from Pinsupa and Nakhon Si, 2010).

2.2.2 Experimental Treatments

The three treatment groups were as follows:

1. Control group 1 (Manual weeding): Weeds were removed by hand-pulling every 10 days to serve as a positive control representing traditional, non-chemical weed management.

2. Control group 2 (30% ethanol): Pots were sprayed with 10 mL of 30% ethanol solution without chili extract.

3. Experimental group (Chili extract in 30% ethanol): Pots were sprayed with 10 mL of the prepared chili extract (in 30% ethanol) every 10 days.

2.2.3 Application Method

For spray treatment (Groups 2 and 3), the 10 mL solution was applied using a fine-mist spray bottle, targeting the weeds growing around the base of the eggplant plants. Care was taken to minimize direct spraying onto the eggplant foliage to assess the selective nature of the extract. Applications were carried out every 10 days for a total duration of 90 days.

2.2.4 Data Collection and Measurements:

1) Weed germination and growth: The number of newly grown weeds, or germinated weeds, was counted and recorded every 10 days. At 30 days after initial weed planting, the dry weight of weed stems (barnyard grass and sensitive plants) was measured by carefully excising the weeds at the soil surface, drying them in an oven at 60°C for 48 hours, and then weighing.

2) Eggplant growth and yield: The height of Thai eggplant, measured from the soil surface to the highest growing point, was recorded every 10 days. The number of eggplant fruits was counted during the harvest, which commenced 60 days after transplanting and continued until 90 days. The percentage of fruit set after flower bloom could not be accurately assessed in this experimental setup; thus, the total fruit count per plant served as the primary yield indicator.

2.2.5 Comparison with Chemical Herbicides:

This study intentionally focused on evaluating the efficacy of a natural, plant-based extract as a sustainable and organic alternative to conventional herbicides. While chemical herbicides are widely used, direct comparison was omitted to specifically highlight the potential of the chili extract within an organic or reduced-chemical farming context. The manual weeding control (Group 1) served as a practical benchmark for comparison, representing a common and effective non-chemical weed control method often employed by organic farmers. The primary goal was to find a bio-alternative that could potentially reduce the labor intensity of manual weeding and mitigate the environmental concerns associated with synthetic chemicals.

2.3 Statistical Analysis

All collected data were subjected to Analysis of Variance (ANOVA) to determine significant differences among treatment groups. When a significant F-test result was obtained ($p < 0.05$), the means of treatments were further compared using the Least Significant Difference (LSD) test at the 0.05 probability level. All statistical analyses were conducted using SAS statistical software.

3. Results and Discussion

3.1 Characteristics of Chili Extract

The chili extract prepared in this study was observed to be a homogeneous, bright orange-red solution, as shown in Figure 1, with a distinctive pungent chili odor, indicating no phase separation. Its pH value was measured at 6.04 ± 0.05, which is notably close to the pH of pure capsaicinoids solution (5.90 ± 0.03), as reported by Kaewnoi *et al.* (2018). These physicochemical properties confirm that the extraction method successfully yielded an extract with characteristics appropriate for the study, suggesting a stable and consistent formulation. The similarity in pH indicates that the active compounds, primarily capsaicinoids, were effectively extracted and retained their inherent acidic properties.

3.2 Effect of Chili Extract on Weed Germination and Growth

The efficacy of chili extract in controlling weed populations was evaluated over a 90-day period. Figure 2 illustrates the dynamic changes in the number of newly germinated weeds for both barnyard grass and sensitive plant across the experimental groups.

Figure 1 The homogeneous chili extract used in this research after 24 hours maceration

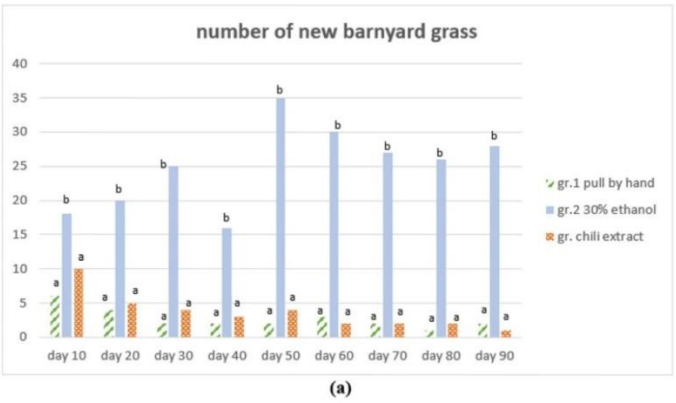

Figure 2 Effect of chili extract on the number of new germinated weeds: (a) barnyard grass and (b) sensitive plant The x-axis is time(day), and y-axis is number of new weeds (plants/area)

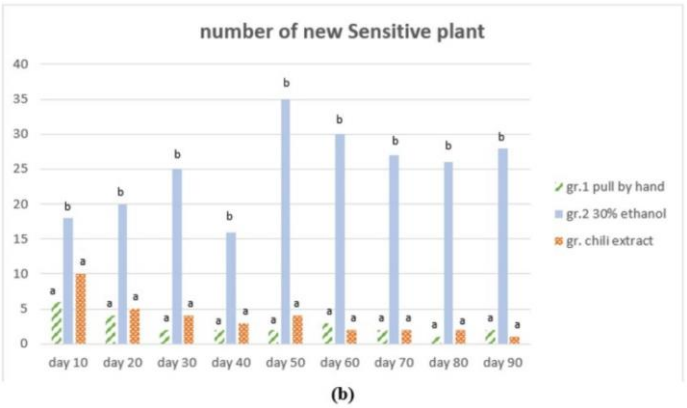

Figure 2 (Continuous)

As depicted in Figure 2, the application of chili extract significantly suppressed the germination and subsequent emergence of new weed seedlings for both barnyard grass and sensitive plant, particularly becoming evident from 20-day post-application onwards. The rate of new weed emergence in the chili extract group was markedly lower compared to the 30% ethanol-only group (Control Group 2). Importantly, the effectiveness of the chili extract treatment in reducing new weed germination was comparable to that achieved by manual weeding (Control Group 1), indicating its strong potential as a natural alternative to labor-intensive physical removal.

Further assessment of weed control focused on dry weight of weed stems at 30 days of age, as presented in Table 1.

Table 1 Effect of chili extract on dry weight of weed stem at 30 days of age

Treatment	Dried weight of Barnyard grass (mean±S.D., mg/Area)[1]	Dried weight of sensitive plant (mean±S.D., mg/Area)[1]
Pulling weeds by hand	N/A	N/A
30% ethanol	128.25±0.52b	95.52±0.41b
Chili extract	55.00±0.10a	11.00±0.19a
F-test	*	**
C.V. (%)	36.09	21.77

1 : Means followed by different letters in the same column are significantly different by LSD.

* = significant at $p < 0.05$

** = significant at $p < 0.01$

Note: N/A (Not applicable) for the "Pulling weeds by hand" group indicates the weeds were physically removed, hence no dry weight data was collected for comparative analysis of growth in this specific measurement.

Table 1 clearly illustrates that the chili extract significantly reduced the dry weight of weed stems for both barnyard grass and sensitive plant when compared to the 30% ethanol control. For barnyard grass, the dry weight decreased from 128.25 mg to 55.00 mg per stem, while for sensitive plant, it dropped from 95.52 mg to a remarkable 11.00 mg per stem. This substantial reduction in biomass further confirms the potent inhibitory effect of the chili extract on weed growth. The observed efficacy aligns with findings from other studies demonstrating that crude plant extracts, in both water and methanol, can inhibit weed growth and biomass accumulation (Sukkhang *et al.*, 2019); tamarind, lemongrass, and citronella grass extracts can inhibit Minnie root growth and dried weight. Furthermore, the properties of the chili extract in this study, which yielded a slightly weaker acid compared to standard capsaicinoids but retained its efficacy in an alcoholic solution, are consistent with the research by Mensin *et al.* (2021), which found that mixed peppermint extracts in alcohol could effectively inhibit goose grass germination. This suggests that the combination of active capsaicinoids and the ethanol solvent create a potent bio herbicidal action.

3.3 Effect of Chili extract on Thai Eggplant growth and Yield

The impact of chili extract application on the growth and yield of Thai eggplant was also critically assessed. Table 2 presents the summary of eggplant height and fruit yield across the treatment groups.

Table 2 Effect of chili extract on growth and yield of Thai eggplant

Treatment	Plant height (mean±SD, cm)[1]	Number of fruit/plant (mean±SD)[1]
Pulling weeds by hand	17.87±0.22b	5.25±0.30b
30% ethanol	10.59±0.20a	0.00±0.00a
Chili extract	16.48±0.63b	4.15±0.08b
F-test	*	*
C.V. (%)	5.71	1.93

1 : Means followed by different letters in the same column are significantly different by LSD.

* = significant at $p < 0.05$

As shown in Table 2, eggplant plants in the chili extract experimental group exhibited significantly higher average height (16.48 cm) compared to the 30% ethanol-only group (10.59 cm). Notably, the height achieved in the chili extract group was statistically comparable to that of the manual weeding control group (17.87 cm). This indicates that the chili extract did not negatively impact eggplant vegetative growth.

Moreover, the fruiting performance of eggplant was profoundly affected by the treatments. In the chili extract group (group 3), eggplant plants produced a substantial number of fruits, with an average of 4 fruits per plant harvested between 60 and 90 days after planting. This yield was significantly higher than the 30% ethanol-only group (group 2), where plants produced no collectible fruits, and many flowers aborted or failed to bloom.

Crucially, the fruit yield in the chili extract group was statistically comparable to that of the manual weeding control group (Group 1).

The observed beneficial effect on eggplant growth and yield, coupled with effective weed control, can be attributed to the properties of the chili extract and its solvent. Ethanol, as a solvent for chili extract, serves a dual purpose. Firstly, its polarity is congruent with capsaicinoids, facilitating the extraction of a high concentration of these active compounds. As discussed, these capsaicinoids, even in a slightly less acidic form than pure capsaicinoids, contribute to weed inhibition. Secondly, ethanol acts as a dehydrating agent, drawing water out of plant cells. This mechanism is particularly effective against tender weed cells, leading to their inhibition or death, similar to how fermented water containing alcohol and acid can control weeds in cassava fields without harming the main crop (Sila-on, 2021). This effect on weeds, combined with the normal growth of eggplant, suggests a degree of selectivity or a rapid degradation of the extract's phytotoxic effect on the more established crop. While previous research (Poonpiboonpipat and Wachoo, 2020) suggests that weak acid extracts may not offer permanent weed control and re-infestation can occur if weeds receive sufficient water, the integration of chili extract provides a promising approach that minimizes reliance on manual labor and harmful chemicals, without compromising crop yield.

4. Conclusion

This study definitely demonstrated the efficacy of using ethanol extract of leftover chili as an effective natural herbicide. The findings revealed that this ethanol extract of leftover chili significantly suppressed the germination and subsequent growth of key weeds like barnyard grass and sensitive plants. Quantitative analysis showed a remarkable reduction in weed dry weight, with barnyard grass decreasing from 128.25 to 55 milligrams per stem and sensitive plants from 95.52 to 11 milligrams per stem, when compared to the ethanol-only control group. Crucially, the weed control achieved through the ethanol extract application was comparable to that of laborious manual weeding, a traditional and time-consuming method.

Beyond just weed suppression, the research also confirmed the safety and beneficial impact of the ethanol extract of leftover chili on the main crop. Eggplant plants treated with the ethanol extract of leftover chili exhibited normal and even superior growth, demonstrating the highest average height and yielding more flowers and fruits. Specifically, eggplants in the experimental group produced an average of four fruits per plant, a yield significantly higher than the ethanol-only group and not statistically different from the manually weeded control group. This positive outcome on crop yield, coupled with effective weed control, highlights the extract’s potential as a selective herbicide that targets weeds without harming the desired crop.

These findings strongly suggest that the ethanol extract of leftover chili presents a variable and environmentally friendly alternative for weed control. It is particularly suitable for pre-planting weed control in agricultural plots, preparing the ground for optimal crop growth. Furthermore, for post-emergence weed control in established crops or seedlings, the targeted application of the ethanol extract of leftover chili directly onto weeds, while carefully avoiding contact with the main plants, can effectively control or reduce weed proliferation. The use of ethanol as a solvent facilitated the extraction of potent capsaicinoids and contributed to the weed suppression mechanism by dehydrating plant cells, a process consistent with observation from other alcohol-containing natural herbicides (Sila-on, 2021).

While this study offers compelling evidence for the effectiveness of ethanol extract of leftover chili as a natural weed control agent, its application needs further validation. Therefore, comprehensive testing in larger, diverse agricultural settings and under varying environmental conditions in highly recommended before its widespread adoption by farmers. This will ensure its consistent efficacy and practicality, paving the way for a sustainable and chemical-free approach to weed control in modern agriculture.

5. References

IFOAM Organics International. 2024. **The Principle of Health.** Available Source: https://www. ifoam.bio/why-organic/principles-organic-agriculture/principle-health, June 23, 2025.

Jirapong, L. 1999. **Preparation and Use of Herbal Plant for Pests Control.** Institute for the Promotion of Organic Agriculture and Farmer Schools, Department of Agricultural Extension, Bangkok. (in Thai)

Kaewnoi, A., Manok, S., Duanyai, S. and Hongprom, Y. 2018. Development of Capsaicin Extract from Rangsima Chili for Use in Making Chili Gel Product. **Chalermkanjana Academic Journal** 5(1): 48-54. (in Thai)

Kongsaengdao, S., Sukprasit, A. and Kongjiang, K. 2010. **Weed Control in Eggplant.** Experimental Report. Weed Research Group, Plant Protection Research and Development Office and Horticultural Research Center, Kanchanaburi. (in Thai)

Mensin, S., Boonkhan, W., Burutpakdi, W. and Promsorn, W. 2021. **Research Report on Biological and Substitute for Agricultural Chemicals for Cultivation of Environmentally Friendly Plants of High Areas.** High Area Research and Development Institute (Public Organization). (in Thai)

Nicholson, J. 2022. **The Effect of Alcohol on Plants.** Available Source: https://sciencing.com/ effect-alcohol-plants-8006187.html, August 30, 2024.

Pinsupa, J. and Nakhon Si, K. 2010. **Research Report on Research and Development of Substances from the Wild Spikenard for Weeds Prevention and Elimination.** Department of Agriculture (DOA). (in Thai)

Poonpiboonpipat, T. and Wachoo, M. 2020. The Efficiency of Certain Types of Weeding Substances on the Control of Nut Grass and Toxicity to Corn. **Journal of Agriculture Naresuan** 17(1): 48-57. (in Thai)

Preedapatarapong, N. 1994. **Production of Oleoresin and Oil Plant from Chili.** Graduate School, Kasetsart University, Bangkok. (in Thai)

Radosevich, S., Holt, J. and Ghersa, C. 2007. **Ecology of Weeds and Invasive Plants: Relationship to Agriculture and Natural Resource Management.** Wiley, New York.

Saeung, P. and Punya, N. 2022. Effects of *Ocimum canum* SIMS. Extract on Seed Germination and Growth of Plants. **Journal of Research and Development, Valaya Alongkorn Rajabhat University under the Royal Patronage (Science and Technology)** 17(2): 61-71. (in Thai)

Salzer, U.J. 1977. The analysis of Essential Oils and Extracts (Oleoresin) from Seasonings – a Critical Review. **CRC Critical Review in Food Science and Nutrition** 9(4): 345-373.

Sardana, V., Mahajan, G., Jabran, K. and Chauhan, B.S. 2017. Role of Competition in Managing Weeds. **Crop Protection** 95(Special Issue): 1-7.

Sayan, P. and Suwanprateep, S. 2015. **Research Report on Analysis of Capsaicin Content in Chili by Fourier Transform Infrared Spectroscopy.** Rajamangala University of Technology Suvarnabhumi. (in Thai)

Sila-on, P. 2021. Wisdom of the land | Bio-extract for grass knock out. **Golden Jubilee Museum of Agriculture.** Available source: http://www.youtube.com/watch?v=asGtUQ-sldc, October 28, 2021. (in Thai)

Soiklom, S., Prommais, P. and Klinchan, S. 2013. Efficiency of Pepper Extracts with Anti-bacterial Activity, pp. 286-291. *In* **Proceedings of the 51st Kasetsart University Annual Conference: Plant Science.** Kasetsart University, Bangkok. (in Thai)

Sukkhang, S., Promdaeng, S., Saejiew, A. and Suwanwong, S. 2019. Crude Extracts from Tamarind Shells (*Tamarindus indica* L.), Lemon Grass (*Cymbopogon citratus* Stapf.) and Citronella Grass (*Cymbopogon nardus* Rendle.) Inhibit Germination and Growth of Minnieroot (*Ruellia tuberosa* Linn.). **Agricultural Science and Management** 2(3): 29-36. (in Thai)

Tosena, K., Thumsaen, B., Songsri, P. and Konkhamdee, S. 2018. Growth Inhibitors of Some Weeds and Crops by Using Wood Vinegar in Combination with Pre-Emergence Herbicides. **Kaen Kaset Journal** 46(5): 901-910. (in Thai)

Urit, T. 2020. **Research Report on Adding Value to Organic Pepper Leaves from Agricultural Waste into Commercial Prebiotic Herbal Fermentation Products.** Naresuan University. (in Thai)

Recent Science and Technology

Journal homepage: https:// www.tci-thaijo.org/index.php/rmutsvrj/index

ISSN: 3057-0786 (Online)

Research Article

Growth Performance of Green Oak, Red Oak, and Green Cos in a Deep Flow Technique Hydroponic System

Poonnanan Phankaen [a *] and Warawut Kumpanuch [b]

[a] *Valaya Alongkorn Rajabhat University under the Royal Patronage Sa kaeo, Valaya Alongkorn Rajabhat University under the Royal Patronage, Pathum Thani 13180, Thailand.*

[b] *Administration Program, Faculty of Humanities and Social Sciences, Valaya Alongkorn Rajabhat University under the Royal Patronage, Pathum Thani 13180, Thailand.*

Article history:

Received: 2024-12-08
Revised: 2025-06-25
Accepted: 2025-07-07

Keywords:

Green Oak;
Red Oak;
Green Cos;
Deep Flow Technique

ABSTRACT

This study examined the growth performance and economic returns of three types of salad vegetables grown in a closed greenhouse using a deep flow technique (DFT) hydroponic system and adjusted to an electrical conductivity (EC) of 1.2–1.8 mS/cm and a pH of 5.6–6.5. The solution contained two balanced stock solutions: Stock A (N, P, K, Mg, S, Mo, B, Zn, Cu, and Mn) and Stock B (Ca and Fe). The study was conducted in Non Mak Khaeng, Watthana Nakhon, Sa Kaeo, Thailand, from March to April, 2024, utilizing a completely randomized design (CRD) with salad vegetable types as the treatment factor. Three lettuce varieties were tested: Green Oak, Red Oak, and Green Cos, with five replications of 10 plants each. The results revealed that Green Cos exhibited the highest growth performance in terms of root length (30.97 ± 0.32 cm), canopy height (19.33 ± 0.25 cm), and weight per plant (162.40 ± 5.29 g), with statistically significant differences ($p<0.05$) compared with Green Oak and Red Oak. However, Green Oak was recorded for the highest number of leaves (22.00 ± 1.00 leaves per plant). Survival rates were consistent at 100% across all three types. From an economic perspective, Green Cos yielded the highest profit of 4,872.54 THB, followed by Green Oak and Red Oak with profits of 4,526.94 THB and 3,867.88 THB, respectively. This research can be applied to the planning of salad vegetable production in a DFT hydroponic system to align with market goals. For example, it can help increase yields to meet the demands of health-conscious consumers, enhance competitiveness in the market, and ensure stable long-term income. Additionally, this approach supports the development of sustainable agricultural practice.

1. Introduction

Lettuce (*Lactuca sativa* L.), a plant commonly known as lettuce, is one of the most renowned leafy greens in the world and is in high demand both for consumption and export. This is due to its diverse nutritional value and beneficial antioxidant properties that promote health. Popular varieties of lettuce include Green Oak, Red Oak, and Green Cos, which are widely appreciated for their unique flavors and vibrant colors (Jiangseubchatveera *et al.*, 2023; Shi *et al.*, 2022). Additionally, lettuce is predominantly consumed fresh, making meticulous care essential throughout the cultivation process. Proper attention ensures that consumers receive high-quality produce that is free from toxic residues and contamination by harmful chemicals or microorganisms. These factors are crucial to lettuce cultivation and are the foundation for ensuring consumer confidence in the safety and quality of the produce (Lita, 2020).

In modern agriculture, farmers face numerous challenges that impact both the quantity and quality of production. Common issues include water scarcity, limited arable land, unpredictable climate changes, and outbreaks of plant diseases and pests. These factors often drive farmers to extensively use chemicals

* **Corresponding author.**

E-mail address: *poonnanan@vru.ac.th*

Cite this article as:

Phankaen, P. and Kumpanuch, W. 2026. Growth Performance of Green Oak, Red Oak, and Green Cos in a Deep Flow Technique Hydroponic System. **Recent Science and Technology** 18(1): 265591.

https://doi.org/10.65411/rst.2026.265591

in cultivation, resulting in chemical residues in soil and crops, environmental toxicity, and health risks for both farmers and consumers. Additionally, traditional soil-based cultivation is susceptible to contamination by microorganisms, particularly in plant parts that come into direct contact with the soil (Siringam *et al.*, 2015). These challenges make achieving sustainable and efficient agricultural production increasingly difficult. Therefore, lettuce producers must carefully plan their cultivation to maximize returns in terms of yield, quality, and consumer benefits. In recent years, hydroponic technology has been adopted by farmers for its ability to accurately calculate fertilizer and nutrient formulas, preventing toxic or heavy metal residues in crops. This method aligns with policies aimed at reducing chemical use in pest management, enabling the production of high-quality crops that better meet market demands (Ekoungoulou and Mikouendanandi, 2020).

One of the most popular hydroponic techniques is the Deep Flow Technique (DFT), which continuously circulates nutrient-enriched water through plant roots. This technique ensures a steady supply of nutrients and oxygen to the roots, reduces water usage, and enhances plant growth efficiency. Furthermore, the DFT hydroponic system allows for easy environmental adjustments, making it suitable for cultivating various crops. In hydroponic systems, nutrient solutions are regulated by two key parameters, including pH and electrical conductivity (EC). Maintaining a stable pH level is crucial for optimal nutrient absorption by the roots. Exposure to solutions with excessively low pH can damage plants, while EC levels measure the nutrient concentration in the solution, requiring regular monitoring to ensure adequate nutrient supply. Each crop has specific optimal ranges for pH and EC, which must be managed carefully for successful cultivation (Pramono *et al.*, 2020).

The evaluation focuses on key parameters such as the number of leaves, root length, plant weight, canopy height, survival rate, and economic returns from the sale of the produce. The findings of this research are expected to provide valuable insights for farmers and agricultural entrepreneurs seeking to adopt hydroponic systems for lettuce production. Moreover, integrating innovative techniques like hydroponics into agricultural practices is anticipated to improve efficiency and foster sustainable farming.

2. Materials and Methods

2.1 Experimental Design

The study on the growth, yield quality, and economic returns of three lettuce varieties was conducted at the researchers would like to express their gratitude to Agricultural Learning Center of General Prem Tinsulanonda Statesman Foundation, Non Mak Khaeng Subdistrict, Watthana Nakhon District, Sa Kaeo province, Thailand. The experiment was designed using a completely randomized design (CRD), with three lettuce varieties as treatments: Green Oak, Red Oak, and Green Cos. Each treatment was replicated five times, with 10 plants per replication. The study aimed to analyze the number of leaves, root length, canopy height, fresh plant weight, and survival rate of the lettuce varieties, as well as to compare the profits generated from cultivating the three lettuce varieties per production cycle in the experimental greenhouse.

2.2 Preparation of the Greenhouse for Lettuce Cultivation in a Deep Flow Technique (DFT) Hydroponic System

The greenhouse used in this experiment had dimensions of 6 x 12 x 3 meters (width x length x depth), providing an internal area of 72 square meters. The roof was covered with 150-micron plastic, and insect nets with a mesh size of 40 were installed to protect the crops. The cultivation was conducted using DFT hydroponic system in which plant roots are immersed in nutrient solution containers with a solution depth of approximately 0.15 – 0.20 meters.

For this study, the greenhouse housed aluminum planting channels capable of accommodating 288 lettuce plants. There were four planting channels, each measuring 0.45 x 11 x 0.25 meters (width x length x depth). Each channel contained 72 planting holes spaced 0.15 meters apart in a staggered arrangement.

The irrigation system operated as a recirculating system, where nutrient solution flowed through each channel and drained into a 500-liter mixing tank. The water level in the tank was controlled by a float valve, and a pump circulated the solution back to the planting channels. The pump's pressure distributed nutrients evenly and increased oxygen levels for the plant roots, as illustrated in Figure 1.

Figure 1 Characteristics of a vegetable cultivation greenhouse (a) greenhouse, (b) growing trough, and (c) tank for mixing fertilizers A and B.

2.3 Nutrient Management and Application

The plant nutrient solution consists of two stock solutions. Stock A contains N, P, K, Mg, S, Mo, B, Zn, Cu, and Mn, while Stock B contains Ca and Fe. These two stock solutions must be prepared separately. To prepare the stock solutions, dissolve 1 kilogram of fertilizer in 10 liters of clean water, stir until completely dissolved, then seal the container and store it in a shaded area. When ready to use, measure equal amounts of Stock A and Stock B. Add Stock A to the mixing tank first, stir thoroughly until the solution is well-mixed, then add Stock B and stir again.

The adjustment of Stock A and Stock B is a crucial step in managing the nutrient levels for lettuce in the hydroponic system. In this study, a 500-liter mixing tank was used to

prepare the solution, and an electrical conductivity (EC) meter was employed to measure the total nutrients in the solution. The nutrient solution was adjusted to an EC range of 1.2–1.8 mS/cm, which is suitable for lettuce growth. Subsequently, the pH was adjusted to a range of 5.6-6.5 by gradually adding nitric acid. Nutrient adjustments were conducted daily at 6:00 AM and 6:00 PM to maintain consistent nutrient levels and ensure optimal growing conditions for the lettuce.

2.4 Lettuce Cultivation Method in a Hydroponic System

The seed germination process begins by soaking sponge growing media in clean water for 24 hours to ensure sufficient moisture. Seeds are then placed into the prepared sponge holes, pressing them lightly to a depth of approximately 0.5 centimeters to position them optimally for germination. The sponges are placed in seedling trays and covered with clear plastic to maintain appropriate humidity and temperature. The trays are kept in a shaded area, away from direct sunlight, which provides an ideal environment for lettuce germination. Moisture levels in the sponge media are regularly checked, and distilled water is added as needed to prevent dryness or over-saturation. On the fourth day, when seeds begin to germinate and develop cotyledons, the plastic cover is removed to allow the seedlings to receive adequate light and air circulation. Germinated seedlings are then transferred to a location with soft natural light to prevent elongation and encourage the development of roots and true leaves.

At 14 days old, the seedlings will have developed 2–3 true leaves and a fully established root system. The seedlings are carefully transplanted into the DFT hydroponic system to avoid damage to the roots and stems. After transplanting, the plants are consistently monitored and maintained. Daily inspections are conducted to observe growth and address any issues such as plant diseases or nutrient deficiencies. Any identified problems are resolved immediately. To prevent pest infestations, a diluted wood vinegar solution is sprayed once a week. At 42 days old, when the lettuce plants reach maturity and are ready for harvest, fertilizer application is stopped 5 days before harvesting to minimize chemical residues in the produce. Observations of lettuce growth are conducted at key stages of development, specifically at 7, 14, 28, and 42 days, as illustrated in Figure 2.

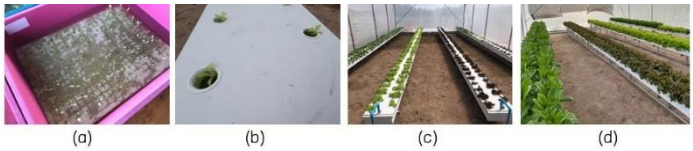

Figure 2 Vegetable cultivation (a) seedling nursery (7 days) (b) transferring seedlings to planting channels (14 days) (c) 28 days and (d) harvesting the produce (42 days)

2.5 Survival Rate and Economic Returns of Three Lettuce Varieties

The economic returns from the sale of three lettuce varieties per production cycle were calculated for a single greenhouse. Each greenhouse can accommodate 288 lettuce plants per cycle, with an average production cost of approximately 740 THB per cycle. The production cost includes materials such as seeds, AB fertilizer, sponges, and wood vinegar. The calculation excludes the costs of greenhouse construction, the hydroponic system, water, electricity, and labor. The lettuce is sold at a price of 120 THB per kilogram. The survival rate of the lettuce and the profit from sales are calculated as follows:

1. Number of surviving plants per cycle = (Survival rate (%) ×100)/288 plants

2. Revenue per greenhouse = Number of surviving plants per cycle × (Average plant weight (g)/1000 kg) × Selling price

3. Profit per greenhouse = Revenue per greenhouse - Production cost

2.6 Data Analysis

The recorded growth data, including the number of leaves, canopy height, root length, and fresh weight of lettuce, were analyzed for variance (Analysis of Variance; ANOVA). The mean values from the experiments were compared using Duncan's New Multiple Range Test (DMRT) at a 95% confidence level, performed with statistical software.

3. Results and Discussion

3.1 Comparison of Leaf Count, Root Length, Canopy Height, and Weight of Green Oak, Red Oak, and Green Cos Lettuce Grown in a Deep Flow Technique Hydroponic System

Each treatment was replicated 5 times with 10 plants per replicate to compare the leaf count, root length, canopy height, and weight of the lettuce varieties grown in a DFT hydroponic system. The findings are presented in Table 1.

The experiment measuring leaf count revealed that Green Oak had the highest average number of leaves at 22.00 ± 1.00 leaves per plant, which was significantly different ($p < 0.05$) from Red Oak and Green Cos, with average leaf counts of 15.33 ± 0.58 and 16.67 ± 1.15 leaves per plant, respectively. This suggests that Green Oak has a greater ability to produce leaves, potentially due to genetic and physiological factors that promote leaf growth. Leaves are critical for plants as they play a key role in photosynthesis, energy production, and nutrient provision for growth and development (Maren and Sergi, 2021). However, the experiment also showed that Green Cos exhibited the highest average canopy height at 19.33 ± 0.25 cm, which was significantly different ($p < 0.05$) compared to Green Oak and Red Oak, with average heights of 14.30 ± 0.26 cm and 13.53 ± 0.15 cm, respectively. This could be attributed to genetic factors and the superior vertical growth potential of Green Cos. A taller canopy height enhances light interception for photosynthesis, reduces evapotranspiration, and helps maintain temperature balance in the environment. Farmers often use canopy height and leaf density as key indicators for assessing plant growth,

yield potential, and planning crop management strategies (Buelvas *et al.*, 2019).

In Deep Flow Technique (DFT) hydroponic systems, efficient plant spacing is essential to maximizing yield and maintaining plant health. One of the key morphological traits that should guide spacing decisions is canopy height, which refers to the vertical extension of the plant's foliage. The average root length of Green Cos was the highest, measuring 30.97 ± 0.32 cm, which was significantly different ($p < 0.05$) from Green Oak and Red Oak, with root lengths of 27.10 ± 0.79 cm and 24.30 ± 0.97 cm, respectively. In DFT, plant roots are suspended in a continuously flowing nutrient solution, making root length and health critical for nutrient uptake. The extended root length of Green Cos increases the root surface area, allowing for greater contact with the nutrient solution. This enhances the plant's ability to absorb water and essential nutrients more efficiently. Plant roots play a critical role in water and nutrient absorption, which are essential factors for growth and yield. Longer and well-developed roots provide a larger surface area for nutrient uptake and enable plants to access nutrients in the solution more effectively compared to shorter roots. Therefore, the longer roots of Green Cos indicate a higher nutrient absorption potential, resulting in healthier growth and the highest weight per plant among the lettuce varieties studied in this research (Cochavi *et al.*, 2020). The average weight per plant also showed that Green Cos had the highest weight at 162.40 ± 5.29 grams, which was significantly different ($p < 0.05$) from Green Oak and Red Oak, with weights of 152.40 ± 5.29 grams and 133.33 ± 16.65 grams per plant, respectively. A higher weight per plant indicates greater yield, making Green Cos the most suitable choice for hydroponic production aimed at commercial sales.

3.2 Survival Rate and Profit Comparison of Three Lettuce Varieties

A comparison of the survival rate, total revenue, and profit of three lettuce varieties including Green Oak, Red Oak, and Green Cos grown in a DFT hydroponic system revealed that all three varieties had a survival rate of 100%. This indicates that the cultivation processes, fertilization, and environmental controls in this study were well-suited to support the growth of all three varieties.

Economic calculations in this study were based on one production cycle within a single greenhouse unit covering 72 m² and accommodating 288 lettuce plants. Green Cos generated the highest profit at 4,872.54 THB, followed by Green Oak with a profit of 4,526.94 THB, and Red Oak with the lowest profit at 3,867.88 THB (Table 2). These results highlight that Green Cos is the most commercially valuable lettuce variety, particularly for cultivation that prioritizes high yields and profitability. Green Oak, while slightly less profitable, is well-suited for markets that value lettuce with dense leaf production. In contrast, Red Oak, although yielding lower profits, stands out for its vibrant and appealing coloration, making it attractive for premium and decorative markets. Green Cos exhibited unique characteristics, including vertical growth, dark green leaves, and tightly layered foliage, with the tallest canopy height among the three varieties (Figure 3). These features make Green Cos an optimal choice for hydroponic production focused on maximizing both yield and economic returns.

Table 1 Comparison of leaf count, root length, canopy height and weight of Green Oak, Red Oak, and Green Cos lettuce grown in a deep flow technique hydroponic system

Cultivars	Number of leaves per plant	Root Length (cm)	Canopy Height (cm)	Weight /Plant (g)
Green Oak	22.00 ± 1.00^{a}	27.10 ± 0.79 ^{b}	14.30 ± 0.26^{b}	152.40 ± 5.29 ^{b}
Red Oak	15.33 ± 0.58^{b}	24.30 ± 0.97 ^{c}	13.53 ± 0.15^{c}	133.33 ± 16.65^{c}
Green Cos	16.67 ± 1.15^{b}	30.97 ± 0.32^{a}	19.33 ± 0.25^{a}	162.40 ± 5.29^{a}

^{a,b,c} Statistically significant differences at the 95% ($p < 0.05$) were determined using Duncan' new multiple rang test (DMRT)

Table 2 Survival rate of lettuce and comparison of profitability for growing three types of lettuce per production cycle

Cultivars	% Survival	Survival/ Greenhouse (plant)	Weight (g)	Income (Bath)	Profit (Bath)
Green Oak	100	288	152.40	5266.94	4,526.94
Red Oak	100	288	133.33	4,607.88	3,867.88
Green Cos	100	288	162.40	5612.54	4,872.54

(a) (b) (c)

Figure 3 Characteristics of (a) Green Oak (b) Red Oak and (c) Green Cos grown in a deep flow technique hydroponic system

4. Conclusion

The experiment comparing the growth of Green Oak, Red Oak, and Green Cos lettuce in a DFT hydroponic system found that Green Cos exhibited the most outstanding performance in terms of root length (30.97 ± 0.32 cm), canopy height (19.33 ± 0.25 cm), and weight per plant (162.40 ± 5.29 g). This reflects its superior nutrient absorption efficiency and growth potential, making it highly suitable for commercial production. However, Green Oak had the highest number of leaves (22.00 ± 1.00 leaves per plant), making it ideal for markets demanding products with dense leaf structures. Although Red Oak yielded less than the other two varieties, it stood out for its vibrant coloration and visual appeal, making it well-suited for niche markets that prioritize attractive appearance. In terms of profitability, Green Cos generated the highest profit at 4,872.54 THB, followed by Green Oak at 4,526.94 THB, and Red Oak at 3,867.88 THB. These results indicate that Green Cos is the most suitable lettuce variety for commercial production, particularly for achieving high yields and profits. This research provides valuable insights for planning lettuce production in hydroponic systems to align with market goals, such as increasing yields for general markets, developing premium-grade products, or catering to health-conscious consumers.

For farmers, the findings highlight the advantages and limitations of each lettuce variety, enabling efficient crop planning. This includes selecting suitable lettuce varieties based on available resources and production goals, reducing costs by optimizing cultivation processes tailored to each plant's characteristics, and managing yields to meet market demand. Moreover, the research supports the adoption of hydroponic systems for sustainable agriculture by reducing water and chemical usage, minimizing pest risks, and adding value to products for export or premium markets. It also serves as a guide for advancing the agricultural profession in an era where consumers emphasize food quality and safety.

5. Acknowledgments

The researchers would like to express their gratitude to the researchers would like to express their gratitude to Agricultural Learning Center of General Prem Tinsulanonda Statesman Foundation, Non Mak Khaeng Subdistrict, Watthana Nakhon District, Sa Kaeo province, Thailand for providing the research facilities.

6. References

Buelvas, R.M., Adamchuk, V.I., Leksono, E., Tikasz, P., Lefsrud, M. and Holoszkiewicz, J. 2019. Biomass estimation from canopy measurements for leafy vegetables based on ultrasonic and laser sensors. **Computers and Electronics in Agriculture** 164(104896): 104896.

Cochavi, A., Cohen, I.H. and Rachmilevitch, S. 2020. The role of different root orders in nutrient uptake. **Environmental and Experimental Botany** 179(104212): 104212.

Ekoungoulou, R. and Mikouendanandi, E.B.R.M. 2020. Lettuce (*Lactuca sativa* L.) production in republic of Congo using hydroponic system. **OAlib** 7(5): 1-17.

Jiangseubchatveera, N., Saechan, C., Petchsomrit, A., Treeyaprasert, T., Leelakanok, N. and Prompanya, C. 2023. Phytochemicals and antioxidant activities of red oak, red coral and butterhead. **Tropical Life Sciences Research** 34(1): 1-17.

Lita, B.C. 2020. Growth and yield performance of lettuce (*Lactuca sativa* L.) fertilized with varying levels of compost. **International Journal of Advances in Social and Economics** 4(2): 50-56.

Maren, M. and Sergi, M. 2021. Hormonal impact on photosynthesis and photoprotection in plants. **Plant Physiology** 185(4):1500-1522.

Pramono, S., Nuruddin, A. and Ibrahim, M.H. 2020. Design of a hydroponic monitoring system with deep flow technique (DFT). **AIP Conference Proceedings** 2217: 030195.

Shi, M., Gu, J., Wu, H., Rauf, A., Emran, T.B., Khan, Z., Mitra, S., Aljohani, A.S.M., Alhumaydhi, F.A., Al-Awthan, Y.S., Bahattab, O., Thiruvengadam, M. and Suleria, H. A.R. 2022. Phytochemicals, nutrition, metabolism, bioavailability, and health benefits in lettuce A comprehensive review. **Antioxidants (Basel, Switzerland)** 11(6): 1158.

Siringam, K., Jirasutas, P. and Sawaengmee, W. 2015. Effect of growing methods on growth aad pigment concentrations of leaf lettuce (*Lactuca sativa* var. *crispa* L.). **Phranakhon Rajabhat Research Journal** 10(1): 82-95.

Recent Science and Technology 18(1): 263551

Recent Science and Technology

Journal homepage: https:// www.tci-thaijo.org/index.php/rmutsvrj/index

ISSN: 3057-0786 (Online)

Research Article

Effects of Seed Soaking in Cucumber and Carrot Aqueous Extract on Germination and Vigor of Rice Seeds

Pharadee Saeung *

Agricultural Program, Science and Technology Faculty, Phranakhon Si Ayutthaya Rajabhat University, Phra Nakhon Si Ayutthaya, Phra Nakhon Si Ayutthaya 13000, Thailand.

Article history:

Received: 2024-05-30
Revised: 2025-11-03
Accepted: 2025-11-26

Keywords:

Seed soaking;
Cucumber aqueous extract;
Carrot aqueous extract;
RD 49 rice variety

ABSTRACT

Rice seed production in Thailand faces problems related to poor seed quality, resulting in yields not meeting farmers' expectations. This research studies the effects of soaking rice seeds in cucumber and carrot extracts prior to planting on their germination and vigor qualities. The hypothesis for this pre-treatment is that the technique could enhance seeding growth and increase their average yield. The rice seed variety tested was RD49. The experiment consisted of eight treatments: (1) no soaking, (2) soaking in distilled water, (3) soaking in 10% cucumber aqueous extract, (4) soaking in 20% cucumber aqueous extract, (5) soaking in 30% cucumber aqueous extract, (6) soaking in 10% carrot aqueous extract, (7) soaking in 20% carrot aqueous extract, and (8) soaking in 30% carrot aqueous extract. The results showed no statistical differences in terms of germination percentage among eight seed soaking treatments. However, soaking in 20% cucumber aqueous extract (treatment 4) improved seed vigor. The seedling growth rate (8.83 mg/plant) under this treatment was higher than that of treatments (1) and (2), in which the seeds underwent no treatment and were soaked in distilled water. Seedling growth, measured in terms of plant length (7.52 cm) and root length (8.52 cm), was highest in treatment (4) compared with all other treatments (1-3 and 5-8).

1. Introduction

Rice is an important food crop for Thai people. Farmers produce rice for both domestic and international markets. In 2023, the production of main-season and off-season rice reached as high as 33,852 thousand tons (Office of Agricultural Economics, 2024). Currently, rice seed production is insufficient to meet demand, and the use of poor-quality seeds has adverse effects on both yield and grain quality (Khatsakan and Kochsamrong, 2023).

The current situation of rice seed production for distribution to farmers shows that the types of seeds produced often do not match grower demand, resulting in surplus seed stocks that deteriorate in quality (Prasertsak *et al.*, 2010). These seeds exhibit low germination percentages and weak seedling vigor. At present, rice seeds produced by government and private sectors total approximately 265,000 tons per year, accounting for only 26.50% of total seed demand. Thus, Thailand's rice production system still lacks a significant quantity of high-quality rice seeds for cultivation each year (Pecharvut *et al.*, 2022). The estimated annual demand for rice seeds through market circulation is about 600,000 tons (Prasertsak, 2022).

In addition, rice and agricultural production in Thailand heavily rely on the use of chemical inputs. In 2022, the import volume of agricultural hazardous substances exceeded 113,640 tons (Office of Agricultural Regulation, 2023). If farmers apply these chemicals without a proper control, it may lead to chemical residue accumulation in agricultural products and farmland. Therefore, promoting good agricultural practices is one approach to help reduce chemical use in rice production.

One example is the pre-germination treatment of rice seeds to enhance germination ability and seed quality using water or certain chemical solutions (Wetchakama and Khaengkhan, 2018). High-quality seeds directly improve both the yield and quality of rice production. For instance, soaking rice or maize seed and cassava stalks in boron and zinc solutions enhances

* **Corresponding author.**

E-mail address: *parad.nuch@gmail.com*

Cite this article as:

Saeung, P. 2026. Effects of Seed Soaking in Cucumber and Carrot Aqueous Extract on Germination and Vigor of Rice Seeds. **Recent Science and Technology** 18(1): 263551.

their strength and nutrient uptake, especially in sandy soils (Mongon *et al.*, 2017). Similarly, soaking glutinous rice seeds ("Khao Niao Khiew Ngu") in bio-fermented liquid fertilizer increases germination and seedling growth compared to soaking in plain water (Junta *et al*., 2018).

Soaking seeds in water or plant extracts is therefore an interesting method to improve seed quality prior to planting. The germination process begins when seeds absorb moisture, followed by biochemical changes leading to seedling and strong plant development. For example, soaking rice seeds in pig manure extract accelerates germination and promotes rapid shoot and root growth (Aroonrungsikul *et al*., 2014).

In this study, cucumber and carrot were selected as target plants for extract preparation. Cucumber is an easily cultivated vegetable that can be grown all year round. Its major nutritional composition includes 83.19% moisture content, 3.45% protein, 1.05% fat, and 11.45 °Brix sugar content (Minh, 2019). It also contains dietary fiber, vitamins, and natural antioxidants (Insanu *et al*., 2002). Carrot, on the other hand, is rich in beta-carotene, vitamin A, and other nutrients (Chainok, 2011). Extracts from these plants have been reported to enhance plant growth. For example, Abou El-Ghit (2016) tested cucumber and carrot seed extracts at concentrations of 10%, 30%, and 60%, and found that these extracts increased germination and growth in beans, possibly due to the auxin-like effect of the extracts.

Therefore, this research aims to investigate the effects of soaking rice seeds in cucumber and carrot extracts on seed germination and vigor. The findings of this study could serve as a guideline for improving rice seed quality using natural plant-based extracts, reducing production costs, adding value to agricultural products, and promoting higher rice productivity in the future.

2. Materials and Methods

The rice seeds used in this experiment were of the RD49 variety, which were provided by the Phra Nakhon Si Ayutthaya Rice Research Center. The seeds were harvested in May 2022 and stored in a temperature-controlled room at 5°C. The experiment was conducted during May–June 2023 in the laboratory of the Department of Agricultural Science, Faculty of Science and Technology, Phra Nakhon Si Ayutthaya Rajabhat University.

Preparation of cucumber and carrot extracts was modified from the methods of Teixeira *et al*. (2021) and Chatiyanon *et al*. (2014). Fresh cucumber and carrot fruits were peeled and finely chopped into pieces approximately 2 millimeters in size. The chopped materials were soaked in distilled water at a ratio of 5% (w/w) (20 g of cucumber or carrot per 400 mL of distilled water) for 12 hours. The mixtures were then filtered through muslin cloth to obtain the crude aqueous extracts. These extracts were subsequently diluted with distilled water to achieve the desired concentrations according to the experimental treatments, which were as follows:

1) No soaking (control),
2) Soaking in distilled water
3) Soaking in 10% cucumber extract soaking
4) Soaking in 20% cucumber extract
5) Soaking in 30% cucumber extract
6) Soaking in 10% carrot extract
7) Soaking in 20% carrot extract
8) Soaking in 30% carrot extract

For the soaking treatments, rice seeds were soaked in the prepared solutions for 24 hours. After soaking, the seeds were incubated by placing them on moist germination paper and wrapping them for 48 hours before sowing (Tipparak and Aroonrungsikul, 2011).

Statistical analysis was conducted using a Completely Randomized Design (CRD). Mean comparisons were performed using Duncan's New Multiple Range Test (DMRT).

Seed quality testing was performed according to standard procedures for seed quality assessment as follows:

1. Seed Germination Test

Germination was tested using 100 seeds per replicate, with four replications, following the *Top of Paper* method at 25°C under 12 hours of lighting. Normal seedlings those that germinated completely with all essential structures intact were counted. The first count was taken on day 5 after sowing, and the final count on day 14 after sowing. The total number of normal seedlings was recorded and reported as germination percentage, according to the International Seed Testing Association (ISTA, 2011).

2. Seed Vigor

2.1 Germination Index (GI)

The germination index was tested in the same way as the standard germination test. However, for this parameter, the number of normal seedlings was recorded daily throughout the test period (from day 1 to day 14 after sowing), following the method of Duangpatra (1986). The germination index was calculated using the formula:

$$GI = \sum \left\{ \frac{\text{Number of normal seedlings}}{\text{Days after sowing}} \right\}$$

2.2 Seedling Growth Rate (SGR)

After completion of the standard germination test, normal seedlings were collected, and both shoots and roots were separated. These were oven-dried at 80°C for 24 hours. The seedling growth rate was calculated as:

$$SGR = \frac{\text{Dry weight of normal seedlings}}{\text{Number of normal seedlings}}$$

2.3 Seedling Growth Measurement

Seeds were germinated using the *Top of Paper* method in darkness at 25°C for 7 days. After germination, normal seedlings were selected and measured for shoot length, which was reported as average shoot length (ISTA, 1995). Root length was also measured and reported as average root length.

3. Results and Discussion

The results of soaking rice seeds in cucumber and carrot extracts on seed germination (Table 1) showed that soaking seeds in 20% cucumber extract, as well as in 10%, 20%, and 30% carrot extracts, distilled water, and the unsoaked control, produced no statistically significant differences in germination percentage, which ranged from 97% to 100%. In contrast, soaking in 10% and 30% cucumber extracts resulted in slightly lower germination percentages (95%). Overall, the germination percentages among all treatments were relatively similar. This may be because the rice seeds used in the experiment had high initial viability, resulting in limited observable differences in germination response among treatments. This finding is consistent with the study by Naenfan and Pagamas (2020), who examined the seed priming of *Tagetes patula* (French marigold) and found that freshly produced, high-vigor seeds exhibited high germination regardless of the priming treatments applied.

3.1 Seed Vigor

The effects of soaking rice seeds in cucumber and carrot extracts on seed vigor included the germination index, seedling growth rate (Table 2), shoot length, and root length (Figure 1).

For the germination index, soaking seeds in 20% carrot extract resulted in the highest germination index (44.67). All soaking treatments, whether using distilled water or various extract concentrations, showed higher germination index values than the unsoaked control.

Regarding the seedling growth rate, soaking rice seeds in different concentrations of the extracts produced growth rates ranging from 8.20 to 9.23 mg per seedling, which were higher than those of seeds soaked in distilled water and those without soaking.

For shoot length, soaking seeds in cucumber extract at concentrations of 10%, 20%, and 30% resulted in the highest average shoot lengths (6.89–7.60 cm), which were greater than those obtained from soaking in carrot extract, distilled water, or without soaking.

As for root length, soaking in 20% cucumber extract yielded the greatest average root length (8.52 cm), exceeding that of the 10% and 30% cucumber extract treatments, as well as those using carrot extract, distilled water, and the untreated control.

The results of this study revealed that soaking rice seeds in cucumber and carrot extracts did not significantly affect seed germination percentage. However, it enhanced seed vigor, as indicated by higher germination index, seedling growth rate, and seedling development compared with the unsoaked control. Among the treatments, soaking seeds in 20% cucumber extract produced the highest germination percentage and seed vigor, surpassing those soaked in distilled water or other extract concentrations.

Table 1 Effects of cucumber aqueous extracts and carrot aqueous extracts on germination of rice seed RD49 variety

Soaking Treatments	Germination (%)
no soaking	97 ab
soaking in distilled water	98 ab
10% cucumber aqueous extract	95 b
20% cucumber aqueous extract	98 ab
30% cucumber aqueous extract	95 b
10% carrot aqueous extract	99 a
20% carrot aqueous extract	99 a
30% carrot aqueous extract	100 a
F-test	*
C.V.(%)	2.1

Means within the same column followed by the same letters indicate no significant differences among treatment using by DMRT, * Significant different at 0.05 (P=0.019)

Table 2 Effects of cucumber aqueous extracts and carrot aqueous extracts on germination index and seedling growth rate of rice seed RD49 variety

Soaking Treatment	Germination Index	Seedling Growth Rate (SGR) (mg per plant)
no soaking	25.95 e	7.25 c
soaking in distilled water	38.00 bc	7.35 c
10% cucumber aqueous extract	39.08 ab	9.23 a
20% cucumber aqueous extract	37.67 bc	8.83 ab
30% cucumber aqueous extract	30.42 de	8.75 ab
10% carrot aqueous extract	32.00 cd	8.40 ab
20% carrot aqueous extract	44.67 a	8.20 b
30% carrot aqueous extract	33.82 bcd	8.78 ab
F-test	**	**
C.V.(%)	11.1	6.9

Means within the same column followed by the same letters indicate no significant differences among treatment using by DMRT, ** Significant different at 0.01 (P=<0.001)

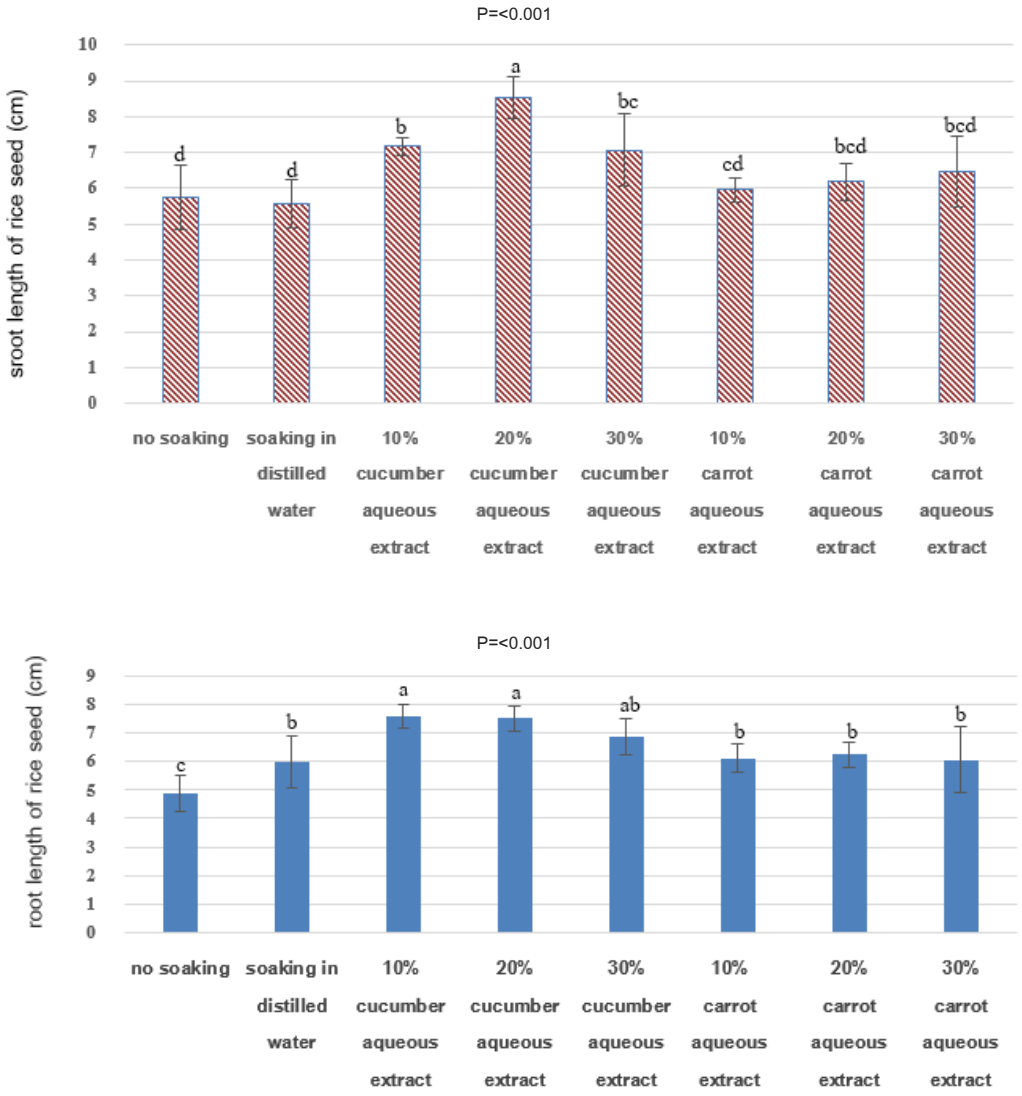

Figure 1 Effects of cucumber aqueous extracts and carrot aqueous extracts on shoot length and root length of rice seed RD49variety (Means within the same label bar followed by the same letters indicate no significant differences among treatment using by DMRT, ** Significant different at 0.01

This finding is consistent with U-sungnoen *et al*. (2012), who reported that soaking rice seeds in diluted pig manure extract (1:20 ratio) did not affect seed germination percentage but improved seed vigor and seedling quality. However, higher extract concentrations reduced rice seedling growth.

Furthermore, Yunusa *et al*. (2018) found that aqueous cucumber extracts contained total phenolic compounds (TPC) of 10.02 mg GAE/g. Phenolic compounds play an important role in regulating metabolic processes related to protein synthesis and the production of antioxidant-related enzymes. These antioxidants scavenge free radicals generated within cells during seed germination (Hayat *et al*., 2010). The presence of antioxidant compounds helps maintain the integrity of cellular membranes, thereby enhancing photosynthesis and metabolic efficiency in rice seedlings. In addition, cucumbers contain approximately 20 mg of vitamin C per 100 g of edible portion, while carrots contain about 3 mg per 100 g (Department of Health, 2018). Vitamin C is a small-molecule antioxidant derived from dietary sources (Sawadsitung, 2025). It acts as a free radical scavenger, preventing oxidative damage to cellular components within the seed, thereby reducing seed deterioration (Siri, 2015). When seed deterioration occurs, structural, physiological, and biochemical changes take place within the seeds, including damage to cell membranes, reduction of enzymatic activity, decrease respiration rate, increase free fatty acid content. The afore-mentioned effects, in turn, course the reduction of germination rate, storability, and seedling vigor (Duangpatra, 1986) and, therefore, minimizing seed deterioration helps preserve seed quality, maintaining high germination and vigor.

4. Conclusion

The results of this study indicate that soaking rice seeds in cucumber and carrot extracts influenced seed vigor. Soaking seeds in 20% cucumber extract produced the highest seed vigor, particularly in terms of seedling growth, compared with the unsoaked control, soaking in distilled water, soaking in carrot extract, and other concentrations of cucumber extract. In addition, the seedling growth rate of seeds soaked in 20% cucumber extract was higher than that of seeds soaked in distilled water or those that were not soaked.

5. Recommendations

Further studies should include additional concentrations of the extracts, such as 5%, 15%, and 25%, to determine the optimal level for promoting seed vigor and seedling growth. Moreover, it is recommended to extend the experiment to other rice varieties or different plant species to evaluate whether soaking seeds in these extracts produces similar improvements in seed quality and vigor. In addition, field experiments should be conducted to investigate the effects of seed soaking with the extracts on plant growth, yield quantity, and crop quality before applying this novel practice.

6. Acknowledgments

The author would like to express her sincere gratitude to the Ayutthaya Rice Research Center for providing rice seeds used in this study, and to the Faculty of Science and Technology, Phranakhon Si Ayutthaya Rajabhat University, for providing laboratory equipment and research facilities.

7. References

Abou El-Ghit, H.M. 2016. Physiological allelopathic effect of aqueous extracts of cucumber, carrot, onion, and garlic seeds on germination and growth of pea. **Journal of Pharmaceutical, Chemical and Biological Sciences** 4(1): 13-19.

Aroonrungsikul, P., Junkwon, P. and Rodraksa, N. 2014. Seed germination and seedling growth enhancement of suphanburi # 1 rice seed variety, pp 249-259. *In* **Proceedings of 11th National seed conference 2014.** Text and Journal Publication Company Limited, Bangkok. (in Thai)

Chainok, K. 2011. Vegetable and fruit juices for health. **Medicinal Plant Newsletter** 28(4): 9-20. (in Thai)

Chatiyanon, B., Wongwattana, C. and Phornphisutthimas, S. 2014. The effect of aqueous extract from some plant leaves of lamiaceae on seed germination and seedling growth of *Pennisetum setosum* L. **Princess of Naradhiwas University Journal** 6(3): 121-132. (in Thai)

Department of Health. 2018. **Food Composition Table of Thai Food.** War Veterans Organization Officer of Printing Mill, Bangkok. (in Thai)

Duangpatra, J. 1986. **Seed Technology** (2nded). Agriculture Book Group, Bangkok. (in Thai)

Hayat, Q., Hayat, S., Irfan, M. and Ahmad, A. 2010. Effect of exogenous salicylic acid under changing environment: A Review. **Environmental and Experimental Botany** 68(1): 14-25.

Insanu, M., Zahra, A.A., Sabila, N., Silviani, V., Haniffadl,i A., Rizaldy, D. and Fidrianny, I. 2002. Phytochemical and antioxidant profile: cucumber pulp and leaves extracts. **Journal of Medical Sciences** 10(A): 616-622.

International Seed Testing Association (ISTA). 1995. **Handbook of Vigour Test Method 3rd Edition 1995**. International Seed Testing Association, Zurich, Switzerland.

International Seed Testing Association (ISTA). 2011. **International Rules for Seed Testing.** International Seed Testing Association, Bassersdorf, Switzerland.

Junta, K., Pokyada, S. and Buayen, N. 2018. Effects of bio-extract on the germination of rice seed (Kiaw Ngu Glutinous Rice). **Science and Technology RMUTT Journal** 8(1): 152-164. (in Thai)

Khatsakan, O. and Kochsamrong, M. 2023. The study on rice seed quality control system of Thai farmer. **Thai Rice Research Journal** 14(1): 89-101. (in Thai)

Minh, N.P. 2019. Production of cucumber (*Cucumis sativus* var. conomon) juice. **Research on Crops** 20(2): 369-375.

Mongon, J., Premprungwit, S., Senaphol, W. and Jantasorn, A. 2017. Increasing seedling vigor of rice, maize and cassava by soaking seeds and stem cuttings in Ca B And Zn solution. **Srinakharinwirot University Journal of Sciences and Technology** 9(18): 49-62. (in Thai)

Naenfan, S. and Pagamas, P. 2020. Effect of Nano-bubble priming on seed germination and seedling growth of France marigold. **Khon Kaen Agriculture Journal** 48(3): 515-526. (in Thai)

Office of Agricultural Economics. 2024. **Agricultural Statistics of Thailand 2025.** Ministry of Agriculture and Cooperatives, Bangkok. (in Thai)

Office of Agricultural Regulation. 2023. **Summary report on agricultural hazardous substances import in 2022 (Type of use).** Available Source: https://www.doa.go.th/ard/?page_id=386, December 15, 2023. (in Thai)

Pecharvut, W., Seesawat, N., Kesbut, D., Jirattivarutkul, K., Tongoun, S., Sriviroj, J. and Engchoun, P. 2022. **Research Report on Study on Rice Seed Production and Distribution for 2022 Year Final Report: Factors Affecting the Demand Rice Seed of Farmers in the Pak Phanang River Basin Project.** Rice Department, Bangkok. (in Thai)

Prasertsak, A. 2022. Rice seed multiplication system. **Thai Rice Research Journal** 13(1): 106-117. (in Thai)

Prasertsak, U., Wongkasame, O., Thavong, P. and Palavisut, W. 2010. **Research Report on Research and Development on Rice Seed Technology.** Rice Department, Bangkok. (in Thai)

Sawadsitung, P. 2025. **Measurement of antioxidant capacity of plant extracts** (4th ed). Odeonstore company limited, Bangkok. (in Thai)

Siri, B. 2015. **Seed Conditioning and Seed Enhancements.** Klungnavittaya Press, Khon Kaen. (in Thai)

Teixeira, S.B., Pires, S.N., Gabriele Espinel Ávila, G.E., Silva, B.E.P, Schmitz, V.N., Deuner, C., Armesto, R.S., Moura, D.S. and Deuner, S. 2021. Application of vigor indexes to evaluate the cold tolerance in rice seeds germination conditioned in plant extract. **Scientific Reports** 11: 11038.

Tipparak, S. and Aroonrungsikul, Ch. 2011. Effect of plant supplement on seed germination and seed vigor of KDML 105 rice variety. **Agricultural Science and Innovations Journal** 42(2)(Suppl.): 149-152. (in Thai)

U-sungnoen, P., Aroonrungsikul, C. and Juttupornpong, S. 2012. Effect of pig manure tea to seed germination and seed quality enhancement of emergence stage in rice (*Oryza sativa* L.) varieties RD 31, pp. 162-170. *In* **Proceedings of 50th Kasetsart University Annual Conference: Agricultural Extension and Home Economics, Plants.** Kasetsart University, Bangkok. (in Thai)

Wetchakama, N. and Khaengkhan, P. 2018. Improvement of seed qualities with seed priming techniques. **Prawarun Agricutural Journal** 15(1): 17-30. (in Thai)

Yunusa, A.K., Dandago, M.A., Ibrahim, S.M., Abdullahi N., Rilwan, A. and Barde, A. 2018. Total phenolic content and antioxidant capacity of different parts of cucumber (*Cucumis sativus* L.). **Acta Universitatis Cibiniensis Series E Food Technology** 22(2): 13-20.

Recent Science and Technology 18(1): 266457

Recent Science and Technology

Journal homepage: https:// www.tci-thaijo.org/index.php/rmutsvrj/index

ISSN: 3057-0786 (Online)

Research Article

Application of Silver/Carbon-based Composite Nanofiber Membrane for Improvement of Microfiltration System

Tanayt Sinprachim [a*], Kattinat Sagulsawasdipan [b] and Somchai Sonsupap [c]

[a] *Department of General Education, Faculty of Science and Fisheries Technology, Rajamangala University of Technology Srivijaya, Sikoa, Trang 92150, Thailand.*

[b] *Department of Marine Science and Environment, Faculty of Science and Fisheries Technology, Rajamangala University of Technology Srivijaya, Sikoa, Trang 92150, Thailand.*

[c] *College of Innovation and Industrial Management, King Mongkut's Institute of Technology Ladkrabang, Ladkrabang, Bangkok 10520, Thailand.*

Article history:

Received: 2025-03-27
Revised: 2025-06-18
Accepted: 2025-08-04

Keywords:

Carbon composite;
Nanofibers;
Microfiltration;
Membrane;
Filtration

ABSTRACT

In this study, silver-reinforced carbon nanofiber membranes (CNF@Ag) were fabricated through a binder-free extrusion process. A precursor mixture of carbon nanofibers (CNF) and silver nitrate ($AgNO_3$) was extruded at 40 MPa, followed by sintering at 800°C in an argon atmosphere for 4 hours to enhance the membrane structure. The physical properties of the CNF@Ag membranes, including porosity, wettability, morphology, and microfiltration efficiency, were systematically analyzed. The results demonstrated that the CNF@Ag membranes exhibited effective microfiltration properties with pore sizes ranging from 9.21 to 21.99 nm. These membranes achieved a turbidity removal efficiency of up to 92.69%, indicating their potential as an effective pre-treatment step for seawater desalination. This study highlights the promising application of CNF@Ag membranes in water purification processes, particularly for turbidity removal in desalination systems.

1. Introduction

The rapid growth of the global population, coupled with the impacts of climate change, has significantly increased the demand for fresh and clean water, especially in urban areas (Flörke *et al.*, 2018). By 2025, many regions are expected to experience severe water shortages, threatening public health, economic stability, and social development (Boretti and Rosa, 2019). As a result, the efficient management of available water resources and the advancement of effective filtration technologies have become critical priorities in addressing global water crises (Brown *et al.*, 2015).

Microfiltration, a membrane filtration technology, has gained significant attention as a solution for improving water quality by removing particulate matter, bacteria, and other contaminants from water sources. Unlike desalination, which primarily targets the removal of salts from seawater or brackish water, microfiltration focuses on separating larger particles, microorganisms, and colloidal matter, making it a crucial process for ensuring access to safe drinking water in both urban and rural settings (Gude, 2016). Microfiltration is particularly advantageous due to its low energy consumption, cost-effectiveness, and scalability compared to other advanced water treatment methods such as reverse osmosis and distillation (Williams, 2022). However, challenges such as membrane fouling and contamination still hinder the efficiency and longevity of filtration systems, limiting their widespread use.

*** Corresponding author.**

E-mail address: *tanayt65@hotmail.com*

Cite this article as:

Sinprachima, T., Sagulsawasdipan, K. and Sonsupap, S. 2026. Application of Silver/Carbon-based Composite Nanofiber Membrane for Improvement of Microfiltration System**. Recent Science and Technology** 18(1): 266457.

https://doi.org/10.65411/rst.2026.266457

In response to these challenges, the incorporation of nanomaterials into membrane technologies has emerged as a promising approach to enhance filtration performance. Nanomaterials, particularly carbon-based nanocomposites, have shown great potential due to their high surface area, excellent porosity, and customizable properties (Gong *et al.*, 2024; Yang and Mi, 2013). These materials offer an enhanced filtration capacity and can be modified with nanoparticles such as silver (Ag) (Yu *et al.*, 2022; Andrade *et al.*, 2015) or titanium dioxide (TiO_2) (Davari *et al.*, 2021; Razmjou *et al.*, 2011; Rahimpour *et al.*, 2008) which impart antimicrobial properties, further improving the effectiveness of filtration systems against microorganisms.

Porous carbon-based nanocomposite materials, particularly those containing carbon nanofibers, have attracted considerable attention for their versatility and broad range of applications. These include uses in energy storage devices (e.g., supercapacitors, lithium-ion batteries, and hydrogen fuel cells) and biomedical fields (Levchenko *et al.*, 2023). In the context of water filtration, these materials have demonstrated great promise in reducing fouling and improving the overall filtration process, especially in applications requiring the removal of bacteria, suspended solids, and other contaminants (Noamani *et al.*, 2019; Idumah and Hassan, 2016; Oladunni *et al.*, 2018). Furthermore, carbon nanofibers, which are key components of these materials, can be fabricated using various methods, such as self-assembly, template synthesis (Pavlenko *et al.*, 2022), chemical vapor deposition (CVD) (Hulicova-Jurcakova *et al.*, 2008), and electrospinning (Inagaki *et al.*, 2012). Among these, electrospinning is particularly noteworthy for its ability to produce highly porous and uniform fibers with tunable properties, making it an ideal technique for fabricating advanced filtration membranes.

This study focuses on the development of carbon nanocomposite membranes containing varying ratios of silver nanoparticles (0, 10, 20, 40, and 200%) in carbon nanofiber composites (CNF, CNF@Ag-10, CNF@Ag-20, CNF@Ag-40, CNF@Ag200). This aims to address gaps in the use of CNF@Ag membranes for microfiltration, particularly in desalination and fouling resistance. While CNF-based membranes have shown potential in turbidity removal and microbial filtration, their effectiveness in removing salts from seawater and long-term stability remain underexplored. The impact of silver nanoparticle concentration on filtration performance was studied. Structural, chemical, surface, and porosity analyses of these membranes were conducted using techniques such as X-ray diffraction (XRD), Raman spectroscopy, scanning electron microscopy (SEM), transmission electron microscopy (TEM), and Brunauer-Emmett-Teller (BET) surface area analysis. The composite membranes were then evaluated in a comparative study to assess their ability to filter and improve the quality of contaminated water, focusing on key water quality parameters such as salinity, turbidity, odor, and color.

2. Materials and Methods

2.1 Preparation of metal oxide carbon nanocomposite fiber membrane material

Figure 1 illustrates the synthesis of carbon nanofibers reinforced with silver particles. Carbon nanofibers (CNF; Changsha Easchem. Co., Ltd, China) and silver nitrate ($AgNO_3$), Sigma-Aldrich, USA) were dissolved separately in ethanol at the ratios shown in Table 1 and stirred on a hot plate for at least 2 h to ensure that the carbon nanofibers were evenly distributed in ethanol and the silver nitrate was completely dissolved. Next, the two solutions were mixed together and stirred for another 2 h to obtain the CNF@$AgNO_3$ mixture, which was then dried at room temperature for 1 night and pressed into a membrane with a diameter of 26 mm using a hydraulic press at a pressure of 40 Mpa for 2 min to obtain a membrane pellet with a thickness of 5–15 mm. After pressing, the membrane pellet was sintered at 800 °C under an argon gas atmosphere with a flow rate of 300 ml/min.

2.2 Sample characterizations

In this work, powder X-ray diffraction analysis (XRD, Bruker D2 PHASER (USA)) with Cu Kα radiation (λ = 0.15406 nm) was used to determine the crystal structure of all samples. The particle size and morphology were characterized by transmission electron microscopy (TEM, EM902 Zeiss, West Germany), while the chemical composition was studied using dispersive Raman spectrometry (Bruker, UK). The CNFs@Ag nanocomposites showed high specific surface area, and pore volumes were investigated by the gas absorption technique (BET).

Table 1 Precursor ratios used for the preparation of membrane composite materials under each condition.

Sample	CNF (g)	$AgNO_3$ (g)	Ethanol (ml)
CNF	10	-	100
CNF@Ag10	10	1	100
CNF@Ag20	10	2	100
CNF@Ag40	10	4	100
CNF@Ag200	10	20	100

CNF= Carbon nanofibers, Ag= silver content added in nanofibers; 0%, 10%, 20%, 40% and 200%

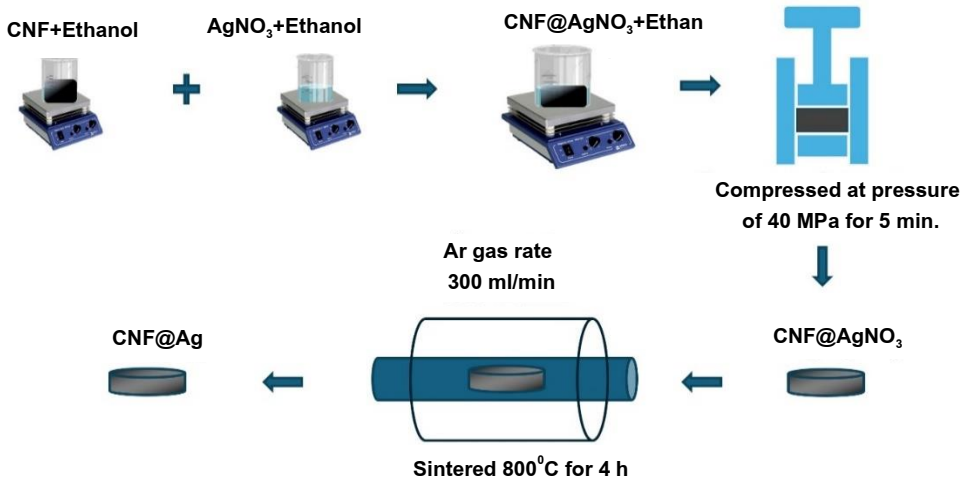

Figure 1 Precursor preparation process and membrane extrusion

2.3 Filtration rate test

The flow rate of water through the experimental membrane was tested using seawater and filtered using a Buchner filter set as shown in Figure 2, which was a dead-end filtration method. The solution was fed in perpendicular to each CNF@Ag membrane. The water was filtered using a vacuum pump at a constant pressure of -60 PSI, allowing water to flow through the membrane until it was soaked, and then the timer was started. Each membrane was timed for 30 min of filtration. The water obtained was measured with a measuring cylinder and the flow rate was calculated using the equation.

$$Q = \frac{V}{t} \quad (1)$$

Q is the flow rate of water through the membrane in m^3/min, V is the volume in m^3, and t is the time in min. While the flux of water through the membrane can be calculated from

$$\Phi = \frac{V}{AtP} \quad (2)$$

Φ is the water flow flux through the cross-section of the membrane in l/m^2h bar. A is the cross-sectional area of the membrane in m^2, t is the time in hours, and *P* is the pressure in bar.

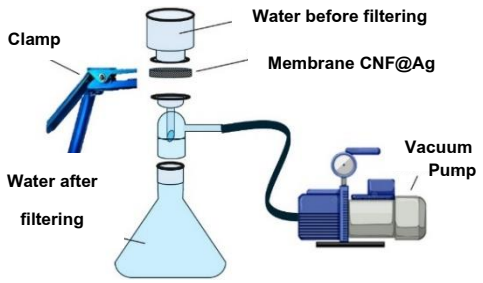

Figure 2 Water filter set with composite carbon nanofibers reinforced with

2.4 Study of the efficiency of turbidity removal in water

The efficiency of turbidity removal was studied after the water was filtered through each carbon nanofiber membrane reinforced with silver particles (CNF@Ag). The water filter setup was a modified Buchner vacuum filtration unit. Using the pressure reduction set up sped up the filtration, making it faster than normal filtration. The Buchner flask was connected to the membrane and funnel with a Buchner funnel clamp, with the filter funnel placed on top, and each CNF@Ag filter medium was placed between the funnel and the small arm, as can be seen in Figure 2. The small arm at the neck of the flask was connected to a vacuum pump to remove air from the flask.

2.5 Study of the efficiency of seawater salinity removal

The efficiency of removing salinity from seawater when filtered with the CNF@Ag composite carbon nanofiber membranes was studied. Seawater samples were collected in front of the lighthouse at Rajamangala University of Technology Srivijaya, Trang Campus, as shown in Figure 3.

Various parameters of seawater were measured before filtration, including temperature, pH, ORP, conductivity, turbidity, dissolved oxygen (DO), total dissolved solids (TDS), and salinity, using a Water Quality Monitor (Horiba). Then, after filtration, the seawater was tested again to measure the filtration efficiency of the experimental CNF@Ag membranes that had been incorporated into the Buchner filter setups.

3. Results and Discussion

3.1 Morphology of the membrane material of metal oxide carbon nanocomposite fibers

After being pressed by a hydraulic press at a pressure of 40 Mpa for 5 min and sintered at 800 °C under an argon gas atmosphere at a flow rate of 300 ml/min for 4 h, the membranes, with a diameter of approximately 26 mm and a thickness between 4-9 mm, were obtained as shown in Figure 4. The fabricated membranes had densities in the range of 2.36×10^{-6} -

2.96×10^{-6} kg/m^3, and the density values also increased with increasing amounts of silver particles.

Detailed analysis was conducted by mounting the membrane samples on a steel base before coating them with gold of a thickness of approximately 5 nm to increase their electrical conductivity. High- magnification images were taken using a scanning microscope. The scanning microscope images at magnifications of 1000x and 10,000x of the CNF@Ag fibers using 0%, 10%, 20%, 40% and 200% silver nitrate precursor are shown in Figure 5. The fibers of all samples had a random arrangement with no definite direction. The fiber sizes are analyzed using the ImageJ program; the average fiber size was 84.42±14.14 nm and the nanoparticles formed and distributed in the composite nanofiber can be observed adhering to the fiber surfaces, as clearly seen in Figure 6. The sizes of the fibers before and after calcination are summarized in Table 2.

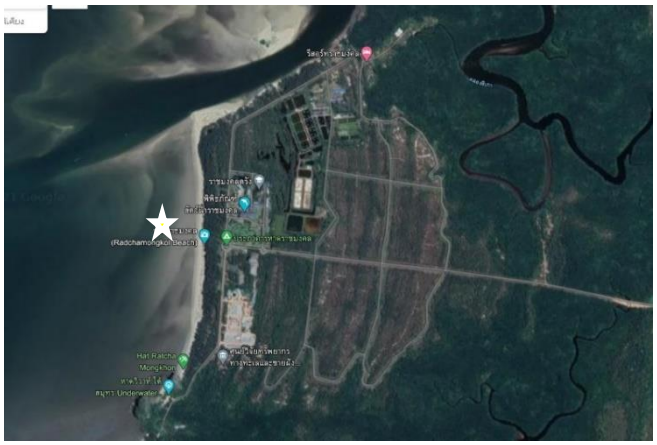

Figure 3 The points where seawater samples were collected from satellite imagery maps within Rajamangala University of Technology Srivijaya (Trang Campus)

Figure 4 Appearance and dimensions of a sintered membrane

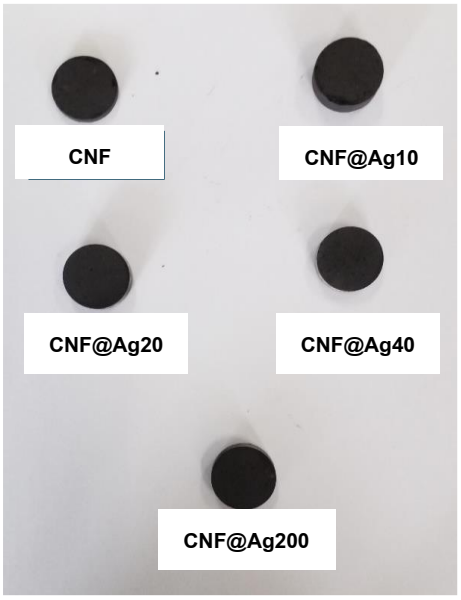

Figure 5 Membranes fabricated from CNF@Ag fibers with different silver particle addition rates. CNF= Carbon nanofiber, Ag= silver content added to the nanofibers; 0%, 10%, 20%, 40% and 200%

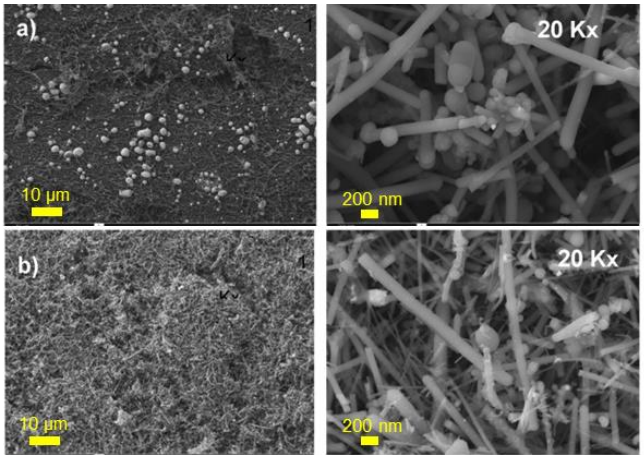

Figure 6 Scanning electron microscope images of the fabricated CNF@Ag metal oxide carbon nanocomposite membranes prepared using different concentrations of precursor: a) CNF@Ag200, b) CNF@Ag40, c) CNF@Ag20, d) CNF@Ag10, and e) CNF

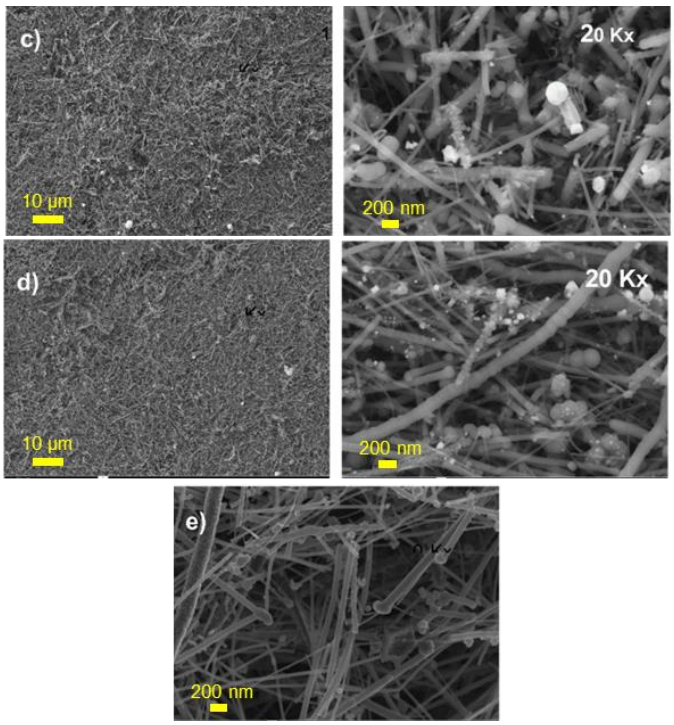

Figure 6 (Continuous)

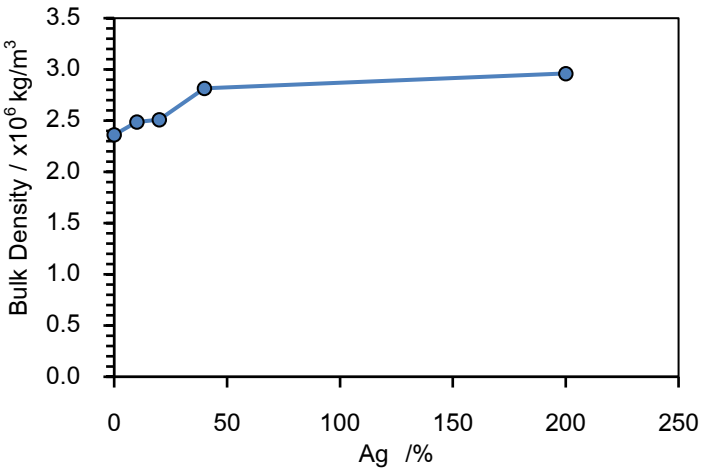

Figure 7 Density of membranes reinforced with different concentrations of silver particles

After degassing the samples at 300 C for 1 night, the specific surface area and porosity properties were measured using a Brunauer-Emmett-Teller analyzer at 77 K. The surface area and porosity were then evaluated by the BET method. It was found that the fibers reinforced with silver particles as shown in Figure 8 exhibited a hysteresis loop type IV adsorption and desorption pattern due to the condensation of nitrogen gas molecules in the mesoporous pores (Sinprachim *et al.*, 2016). The knee-shaped region at low pressure also indicated the presence of a large number of small pores, resulting in a higher specific surface area of the membrane compared to the CNF membrane without silver reinforcement. The low specific surface area of the membrane made from pure CNF may be due to the absence of silver particles, which made the pure CNF more homogeneous and dense when the membrane was compressed at a high pressure of 60 MPa. Meanwhile, compared to the membrane reinforced with particles, the membrane reinforced with fewer silver particles had a larger surface area because the silver nanoparticles were inserted between the fiber slits. Increasing the size and number of junctions between carbon nanofibers resulted in an increase in the pore volume, which had an effect on the increase in the specific surface area. However, the specific surface area decreased with an increase in the silver addition concentration. The membranes had specific surface areas ranging from 14.95 to 65.63 m2/g and pore sizes ranging from 9.21 to 21.99 nm, which might be due to the increase in the amount of silver particles, a very dense metal compared to the lightweight carbon fibers, causing the overall mass to increase significantly. Therefore, the calculated surface area to mass ratio was lower with the increase in the silver fraction, as summarized in Table 3.

Table 2 General properties of membranes.

Membranes	% of Ag composited	Mass (g)	Diameter (mm)	Thickness (mm)	Cross-sectional area ($x10^{-4}$ m^2)	Density ($x10^{-6}$ kg/m^3)
CNF	0	1.35	26±1.02	7.0±0.66	5.31	2.36
CNF@Ag10	10	1.32	26±1.24	6.5±0.88	5.31	2.42
CNF@Ag20	20	0.82	26±0.68	4±0.94	5.31	2.51
CNF@Ag40	40	0.92	26±0.72	4±0.28	5.31	2.82
CNF@Ag200	200	1.33	26±0.84	5.5±0.74	5.31	2.96

Table 3 Surface area and porosity of membranes fabricated with CNF@Ag composite at Ag concentrations of 0%, 10%, 20%, 40%, and 200%

Membranes	S_{BET} (m^2/g)	D_{mean} (nm)	V_{pore} (cm^3/g)
CNF	14.95	21.08	0.078
CNF@Ag10	65.63	9.21	0.151
CNF@Ag20	27.18	15.24	0.104
CNF@Ag40	20.21	18.46	0.093
CNF@Ag200	18.82	21.99	0.104

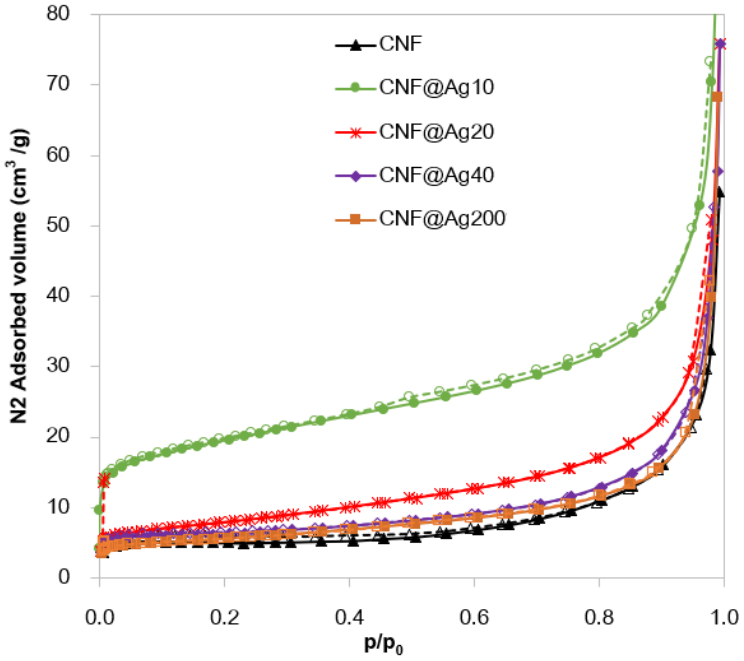

Figure 8 Graphs showing the adsorption and desorption of CNF fibers CNF@Ag10, CNF@Ag20, CNF@Ag40, and CNF@Ag200. CNF= Carbon nanofibers, Ag= silver content added to nanofibers: 0%, 10%, 20%, 40% and 200%

3.2 Structural analysis using X-ray diffraction technique

The study of structural property analysis was conducted using the X-ray diffraction technique with Cu-K radiation (λ = 0.15406 nm) in the range of 20-90°. From Figure 9, the X-ray diffraction pattern curves show the positions of carbon peaks at approximately 26° and 44°, representing the (002) and (101) diffraction planes, respectively, as per the carbon standard file PDF# 75-1621 (Shalaby *et al.*, 2015). In the case of CNF@Ag samples, the diffraction peaks of Ag were found at approximately 38.2°, 44.4°, 64.6°, 77.5°, and 81.7°, corresponding to the (111), (200), (220), (311), and (222) diffraction planes, respectively, of the silver standard file PDF# 87-0720 (Yuwen *et al.*, 2014), which were presumably consistent with the diffraction peaks of cubic Ag that was distributed in different positions according to the standard file as shown in Figure 9. It is noticeable that Ag did not form an oxide structure because it is an inert element. The effect of preparation with different concentrations of precursors did not affect the diffraction pattern but affected the intensity value, which was consistent with the samples of higher Ag concentration having higher spectral intensity (Dubey *et al.*, 2009).

3.3 Characterization of carbon using Raman spectroscopy

The Raman spectra were measured in the range of 100 – 4000 cm^{-1} using a 532 nm laser and are shown in Figure 10. The Raman spectra of the CNF and CNF metal oxide nanocomposites display common peaks related to carbon, namely, the G-Band peak at approximately 1590 cm^{-1} and the D-Band peak at approximately 1340 cm^{-1}. Moreover, for all samples, the peaks overlap and indicate the presence of amorphous carbon (Li *et al.*, 2016). The slightly visible peak in the range of 2600 – 2900 cm^{-1} is due to the phonon vibration of graphite crystals that are mixed in the sample (Kuzmany *et al.*, 2021).

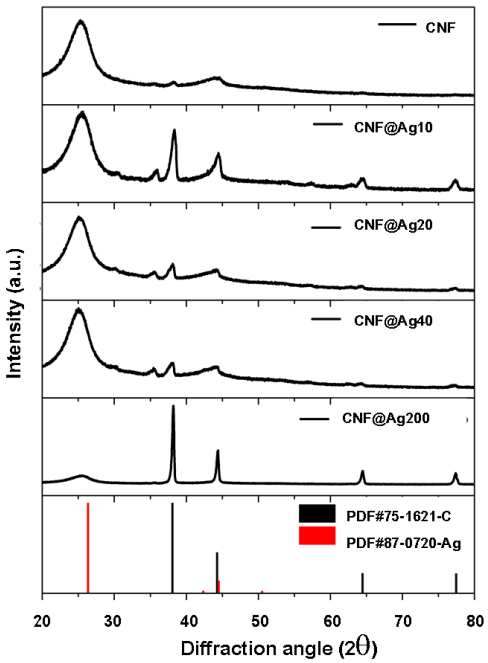

Figure 9 X-ray diffraction patterns of samples at different compositions and concentrations. CNF= Carbon nanofibers, Ag= silver content added to nanofibers; 0%, 10%, 20%, 40% and 200%

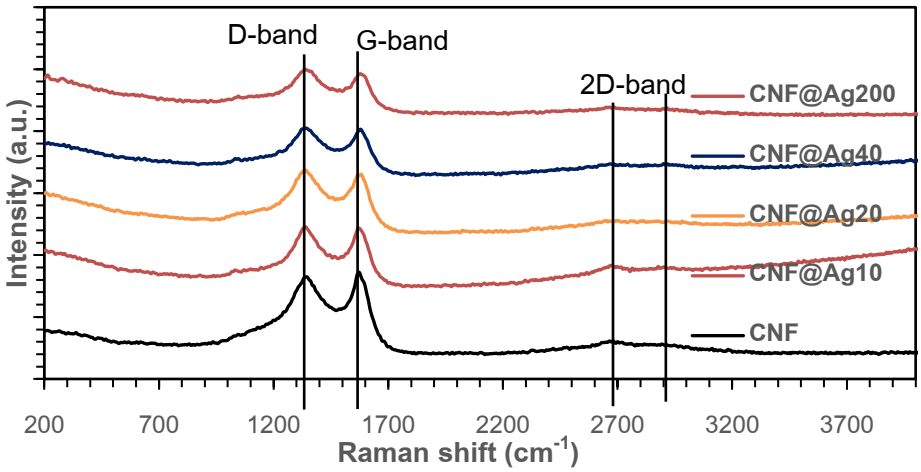

Figure 10 Raman spectra of the CNF carbon nanocomposite metal oxide fiber materials of CNF fibers CNF@Ag10%, CNF@Ag20%, CNF@Ag40%, and CNF@Ag200%. CNF= Carbon nanofibers, Ag= silver content added in nanofibers; 0%, 10%, 20%, 40% and 200%

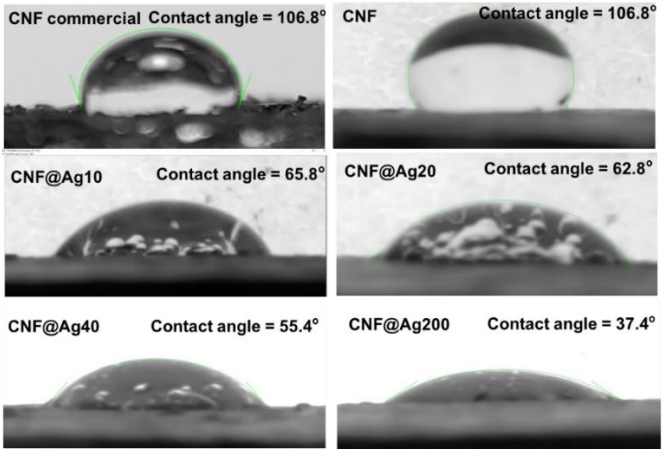

Figure 11 Images of water droplets on the surface of the prepared membrane. CNF= Carbon nanofibers, Ag= silver content added to nanofibers: 0%, 10%, 20%, 40% and 200%

3.4 Water absorption capacity of the membranes and wettability of the surface

The contact angle measurement experiment was used to study the wetting properties of the membranes. As shown in Figure 11, the CNF-based membranes had the highest contact angle value of only 106.8°, which highlighted the hydrophobic surface properties of the pure CNF (Zhang *et al.*, 2020). Meanwhile, in the case of the CNF-Ag composites, the contact angle values decreased with the increasing proportion of silver particles as shown in Figure 12. In other words, with the addition of silver particles, the membranes were better wet. However, after immersion in water for 15 h, the water absorption properties of the membranes were found to be close, in the range of 279.34–288.27%, as shown in Table 4, which may have been because the membranes had similar specific surface areas, and the immersion time of up to 15 h was long enough for the membranes to fully absorb water.

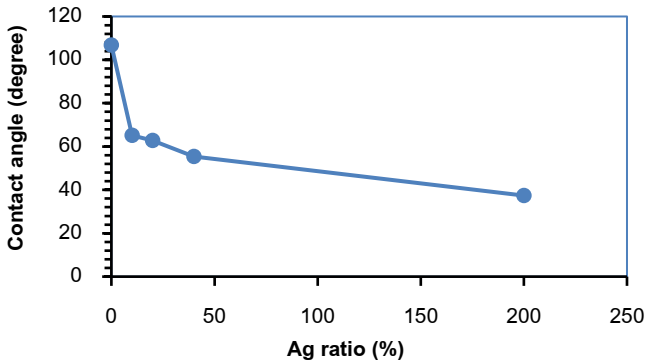

Figure 12 Graph showing the relationship between contact angle and Ag addition amount

Table 4 Water absorption and contact angle measurements of the prepared membranes.

Membranes	Water absorption rate compared to the mass of the membrane (%)
CNF	281.61
CNF@Ag10	286.59
CNF@Ag20	288.27
CNF@Ag40	279.34
CNF@Ag200	287.26

CNF= Carbon nanofibers, Ag= silver content added to the nanofibers; 0%, 10%, 20%, 40% and 200%

Table 5 Results of the study on water flow rate through CNF and CNF@Ag membranes.

Membranes	Flow rate (ml/min)	Flux (l/m^{2}hbar)
CNF	5.56	50.04
CNF@Ag10	4.17	113.74
CNF@Ag20	5.08	138.43
CNF@Ag40	5.39	146.23
CNF@Ag200	5.56	151.65

Table 6 Seawater parameters before CNF and CNF@Ag membrane filtration.

Order	Parameter	Value	Unit
1	Temperature	32.57	°C
2	Acidity-Alkalinity	7.66	
3	ORP	198	mV
4	Conductivity	47.4	µs/cm
5	Turbidity	16.5	NTU
6	Dissolved Oxygen (DO)	8.84	mg/L
7	Total Dissolved Solids (TDS)	28.9	g/L
8	Salinity	30.8	ppt

CNF= Carbon nanofibers, Ag= Silver content added to nanofibers; 0%, 10%, 20%, 40% and 200%

3.5 Testing of water flow rate through the membrane

The results of the study of the flow rate of water through the composite nanocarbon fiber membranes were obtained by making the water flow through the vacuum filter set. The water was poured into the vacuum filter funnel, and the pressure was set to -60 PSI. The water slowly flowed through the membrane. The time was set with a stopwatch for 30 min. The volume of water that flowed into the flask was measured with a measuring cylinder. The volume of water obtained was recorded, calculated, and the results were compared as shown in Table 5. It is noticeable that pure carbon gave good flow rate values as well as the silver particle mixture up to 200%, while the mixture of small proportions of nanoparticles gave lower flow rate values respectively. However, this interesting result will be further studied in the future.

3.6 Study of removal rate of specific contaminants

The removal of salt and turbidity from seawater was investigated using a membrane filtration technique to evaluate membrane efficiency under different conditions. In the experiment, the seawater had parameters as listed in Table 6. The turbidity removal efficiency was evaluated by filtering water with an initial turbidity of 33.00 NTU through the experimental membrane using vacuum filtration at a pressure of -60 PSI (Muthuraman and Sasikala, 2014). The results indicated that turbidity could be effectively removed by the CNF@Ag membrane, with removal efficiencies ranging from 71.19% to 92.69% in all cases. Filtration through the experimental membrane yielded water with clarity of less than 10 NTU, which meets the drinking water quality criteria for turbidity set by the Ministry of Public Health (2000, 2011 edition). These results are summarized in Table 7.

The turbidity filtration process was classified as microfiltration, indicating that colloidal particles, emulsions, and suspended

solids were removed through pores with a size range of 0.05 to 20 μm. In addition, the addition of silver particles at higher ratios was found to significantly improve filtration efficiency. This improvement may be attributed to the reduction in interfiber gaps resulting from the insertion of silver nanoparticles, which enhances the capture of colloidal particles, as suggested by Praveen Kamath *et al.* (2023).

However, the experimental results shown in Table 8 indicate that all the membranes are ineffective in reducing salinity. These inefficiencies may be due to the filtration mechanism, which is influenced by the large interfiber gaps of 0.05 to 20 μm, as observed in the high-magnification scanning electron microscope (SEM) images (Figure 6). These gaps are larger than the size of the salt molecules, which is approximately 0.283 nm. In addition, the good wetting properties of the membrane allow water to easily permeate the membrane, enabling the salt molecules to pass through the membrane without being trapped. Therefore, the salinity values before and after filtration are similar, indicating that the salinity is not significantly reduced.

Table 7 Study of water turbidity reduction performance of different types of CNF@Ag membranes.

Membranes	Turbidity before filtration (NTU)	Turbidity after filtration (NTU)	Turbidity removal efficiency (%)
CNF	33.00±0.12	7.53±0.60	76.47
CNF@Ag10	33.00±0.12	9.22±1.88	71.19
CNF@Ag20	33.00±0.12	3.65±0.62	88.59
CNF@Ag40	33.00±0.12	2.56±0.48	92.00
CNF@Ag200	33.00±0.12	2.34±0.26	92.69

CNF= Carbon nanofibers, Ag= silver content added to nanofibers; 0%, 10%, 20%, 40% and 200%

Table 8 Comparison of salinity values before and after filtration with different types of membranes.

Membranes	Salinity before filtration (%)	Salinity after filtration (%)
CNF	30±0.8	30±0.6
CNF@Ag10	30±0.8	30±0.8
CNF@Ag20	30±0.8	30±0.4
CNF@Ag40	30±0.8	30±0.8
CNF@Ag200	30±0.8	30±0.6

4. Conclusion

In this study, a binder-free extrusion process successfully fabricated a membrane, which was sintered at 800 °C, resulting in a cross-sectional area of 2.51 × 10^{-4} m². The membrane exhibited a smooth surface and a uniform distribution of silver nanoparticles on the carbon nanofiber (CNF) structure. The incorporation of silver nanoparticles significantly increased the membrane's density and reduced its specific surface area from 65.63 m²/g to 18.82 m²/g, while also enhancing its hydrophilicity. Filtration tests at -60 PSI revealed water flow rates ranging from 1.83 to 5.56 mL/min, with the membrane achieving a turbidity removal efficiency of 92.69%, thereby meeting drinking water quality standards. However, the membrane was found to be ineffective for desalination due to its pore size range of 9.21 to 21.99 micrometers, which is suitable for microfiltration but inadequate for separating smaller particles, such as salt molecules (0.283 nm). In conclusion, while the CNF@Ag membrane demonstrates promising results for microfiltration applications, further optimization is needed to enhance its desalination performance. Specifically, reducing the pore size and increasing the membrane thickness could improve its ability to filter smaller solutes, such as salts, thereby enabling more efficient desalination.

5. Acknowledgments

This research project was successfully implemented with the support of the research budget by Fundamental Fund (FF) via Rajamangala University of Technology Srivijaya in 2020 (Project code 312). We also acknowledge the editorial team at the Office of Academic Journal Administration, KMITL, for proofreading this manuscript.

6. References

Andrade, P.F., de Faria, A.F., Oliveira, S.R., Arruda, M.A.Z. and do Carmo Gonçalves, M. 2015. Improved antibacterial activity of nanofiltration polysulfone membranes modified with silver nanoparticles. **Water Research** 81: 333-342.

Boretti, A. and Rosa, L. 2019. Reassessing the projections of the world water development report. **NPJ Clean Water** 2(1): 15.

Brown, C.M., Lund, J.R., Cai, X., Reed, P.M., Zagona, E.A., Ostfeld, A., Hall, J., Characklis, G.W., Yu, W. and Brekke, L. 2015. The future of water resources systems analysis: toward a scientific framework for sustainable water management. **Water Resources Research** 51(8): 6110-6124.

Davari, S., Omidkhah, M. and Salari, S. 2021. Role of polydopamine in the enhancement of binding stability of TiO2 nanoparticles on polyethersulfone ultrafiltration membrane. **Colloids and Surfaces A: Physicochemical and Engineering Aspects** 622: 126694.

Dubey, M., Bhadauria, S. and Kushwah, B. 2009. Green synthesis of nanosilver particles from extract of Eucalyptus hybrida (safeda) leaf. **Digest Journal of Nanomaterials and Biostructures** 4(3): 537-543.

Flörke, M., Schneider, C. and McDonald, R.I. 2018. Water competition between cities and agriculture driven by climate change and urban growth. **Nature Sustainability** 1(1): 51-58.

Gong, W., Bai, L. and Liang, H. 2024. Membrane-based technologies for removing emerging contaminants in urban

water systems: Limitations, successes, and future improvements. **Desalination** 590: 117974.

Gude, V.G. 2016. Desalination and sustainability an appraisal and current perspective. **Water Research** 89: 87-106.

Hulicova-Jurcakova, D., Li, X., Zhu, Z., De Marco, R. and Lu, G.Q. 2008. Graphitic carbon nanofibers synthesized by the chemical vapor deposition (CVD) method and their electrochemical performances in supercapacitors. **Energy & Fuels** 22(6): 4139-4145.

Idumah, C.I. and Hassan, A. 2016. Emerging trends in graphene carbon based polymer nanocomposites and applications. **Reviews in Chemical Engineering** 32(2): 223-264.

Inagaki, M., Yang, Y. and Kang, F. 2012. Carbon nanofibers prepared via electrospinning. **Advanced materials** 24(19): 2547-2566.

Kuzmany, H., Shi, L., Martinati, M., Cambré, S., Wenseleers, W., Kürti, J., Koltai, J., Kukucska, G., Cao, K. and Kaiser, U. 2021. Well-defined sub-nanometer graphene ribbons synthesized inside carbon nanotubes. **Carbon** 171: 221-229.

Levchenko, I., Baranov, O., Riccardi, C., Roman, H.E., Cvelbar, U., Ivanova, E.P., Mohandas, M., ŠČajev, P., Malinauskas, T. and Xu, S. 2023. Nanoengineered Carbon‐Based Interfaces for Advanced Energy and Photonics Applications: A Recent Progress and Innovations. **Advanced Materials Interfaces** 10(1): 2201739.

Li, Y., Hu, Y.S., Li, H., Chen, L. and Huang, X. 2016. A superior low-cost amorphous carbon anode made from pitch and lignin for sodium-ion batteries. **Journal of Materials Chemistry A** 4(1): 96-104.

Muthuraman, G. and Sasikala, S. 2014. Removal of turbidity from drinking water using natural coagulants. **Journal of Industrial and Engineering Chemistry** 20(4): 1727-1731.

Noamani, S., Niroomand, S., Rastgar, M. and Sadrzadeh, M. 2019. Carbon-based polymer nanocomposite membranes for oily wastewater treatment. **NPJ Clean Water** 2(1): 20.

Oladunni, J., Zain, J.H., Hai, A., Banat, F., Bharath, G. and Alhseinat, E. 2018. A comprehensive review on recently developed carbon based nanocomposites for capacitive deionization: from theory to practice. **Separation and Purification Technology** 207: 291-320.

Pavlenko, V., Żółtowska, S., Haruna, A., Zahid, M., Mansurov, Z., Supiyeva, Z., Galal, A., Ozoemena, K., Abbas, Q. and Jesionowski, T. 2022. A comprehensive review of template-assisted porous carbons: Modern preparation methods and advanced applications. **Materials Science and Engineering: R: Reports** 149: 100682.

Praveen Kamath, P., Sil, S., Truong, V.G. and Nic Chormaic, S. 2023. Particle trapping with optical nanofibers: a review. **Biomedical Optics Express** 14(12): 6172-6189.

Rahimpour, A., Madaeni, S., Taheri, A. and Mansourpanah, Y. 2008. Coupling TiO2 nanoparticles with UV irradiation for modification of polyethersulfone ultrafiltration membranes. **Journal of Membrane Science** 313(1-2): 158-169.

Razmjou, A., Mansouri, J. and Chen, V. 2011. The effects of mechanical and chemical modification of TiO2 nanoparticles on the surface chemistry, structure and fouling performance of PES ultrafiltration membranes. **Journal of Membrane Science** 378(1-2): 73-84.

Shalaby, A., Nihtianova, D., Markov, P., Staneva, A., Iordanova, R. and Dimitriev, Y. 2015. Structural analysis of reduced graphene oxide by transmission electron microscopy. **Bulgarian Chemical Communications** 47(1): 291-295.

Sinprachim, T., Phumying, S. and Maensiri, S. 2016. Electrochemical energy storage performance of electrospun AgO_x-MnO_x/CNF composites. **Journal of Alloys and Compounds** 677: 1-11.

Williams, J. 2022. Desalination in the 21st century: a critical review of trends and debates. **Water Alternatives** 15(2): 193-217.

Yang, Q. and Mi, B. 2013. Nanomaterials for membrane fouling control: accomplishments and challenges. **Advances in Chronic Kidney Disease** 20(6): 536-555.

Yu, Y., Zhou, Z., Huang, G., Cheng, H., Han, L., Zhao, S., Chen, Y. and Meng, F. 2022. Purifying water with silver nanoparticles (AgNPs)-incorporated membranes: Recent advancements and critical challenges. **Water Research** 222: 118901.

Yuwen, L., Xu, F., Xue, B., Luo, Z., Zhang, Q., Bao, B., Su, S., Weng, L., Huang, W. and Wang, L. 2014. General synthesis of noble metal (Au, Ag, Pd, Pt) nanocrystal modified MoS 2 nanosheets and the enhanced catalytic activity of Pd–MoS 2 for methanol oxidation. **Nanoscale** 6(11): 5762-5769.

Zhang, S., Huang, X., Wang, D., Xiao, W., Huo, L., Zhao, M., Wang, L. and Gao, J. 2020. Flexible and superhydrophobic composites with dual polymer nanofiber and carbon nanofiber network for high-performance chemical vapor sensing and oil/water separation. **ACS Applied Materials & Interfaces** 12(41): 47076-47089.

Recent Science and Technology

Journal homepage: https:// www.tci-thaijo.org/index.php/rmutsvrj/index

ISSN: 3057-0786 (Online)

Research Article

Characterization of Soluble Polysaccharides from Coconut Residue of Virgin Coconut Oil Production

Viriya Nitteranon * **and Ananthaya Sansawat**

Department of Food Science and Technology, Rajamangala University of Technology Tawan-ok, Sriracha, Chonburi 20110, Thailand.

Article history:

Received: 2025-05-01
Revised: 2025-08-27
Accepted: 2025-10-17

Keywords:

Cold-pressed coconut oil;
Defatted coconut residue;
Polysaccharides;
Prebiotics

ABSTRACT

This study aimed to explore the potential of soluble polysaccharides extracted from defatted coconut residue (DCR) as a prebiotic. Our findings reveal that the defatting process of coconut residue (CR) changes its chemical composition of coconut residue in terms of moisture content (7.04 ± 0.04%), fat (3.99 ± 0.55%), protein (2.93 ± 0.18%), ash (0.76 ± 0.04%), and carbohydrate contents (46.58 ± 1.05%). The percentage of soluble polysaccharide was 2.50 ± 0.40. The extraction of soluble polysaccharides (SP) from DCR resulted in increased total sugar contents and non-reducing sugars. Structural analysis of SP by Fourier transform infrared (FT-IR) analysis showed a predominantly polysaccharide composition. High performance liquid chromatography (HPLC) analysis further identified mannose (27.87%) and glucose (25.00%) as the major monosaccharides present in SP. Remarkably, SP exhibited stronger resistance (92.42% resistance) to acidic condition in the human stomach compared to inulin (25.52% resistance) at pH 1. Furthermore, SP demonstrated prebiotic properties by promoting the growth of *Lactobacillus acidophilus* TISTR 2365. These findings confirmed the promising prebiotic properties of coconut residue after cold-pressed coconut oil processing, which may be used as an ingredient in functional foods and nutraceutical products.

1. Introduction

In the current health food market, particularly in those aimed at boosting the body's immune system against microbial pathogens, there has been a notable increase in the incorporation of prebiotics into these products. Prebiotics are essentially non-digestible food ingredients, mainly dietary fiber, oligosaccharides, and polysaccharides that can substantially affect the consumer health by promoting a healthy balance of beneficial bacteria in the large intestine, thereby enhancing the immune response (Kolida *et al*., 2002). Prebiotics are not digested in the stomach and small intestine; instead, they enter the large intestine, where they serve as specific food for beneficial bacteria, particularly *Bifidobacteria* and *Lactobacillus*. These bacteria aid in inhibiting harmful bacterial growth (Bamigbade *et al*., 2022). In 2016, the International Scientific Association for Probiotics and Prebiotics redefined prebiotics as substances that can be selectively used and transformed by the host intestinal flora under the premise that they are beneficial to host health. Therefore, the new definition of prebiotics includes oligosaccharide carbohydrate and non-carbohydrates (Gibson *et al*., 2017). In the large intestine, prebiotics are fermented to produce short-chain fatty acids (SCFAs) such as acetate, propionate, and butyrate. SCFAs influence the structure of the large intestine, provide energy to intestinal cells, reduce pH levels, stimulate water and mineral absorption, and support the influx of beneficial probiotics (Peredo Lovillo *et al*., 2020). The demand for prebiotics has been on the rise, with the global prebiotics market reaching a value of 7.99 billion US dollars in 2023 (Pulidindi and Ahuja, 2024). Reflecting this trend, the prebiotics markets in Thailand and the Asia Pacific were valued at 73.4 and 2,468 million US dollars in 2023, respectively (Prebiotics market size, 2023). This growth can be attributed to various factors, including increased awareness due to the global

* **Corresponding author.**

E-mail address: *viriya_ni@rmutto.ac.th*

Cite this article as:

Nitteranon, V. and Sansawat, A. 2026. Characterization of Soluble Polysaccharides from Coconut Residue of Virgin Coconut oil Production. **Recent Science and Technology** 18(1): 267472.

https://doi.org/10.65411/rst.2026.267472

COVID-19 pandemic situation, which has prompted global populations to pay more attention to health.

The coconut residue (CR) is obtained from the extraction of coconut oil or mechanical squeezing to produce coconut milk. Currently, this remaining coconut residue is primarily used as fertilizer and low-cost animal feed (Sulaiman *et al*., 2013). Typically, coconut residue is a source of carbohydrate, accounting for 43-45% of its composition, particularly in the form of oligosaccharides, such as mannan-oligosaccharides (MOS), along with other sugars like mannose, glucose, galactose, and arabinose (Khuwijitjaru *et al*., 2012). MOS are composed of linear chains of mannose sugars and have attracted considerable interest as prebiotics. MOS extracted from yeast cell wall are effective in enhancing the immune system of animals and are already widely applied in the feed industry (Yamabhai *et al*., 2014). Interestingly, mannan-rich plants including copra meal showed potential as prebiotics and have health-promoting effects including antibacterial properties and the ability to promote the growth of probiotic bacteria in both humans and livestock (Intaratrakul *et al*., 2022; Asbury and Saville, 2025). Nowadays, researchers have recognized the benefits and potential of utilizing discarded coconut residue to produce functional food ingredients rich in dietary fiber. Previous studies have shown that polysaccharide extracts from coconut residue can resist artificial human gastric juices and enhance the growth of *Lactobacillus casei* Shirota and *L. bulgaricus* (Mohd Nor *et al*., 2017).

Therefore, this research focused on utilizing coconut residue, an abundant, fiber-rich by-product derived from the cold-pressed coconut oil extraction process of a community enterprise. The objective is to investigate the prebiotic potential of crude soluble polysaccharides (SP) extracted from defatted coconut residue (DCR), with the aim of advancing its development as a functional food ingredient. The use of coconut residue offers a compelling prospect owning to their cost-effectiveness as a raw material for prebiotic production, thereby enhancing the economic value of coconut residue.

2. Materials and Methods

2.1 Chemical and bacterial strains

Inulin and 3,5-dinitrosalycylic acid (DNS) were obtained from TCI (Tokyo, Japan). Trifluoroacetic acid (TFA) was purchased from Fisher Scientific (PA, USA). α-Amylase from porcine pancreas was obtained from Sigma (MO, USA). De Man, Rogosa, and Sharpe (MRS) broth and agar were obtained from Himedia (Mumbai, India). 98% Sulfuric acid and D-glucose were obtained from Ajax Finechem (Sydney, Australia). All chemicals used were of analytical grade. *Lactobacillus acidophilus* TISTR 2365 was obtained from Thailand Institute of Scientific and Technological Research (TISTR, Thailand).

2.2 Preparation of coconut residue (CR) and defatted coconut residue (DCR)

The coconut residue was obtained from a local community "Takien Tia", Chonburi, Thailand. The coconut residue was oven-dried at 60 °C for 7 h using a tray dryer (OFM, Thailand). Subsequently, it was ground into powder using an electric grinder (Panasonic, Japan) to obtain coconut residue (CR) powder, which was then passed through a 50-mesh sieve. CR was kept in a sealed plastic bag and stored at room temperature (Thongsook and Chaijamrus, 2018).

To obtain defatted coconut residue (DCR), CR powder was subjected to fat removal by mixing 100 g of dried CR powder with 1 L of hexane for 18 h at room temperature. After hexane removal, the coconut residue was dried in a hot air oven (Memmert, Germany) at 45 °C for 3 h to evaporate any remaining hexane (Raghavendra *et al*., 2004). The DCR was stored in an airtight package for further analysis.

2.3 Proximate analysis of CR and DCR

The coconut residue powder (CR) and defatted coconut residue powder (DCR) samples were subjected to proximate analysis following the AOAC (2002) method. The components analyzed included moisture content, protein, fat, ash, and fiber. Total carbohydrate (% wet basis) was calculated using the following formula:

Total carbohydrate (%) = 100 – [protein content (%) + crude fat (%) + moisture (%) + ash (%) + fiber (%)]

2.4 Extraction of crude soluble polysaccharides using hot water

The extraction process followed the method outlined by Bello *et al*. (2018) with some modifications. Initially, DCR was subjected to extraction using distilled hot water at a ratio of 1:20 w/v at 80 ºC for 2 h. The mixture was subsequently filtered through a cheese cloth. This extraction process was repeated twice to ensure the removal of any residual polysaccharides. The extracts were combined and concentrated using a rotary evaporator to reduce the volume to 1/5 of original. Subsequently, 95% (v/v) ethanol was added four times of the original volume to precipitate the polysaccharides. The mixture was then refrigerated at 4 ºC overnight. Following precipitation, the water-soluble polysaccharide was isolated by centrifugation at 9300 xg for 15 min at 4 ºC. The supernatant was decanted, and the obtained sample was subjected to freeze-drying to obtain a dry sample. Finally, the dried sample was stored at room temperature for further analysis.

2.5 Determination of total sugar content, reducing sugar, and non-reducing sugar

2.5.1 Determination of total sugar content

Total sugar content was assessed using the phenol-sulphuric method as described by Dubois *et al*. (1956). Initially, 2 mL of the sample solution was combined with 5% (v/v) phenol

and 5 mL of concentrated 98% sulfuric acid (H_2SO_4). The mixture was vortexed and incubated at room temperature for 30 min. Subsequently, the absorbance of solution was measured at 490 nm using a UV-Vis spectrophotometer (Shimadzu, Japan). Total sugar content was determined based on a standard curve generated using D-glucose and expressed as mg/g extract.

2.5.2 Determination of reducing sugar and non-reducing sugar

The reducing sugar assay was performed following the method described by Robertson *et al*. (2001). One milliliter of the sample was mixed with 3,5-dinitrosalicylic acid (DNS) reagent and boiled for 5 min. Subsequently, the sample was allowed to cool to room temperature for 5 minutes before adding 7 mL of distilled water. The absorbance was then measured at 540 nm using a UV-Vis spectrophotometer (Shimadzu, Japan). Total reducing sugar was calculated with D-glucose as a standard and expressed as mg/g extract. Non-reducing was calculated using the following formula:

Non-reducing sugar (mg/g) = Total sugar content (mg/g) – Reducing sugar content (mg/g)

2.6 Analysis of structural properties of soluble polysaccharides

The structure of soluble polysaccharides (SP) was determined using the Fourier transform infrared (FT-IR) spectroscopy. Infrared spectra were acquired using a Nicolet 6700 FT-IR spectrum analyzer (Thermo Scientific, USA) over the range of 4000-400 cm^{-1}. Samples were prepared by grinding 1 mg of SP with potassium bromide (KBr) and pressing the mixture into a pellet for FT-IR analysis (Mohd Nor *et al*., 2017).

2.7 Analysis of monosaccharide composition of soluble polysaccharides

Soluble polysaccharides (SP) were subjected to hydrolysis prior to monosaccharide determination. In brief, 10 mg of SP was dissolved in 10 mL of 2M trifluoroacetic acid (TFA) and incubated at 95 ºC for 6 h. The resulting mixture was then centrifuged at 9300 xg for 5 min. The supernatant was collected and evaporated using a rotary evaporator at 60 ºC to remove TFA. The hydrolysate was dissolved in 1 mL of distilled water. High-performance liquid chromatography (HPLC) equipped with a refractive index detector (Hitachi, Japan) was used to analyze the monosaccharide composition. The HPLC system employed with a BP-800 Ca column, with HPLC-grade water serving as the mobile phase, pumped at a flow rate of 0.6 mL/min at 85 ºC for 20 min. A 10 µL injection volume was used for each sample. The concentration of each sugar was determined by comparing peak areas with those of standard sugars, including glucose, fructose, rhamnose, mannose, and xylose.

2.8 Determination of prebiotic activity of soluble polysaccharides on Lactobacillus acidophilus TISTR 2365

The prebiotic effect of SP was evaluated through the *L. acidophilus* TISTR 2365 growth. MRS medium was used as a basal growth medium. *L. acidophilus* TISTR 2365 was cultured at 35°C with samples of SP at concentrations of 0.1 %. Following incubation for 0, 24, 48, 72, 96, 120, 144, 168, 192, 216, and 240 h at 35 ºC, sampling was collected. The total plate count was determined using MRS agar for enumeration. Plates were incubated at 35 °C for 48 h. The number of bacteria were counted, calculated, and expressed as log CFU/mL (Torshabi *et al*., 2023).

2.9 Determination the effect of artificial human gastric juice on hydrolysis of soluble polysaccharides

The effect of artificial human gastric juice on hydrolysis of SP was determined as described by Korakli *et al*. (2002). Initially, SP was dissolved in distilled water to make a concentration of 1 % (w/v). Artificial human gastric juice was prepared by dissolving 8 g of NaCl, 0.2 g of KCl, 8.25 g of $Na_2HPO_4.2H_2O$, 14.35 g of $NaHPO_4$, 0.1 g of $CaCl_2.2H_2O$, and 0.18 g of $MgCl_2.6H_2O$ in distilled water to make a 1 L solution. The pH of the solution was adjusted to 1, 2, 3, 4, and 5 using 6 M HCl, respectively. For the hydrolysis assay, 5 mL of the solution at each pH level was mixed with 5 mL of SP sample. The mixture was then incubated in a water bath at 37 °C for 6 h. Samples were collected at 0, 30 min, 1, 2, 3,4, 5, and 6 h to determine the total and reducing sugar contents. Inulin was used as a positive control for comparison. The percentage of hydrolysis degree was calculated using the following formula:

$$\text{Hydrolysis degree (\%)} = \frac{\text{Reducing sugar} \times 100}{\text{Total sugar content-initial reducing sugar content}}$$

2.10 Statistical analysis

Each experiment was performed three times and the results were reported as ± standard deviation (SD). Data were analyzed by one-way ANOVA using SPSS statistics 17.0 (SPSS Inc., Chicago, IL, USA). All statistics were based on a confidence level of 95 %, and $p < 0.05$ was considered statistically significant.

3. Results and Discussion

3.1 Chemical composition of coconut residue (CR) and defatted coconut residue (DCR)

The chemical composition of CR and DCR is presented in Table 1. Carbohydrate and fiber were identified as the major components in both CR and DCR. The defatting process resulted in a significant reduction in fat content in coconut residue ($p < 0.05$), decreasing from 16.35 ± 0.36 % in CR to 3.99 ± 0.55 % in DCR. Similarly, there was a notable decrease in protein content from 4.56 ± 0.32 % CR to 2.93 ± 0.18 % in DCR. Additionally, the ash content in DCR (0.76 ± 0.04 %) was

found to be lower than that in CR (1.24 ± 0.01 %). The extraction of fat from coconut residue resulted in changes in its chemical composition, including lower fat, protein, and ash contents, while the carbohydrate content was higher compared to CR. Specifically, the fat content of DCR in this study was significantly lower than the findings reported by Mohd Nor *et al*. (2017), who observed a fat content of 17.26 % in defatted coconut residue. The difference in lipid contents might be due to the variety of coconut, growing conditions, and processing methods.

Hot water extraction followed by precipitation with alcohol is the most widely used method for extracting polysaccharides (Sritrakul and Keawsompong, 2021; Gunarathne *et al*., 2024). Soluble polysaccharides (SP) were obtained from DCR as a water-soluble white water-soluble as shown in Figure 1. In this study, the percentage yield of SP was 2.50 ± 0.40 which exceeded that reported by Abbasiliasi *et al*. (2019) (% yield: 1.33 ± 0.30) and Mohd Nor *et al*. (2017) (% yield: 0.73 ± 0.04). The variation of extraction yield may be attributed to several factors, including the extraction method employed, the ratio of water to raw material, extraction duration, and extraction temperature (Cai *et al*., 2008).

A B C

Figure 1 A) Coconut residue (CR) B) Defatted coconut residue (DCR) and C) Soluble polysaccharides (SP)

3.2 Total sugar content, reducing sugar, and non-reducing sugar

As shown in Table 2, the removal of fat from CR resulted in a remarkable increase in the total sugar content of DCR, rising from 63.31 ± 7.39 mg/g to 85.77 ± 5.71 mg/g. Furthermore, the percentage yield of soluble polysaccharides (SP) obtained in this study was 4.40 ± 0.11 %. Subsequently analysis revealed that the total sugar content of SP was 397.29 ± 66.24 mg/g, with a reducing sugar content of 27.47 ± 0.67 mg/g. Accordingly, the non-reducing sugar content of SP was calculated to be 369.82 ± 66.42 mg/g. Remarkably, SP exhibited the highest content of both total sugar and non-reducing sugar ($p < 0.05$) compared to other samples. The extraction of soluble polysaccharides from DCR had the highest proportion of non-reducing sugars. This observation suggests that the SP may contain a higher proportion of oligosaccharides or polysaccharides compared to monosaccharides. The determination of non-reducing sugar is indicative of the presence of oligosaccharides (Thungchoho, 2012).

3.3 Monosaccharides content of soluble polysaccharides

The monosaccharide composition of soluble polysaccharides (SP) comprises two major sugars: mannose, accounting for 27.87 % and glucose, comprising 25.00 %. Fructose also presented a smaller proportion of 7.10 %. This result agrees with the study by Thongsook and Chaijamrus (2018), who found that glucose and mannose were the major sugars detected in the copra meal hydrolysis. The study on extracted polysaccharides by Sritrakul and Keawsompong (2021) reported that mannose was the main sugar accounting for 99 % of total monosaccharides. A study reported that copra meal is a main source of galactomannan (Rungruangsaphakun and Keawsompong, 2018). Other previous studies showed that the composition of polysaccharides in coconut residue was glucose (1.66 %) and fructose (19.16 %) (Mohd Nor *et al*., 2017). It was revealed that geographical area and seasonal harvest of the plant sources could contribute to the variation in the monosaccharide composition (Ng *et al*., 2010).

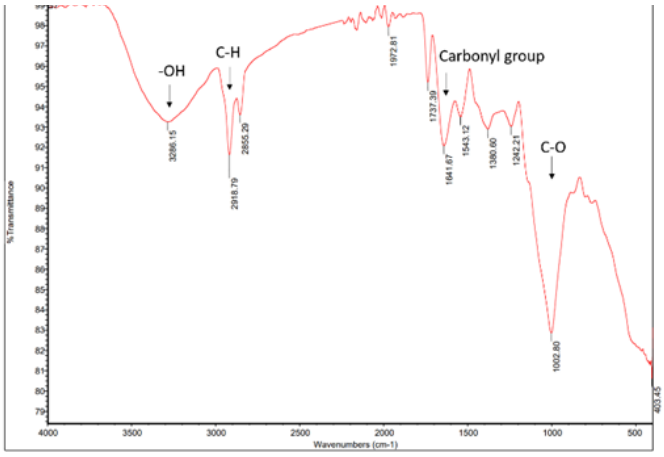

Figure 2 FTIR spectrum of soluble polysaccharides

3.4 FT-IR Analysis of SP

Combining data from chemical analysis with FT-IR spectroscopy allows for the approximate identification of compounds as shown in Figure 2. In this study, a broad band centered at 3286.15 cm-1 was attributed to hydroxyl (OH) group, while the band observed at 2918.79 cm^{-1} indicated C-H stretching, suggesting the presence of polysaccharides. Additionally, a band in the region of 1641.67 cm^{-1} represented the stretching vibration of the carbonyl group. Adsorption at 1002.80 cm^{-1} indicated CO stretching vibration. Taken together, these findings indicate that SP is mainly composed of polysaccharides.

3.5 Effect of artificial human gastric juice on hydrolysis of soluble polysaccharides

According to the requirement for prebiotic products, it is essential that they are not hydrolysed under acidic conditions to ensure their passage to the intestine where they can facilitate the proliferation of beneficial gut bacteria (probiotics). SP containing non-reducing sugar exhibits characteristics indicative

of an oligosaccharide with potential prebiotic characteristics. To assess its resistance to hydrolysis, SP and inulin (used as a positive control) were subjected to incubation with artificial human gastric juice at various pH levels (Figure 3). For inulin, the degree of hydrolysis after 5 h of incubation at pH 1, 2, 3, 4, and 5 were 74.48, 10.65, 0.45, 0.42, and 0.16 %, respectively (Figure 3A). For SP, the degree of hydrolysis at pH 1, 2, 3, 4, and 5 were 7.58, 9.58, 6.86, 6.81, and 0.60 %, respectively (Figure 3B). Notably, at pH 1 (lowest pH), the degree of hydrolysis of SP was lower compared to inulin. The hydrolysis of polysaccharides with human gastric juice was influenced by their monosaccharide compositions, ring configurations, and types of glycosidic linkages (Wang *et al*., 2015). In this study, the main composition of SP was mannose. A previous study has reported that a high mannose content could resist digestive enzymes (Asano *et al*., 2003). In addition, a pH level below 2 has been reported to degrade inulin and lead to an increase in reducing sugar due to the β-(2-1) glycosidic bonds in inulin being susceptible to acid hydrolysis (Lin *et al*., 2024). In the present study, at pH 2, no significant differences of acid stability were observed between SP (~90% resistance) and inulin (~89% resistance). Therefore, at pH 2, both SP and inulin were hydrolyzed slowly, and their structures remained relatively intact. Furthermore, the degree of hydrolysis of SP decreased with increasing pH from 1 to 5. It was found that soluble polysaccharides can resist simulated human gastric juice.

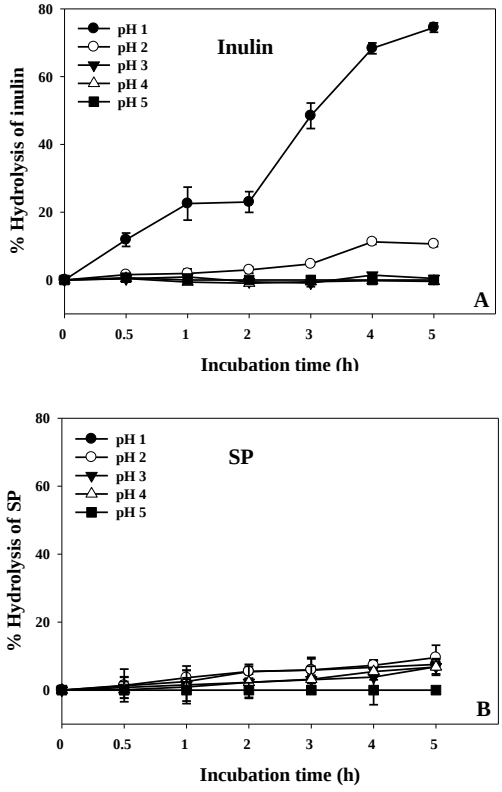

Figure 3 Hydrolysis of inulin (A) and SP (B) after treatment with artificial human gastric juice

In this study revealed that both soluble polysaccharides (SP) and inulin exhibited a higher degree of hydrolysis at low pH compared to high pH. The increased hydrolysis observed at low pH can be attributed to the stomach. Under these acidic conditions, the glycosidic linkages in the polysaccharides are more susceptible to rupture, leading to partial hydrolysis. Consequently, the polysaccharides may degrade into smaller molecules. Prolonged incubation times in acidic conditions further caused the hydrolysis of polysaccharides to monosaccharides or disaccharides (Mohd Nor *et al*., 2017; Wang *et al*., 2015). The digestibility of polysaccharides during the initial two-hour period was a high degree of hydrolysis at pH 1 and 2. The percentage of SP that resisted human gastric digestion at pH 1 was approximately 92 %, which markedly exceeded that of inulin (25 %). It might be due to the differences in their monosaccharide compositions. SP predominantly consists of mannose, a monosaccharide that has been reported to exhibit resistance to digestive enzymes (Asano *et al*., 2003). Conversely, inulin is primarily composed of fructose molecules (Prosky, 1999). Consequently, there is a possibility that most of the SP is not digested, enabling it to transit to the large intestine where it can serve as a substrate for native probiotics.

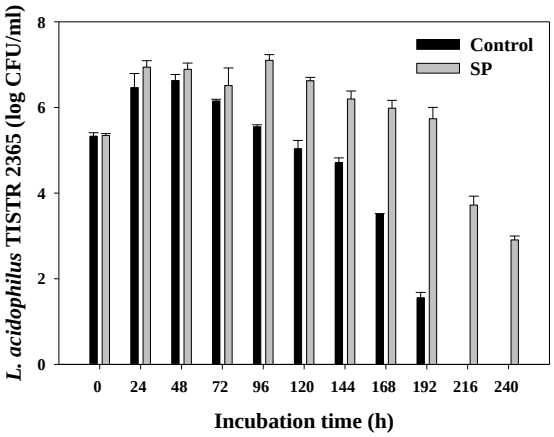

Figure 4 Proliferation of *L. acidophilus* TISTR 2365 on SP

3.6 Prebiotic activity of SP on Lactobacillus acidophilus TISTR 2365

Figure 4 depicts the ability of 0.1 % SP to promote the growth of probiotic bacteria, *Lactobacillus acidophilus* TISTR 2365, following incubation periods ranging from 0 to 240 h. The concentration of prebiotics is also an important factor affecting the production of short-chain fatty acids (SCFAs) by probiotics. The increase of SCFAs leads to a decrease in the pH of the intestine and is beneficial to human health (You *et al*., 2022). In this study, using 0.1 % SP powder is an optimal concentration to lower intestinal pH and promote the growth of *Lactobacillus* acidophilus TISTR 2365.

A significance difference ($p < 0.05$) was observed between the control group (MRS only) and MRS supplemented with SP. Specifically, the addition of SP was found to enhance the growth of *L. acidophilus* TISTR 2365 compared to the control group.

L. acidophilus was able to utilize various oligosaccharides and polysaccharides (Dong *et al*., 2024). In the control group, the cell count decreased after 96 h, whereas in the SP treatment, the population of *L. acidophilus* TISTR 2365 remained higher. Following nutrient depletion in the MRS medium, SP served as an additional carbon source. As a result, the decline in cell counts was delayed until 240 h when compared with the control. The enhanced proliferation of probiotics in SP-supplemented media may be attributed to the sugar content present in polysaccharides, including mannose, glucose, fructose, which serve as substrates for bacterial growth. Furthermore, soluble polysaccharides are more effective for bacterial utilization. These polysaccharides can be readily hydrolyzed by bacterial enzymes, releasing sugars that can be metabolized by probiotics and become more beneficial for gut health (Mohd Nor *et al*., 2017).

Table 1 Chemical composition of coconut residue (CR) and defatted coconut residue (DCR)

Parameters	Composition (%)	
	Coconut residue (CR)	Defatted coconut residue (DCR)
Moisture content	4.51 ± 0.21[a]	7.04 ± 0.04[b]
Crude protein	4.56 ± 0.32[b]	2.93 ± 0.18[a]
Crude fat	16.35 ± 0.36[b]	3.99 ± 0.55[a]
Ash content	1.24 ± 0.01[b]	0.76 ± 0.04[a]
Crude fiber	39.31 ± 0.96a	38.70 ± 1.48[a]
Carbohydrate	34.03 ± 1.51a	46.58 ± 1.05[b]

Table 2 Total sugar, reducing sugar, and non-reducing sugar of CR, DCR, and SP

Samples	Total sugar (mg/g)	Reducing sugar (mg/g)	Non-reducing sugar (mg/g)
CR	63.31 ± 7.39[a]	48.50 ± 4.23[c]	14.81 ± 5.08[a]
DCR	85.77 ± 5.71[b]	19.69 ± 2.77[a]	66.08 ± 2.98[b]
SP	397.29 ± 66.24[c]	27.47 ± 0.67[b]	369.82 ± 66.42[c]

4. Conclusion

The soluble polysaccharides (SP) from defatted coconut residue were obtained. These findings confirm the potential of SP as a prebiotic ingredient due to its resistance to gastric digestion and its subsequent availability for fermentation by gut microbiota in the colon. Therefore, this study highlights the sustainability aspect of utilizing coconut residue, which encourages the efficient use of agricultural waste and enhances economic feasibility. This contributes to its significant potential for large-scale commercial applications. Further study to confirm the characteristics of MOS could be performed by molecular weight distribution analysis using HPAEC-PAD, linkage type analysis by methylation followed by GC-MS and NMR, and evaluation of prebiotic activity through human fecal fermentation.

5. Acknowledgment

This research was supported by the Science, Research and Innovation Promotion Fund, Thailand Science Research and Innovation (TSRI), through Rajamangala University of Technology Tawan-ok (Grant No.: FRB619/2566).

6. References

Abbasiliasi, S., Tan, J.S., Bello, B., Ibrahim, T.A.T., Tam, Y.J., Ariff, A. and Mustafa, S. 2019. Prebiotic efficacy of coconut kernel cake's soluble crude polysaccharides on growth rates and acidifying property of probiotic lactic acid bacteria in vitro. **Biotechnology & Biotechnological Equipment** 33(1):1216-1227.

AOAC. 2002. **Official Methods of Analysis of AOAC International** (17thed). Association of Analytical Chemists. Gaithersburg, USA.

Asano, I., Hamaguchi, K., Fuji, S. and Iino, H. 2003. In vitro digestibility and fermentation of mannooligosaccharides from coffee mannan. **Food Science and Technological Research** 9: 62-66.

Asbury, R.E. and Saville, B.A. 2025. Manno-oligosaccharides as a promising antimicrobial strategy: pathogen inhibition and synergistic effects with antibiotics. **Frontiers in Microbiology** 16: 1529081.

Bamigbade, G.B., Subhash, A.J., Kamal-Eldin, A., Nyström, L. and Ayyash, M. 2022. An Updated review on prebiotics: Insights on potentials of food seeds waste as source of potential prebiotics. **Molecules** 27(18): 5947.

Bello, B., Mustafa, S., Tan, J.S., Ibrahim, T.A.T., Tam, Y.J., Ariff, A.B., Manap, M.Y. and Abbasiliasi, S. 2018. Evaluation of

the effect of soluble polysaccharides of palm kernel cake as a potential prebiotic on the growth of probiotics. **3 Biotech** 8(8): 346.

Cai, W., Gu, X. and Tang, J. 2018. Extraction, purification, and characterization of the polysaccharides from *Opuntia milpa alta*. **Carbohydrate Polymers** 71: 403-410.

Dong, Y., Han, M., Fei, T., Liu, H. and Gai, Z. 2024. Utilization of diverse oligosaccharides for growth by *Bifidobacterium* and *Lactobacillus* species and their in vitro co-cultivation characteristics. **International Microbiology** 27: 941-952.

Dubois, M., Gilles, K.A., Hamilton, J.K., Rebers, P.A. and Smith, F. 1956. Colorimetric method for determination of sugars and related substances. **Analytical Chemistry** 28(3): 350-356.

Gibson, G.R., Hutkins, R., Sanders, M.E., Prescott, S.L., Reimer, R.A., Salminen, S.J., Scott, K., Stanton, C., Swanson, K.S., Cani, P.D., Verbeke, K. and Reid, G. 2017. Expert consensus document: The International Scientific Association for Probiotics and Prebiotics (ISAPP) consensus statement on the definition and scope of prebiotics. **Nature reviews. Gastroenterology & Hepatology** 14(8): 491-502.

Gunarathne, R., Wijenayake, S., Yalegama, C., Marikkar, N.M. and Lu, J. 2024. Exploring the prebiotic characteristics of crude polysaccharides from coconut testa flour: A comparative analysis of local cultivar. **Heliyon** 10(9): e30256.

Intaratrakul, K., Nitisinprasert, S., Nguyen, T.H., Haltrich, D. and Keawsompong, S. 2022. Manno-oligosaccharides from copra meal: Optimization of its enzymatic production and evaluation its potential as prebiotic. **Bioactive Carbohydrates and Dietary Fibre** 27: 100292.

Khuwijitjaru, P., Watsanit, K. and Adachi, S. 2012. Carbohydrate content and composition of product from subcritical water treatment of coconut meal. **Journal of Industrial Engineering Chemistry** 18: 225-229.

Kolida, S., Tuohy, K. and Gibson, G.R. 2002. Prebiotic effects of inulin and oligofructose. **The British Journal of Nutrition** 87: S193-S197.

Korakli, M., Gänzle, M.G. and Vogel, R.F. 2002. Metabolism by bifidobacteria and lactic acid bacteria of polysaccharides from wheat and rye, and exopolysaccharides produced by *Lactobacillus sanfranciscensis*. **Journal of Applied Microbiology** 92(5): 958-965.

Lin, X., Zhang, X. and Xu, B. 2024. Differences in physicochemical, rheological, and prebiotic properties of inulin isolated from five botanical sources and their potential applications. **Food Research International** 180: 114048.

Mohd Nor, N.N., Abbasiliasi, S., Marikkar, M.N., Ariff, A., Amid, M., Lamasudin, D.U., Abdul Manap, M.Y. and Mustafa, S. 2017. Defatted coconut residue crude polysaccharides as potential prebiotics: study of their effects on proliferation and acidifying activity of probiotics in vitro. **Journal of Food science and Technology** 54(1):164-173.

Ng, S.P., Tan, C.P., Lai, O.M., Long, K. and Mirbosseini, H. 2010. Extraction and characterization of dietary fiber from coconut residue. **Journal of Food, Agriculture & Environment** 8(2): 172-177.

Peredo Lovillo, A., Romero Luna, H.E. and Jiménez Fernández, M. 2020. Health promoting microbial metabolites produced by gut microbiota after prebiotics metabolism. **Food Research International** 136: 109473.

Prebiotics market size. 2023. **Thailand Prebiotics Market Size & Outlook, 2023-2030**. Available Source: https://www.grandview research.com/ horizon/outlook/prebiotics-market/thailand, June 15, 2025.

Prosky, L. 1999. Inulin and oligofructose are part of the dietary fiber complex. **Journal of AOAC International** 82(2): 223-226.

Pulidindi, K. and Ahuja, K. 2024. Prebiotics Market Size. **Global Market Insights.** Available Source: https://www. gminsights.com/industry-analysis/prebiotics-market, July 13, 2024.

Raghavendra, S.N., Rastogi, N.K., Raghavarao, K.S.M.S. and Tharanathan, R.N. 2004. Dietary fibre from coconut residue: effects of different treatments and particle size on the hydration properties. **European Food Research and Technology** 218: 563-567.

Robertson, J.A., Ryden, P., Botham, R.L., Reading, S., Gibson, G. and Ring, S.G. 2001. Structural properties of diet-derived polysaccharides and their influence on butyrate production during fermentation. **LWT-Food Science and Technology** 34(8): 567-573.

Rungruangsaphakun, J. and Keawsompong, S. 2018. Optimization of hydrolysis conditions for the mannooligosaccharides copra meal hydrolysate production. **3 Biotech** 8(3): 1-9.

Sritrakul, N. and Keawsompong, S. 2021. Polysaccharides in copra meal: extraction conditions, optimization and characterization. **International Journal of Agricultural Technology** 17(1): 337-348.

Sulaiman, S., Abdul Aziz, A.R. and Aroua, M.K. 2013. Optimization and modeling of extraction of solid coconut waste oil. **Journal of Food Engineering** 114(2): 228-234.

Thongsook, T. and Chaijamrus, S. 2018. Optimization of enzymatic hydrolysis of copra meal: compositions and properties of the hydrolysate. **Journal of Food Science and Technology** 55(9): 3721-3730.

Thungcholo, K. 2012. Non-reducing sugar extraction in laboratory and pilot plant scale and evaluation of the resistance to digestion in simulated upper gut condition. Master of Science, Prince of Songkla University, Thailand.

Torshabi, M., Bardouni, M.M. and Hashemi, A. 2023. Evaluation of antioxidant and antibacterial effects of lyophilized cell-free probiotic supernatants of three *Lactobacillus* spp. and their cytocompatibility against periodontal ligament stem cells. **Iranian Journal of Pharmaceutical Research** 22(1): e136438.

Wang, X., Huang, M., Yang, F., Sun, H., Zhou, X., Guo, Y., Wang, X. and Zhang, M. 2015. Rapeseed polysaccharides as prebiotics on growth and acidifying activity of probiotics in vitro. **Carbohydrate Polymers** 125: 232-240.

Yamabhai, M., Sak-Ubol, S., Srila, W. and Haltrich, D. 2014. Mannan biotechnology: From biofuels to health. **Critical Reviews in Biotechnology** 15: 1-11.

You, S., Ma, Y., Yan, B., Pei, W., Wu, Q., Ding, C. and Huang, C. 2022. The promotion mechanism of prebiotics for probiotics: A review. **Frontiers in nutrition** 9: 1000517.

Recent Science and Technology

Journal homepage: https:// www.tci-thaijo.org/index.php/rmutsvrj/index

ISSN: 3057-0786 (Online)

Research Article

Effects of Cannabis (*Cannabis sativa* L.) Leaf Supplementation in Broiler Diets on Growth Performance, Carcass Characteristics, and Meat Quality

Piphat Chanataepaporn [a], Janjira Tohkwankaew [a], Chalermpan Tantara [b] and Rattanakorn Saenthumpol [a *]

[a] *Program of Agriculture, Faculty of Agricultural Technology and Industrial Technology, Phetchabun Rajabhat University, Phetchabun 67000, Thailand.*
[b] *Department of Animal Science, Faculty of Agriculture at Kamphaeng Saen, Kasetsart University, Nakhon Pathom 73140, Thailand.*

Article history:

Received: 2025-02-25
Revised: 2025-08-10
Accepted: 2025-08-13

Keywords:

Broiler;
Cannabis;
Growth performance;
Carcass characteristics;
Meat quality

ABSTRACT

This study investigated the effects of supplementing broiler diets with *Cannabis sativa L.* leaves on growth performance, carcass characteristics, and meat quality. A total of 150 unsexed broiler chicks (aged 7 days) were randomly assigned to five dietary treatments with three replicates per treatment and 10 birds per replicate. The treatments included a control group fed a basal diet and four experimental groups receiving the basal diet supplemented with 0.5%, 1%, 1.5%, and 2% cannabis leaf powder, respectively. The birds were raised in an open-house system with ad libitum access to feed and water throughout the trial. The results showed that cannabis leaf supplementation had no significant effect on feed intake and feed conversion ratio (FCR) ($P > 0.05$). However, supplementation at 0.5% significantly increased final body weight and average daily gain (ADG) ($P < 0.01$), while the 2% supplementation level resulted in a significant reduction in these parameters ($P < 0.01$). Regarding carcass characteristics, the 0.5% supplementation level increased the percentage of breast and tenderloin yields ($P < 0.01$), whereas the 2% level reduced neck yield ($P < 0.05$). Meat quality parameters, including pH, water-holding capacity, and sensory attributes, were unaffected by dietary cannabis supplementation ($P > 0.05$). However, the 1% supplementation level resulted in a significantly higher b* value in drumstick meat ($P < 0.05$). In conclusion, supplementing broiler diets with 0.5% cannabis leaf powder may enhance growth performance and improve carcass characteristics without negatively affecting meat quality. Further studies are recommended to determine the optimal inclusion level for practical applications in poultry nutrition.

1. Introduction

The broiler industry has undergone rapid advancements in multiple aspects, including genetic improvements, high-quality feed development, and modernized farm management systems. Selective breeding has enabled faster growth rates, while advancements in nutrition and farm management efficiency have further enhanced production potential. As a result, the industry has been able to adequately meet consumer demand and improve overall productivity. Despite these advancements, chemical feed additives (FAs) continue to be widely used in poultry production. Among them, antibiotic growth promoters (AGPs) are commonly added to broiler diets to reduce mortality rates and enhance growth performance. However, the prolonged use of AGPs raises concerns about antimicrobial residues in poultry products, food safety risks, and potential trade restrictions on chicken exports.

To address these concerns, animal nutritionists have turned their attention to natural alternatives, particularly the incorporation of local medicinal herbs in animal feed, such as basil, garlic, and ginger (Khajaren, 2013). These natural additives reduce chemical residues in poultry products while enhancing food safety. Among these, Cannabis sativa has gained interest due to its long history of use in both human and animal nutrition, traditional medicine, textiles, and other applications. Cannabis

* **Corresponding author.**
E-mail address: *rattanakorn.sae@pcru.ac.th*

Cite this article as:

Chanataepaporn, P., Tohkwankaew, J., Tantara, C. and Saenthumpol, R. 2026. Effects of Cannabis (*Cannabis sativa* L.) Leaf Supplementation in Broiler Diets on Growth Performance, Carcass Characteristics, and Meat Quality. **Recent Science and Technology** 18(1): 266476.

https://doi.org/10.65411/rst.2026.266476

contains over 750 bioactive compounds, with cannabinoids such as Tetrahydrocannabinol (THC) and Cannabidiol (CBD) being the most prominent. These compounds exhibit medicinal properties and have been extensively studied for their potential in treating multiple sclerosis, epilepsy, and cancer. Additionally, cannabis is used as an appetite stimulant, an antiemetic (anti-vomiting agent), and a pain reliever (Hazekamp *et al*., 2007; Bernstein *et al*., 2019).

While research on cannabis supplementation in animal feed remains limited, previous studies suggest potential benefits in broiler production. Cannabis supplementation has been found to reduce disease incidence by lowering serum aspartate aminotransferase (AST) levels, an enzyme associated with liver toxicity (Vispute *et al*., 2019); improve product quality by enhancing chemical composition and meat color attributes (Goldberg *et al*., 2012); and enhance production efficiency, leading to increased body weight and improved feed conversion (Khan *et al*., 2010). However, these findings are not yet conclusive, and further research is needed to determine the optimal supplementation levels and long-term effects of cannabis in broiler diets. Therefore, this study aims to evaluate the effects of cannabis leaf supplementation on growth performance, carcass characteristics, and meat quality in broilers. The findings from this research could provide guidelines for the efficient utilization of local cannabis leaves in poultry nutrition. If proven effective, cannabis leaf supplementation could enhance broiler production performance, generate additional income for farmers, and promote sustainability within the poultry industry.

2. Materials and Methods

2.1 Preparing cannabis leaves

The cannabis leaves used in this study were prepared by washing with clean water to remove any contaminants. The fresh leaves were then weighed and dried at 50°C for 48 hours until they were completely dry. The dry weight was recorded, and the leaves were ground into a fine powder using a blender. The powder was then sieved through a 1-millimeter mesh to ensure uniform particle size. Finally, the bioactive compounds in the cannabis leaf powder were analyzed using High-Performance Liquid Chromatography (HPLC), with the results measured using a Diode Array Detector (DAD). The composition of the bioactive compounds is presented in Table 1.

Table 1 Phytochemical content of cannabis leaves

Item	Value (%w/w)
Cannabidiolic Acid (CBDA)	0.5524
Cannabigerol (CBG)	0.0038
Cannabidiol (CBD)	0.0579
Cannabinol (CBN)	-
Delta-9-tetrahydrocannabinol (A9-THC)	0.1557
Delta 9-Tetrahydrocannabinolic Acid (THCA)	0.6320
Total THC	0.7093

2.2 Experimental animals

This experiment was approved for the use of animals in scientific research by the Faculty of Agricultural Technology and Industrial Technology, Phetchabun Rajabhat University, under approval document number (PCRU/2567/101). The study utilized 150 unsexed Arbor Acres broilers, aged 7 days, in a completely randomized design (CRD). The broilers were randomly assigned to five dietary treatments, with three replicates per treatment and 10 broilers per replicate (6 males and 4 females per replicate). The experimental groups were as follows: Group 1 (CON): basal diet (control). Groups 2–5: basal diet supplemented with 0.5%, 1%, 1.5%, and 2% cannabis leaf powder, respectively. The basal diet consisted of commercial feed base on the nutrient requirements of poultry (Aviagen, 2022), divided into two formulations: starter diet (0–21 days), containing at least 21% crude protein; and finisher diet (22–42 days), containing at least 19% crude protein. All broilers had *ad libitum* access to feed and water throughout the experimental period.

2.3 Broiler Management

The experimental broilers were housed in communal pens, each measuring 1 × 1 meter, with a total of 15 pens (10 birds per pen). They were raised under an open-house system at Phetchabun Rajabhat University, where the average temperature ranged from 21 to 34°C, and the relative humidity averaged 83%. The experiment lasted for five weeks.

2.4 Growth Performance and Carcass Characteristics

Data on body weight, daily feed intake, and mortality rate were recorded throughout the experimental period. At the end of the trial (42 days of age), broilers with body weights closest to the average of each replicate were randomly selected (four birds per replicate: two males and two females) for slaughter. Carcass weight (weight after slaughter, including feet and neck but excluding head and internal organs) was measured following the method described by Faria *et al*. (2010).

The following calculations were performed:

$$\text{Average Daily Gain (ADG)} = \frac{\text{Final weight - Initial weight}}{\text{Number of rearing days}}$$

$$\text{Feed Conversion Ratio (FCR)} = \frac{\text{Total feed intake}}{\text{Body weight gain}}$$

$$\text{Carcass yield percentage (\%)} = \frac{\text{Carcass weight (excluding internal organs)} \times 100}{\text{Live weight}}$$

$$\text{Cut-up part yield percentage (\%)} = \frac{\text{Part weight} \times 100}{\text{Carcass weight}}$$

2.5 Meat Quality Evaluation

On the final day of the experiment, broilers were slaughtered, defeathered, and eviscerated, and breast and drumstick meat samples were collected. The samples were then stored in a

refrigerator at 4°C for 24 hours for further analysis of meat pH, color, drip loss, cooking loss, and sensory attributes. The pH value of the meat was measured using a pH meter (Model G0842, Schott AG, Germany), while color parameters (L*, a*, and b*) were analyzed using a Hunter Lab MiniScan EZ (Virginia, USA). For drip loss measurement (AOAC, 1990), meat samples were trimmed to remove fat tissue, weighed, and sealed in airtight plastic bags to prevent moisture evaporation and oxidation. The samples were then suspended in a refrigerator at 4°C for 24 hours, after which they were weighed again after gently blotting the excess liquid. Cooking loss measurement (Lawrie and Ledward, 2006) was performed by weighing meat samples, sealing them in poly-bag zipper plastic bags, and boiling them in a water bath at 80°C for 10 minutes. After cooling to room temperature, the samples were weighed again, and cooking loss percentage was calculated. Sensory attributes were evaluated using the 9-point hedonic scale (Chompreeda, 1993). A panel of 30 untrained consumers, aged 18–22 years, assessed color, odor, taste, and texture, following the method described by Wiriyacharee (2018).

The following calculations were performed:

$$\text{Drip loss} = \frac{\text{Initial weight} - \text{Final weight} \times 100}{\text{Initial weight}}$$

$$\text{Cooking loss} = \frac{\text{Initial weight} - \text{Final weight} \times 100}{\text{Initial weight}}$$

2.6 Statistical Analysis

The collected data were analyzed using Analysis of Variance (ANOVA), and mean differences were tested using the Least Significant Difference (LSD) method with SPSS statistical software. The results were presented as mean ± standard error of the mean (Mean ± SEM). Statistical significance was determined at $P < 0.05$.

3. Results and Discussion

3.1 Bioactive Compound Composition in Broiler Meat

The bioactive compounds detected in broiler meat are presented in Table 2. The study found that cannabis leaf supplementation did not result in detectable residues of tetrahydrocannabinol (THC), a compound that could potentially impact consumers. However, at the 2% supplementation level, a trace amount of cannabidiol (CBD) was detected, measuring 0.0011% of the total meat weight. CBD is a naturally occurring compound in cannabis and is generally recognized as safe. It has no reported adverse effects on physiology, biochemistry, behavior, or addiction in both animals and humans. According to the World Health Organization (WHO, 2018), the amount of CBD required to potentially affect humans must reach 150 mg and be consumed continuously over an extended period. Therefore, the presence of CBD in broiler meat due to cannabis leaf supplementation is unlikely to pose any health risks to consumers.

Table 2 Phytochemical content in broilers meat products supplemented with cannabis leaves

Item (%w/w)	Levels of dietary cannabis leaves (%)				
	CON[1]	0.5	1	1.5	2
Cannabidiol (CBD)	-	-	-	-	0.0011
Delta-9-tetrahydrocannabinol	-	-	-	-	-
Delta-9-tetrahydrocannabinol Acid	-	-	-	-	-

Remark:[1] CON = Control diet.

3.2 Growth Performance

As shown in Table 3, cannabis leaf supplementation did not affect feed intake or feed conversion ratio (FCR; $P > 0.05$). This finding is consistent with the study by Sopian *et al*. (2024), which investigated the supplementation of cannabis by-products (leaves and stems) in broiler diets at levels of 0%, 0.5%, 1%, and 2%, reporting no significant impact on FCR ($P > 0.05$). However, their study observed a reduction in feed intake, which differs from the findings of He *et al*. (2024), who supplemented hemp seeds in the diets of 50-day-old Three-Yellow chickens at 0%, 5%, 10%, and 20% levels, resulting in increased feed intake.

Regarding final body weight, weight gain, and average daily gain (ADG), the highest values were observed in broilers supplemented with 0.5% cannabis leaves (1,571.70 g and 54.53 g/bird/day, respectively), whereas the lowest values were recorded in the 2% supplementation group (1,476.34 g and 51.16 g/bird/day, respectively; $P < 0.01$). The increase in body weight and ADG may be attributed to cannabinoid compounds, particularly Tetrahydrocannabinol (THC), which stimulates appetite by promoting ghrelin (hunger hormone) secretion (Famii and Oluwafeyikemi, 2024).

However, high levels of cannabis leaf supplementation may alter feed palatability, leading to reduced feed intake (Sopian *et al*., 2024). These findings align with the study by Famii and Oluwafeyikemi (2024), which supplemented cannabis leaves in broiler diets at levels of 0%, 0.1%, 0.2%, 0.4%, and 0.8%, reporting that broilers in the 0.8% supplementation group exhibited significantly higher body weight than other groups ($P < 0.05$), Additionally, Beiń *et al*. (2024) supplemented cannabidiol (CBD) extract in broiler diets under bacterial stress from Clostridium perfringens at 3% of feed, finding that broilers maintained higher body weights despite being under stress ($P < 0.05$).

Table 3 Effects of cannabis leaves supplementation in broilers diets on broilers growth performance

Items[1]	Levels of dietary cannabis leaves (%)					P-value
	CON[2]	0.5	1	1.5	2	
IBW (g/b)	43.80 ± 0.38	44.93 ± 1.56	44.43 ± 0.91	43.98 ± 2.18	44.03 ± 0.27	0.8220
FBW (g/b)	1,554.49 ± 12.19^{ab}	1,571.70 ± 19.96^{a}	1,546.53 ± 46.58^{ab}	1,515.83 ± 14.41^{bc}	1,476.34 ± 19.00^{c}	0.0078
BWC (g/b)	1,510.69 ± 12.49^{ab}	1,526.76 ± 19.22^{a}	1,502.09 ± 46.42^{ab}	1,471.85 ± 13.86^{bc}	1,432.32 ± 19.00^{c}	0.0078
FI (g/b/d)	71.24 ± 2.16	70.80 ± 2.51	70.66 ± 2.19	68.72 ± 2.14	67.50 ± 0.05	0.1895
ADG (g/b/d)	53.96 ± 0.45^{ab}	54.53 ± 0.69^{a}	53.65 ± 1.66^{ab}	52.57 ± 0.49^{bc}	51.16 ± 0.6^{c}	0.0079
FCR	1.32 ± 0.05	1.30 ± 0.06	1.32 ± 0.01	1.31 ± 0.04	1.32 ± 0.02	0.9575

Remark: [a-c] Mean values in same row with different superscripts differ significantly (P<0.05).

[1] IBW, initial body weight; FBW, final body weight; BWC, Body weight change; FI, feed intake; ADG, average daily gain; FCR, feed conversion ratio.

[2] CON = Control diet.

Table 4 Effects of cannabis leaves supplementation in broilers diets on broilers carcass characteristics

Items	Levels of dietary cannabis leaves (%)					P-value
	CON[1]	0.5	1	1.5	2	
Live weight (g)	1,557.92 ± 7.24^{ab}	1,573.46 ± 2.37^{a}	1,546.43 ± 6.66^{b}	1,520.29 ± 5.25^{c}	1,481.50 ± 20.28^{d}	<.0001
Carcass weight (g)	1,440.75 ± 6.52^{a}	1,458.38 ± 3.48^{a}	1,440.60 ± 4.72^{a}	1,417.63 ± 7.16^{b}	1,384.76 ± 19.67^{c}	<.0001
Carcass yield (%)	80.66 ± 0.40^{c}	80.85 ± 0.15^{c}	81.17 ± 0.38^{bc}	81.49 ± 0.14^{ab}	81.89 ± 0.50^{a}	0.0090
Head	2.89 ± 0.05	2.95 ± 0.09	2.90 ± 0.06	2.85 ± 0.05	2.77 ± 0.10	0.0851
Neck	3.93 ± 0.07^{a}	3.96 ± 0.09^{a}	3.84 ± 0.23^{a}	3.82 ± 0.09^{ab}	3.61 ± 0.02^{b}	0.0394
Leg	3.91 ± 0.02	3.90 ± 0.04	3.86 ± 0.03	3.84 ± 0.09	3.88 ± 0.05	0.1369
Breast	22.81 ± 0.73^{ab}	23.73 ± 1.41^{a}	21.56 ± 0.46^{bc}	20.52 ± 0.72^{c}	18.76 ± 0.18^{d}	0.0002
Thigh	15.43 ± 0.47	16.09 ± 0.85	14.69 ± 0.82	12.36 ± 3.33	13.48 ± 0.33	0.0980
Drumstick	11.53 ± 0.10^{a}	11.60 ± 0.10^{a}	11.01 ± 0.04^{b}	11.15 ± 0.13^{b}	11.03 ± 0.06^{b}	<.0001
Wing	11.23 ± 0.39^{a}	11.17 ± 0.32^{a}	10.02 ± 0.18^{b}	9.06 ± 0.15^{c}	8.72 ± 0.06^{c}	<.0001
Tenderloin	3.79 ± 0.06^{b}	3.81 ± 0.09^{a}	3.69 ± 0.13^{a}	3.53 ± 0.05^{b}	3.29 ± 0.02^{c}	<.0001

Remark: [a-d] Mean values in same row with different superscripts differ significantly (P<0.05).

[1] CON = Control diet.

3.3 Carcass Characteristics

The evaluation of broiler carcass quality, as presented in Table 4, revealed that cannabis leaf supplementation significantly influenced live weight, carcass weight, and carcass yield percentage ($P < 0.01$), as well as the average organ weights ($P < 0.05$). The highest average live weight was recorded in broilers fed 0.5% cannabis leaves (1,573.46 g), while the lowest was found in the 2% supplementation group (1,481.50 g). These results align with feed intake and growth performance data from this study. However, high levels of cannabis leaf supplementation may alter feed palatability, leading to reduced feed intake and consequently affecting broiler body weight (Sopian *et al*., 2024). Previous studies on cannabis supplementation in animals reported similar findings. Abey (2018) found that supplementing 5% and 10% cannabis leaves in rat diets resulted in reduced body weight, whereas Maqbool *et al*. (2023) observed no impact on feed intake or body weight in rats fed cannabis leaves.

Regarding carcass weight, broilers supplemented with 1.5% and 2% cannabis leaves had significantly lower carcass weights than other groups ($P < 0.01$). However, when comparing carcass yield percentage, the 1.5% and 2% supplementation groups exhibited significantly higher carcass yield percentages than other groups ($P < 0.01$). Although these groups showed reduced feed intake, the increased carcass yield percentage could be attributed to improved nutrient digestion and absorption. Cannabinoid compounds are known to play a key role in reducing nutrient malabsorption disorders, regulating gut microbiota balance, reducing intestinal inflammation, and enhancing gut immune function (Karoly *et al*., 2019).

When evaluating individual carcass parts, broilers supplemented with 2% cannabis leaves exhibited a lower neck percentage compared to other groups ($P < 0.05$). Meanwhile, the 0.5% supplementation group showed the highest breast percentage, which decreased as the supplementation level increased ($P < 0.01$). Additionally, thigh and wing percentages were significantly lower in broilers supplemented with 1%, 1.5%, and 2% cannabis leaves compared to the control group ($P < 0.01$). Moreover, the tenderloin percentage was significantly higher in the 0.5% and 1% supplementation groups compared to others, but was lowest in the 2% group ($P < 0.01$). This decrease in tenderloin percentage was consistent with lower feed intake and carcass weight in the 2% cannabis supplementation group. However, these findings

contrast with those of Tufarelli *et al*. (2023), who investigated hemp seed meal supplementation in male Hubbard broilers at levels of 0%, 5%, and 10%, reporting no significant effects on carcass quality. Similarly, Sopian *et al*. (2024) found that supplementing cannabis by-products (leaves and stems) at levels of 0%, 0.5%, 1%, and 2% in broiler diets had no significant impact on carcass quality. However, their study observed an increased heart percentage in broilers supplemented with 1% and 2% cannabis by-products, possibly due to the activation of cannabinoid type 1 receptors by Tetrahydrocannabinol (THC), which has been linked to heart enlargement and increased cardiac muscle size (Abey, 2018; Goyal *et al*., 2017).

3.4 Meat Quality

The effects of cannabis leaf supplementation on meat quality, as presented in Table 5, showed that it did not affect the pH values or color parameters (L*, a*, and b*) of breast meat (P > 0.05). This finding is consistent with the study by Kaić *et al*. (2024), which investigated cannabis leaf supplementation (*Cannabis sativa*) in Ross 308 broilers at levels of 1%, 2%, and 3%, reporting no impact on meat pH values. Similarly, Beiń *et al*. (2024) supplemented cannabidiol (CBD) extract in broiler diets under bacterial stress from Clostridium perfringens at 3% of feed, and found no significant effects on L*, a*, or b* values. However, in this study, drumstick meat color was affected by cannabis leaf supplementation, with 1% and 1.5% supplementation increasing the b* (yellowness) value (P < 0.01), while 2% supplementation slightly reduced the b* value compared to 1% and 1.5% levels. The increase in b* value may be due to the high carotenoid content in cannabis leaves, particularly β-carotene, which is responsible for color changes from deep green to yellow in plant-based oils (Kopsell *et al*., 2005; Šťastník *et al*., 2019). However, the mechanism by which high cannabis supplementation levels influence meat color remains unclear, although it is suspected that certain bioactive compounds in cannabis may undergo chemical reactions that affect meat color (Kanbur, 2022).

Regarding water-holding capacity, cannabis leaf supplementation did not affect cooking loss or drip loss, which aligns with the findings of Kaić *et al*. (2024), who supplemented cannabis leaves at 2% and 3% in Ross 308 broiler diets, impacting on meat water-holding capacity.

Table 5 Effects of cannabis leaves supplementation in broilers diets on meat quality in broilers

Item	Levels of dietary cannabis leaves (%)					P-value
	CON[2]	0.5	1	1.5	2	
pH	6.87±0.06	6.56±0.06	6.40±0.20	6.45±0.20	6.53±0.29	0.0753
Breast color[1]						
L*	47.43±5.80	48.33±5.35	48.99±4.88	49.56±5.01	51.87±2.43	0.5235
a*	-0.63±0.88	0.47±0.78	0.57±1.60	0.59±1.56	0.65±1.06	0.4092
b*	11.05±0.84	12.41±0.83	13.86±2.08	14.25±2.12	15.16±2.09	0.0711
Drumstick color[1]						
L*	59.77±6.62	59.53±5.35	59.24±3.30	58.12±4.85	56.58±9.02	0.8287
a*	-3.35±2.15	-3.48±2.23	0.14±0.80	0.22±0.78	-0.36±2.34	0.1257
b*	11.77±2.47^{b}	12.37±1.98^{b}	17.62±1.74^{a}	17.43±1.56^{a}	15.57±1.76^{ab}	0.0438
Water holding capacity (%)						
Cooking loss	0.09±0.00	0.08±0.10	0.10±0.12	0.12±0.00	0.10±0.01	0.5510
Drip loss	0.14±0.01	0.15±0.02	0.78±0.62	0.85±0.64	0.99±0.74	0.2267

Remark:$^{a-b}$ Mean values in same row with different superscripts differ significantly (P<0.05).

[1] L* represents lightness (0 = black, 100 = white); a* represents the redness (-a = green, +a = red); b* represents the yellowness (-b = blue, +b = yellow).

[2] CON = Control diet.

Table 6 Effects of cannabis leaves supplementation in broilers diets on meat sensory evaluation in broilers

Item	Levels of dietary cannabis leaves (%)					P-value
	CON[1]	0.5	1	1.5	2	
Color	3.87±0.97	3.86±0.97	3.77±0.82	3.75±0.78	3.70±0.88	0.7985
Odor	3.47±1.11	3.63±1.00	3.53±0.97	3.58±0.98	3.60±1.10	0.7855
Taste	4.10±0.76	3.90±0.78	3.93±0.74	3.87±0.81	3.67±0.80	0.0945
Texture	3.83±0.91	3.35±0.95	3.33±0.84	3.35±0.885	3.37±0.93	0.0630
Overall	4.10+0.88	4.00±0.80	3.83±0.75	3.98±0.73	3.73±0.64	0.1785

Remark: [1] CON = Control diet.

3.5 Sensory Evaluation of Meat

As shown in Table 6, cannabis leaf supplementation in broiler diets did not affect the sensory attributes of meat, including color, odor, taste, and texture ($P > 0.05$).

This result differs from the findings of Tathong *et al*. (2024), who studied cannabidiol (CBD) supplementation in Boer crossbred goats at levels of 0.1, 0.2, and 0.3 ml per 30 kg of body weight (0.0003%, 0.0007 and 0.001% of body weight) and found that the odor of meat from the supplemented groups was rated higher than that of the control group. This change in odor may be attributed to the presence of phenolic compounds, which exhibit antioxidant properties and inhibit lipid oxidation (Chen *et al*., 2012). As a result, phenolic compounds may contribute to the breakdown of fatty acids and the suppression of volatile organic compounds (VOCs), which are key factors in meat spoilage (Konieczka *et al*., 2022).

4. Conclusion

The supplementation of cannabis leaves in broiler diets did not affect feed intake, feed conversion ratio (FCR), meat pH, water- holding capacity, or sensory evaluation. However, supplementation at 0.5% was found to tend to enhance growth performance by increasing final body weight and average daily gain (ADG), as well as improving breast and tenderloin yield percentages, whereas supplementation at 1% and 1.5% improved the yellowness of meat.

5. Acknowledgment

The authors would like to express their gratitude to the Faculty of Agricultural Technology and Industrial Technology, Phetchabun Rajabhat University, for providing research funding. Sincere appreciation is also extended to the farming community in Phetchabun Province and the agriculture students for their valuable cooperation and support in this research.

6. References

Abey, N.O. 2018. *Cannabis sativa* (Marijuana) alters blood chemistry and the cytoarchitecture of some organs in Sprague Dawley rat models. **Food and Chemical Toxicology** 116(2018): 292-297.

AOAC. 1990. **Official Methods of Analysis of the Association of Analytical Chemists** (40th ed). Washington, D.C., USA.

Aviagen. 2022. **Ross broiler: Nutrition specifications.** The local Aviagen, US.

Bernstein, N., Gorelick, J. and Koch, S. 2019. Interplay between chemistry and morphology in medical cannabis (Cannabis sativa L.). **Industrial Crops and Products** 129: 185-194.

Bień, D., Michalczuk, M., Jóźwik, A., Matuszewski, A. and Konieczka, P. 2024. Effects of *Cannabis sativa* extract on growth performance, meat physicochemical properties, and oxidative status in chickens challenged with *Clostridium perfringens* and lipopolysaccharide. **Animal Science Papers and Reports** 42(1): 21-108.

Chen, T., He, J., Zhang, J., Li, X., Zhang, H., Hao, J. and Li, L. 2012. The isolation and identification of two compounds with predominant radical scavenging activity in hempseed (seed of *Cannabis sativa* L.). **Food Chemistry** 134: 1030-1037.

Chompreeda, P. 1993. **Sensory Evaluation.** Kasetsart University, Bangkok. (in Thai)

Famii, Z.L. and Oluwafeyikemi, E.U. 2024. The effect of feed Supplementation with Cannabis sativa on the Growth rate and Development of Broiler Chicks. **Newport International Journal of Research in Medical Sciences (NIJRMS)** 5(3): 29-33.

Faria, P.B., Bressan, M.C., Souza, X.R., Rossato, L.V., Botega, L.M.G. and Gama, L.T. 2010. Carcass and parts yield of broilers reared under a semi-extensive system. **Brazilian Journal of Poultry Science** 3: 153-159.

Goldberg, E.M., Gakhar, N., Ryland, O., Aliani, M., Gibson, R.A. and House, J.D. 2012. Fatty acid profile and sensory characteristics of table eggs from laying hens fed hempseed and hempseed oil. **Journal of Food Science** 77(4): 153-160.

Goyal, H., Awad, H.H. and Ghali, J.K. 2017. Role of cannabis in cardiovascular disorders. **Journal of Thoracic Disease** 9(7): 2079-2092.

Hazekamp, A., Bastola, K., Rashidi, H., Bender, J. and Verpoorte, R. 2007. Cannabis tea revisited: A systematic evaluation of the cannabinoid composition of cannabis tea. **Journal of Ethnopharmacology** 113(1): 85-90.

He, Q., Zhang, Z., Tian, H., Wang, H., Lu, X., Deng, H., Yang, F., Tang, X., Wang, J., Li, Z., Li, H., Shen, S., Lu, Y. and Huang, J. 2024. Effects of partial replacement of soybean meal with hemp seed (*Cannabis sativa* L.) cake on the growth and meat quality in female three-yellow chickens. **Poultry Science** 104(2025): 104466.

KaiĆ, A., StamiČar, M., Škorput, D., UgarkoviĆ, N.K. and JanjeČiĆ, Z. 2024. The effect of dietary supplementation with leaves of industrial hemp (*Canabis sativa* L.) on the carcass and meat quality traits of broiler breast meat. **Journal of Central European Agriculture** 25(4): 919-931.

Kanbur, G. 2022. Growth-depressing effect of dietary hempseed oil on broiler performance in the starting period and alterations in meat oxidation, serum parameters and abdominal fatty acids. **Animal Science Papers and Reports** 40(2): 203-216.

Karoly, C.H., Mueller, R.L., Bidwell, L.C. and Hutchison, K.E. 2019. Cannabinoids and the Microbiota-Gut-Brain Axis: Emerging Effects of Cannabidiol and Potential Applications to Alcohol Use Disorders. **Alcohol, Clinical and Experimental Research** 44(2): 340-353.

Khajaren, J. 2013. The Application of Herbal Medicine in Thai Animal Feed: Progress Towards ASEAN Standards. **Khon Kaen Agriculture Journal** 41(4): 369-376. (in Thai)

Khan R.U., Durrani, F.R., Chand, N. and Anwar, H. 2010. Influence of feed supplementation with Cannabis sativa on quality of broilers carcass. **Pakistan Veterinary Journal** 30(1): 34-38.

Konieczka, P., Wojtasik-Kalinowska, I., Poltorak, A., Kinsner, M., Szkopek, D., Fotschki, B., JuŚkiewicz, J., Banach, J. and Michalczuk, M. 2022. Cannabidiol affects breast meat volatile compounds in chickens subjected to different infection models. **Scientific Reports** 12: 18940.

Kopsell, D.A., Kopsell, D.E. and Curran-Celentano, J. 2005. Carotenoid and chlorophyll pigments in sweet basil grown in the field and greenhouse. **Horticultural Science** 40: 1230-1233.

Lawrie, R.A. and Ledward, D.A. 2006. **Lawrie's meat science** (7th ed). Woodhead Publishing Limited, England.

Maqbool, J., Anwar, H., Rasul, A., Imran, A., Saadullah, M., Malik, S.A., Shabbir, A., Akram, R., Sajid, F., Zafar, S., Saeed, S., Akram, M.N., Islam, F., Hussain, G. and Islam, S. 2023. Comparative evaluation of ethyl acetate and n-Hexane extracts of *Cannabis sativa* L. leaves for muscle function restoration after peripheral nerve lesion. **Food Science & Nutrition** 11(2023): 2767-2775.

Sopian, Y., Sartsook, A., Sringarm, K., Arjin, C., Umsangkul, C., Sivapirunthep, P. and Chaosap, C. 2024. Dietary supplementation of Cannabis sativa residues in broiler chickens affects performance, carcass characteristics, intestinal morphology, blood biochemistry profile and oxidative stability. **Poultry Science** 103(10): 1-12.

Šťastník, O., Jůzl, M., Karásek, F., Fernandová, D., Mrkvicová, E., Pavlata, zzzl., Nedomová, S., Vyhnánek, T., Trojan, V. and Doležal, P. 2019. The effect of hempseed expellers on selected quality indicators of broiler chicken's meat. **Acta Veterinaria Brno** 88: 121-128.

Tathong, T., Khamhan, S., Soisungwan, S. and Phoemchalard, C. 2024. Effects of hemp-derived cannabidiol supplementation on blood variables, carcass characteristics, and meat quality of goats. **Animals** 14: 1718-1730.

Tufarelli, V., Losacco, C., Tedone, L., Passantino, L., Tarricone, S., Laudadio, V. and Colonna, M.A. 2023. Hemp seed (Cannabis sativa L.) cake as sustainable dietary additive in slow-growing broilers: effects on performance, meat quality, oxidative stability and gut health. **Veterinary Quarterly** 43(1): 1-12.

Vispute, M.M., Sharma, D., Mandal, A.B., Rokade, J.J., Tyagi, P.K. and Yadav, A.S. 2019. Effect of dietary supplementation of hemp (*Cannabis sativa*) and dill seed (*Anethumgraveolens*) on performance, serum biochemicals and gut health of broiler chickens. **Journal of Animal Physiology and Animal Nutrition** 103: 525-533.

WHO. 2018. **CANNABIDIOL** (39th ECDD meeting). Kentucky, USA.

Wiriyacharee, P. 2018. **Sensory Evaluation.** Chiang Mai University, Chiang Mai. (in Thai)

Recent Science and Technology

Journal homepage: https:// www.tci-thaijo.org/index.php/rmutsvrj/index

ISSN: 3057-0786 (Online)

Research Article

Effects of Roughage Feeding Strategies on Growth Performance Carcass Quality and Fatty Acid Composition in Meat Goats

Wanida Maksiri [a*], Warinthorn Maneerat [b], Pitunart Noosen [c], Wisut Maitreejet [d] and Jenjina Tamraungit [a]

[a] *Department of Animal Science, Faculty of Agricultural Technology, Phetchaburi Rajabhat University, Mueng, Phetchaburi 76000, Thailand.*

[b] *School of Agriculture and Cooperatives, Sukhothai Thammathirat Open University, Pak Kret, Nonthaburi 11120, Thailand.*

[c] *Department of Animal Science, Faculty of Natural Resources, Prince of Songkla University, Hat Yai, Songkhla 90110, Thailand.*

[d] *Department of Animal Science, Faculty of Agriculture at Kamphaeng Saen, Kasetsart University, Kamphaeng Saen Campus, Nakhon Pathom 73140, Thailand.*

Article history:

Received: 2025-04-24
Revised: 2025-11-02
Accepted: 2025-11-07

Keywords:

Goat;
Roughage;
Growth Performance;
Fatty Acid

ABSTRACT

This study aimed to compare the effects of three different roughage sources—Leucaena (*Leucaena leucocephala*), Pakchong 1 Napier grass (*Pennisetum purpureum* × *Pennisetum americanum*), and Pangola grass (*Digitaria eriantha*) in combination with concentrate supplementation on production performance, carcass quality, and fatty acid composition in meat goat. The experiment was conducted using a completely randomized design (CRD) involving nine male goats (50% Thai Native × Boer crossbred), approximately four months old, with an average initial body weight of 17.94 ± 1.5 kg. The animals were randomly allocated into three treatment groups (n = 3 per group), each receiving one type of freshly cut roughage *ad libitum* (Leucaena, Pakchong 1 Napier grass or Pangola grass) and supplemented with a 14% crude protein concentrate at 1.5% of body weight. The results indicated that goats fed *Leucaena leucocephala* combined with concentrate exhibited the highest dry matter digestibility, body weight gain, and omega-3 fatty acid accumulation, indicating that Leucaena is the most effective roughage source under the present experimental conditions. Nevertheless, both Pakchong 1 Napier grass and Pangola grass proved to be suitable and sufficient alternatives for goat feeding, particularly in areas where these grasses are readily available. Additionally, these forages contributed to the accumulation of omega-6 (C18:2) fatty acids, which are known to help maintain normal cell function, support immune responses, and reduce the risk of cardiovascular disease when consumed in balanced proportions.

1. Introduction

Meat goat production in Thailand has continued to develop, particularly in rural areas where farmers commonly utilize naturally available roughages such as Leucaena (*Leucaena leucocephala*) and native grasses as primary feed sources. In addition, some farmers cultivate specific forage crops such as Napier grass and Pangola grass to feed their goats. However, the quantity and quality of these forages vary cross season, especially during the rainy season, which spans from June to October and is considered a period of forage abundance. This season offers an opportunity for effective and economical goat feeding management. The information regarding the seasonal variation in forage availability and the types of roughages commonly used by farmers was derived from the authors' long-term field experience and on-farm observations in goat production areas, particularly in central and western Thailand, where seasonal patterns of rainfall strongly influence forage growth. Such practical experience reflects real conditions on smallholder farms and provides useful context for developing

* **Corresponding author.**

E-mail address: *wanida.mak@mail.pbru.ac.th*

Cite this article as:

Maksiri, W., Maneerat, W., Noosen, P., Maitreejet, W. and Tamraungit, J. 2026. Effects of Roughage Feeding Strategies on Growth Performance Carcass Quality and Fatty Acid Composition in Meat Goats. **Recent Science and Technology** 18(1): 267356.

https://doi.org/10.65411/rst.2026.267356

feeding strategies suitable for local production systems. The selection of suitable forage types combined with protein-rich concentrates or feed ingredients such as soybean meal or pelleted legume hulls plays an essential role in improving growth performance, reducing production costs, and enhancing meat and carcass quality, especially the nutritional composition of goat meat.

One important aspect of nutritional quality is the composition of beneficial fatty acids, particularly conjugated linoleic acid (CLA). CLA is an unsaturated fatty acid with antioxidant functions and has been linked to reduced risks of cardiovascular disease, cancer, and inflammatory disorders (Tricon *et al*., 2004). Its formation in meat is associated with the availability of fatty acid precursors in the diet, such as linoleic acid (C18:2n6) and alpha-linolenic acid (C18:3n3).

Different roughage sources, including leucaena, Napier grass, and Pangola grass, contain varying levels of these fatty acids. Leucaena, a leguminous forage, offers high protein content and good nutritional value, making it suitable during the rainy season. Napier grass, although highly productive, generally contains lower protein and higher fiber levels, which can reduce digestibility, therefore supplementation with protein-rich concentrate is often required to maintain a balanced diet.

Previous studies have highlighted the important interaction between forage type and CLA content in meat. Jaturasitha *et al*. (2009) demonstrated that purple guinea grass (*Panicum maximum* TD58) and Hamata stylo (*Stylosanthes hamata*) are rich in alpha-linolenic acid, contributes to increased CLA levels in beef. Furthermore, Saichuer *et al*. (2012) reported that goats fed only fresh purple guinea grass produced meat with higher CLA concentrations than goats receiving concentrate supplementation, despite the latter showing better growth performance.

In recent years, consumer demand for safe, high-quality, and health-promoting foods has increased significantly. Enhancing CLA content in goat meat presents an opportunity to create value-added products and expand access to niche markets such as the halal meat sector. Tailoring feeding strategies to seasonal forage availability may not only improve production efficiency and reduce feed costs but also support the sustainability of goat production systems in Thailand.

These three forages were selected because they are among the most commonly used roughage sources in tropical goat production systems. Leucaena represents a high-protein legume, while Pakchong 1 Napier grass and Pangola grass are widely cultivated grasses differing in digestibility and fiber content. Their comparison provides practical implications for selecting appropriate roughage sources for meat goat production in Thailand.

2. Materials and Methods

2.1 Animals and Experimental Design

The experiment was conducted using a completely randomized design (CRD). A total of nine male crossbred goats (50% Thai Native × Boer), with an average age of approximately 4 months (post-weaning stage) with an average body weight of 17.94 ± 1.54 kg, were used. The goats were randomly allocated into three treatment groups with three replicates per group (one goat per replicate). All goats were fed a concentrate diet containing at least 14% crude protein (commercial concentrate feed) at 1.5% of their body weight. The experimental treatments were as follows: Group 1: goats fed with freshly cut *Leucaena leucocephala*, Group 2: goats fed with freshly cut Pakchong 1 Napier grass, and Group 3: goats fed with freshly cut Pangola grass. The forages used in the experiment were obtained from typical farm-based sources to reflect practical feeding practices. *Leucaena leucocephala* (leucaena) was harvested from naturally growing stands in public areas commonly utilized by local farmers. The upper 1–2 meters of the plants, mainly consisting of tender leaves and branches, were cut and chopped before feeding. Pakchong 1 Napier grass (*Pennisetum purpureum × P. americanum*) and Pangola grass (*Digitaria eriantha*) were harvested from farmer-owned pastures at approximately 60 days of regrowth, which represents the stage most commonly used for ruminant feeding due to optimal balance between yield and nutritive quality. Clean drinking water and mineral blocks were provided *ad libitum*. Prior to the experimental period, all goats underwent a 14-day adaptation phase, during which they were dewormed using a commercial ivermectin-based anthelmintic Ivermec-F® by subcutaneous injection at the recommended dosage. The feeding trial lasted for 90 days. The experiment was conducted in a well-ventilated, raised-floor housing facility with a tiled roof. Each goat was housed individually in a pen measuring 1.5 × 1.5 meters. The environmental conditions inside the housing were monitored throughout the experimental period, with an average temperature of approximately 32°C and relative humidity of around 60%. Ventilation was maintained using natural airflow and supplemental fans to ensure adequate air exchange and minimize heat stress. All pens were cleaned daily, and manure was removed to maintain hygiene and prevent the buildup of harmful gases such as ammonia, which may negatively affect feed intake and growth performance.

2.2 Data Collection and Chemical Analysis

Feed intake was recorded daily by weighing the feed offered and the feed refused in order to calculate the individual daily feed intake. Individual body weights of the experimental goats were recorded at the beginning and at the end of the feeding trial to determine body weight change, average daily gain (ADG), and feed conversion ratio (FCR). Representative samples of each feed were randomly collected for chemical composition analysis. The proximate composition was determined using the standard procedures of the Association of Official Analytical Chemists (AOAC, 2000). Neutral detergent fiber (NDF) and acid detergent fiber (ADF) were analyzed following the method described by Van Soest *et al*. (1991).

Fecal and Feed Sampling for Dry matter digestibility. Determination representative samples of the feed consumed and feces were collected to determine the acid-insoluble ash (AIA), which was used as an internal marker to estimate the apparent dry matter digestibility (DMD). No other nutrient digestibility measurements were performed in this study. The analysis followed the method of Schnieder and Flatt (1975). Fecal samples were collected during the last week of the experimental period for five consecutive days. After each daily collection, samples were stored in a refrigerator. At the end of the 5-day period, the fecal samples from each individual goat were pooled together, and a composite subsample was taken for analysis. This subsample was dried at 105 °C overnight, ground, and passed through a 1 mm sieve before analysis for AIA content.

Rumen Fluid Sampling and VFA Analysis. On the final day of the experiment, rumen fluid samples were collected from each goat at two time points: before feeding (0 h) and 4 hours after feeding. Sampling was conducted using a stomach tube connected to a vacuum pump. Approximately 100 mL of rumen fluid was collected from each animal. The pH of the rumen fluid was measured immediately after collection. The fluid was then filtered through four layers of cheesecloth. A subsample of 50 mL was transferred into a plastic bottle and acidified with 9 mL of 1 M sulfuric acid (H_2SO_4) to halt microbial activity. The acidified samples were centrifuged at 4,400 × g 12 min. The supernatant was collected and stored at -20°C for the subsequent analysis of total volatile fatty acids (VFAs).

Blood Sampling and Analysis. On the final day of the experiment, blood samples were collected at 0 and 4 h after feeding from the jugular vein using a 5 mL syringe. Each sample was divided into two portions. The first portion was placed in a fluoride-coated tube containing sodium fluoride to preserve plasma for the analysis of blood glucose concentrations. The second portion was placed in a plain tube i.e. without anticoagulant to obtain serum for the determination of blood urea nitrogen (BUN). Blood glucose concentione were analyzed using the method described by Henry *et al.* (1974), while BUN concentrations were determined according to the method of Tiffany *et al*. (1972).

Slaughtering Procedure and Carcass Evaluation. At the end of the 90-day feeding trial, two goats from each treatment group were randomly selected for slaughter. The selected animals were fasted for 12 hours prior to slaughter, with free access to clean drinking water. The live weight after fasting was recorded before slaughter. The animals were slaughtered and processed according to a modified procedure based on Kanthapanit (1986), with adjustments made to align with current standard slaughtering and carcass evaluation practices (FAO, 2020). The hot carcass weight was recorded immediately after evisceration, and the dressing percentage was calculated. The longissimus dorsi muscle area was measured at the cross-section of the longissimus dorsi muscle between the 12th and 13th ribs on the left side of each carcass. This was done by tracing the muscle area onto tracing paper twice, and the average area was calculated to determine the loin eye area.

Longissimus Dorsi Sampling and Meat Quality Analysis. Samples of the longissimus dorsi muscle, which is recognized as a high-quality and tender muscle, were collected for the analysis of physical meat quality parameters. These included pH, color values, shear force, drip loss (i.e., weight loss during refrigerated storage), and cooking loss (i.e., weight loss after standardized cooking). In addition, the fatty acid composition and the concentration of CLA in the longissimus dorsi were determined using gas chromatography.

2.3 Statistical Analysis

All collected data were subjected to analysis of variance (ANOVA) to evaluate the effects of different treatments. Differences among treatment means were compared using Duncan's New Multiple Range Test (DMRT) at a significance level of $p<0.05$.

3. Results and Discussion

3.1 Chemical Composition of diets

The chemical composition analysis of the roughages used in this study, Pakchong 1 Napier grass, Pangola grass, *Leucaena leucocephala* (leucaena), and concentrate-revealed that Pakchong 1 Napier grass had the highest moisture content compared to Pangola grass and leucaena. Regarding crude protein content, Pakchong 1 Napier grass and Pangola grass contained 6.51% and 5.82%, respectively, which were considerably lower than that of leucaena, (23.02%). As a leguminous forage, leucaena naturally possesses a high protein content.

Both Pakchong 1 Napier grass and Pangola grass used in this study were harvested as fresh forages at an average cutting age of approximately 60 days. This harvesting stage contributed to the reduced crude protein levels observed in both types of roughage. The fiber contents of the two grasses were relatively similar. The NDF contents of Pakchong 1 Napier and Pangola grasses were 64.71% and 64.30%, respectively, while the ADF contents were 44.50% and 40.29%, respectively. These values were considerably higher than those found in leucaena, which had NDF and ADF values of 37.80% and 32.58%, respectively, as shown in Table 1. The higher protein and lower fiber contents observed in leucaena are attributed to the appropriate cutting stage, which involved harvesting from the top portion down to approximately 1.5 meters-consisting largely of tender branches and leaves rich in nutrients. The results suggest that Pakchong 1 Napier grass and Pangola grass can be classified as moderate-quality roughages due to their crude protein levels

Table 1 Chemical composition of Leucaena, Napier Pakchong 1 grass, Pangola grass and concentrate feed

Chemical composition (%)	Leucaena	Napier Pakchong 1 grass	Pangola grass	Concentrate feed
DM[1]	33.73±0.96	22.96±0.69	38.46±0.82	87.26±0.74
Moisture	66.27±0.69	77.04±0.69	61.54±0.82	12.74±0.74
Ash	8.42±0.12	13.10±0.34	10.91±0.14	15.84±0.29
EE[2]	3.70±0.15	2.12±0.14	1.38±0.01	6.31±0.17
CP[3]	23.02±1.15	6.51±0.83	5.82±0.12	14.44±1.03
NDF[4]	37.80±0.34	64.71±.73	64.03±0.57	-
ADF[5]	32.58±0.43	44.50±0.82	40.29±2.32	-
Gross Energy (cal/gDM)	4,582.50±18.19	3,904.89±17.09	3,89.03±12.28	3,927.96±0.30

[1] Dry matter, [2] Ether extract, [3] Crude protein, [4] Neutral detergent fiber, [5] Acid detergent fiber

being lower than 7%. Such levels are insufficient to meet the protein requirements of rumen microbes, particularly cellulolytic bacteria, which require a minimum of 7% dietary crude protein to maintain optimal metabolic activity (Hennessy, 1980; NRC, 2007; Wanapat, 2014). These nutritional limitations are expected to affect rumen fermentation, dry matter intake, and growth performance, which are further discussed in Section 3.2.

3.2 Feed Intake of goats

The results revealed a statistically significant difference in roughage intake among the treatment groups. Goats fed with leucaena and Pangola grass had higher roughage intake compared to those fed with Pakchong 1 Napier grass (Table 2). All goats were supplemented with a concentrate at 1.5% of their body weight, with an average intake of 261.78 g/head/day on dry matter basis, which accounted for approximately 1.25% of body weight. When considering total dry matter intake, goats in Groups 1, 2, and 3 consumed 1,067.93, 772.93, and 1,109.18 g/head/day, respectively. The total dry matter intake of goats fed with leucaena and Pangola grass was significantly higher ($P<0.05$) than that of goats fed Pakchong 1 Napier grass. This difference may be attributed to the higher moisture content and greater stem proportion in Pakchong 1 Napier grass, which likely led to a reduced palatability and voluntary feed intake.

Goats fed with leucaena supplemented with concentrate exhibited the highest total feed intake. This result corresponds with the high crude protein content of leucaena, which provided an adequate daily protein intake to support optimal growth. Consequently, goats in this group showed superior growth performance compared to the other groups. Moreover, the higher dry matter digestibility observed in goats fed with Leucaena was associated with improved feed utilization efficiency, as reflected by a lower feed conversion ratio (FCR) compared to the other treatments. The enhanced digestibility of Leucaena likely facilitated greater nutrient absorption and energy availability, which translated into higher growth performance per unit of feed consumed. Conversely, goats fed with Pakchong 1 Napier grass and Pangola grass, which contained higher fiber and lower protein levels, exhibited higher FCR values, indicating less efficient conversion of feed into body weight gain. This finding aligns with previous reports that roughages with lower digestibility result in poorer feed efficiency (Atti *et al*., 2004; NRC, 2007). However, when leucaena is used as the primary roughage, concentrate supplementation may not be necessary due to its sufficient nutritional value, especially its high protein content. In contrast, both Pakchong 1 Napier grass and Pangola grass, which contain lower protein levels, require supplementation with concentrate at 1.5% of body weight, in accordance with NRC (2006) recommendations. According to NRC guidelines, growing kids weighing approximately 20 kg require about 95 g of crude protein per day to achieve an average daily gain (ADG) of 100 g/day. Regarding dry matter digestibility, goats in Group 1 (fed with leucaena) had significantly higher digestibility coefficients than those in Groups 2 and 3, which received Pakchong 1 Napier and Pangola grass, respectively ($P<0.05$). This finding is consistent with the lower fiber content of leucaena, which likely enhanced ruminal fermentation and digestion efficiency.

3.3 Body Weight Change and Growth Performance

The initial body weights of meat goats in Groups 1, 2, and 3 were 17.39, 18.17, and 18.28 kg, respectively. At the end of the 90 days feeding period, the final body weights were 26.37, 22.23, and 22.95 kg, respectively. The corresponding body weight gains were 8.98, 4.06, and 4.67 kg, and the average daily gains (ADG) were 100.90, 45.62, and 52.43 g/head/day, respectively. However, no statistically significant differences were observed in body weight gain or ADG among the treatment groups (Table 3). The numerically higher ADG observed in goats fed with Leucaena may be attributed to its superior nutritional composition and ruminal fermentation characteristics. Leucaena contains a balanced proportion of rumen-degradable protein (RDP) and rumen-undegradable protein (RUP), which enhances microbial growth and amino acid flow to the small intestine. This improves nitrogen utilization efficiency and supports muscle protein synthesis. Additionally, the higher digestibility and metabolizable energy content of Leucaena likely increased energy availability for growth, resulting in a better feed conversion efficiency. The moderate tannin concentration in Leucaena may have further contributed to improved nitrogen

retention by reducing excessive protein degradation in the rumen (Silanikove *et al*., 2001; NRC, 2007.) In contrast, Pakchong 1 Napier grass and Pangola grass have higher NDF and ADF contents, resulting in lower digestibility and reduced nutrient utilization. Van Soest *et al*. (1991) indicated that when the NDF content exceeds 60%, it can suppress feed intake and adversely affect the digestive efficiency of ruminants. Furthermore, although all goats in the experiment received the same level of concentrate supplementation (261.78 g/head/day), the efficiency of concentrate utilization also depended on the type of roughage provided. Goats fed with leucaena were better able to utilize protein and energy from the concentrate in conjunction with the roughage, whereas those fed with high fiber grasses showed lower ruminal fermentation and digestibility.

Table 2 Dry matter intake (DMI), total protein intake and dry matter digestibility coefficient of meat goat (Mean ± Standard deviation)

Item	Group[1]			P-value
	group 1	group 2	group 3	
Dry matter intake (g/head/day)				
Roughage	806.15±12.16[a]	511.15±18.51[b]	847.40±72.80[a]	0.0002
Concentrate feed	261.78±0.00	261.78±0.00	261.78±0.00	-
Total	1,067.93±12.16[a]	772.93±18.51[b]	1,109.18±72.80[a]	0.0002
Dry matter intake (%BW)				
Roughage	3.74±0.15[a]	2.50±0.21[b]	4.13±0.48[a]	0.0078
Concentrate feed	1.22±0.07	1.28±0.06	1.27±0.04	0.3999
Total	4.96±0.22[a]	3.79±0.26[b]	5.40±0.52[a]	0.0040
Crude protein intake (g/head/day)				
Roughage	185.58±2.80a	33.28±1.21c	49.32+4.24b	‹.0001
Concentrate feed	37.80+0.00	37.80±0.00	37.80±0.00	-
Total	223.38±2.80a	71.08±1.21c	87.12±4.24b	‹.0001
Feed conversion ratio				
Roughage	9.56±5.35	12.46±4.34	16.95±04.50	0.2380
Concentrate feed	3.09±1.68	6.40±2.30	5.29±1.68	0.1780
Total	6.33±3.52	9.43±3.31	11.12±3.08	0.2739
Dry matter coefficient (%)	67.62±3.24a	55.01±2.11b	57.35±2.77b	0.0029

[a, b] Mean values within a row indicated with different superscripts are significantly different (P < 0.05).

[1] Group 1 = Leucaena; Group 2 = Pakchong 1 Napier grass; Group 3 = Pangola grass.

Table 3 Average body weight and growth rate of meat goats (Mean ± Standard deviation)

Item	Group[1]			P-value
	group 1	group 2	group 3	
Initial weight (kg/head)	17.39±2.48	18.17±1.26	18.28±1.01	0.7931
Final weight (kg/head)	26.37±1.94[a]	22.23±0.79[b]	22.95±0.48[b]	0.0136
Body weight gain (kg/head)	8.98±4.07	4.06±1.78	4.67±1.25	0.1220
Average daily gain (g/head/day)	100.90±45.72	45.62±19.83	52.43±14.08	0.1219

[a, b] Mean values within a row indicated with different superscripts are significantly different (P < 0.05).

[1] Group 1 = Leucaena; Group 2 = Pakchong 1 Napier grass; Group 3 = Pangola grass.

3.4 Blood Metabolites and Volatile Fatty Acids in the Rumen

The blood urea nitrogen levels prior to feeding (0 h) for goats in Groups 1, 2, and 3 were 35.40, 9.57, and 12.70 mg/dL, respectively. At 4 h post-feeding, the BUN values increased to 36.60, 10.37, and 14.63 mg/dL, respectively. The BUN levels differed significantly among treatments (*P<0.05*), as shown in Table 4. The BUN concentrations of goats fed with Pakchong 1 Napier grass and Pangola grass were within the normal physiological range of 6.30–25.50 mg/dL (Wanapat, 1990), which is consistent with the findings of Preston and Leng (1987), who reported that optimal rumen microbial function occurs at ammonia nitrogen concentrations between 5–25 mg/dL. The increase in BUN is directly related to the amount of protein consumed and its conversion to ammonia in the rumen (Kohn *et al*., 2005). The significantly higher BUN concentration observed in goats fed with Leucaena could be explained by the high content of rumen-degradable protein (RDP) in Leucaena, which led to increased ammonia production in the rumen.

Excess ammonia that was not incorporated into microbial protein was absorbed into the bloodstream and converted to urea in the liver, resulting in higher BUN levels. This elevation indicates greater nitrogen turnover associated with high-protein diets. The higher BUN in Group 1 corresponded with greater dry matter digestibility and growth performance, suggesting that a substantial proportion of the degraded nitrogen was efficiently utilized for microbial protein synthesis and tissue growth. However, excessive ruminal ammonia may also imply partial inefficiency in nitrogen utilization, which should be considered in future feeding management (Kohn *et al*., 2005; NRC, 2007).

However, excessively high BUN concentrations may indicate inefficiencies in nitrogen utilization and place additional metabolic load on the liver for urea detoxification. Furthermore, elevated BUN leads to increased urinary nitrogen excretion, which has implications for environmental nitrogen pollution and overall feeding cost efficiency. Therefore, optimizing the balance between protein intake and microbial utilization is crucial to maximize growth performance while minimizing N loss and potential health risks.

The blood glucose concentrations prior to feeding for goats in Groups 1, 2, and 3 were 66.30, 65.00, and 56.67 mg/dL, respectively. Although the differences tended to higher in Group 1, they were not statistically significant (*P=0.078*). At 4 h after feeding, these values increased to 71.33, 66.33, and 62.00 mg/dL, respectively with no significant differences observed among the groups (*P=0.1199*). There were no statistically significant differences among the treatment groups. All measured glucose concentrations remained within the normal physiological range for healthy goats (50–75 mg/dL), as reported by Kaneko (1980) and supported by more recent references (Kaneko *et al*., 2008; Thrall, 2012). This indicates that the diets provided an adequate energy supply, primarily through propionic acid, a major volatile fatty acid (VFA) produced from ruminal carbohydrate fermentation and subsequently utilized for hepatic gluconeogenesis in ruminants (Owens *et al*., 1998). The absence of significant differences in blood glucose concentrations among the treatment groups further reflects the strong regulatory capacity of ruminants to maintain glucose homeostasis, as their blood glucose is tightly controlled by gluconeogenesis rather than direct intestinal absorption, even when fed different roughage sources.

The ruminal pH values before feeding in Groups 1, 2, and 3 were 6.60, 6.60, and 6.20, respectively. Four hours after feeding, the pH values decreased significantly (*P<0.05*) to a range of 5.6 7 –5.9 3 . This decrease indicates intensive fermentation during the postprandial period, particularly within 2-4 h after feeding, when VFA production peaks (Van Soest, 1994). The optimal ruminal pH for the growth and activity of fibrolytic bacteria is typically 6.2–6.8, and a ruminal pH below 6.0 can compromise fiber digestion (Russell and Dombrowski, 1980). However, the rumen has physiological buffering mechanisms, primarily through salivary bicarbonate, which help maintain pH within a functional range. Additionally, appropriate diet formulation such as providing sufficient long fiber and controlling concentrate inclusion may help prevent excessive pH decline and thereby sustain microbial activity and roughage utilization efficiency.

The proportions of volatile fatty acids (VFAs) in the rumen fluid of goats at 4 hours post-feeding showed that acetic acid was the predominant VFA in all treatment groups, ranging from 76.56% to 84.39%. Propionic acid levels were significantly higher (P<0.05) in Group 2 compared to the other groups. The proportions of volatile fatty acids (VFAs) in the rumen fluid of goats at 4 hours post-feeding showed that acetic acid was the predominant VFA in all treatments, indicating that roughage served as the primary fermentative substrate. The variation in acetic and propionic acid proportions among treatments was closely related to differences in roughage intake and nutrient composition. Goats fed with Leucaena and Pangola grass consumed greater amounts of roughage (806.15 and 847.40 g/head/day, respectively) compared to those fed with Pakchong 1 Napier grass (511.15 g/head/day), while the concentrate intake was similar across treatments (261.78 g/head/day). The higher roughage intake in Groups 1 and 3 promoted more fiber fermentation in the rumen, leading to greater acetic acid production, which is a typical end product of cellulose degradation by fibrolytic bacteria (Van Soest, 1994). This explains the higher acetic acid proportions observed in these groups. In contrast, the lower roughage intake but relatively higher proportion of concentrate in Group 2 (Napier grass) favored starch fermentation, which stimulated amylolytic bacteria and resulted in significantly higher propionic acid levels (P<0.05) (France and Dijkstra, 2005). Propionate serves as a major glucogenic precursor, providing more readily available energy in the form of glucose. Although the overall VFA concentrations were within the physiological range reported for ruminants (Wanapat, 1990), the differences in acetic-to-propionic ratios reflected the distinct fermentation patterns among the forage types used. A higher acetic-to-propionic ratio, as observed in the Leucaena and Pangola groups, indicates greater reliance on fiber fermentation and may be associated with lower energy efficiency but improved fiber digestibility. Conversely, the Napier group exhibited a lower acetic-to-propionic ratio, which suggests a more efficient energy conversion process. These findings imply that the type and amount of roughage intake directly influenced rumen fermentation characteristics, energy metabolism, and consequently, the growth performance of goats observed in this study (France and Dijkstra, 2005; NRC, 2007; Van Soest, 1994).

Table 4 Blood chemical composition of meat goats (mean±standard deviation)

Item (mg/dl)	Group[1]			P-value
	group 1	group 2	group 3	
Blood urea nitrogen				
0 h-pre feeding	35.40±6.85[a]	9.57±0.42[b]	12.70±4.20[b]	0.0009
4 h-post feeding	36.60±7.49[a]	10.37±0.23[b]	14.63±4.58[b]	0.0015
Blood glucose				
0 h-pre feeding	66.33±6.65	65.00±4.00	56.67±1.15	0.0785
4 h-post feeding	71.33±5.69	66.33±4.93	62.00±2.65	0.1199

[a, b] Mean values within a row indicated with different superscripts are significantly different (P < 0.05).

[1] Group 1 = Leucaena; Group 2 = Pakchong 1 Napier grass; Group 3 = Pangola grass.

Table 5 pH and volatile fatty acid (VFA) concentration in rumen fluid of meat goats (mean±standard deviation)

Item	Group[1]			P-value
	group 1	group 2	group 3	
Ruminal (pH)				
0 h-pre feeding	6.60±0.10[a]	6.60±6.20[a]	6.20±0.10[b]	0.0203
4 h-post feeding	5.93±0.058[a]	5.77±0.12[ab]	5.67±0.12[b]	0.0448
Total VFA (mmol/dl)				
0 h-pre feeding	16.91±3.85	17.90±4.08	20.22±2.24	0.5269
4 h-post feeding	20.50±4.46	19.84±4.12	21.33±3.69	0.9071
Acetic (% of total VFA)				
0 h-pre feeding	84.39±1.81	83.83±1.34	84.11±1.32	0.9021
4 h-post feeding	80.71±0.87	76.56±2.65	82.20±3.38	0.0786
Propionate (% of total VFA)				
0 h-pre feeding	8.46±0.78[b]	11.21±1.75[a]	7.40±1.23[b]	0.0292
4 h-post feeding	10.63±0.72[b]	16.30±2.68[a]	10.31±1.86[b]	0.0150
Butyrate (% of total VFA)				
0 h-pre feeding	4.27±1.72[ab]	2.88±0.82[b]	6.32±0.78[a]	0.0329
4 h-post feeding	6.40±0.93	5.11±0.87	5.87±1.25	0.3671
Acetate:Propionate				
0 h-pre feeding	10.04±1.03[ab]	7.60±1.19[b]	11.60±2.10[a]	0.0469
4 h-post feeding	7.62±0.55[a]	4.81±0.99[b]	8.14±1.68[a]	0.0267

[a, b] Mean values within a row indicated with different superscripts are significantly different (P < 0.05).

[1] Group 1 = Leucaena; Group 2 = Pakchong 1 Napier grass; Group 3 = Pangola grass

3.5 Carcass Characteristics and Fatty Acid Composition of Goat Meat

The results showed that the use of Leucaena as a roughage source in goat feeding led to a significantly greater Longissimus dorsi muscle area compared to goats fed with Pakchong 1 Napier grass or Pangola grass (*P<0.05*). This finding can be attributed to the higher crude protein content and superior digestibility of Leucaena, which enhanced amino acid availability and metabolizable energy supply for muscle development. The combination of Leucaena with concentrate supplementation provided a more balanced nutrient intake, improving nitrogen utilization efficiency and promoting greater lean tissue accretion. The efficient digestion and utilization of protein from Leucaena likely contributed to higher body weight gain and a more developed loin muscle compared with the grass-fed groups. This result corresponds with the higher average daily gain (ADG) and dry matter digestibility (DMD) observed in Group 1. The better nutritional quality and rumen fermentation pattern of Leucaena promoted microbial protein synthesis, resulting in greater amino acid absorption for muscle protein synthesis. These mechanisms explain the larger loin eye area found in goats fed with Leucaena in this study. Similar trends have been reported by Kongman and Prasanpanich (2016), who found that the type of roughage significantly affects growth and carcass characteristics. Atti *et al*. (2004) also demonstrated that diets with higher protein content improve muscle development, particularly in red muscle regions such as the loin and hind limbs. Moreover, Solomon *et al*. (2008) and Conrad and Hibbs (1968) emphasized that improved digestibility and ruminal fermentation efficiency contribute directly to increased carcass

weight and muscle deposition. The present study supports these findings and highlights Leucaena as an effective protein-rich forage for enhancing muscle growth and carcass yield in goats.

Significant differences (P<0.05) were observed in the fatty acid composition of goat meat among the three dietary treatments (Table 7). Goats fed with Leucaena (Group 1) had a significantly lower proportion of myristic (C14:0), pentadecanoic (C15:0), and palmitic acid (C16:0) but a higher level of stearic acid (C18:0) compared with the other groups. Moreover, the Leucaena group exhibited significantly higher levels of alpha-linolenic acid (C18:3 n3) and trans-oleic acid (C18:1 n9t), resulting in the lowest n6:n3 ratio (3.59). This indicates that Leucaena feeding improved the nutritional quality of meat fat by increasing beneficial unsaturated fatty acids and decreasing the proportion of hypercholesterolemic SFAs. The higher UFA levels in the Leucaena group may be attributed to its higher crude protein content and the presence of secondary plant compounds that reduce ruminal biohydrogenation (Jenkins *et al*., 2008). These factors allow more UFAs, particularly omega-3 fatty acids, to bypass the rumen and deposit in muscle tissue. In contrast, goats fed with Pakchong 1 Napier grass (Group 2) showed the highest proportions of palmitic and myristic acids, likely due to enhanced hydrogenation associated with higher fiber fermentation (Van Soest, 1994). The Pangola grass group (Group 3) showed intermediate values between the Leucaena and Napier groups, reflecting its moderate fiber and protein contents.

In terms of fatty acid composition, the meat from all three experimental goat groups contained palmitic acid (C16:0) and stearic acid (C18:0) as the predominant saturated fatty acids (SFAs), both of which are commonly found in the fat of meat and dairy products (Redah *et al*., 2011). Among the unsaturated fatty acids (UFAs), oleic acid (C18:1 cis-9) was the most abundant. This monounsaturated fatty acid is also widely present in olive oil, avocado oil, and canola oil, and is known for its beneficial effects in reducing the risk of cardiovascular disease, lowering blood cholesterol, and improving blood sugar control (Guasch-Ferré *et al*., 2020).

Although conjugated linoleic acid (CLA) was not detected in this study, all groups contained appreciable levels of beneficial unsaturated fatty acids such as oleic (C18:1), linoleic (C18:2), and alpha-linolenic (C18:3), which are associated with improved lipid metabolism and anti-inflammatory effects in humans (Dhiman *et al*., 2005; Guasch-Ferré *et al*., 2020). The results of this study therefore suggest that feeding Leucaena leucocephala as a primary forage source can improve the nutritional profile of goat meat by increasing omega-3 fatty acid content and reducing the n6:n3 ratio, thereby enhancing its value for human health.

The absence of detectable CLA in the present study may be due to insufficient dietary precursors for CLA synthesis or extensive ruminal biohydrogenation of unsaturated fatty acids prior to absorption. Additionally, it is possible that the detection limit of the analytical method used may not have been sensitive enough to quantify low concentrations of CLA in goat muscle. Further investigation is therefore recommended to optimize dietary strategies that could enhance CLA deposition in meat.

Table 6 Carcass chracteristics and meat quality in goat (mean±standard deviation)

Item	Group[1]			P-value
	group 1	group 2	group 3	
Live weight after fasting (kg)	28.34±2.18	22.64±1.44	21.76±0.06	0.0405
Hot carcass weight (kg)	11.20±0.71	8.88±0.60	7.88±0.46	0.2113
Hot carcass percentage (%)	39.54±0.54	39.20±0.16	34.63±2.21	0.0771
Longissimus muscle area (cm^2)	14.44±0.06[a]	13.15±0.15[b]	13.24±0.39[b]	0.0223
$pH_{0\ min}$	7.41±0.61	6.52±0.21	6.42±0.57	0.2373
$pH_{24\ min}$	7.60±0.45	7.46±0.12	7.10±0.78	0.6566
L^*	36.41±3.29	36.04±3.82	36.35±3.78	0.9941
a^*	13.24±0.60	14.24±0.82	13.96±0.25	0.3591
b^*	11.98±2.25	13.35±0.32	12.78±0.86	0.6616
% cookin loss	22.95±5.68	24.04±2.15	19.01±9.01	0.7267
% drip loss	6.22±1.26	6.46±0.35	8.82±1.67	0.2125
Shear force (กก.)	9.47±2.69	7.22±1.07	11.73±1.52	0.2019

[a, b] Mean values within a row indicated with different superscripts are significantly different (P < 0.05).

[1] Group 1 = Leucaena; Group 2 = Pakchong 1 Napier grass; Group 3 = Pangola grass

Table 7 Fatty acid composition in longissimus dorsi muscle (as % of fatty acid) (mean±standard deviation)

Item	Group[1]			P-value
	group 1	group 2	group 3	
SFA				
C10:0	0.28±0.07	0.22±0.02	10.23±0.03	0.1532
C12:0	1.22±0.13	2.08±1.00	1.85±0.30	0.0671
C14:0	10.64±0.62[b]	15.31±3.39[a]	14.16±0.96[a]	0.0037
C15:0	1.42±0.26[b]	1.85±0.39[a]	1.44±0.22[b]	0.0475
C16:0	47.29±1.94[b]	53.87±3.90[a]	51.52±3.77[a]	0.0121
C18:0	38.90±1.00[a]	26.09±1.27[c]	30.37±2.89[b]	<.0001
C20:0	0.13±0.01	0.21±0.14	0.15±0.06	0.2801
C22:0	0.12±0.03[b]	0.36±0.06[a]	0.27±0.14[a]	0.0013
UFA				
C14:1	0.37±0.03[c]	1.00±0.27[a]	0.70±0.14[b]	<.0001
C16:1	5.68±0.18[b]	9.08±1.14[a]	8.50±0.28[a]	<.0001
C18:1 n9t	6.82±0.16[a]	3.96±0.97[b]	4.72±1.21[b]	0.0002
C18:1 n9c	81.86±0.96	81.14±3.23	81.50±0.90	0.8295
C18:2 n6c	4.05±0.56	4.17±0.74	3.83±0.16	0.5452
C18:3 n3	1.15±0.27[a]	0.41±0.04[c]	0.64±0.08[b]	<.0001
C20:1	0.13±0.00	0.12±0.01	0.11±0.03	0.5984
SFA (mg/g oil)	300.12±7.06	277.03±21.51	316.35±62.73	0.2383
UFA (mg/g oil)	190.67±3.60	206.07±12.56	179.91±14.88	0.0044
n6:n3 ratio	3.59±0.41[c]	10.17±1.67[a]	6.04±0.93[b]	<.0001

[a, b, c] Mean values within a row indicated with different superscripts are significantly different ($P < 0.05$).

[1] Group 1 = Leucaena; Group 2 = Pakchong 1 Napier grass; Group 3 = Pangola grass

4. Conclusion

The present study demonstrated that the type of roughage significantly influenced growth performance, carcass characteristics, and fatty acid composition in meat goats. Among the three treatments evaluated, feeding Leucaena supplemented with concentrate resulted in the most favorable outcomes. Goats in this group exhibited the highest dry matter digestibility, superior growth rate, and the largest *Longissimus dorsi* muscle area, reflecting more efficient nutrient utilization and muscle protein synthesis. Furthermore, the meat from this group contained higher levels of beneficial unsaturated fatty acids, particularly alpha-linolenic acid (C18:3n3), and a more desirable n6:n3 ratio, indicating enhanced nutritional quality.

These results collectively suggest that Leucaena is the most suitable roughage source for improving both production efficiency and meat quality in goats, especially when combined with an appropriate concentrate supplement. However, in areas where Leucaena is not readily available, Pakchong 1 Napier grass and Pangola grass remain practical alternatives, particularly when supplemented with protein-rich concentrates to improve their nutritional balance. The findings highlight the importance of integrating locally available forage resources with suitable concentrate formulations to optimize goat production under tropical feeding systems.

5. Acknowledgments

This research was financially supported by the Science, Research and Innovation Fund (TSRI) under the Fundamental Fund (FF) for Basic Research, Fiscal Year 2024. The authors would like to express their sincere appreciation to the Animal Science Program, Faculty of Agricultural Technology, Phetchaburi Rajabhat University, for providing access to the goat research facility and animal feed analysis laboratory. Special thanks are also extended to Ploy Phet Mook Farm for their generous provision of meat goats for this study.

6. References

AOAC. 2000. **Official Method of Analysis of AOAC International** (17th ed). The Association of Official Analytical Chemists, Virginia.

Atti, N., Rouissi, H. and Mahouachi, M. 2004. The effect of dietary crude protein level on growth, carcass and meat composition of male goat kids in Tunisia. **Small Ruminant Research** 54(1): 89-97.

Conrad, H. and Hibbs, J. 1968. Appreciation of Its Nutritive Value. **Journal of Dairy Science** 51(2): 276-285.

Dhiman, T.R., Nam, S.H. and Ure, A.L. 2005. Factor affecting conjugated linoleic acid content in milk and meat. **Critical Reviews in Food Science and Nutrition** 45(6): 463-482.

FAO. 2020. **Guidelines for humane handling, transport, and slaughter of livestock.** Available Source: https://www.fao.org/3/i5704e/i5704e.pdf, Nonember 23, 2025.

France, J. and Dijkstra, J. 2005. Volatile fatty acid production, pp.157-175. *In* Dijkstra, J., Forbes, J. and France, J., Eds. **Quantitative aspects of ruminant digestion and metabolism.** CABI Publishing, Wallingford.

Guasch-Ferré, M., Li, Y., Willett, W.C., Iruela-Arispe, M.L. and Hu, F.B. 2020. Olive oil consumption and cardiovascular risk in U.S. adults. **Journal of the American College of Cardiology** 75(15): 1729-1739.

Hennessy, D.W. 1980. Protein nutrition of ruminants in the tropical areas of Australia. **Tropical Grasslands** 14: 260-265.

Henry, R.J., Donald, C.C. and James, W.W. 1974. **Clinical Chemistry: Principle and Technique** (2nd ed). Harper and Row Inc., Vergenia, USA.

Jaturasitha, S., Kayan, A. and Wicke, M. 2009. Carcass and meat characteristics of male Thai native cattle (Brahman × Thai native) fattened on different roughage feeding systems. **Meat Science** 83(3): 440-444. (in Thai)

Jenkins, T.C., Wallace, R.J., Moate, P.J. and Mosley, E.E. 2008. Board-invited review: Recent advances in biohydrogenation of unsaturated fatty acids within the rumen microbial ecosystem. **Journal of Animal Science** 86(2): 397-412.

Kaneko, J.J. 1980. **Clinical Biochemistry of Domestic Animals.** Academic Press, New York.

Kaneko, J.J., Harvey, J.W. and Bruss, M.L. 2008. **Clinical Biochemistry of Domestic Animals** (6th ed). Academic Press, Elsevier.

Kanthapanit, C. 1986. **Meat science.** Thai Wattana Panich Publishing, Bangkok. (in Thai)

Kohn, R.A., Dinneen, M.M. and Russek-Cohen, E. 2005. Using blood urea nitrogen to predict nitrogen excretion and efficiency of nitrogen utilization in cattle, sheep, goats, horses, pigs, and rats. **Journal of Animal Science** 83(4): 879-889.

Kongman, P. and Prasanpanich, S. 2016. **Research Report on Effects of various roughage on fattening beef goat in growth rate and carcass quality.** Faculty of Agriculture, Kasetsart University. (in Thai)

NRC. 2006. **Nutrient Requirements of Small Ruminant.** National Academy Press, Washington, DC., USA.

NRC. 2007. **Nutrient requirements of small ruminants: Sheep, goats, cervids, and New World camelids.** National Academies Press, Washington, DC.

Owens, F.N., Zinn, R.A. and Hanson, C.F. 1998. Acidosis in cattle: A review. **Journal of Animal Science** 76(1): 275-286.

Preston, T.R. and Leng, R.A. 1987. **Matching Ruminant Production Systems with Available Resources in the Tropics and Sub-tropics.** Penambull Book Armidale, Australia.

Redah, A.A., Ali, A., Rashed, A. and Mahgoub, O. 2011. Fatty acid composition of muscle and adipose tissues from Omani Jebel Akhdar goat. **Journal of Animal and Veterinary Advances** 10(12): 1551-1556.

Russell, J.B. and Dombrowski, D.B. 1980. Effect of pH on the efficiency of growth by pure cultures of rumen bacteria in continuous culture. **Applied and Environmental Microbiology** 39(3): 604-610.

Saichuer, A., Kongmun, P., Loongyai, W., Poathong, S. and Prasanpanich, S. 2012. Effects of purple Guinea grass combined with different levels of concentrate on production performance and conjugated linoleic acid (CLA) content in meat goats, pp. 107-114. *In* **Proceedings of the 50th Kasetsart University Annual Conference: Animal Science, Veterinary Medicine, and Fisheries.** Kasetsart University, Bangkok. (in Thai)

Schneider, B.H. and Flatt, W.P. 1975. **The Evaluation of Feeding Through Digestibility Experiments.** University of Georgia Press, Athens.

Silanikove, N., Perevolotsky, A. and Provenza, F.D. 2001. Use of tannin-binding chemicals to assay for tannins and their negative post-ingestive effects in ruminants. **Animal Feed Science and Technology** 91(1-2): 69-81.

Solomon, M., Melaku, S. and Tolera, A. 2008. Supplementation of cottonseed meal on feed intake, digestibility, live weight and carcass parameters of Sidama goats. **Livestock Science** 119(1-3): 137-144.

Thrall, M.A., Weiser, G., Allison, R.W. and Campbell, T.W. 2012. **Veterinary hematology and clinical chemistry** (2nd ed). John Wiley and Sons.

Tiffany, T.O., Jansen, J.M., Burtis, C.A., Overton J.B. and Scott, C.D. 1972. Enzymatic kinetic rate and end point analyses of substrate by the use of a GeMSAEC fast analyser. **Clinical Chemistry** 18(8): 829-840.

Tricon, S., Burdge, G.C., Kew, S., Banerjee, T., Russell, J.J., Grimble, R.F., Williams, C.M., Calder, P.C. and Yaqoob, P. 2004. Effects of cis-9, trans-11 and trans-10, cis-12 conjugated linoleic acid on immune cell function in healthy humans. **The American Journal of Clinical Nutrition** 80(6): 1626-1633.

Van Soest, P.J., Robertson, J.B. and Lewis, B.A. 1991. Methods for dietary fiber, neutral detergent fiber and non starch polysaccharides in relation to animal production. **Journal of Dairy Science** 74(10): 3583-3597.

Van Soest, P.J. 1994. **Nutritional ecology of the ruminant** (2nd ed). Comstock Publishing Associates, Cornell University Press, Ithaca, NY.

Wanapat, M. 1990. **Ruminant nutrition.** Department of Animal Science, Faculty of Agriculture, Khon Kaen University. (in Thai)

Wanapat, M. 2014. **Rumen microbiology and ruminant digestion.** Department of Animal Science, Faculty of Agriculture, Khon Kaen University. (in Thai)

Recent Science and Technology
Research and Development Institute,
Rajamangala University of Technology Srivijaya
179 M.3, Maifad, Sikao, Trang 92150, Thailand.
Tel:+66-0922-6004-39 Email: rst.journal@rmutsv.ac.th